2003-2006

China National Report on Physical Sciences of the Oceans

For

The 24rd General Assembly of IUGG

Perugia, Italy, 2-13 July, 2007

By Chinese National Committee for

The International Union of Geodesy and Geophysics

Beijing, China

June, 2007

PREFACE

This quadrennial report is the second report in the new millennium, which is one of the China National Reports (2002-2006), prepared by the Chinese National Committee for IAPSO for the XXIV IUGG General Assembly of the International Union of Geodesy and Geophysics to be held in Perugia, Italy from July 2 to July 13, 2007.

This report can be divided into two parts. The first part consists of the following 6 papers, i.e. Circulation in the East China Sea and Dynamics of the Kuroshio and the Ryukyu Current, Research Progress in the South China Sea Circulation and Local Air-Sea Interaction in 2003-2006, A Review of Ocean-Atmosphere Interaction Studies in China, Advance in Tide and Sea Level Research in China from 2002 to 2006, Internal Waves in China During 2002-2006 and Sea Fog Research of China: A Review. These 6 papers review the main work done and the major progress made in physical oceanography and air-sea interaction in Mainland China.

The second part covers such 6 papers as Marine Sediment Dynamics and Related Research in China, 2002-2006, Progress of Chemical Oceanography in China (2002-2006), Progress of Oceanic Remote Sensing by Satellite Altimetry in China,2002-2006, Advances in Marine Microwave Remote Sensing in China, Progress of Ocean Color Sensing in China and Progress and Perspective in the Ocean Information Technology in China. They represent a new trend that the physical sciences of the ocean are becoming multi-disciplinary sciences, although researches into sediment dynamics, ecosystem dynamics and biogeochemistry of the ocean are still at their initial stage in China. It should be noted that this report only provides an overview of the subjects mentioned in the above papers, but it does show encouraging progress in physical sciences of the oceans in Mainland China over the past four years. It is pleasant to see the fact that most of papers in this report have been written by the younger scientists, which shows that the younger generation of marine scientists in China has grown up.

I would like to take this opportunity, on behalf of the Chinese National Committee for IAPSO, to express my deep appreciation to all the authors for their contributions, to Prof. ZHAO Jingping, Vice-Chairman of the Chinese National Committee for IAPSO, who made a great contribution to

organizing the writing group for this report, and to Mr. HU Bo and Ms. WANG Hong, who carefully corrected mistakes in texts of some papers. Finally, the editing of this report was supported by the two key projects of the National Natural Science Foundation of China: Study on the structure of Arctic Circumpolar Boundary Current and its impact on climate change (Grant No. 40631006) and The non-linear features of the key dynamic processes and their predictive methods in the Kuroshio region of the China seas (Grant No.90411013).

LE Kentang

Editor-in-Chief

Chairman, Chinese National Committee for IAPSO

CIRCULATION IN THE EAST CHINA SEA AND DYNAMICS OF THE KUROSHIO AND THE RYUKYU CURRENT

YUAN Yao-chu

State Key Laboratory of Satellite Ocean Environment Dynamics, Second Institute of Oceanography, State Oceanic Administration, Hangzhou 310012, China

On the study of the circulation in the East China Sea (ECS), the Kuroshio and the Ryukyu Current, a lot of the works were made and reviewed by the Chinese scientists during July of 2002-July of 2006. In this paper these works will be reviewed and can be divided into three aspects, namely the circulation in the East China Sea (ECS) and the Kuroshio in the ECS, the circulation and Kuroshio east of Taiwan and the currents east of the Ryukyu Islands.

Ⅰ. CIRCULATION AND THE KUROSHIO IN THE EAST CHINA SEA (ECS)

1.1 Numerical computed results with the observed currents and hydrographic data

On the basis of hydrographic data and the current measurements with the mooring system, the vessel-mounted ADCP and toward ADCP data were obtained by the cooperative study between Chinese (inclusive of Chinese Taibei) and Japanese Scientists during June 4 to 19, 1999 onboad the R/V Xiangyanghong 14 (hereafter called cruise 1), the circulation in the southern Huanghai Sea (HS) and northern East China Sea (ECS) are computed by using the modified inverse method (Yuan et al., 2003a) and the three dimensional non-linear diagnostic, semidiagnostic and prognostic models in the sigma coordinate (Wang et al., 2003), respectively. The following results had been obtained by them. 1) The Kuroshio flowed northeastward through an eastern part of the investigated region and had main core at Section PN. There was also a northward flow at the easternmost part of Section PN, and there was a weaker anti-cyclonic eddy between these two northward flows. There was a weak cyclonic eddy at the western part of Section PN. The above current structure is one type of the current structures at Section PN in ECS. 2) The net northward volume transport(VT) of the Kuroshio and the offshore branch of Taiwan Warm Current(TWCOB) through Section PN was about $26.2\times10^6 m^3/s$ in June 1999.The VT of inshore branch of Taiwan Warm Current(TWCIB) through the investigated region was about $0.4\times10^6 m^3/s$.The Taiwan Warm Current (TWC) had a great effect on the currents over the continental shelf. 3) The Huanghai Sea Coastal Current (HSCC) flowed southeastward and enters into the northwestern part of investigated region, and flowed to turn cyclonically, and then it flowed northeastward, which was due to the influence of the Taiwan Warm Current and topography. 4) There was a cyclonic eddy southwest of the Cheju Island. It had the feature of high dense and cold water. 5) The homogeneous cold water appeared in the layer from about 30 m level to the bottom between stations C3-6 and C3-11 at the northernmost Section C3.It was a southwestern part of the Huanghai Sea Cold Water Mass (HSCWM). 6) A comparison between the computed velocities and the observed currents at the mooring station showed that they agreed each other.

On the basis of hydrographic data obtained in June 17 to 25, 1999 on board the R/V *Eardo*, Korea (hereafter called cruise 2), the circulation in the southern Huanghai Sea and East China

Sea were computed by using the modified inverse method (Yuan et al, 2004a). A comparison between above the two computed results in cruise 1 and cruise 2 showed following variability of circulation between cruises 1 and 2 (Yuan et al, 2004a). 1) The position of the Kuroshio core in cruise 2 was slightly to the east of that in cruise 1; 2) The high dense and cold water (HDCW) occurred in the region south of Cheju Island between 125°30′E and 127°E during the second cruise. The circulation in the region of HDCW was cyclonic. Comparing the position of HDCW during cruise 2 with that during cruise 1, its position in cruise 2 moved slightly northward. It is worthy of note that the time difference between cruises 1 and 2 was about two weeks.

The direct measurements of current velocity and water temperature were taken at the mooring station M (125º29.38' N, 31 º49.70' E) in the continental shelf area of the East China Sea during June 1999 by R/V Xianyanghong No. 14 (see Liu et al., 2004). The relationship between oceanic fluctuations at different depths were calculated by the spectra analysis. The major results are as follows (see Liu et al., 2004): 1) the mean flows are southeastward at both the 30 m and 45m depths. The currents became stronger gradually during the observation period. This may be mainly attributed to the transition of the tidal currents from neap to spring. 2) The local inertial period was close to the period of diurnal fluctuation, and an inertial motion is clockwise. Thus, the local inertial motion combines with diurnal fluctuation, and makes the spectral peak in clockwise components much higher than those in counterclockwise ones. Besides the fluctuations of above main periods, there exists also a peak at the 3d period for counterclockwise components in the upper and lower layers. 3) The computed cross spectra between two time series of current velocities at the 30m and 45m depths show that the current fluctuations at the both 30m and 45m depths are much alike, i. e., they are synchronous. This means that the flow field here is rather vertically uniform. 4) Plots of temperature time series at the 16m, 30m, 35m, 45m and 50m depths show that the temporal variations of temperature at these depths are synchronous, just as those in the velocity field; the temperature records also show a gradual rise in temperature, just like those in velocity field.

Based on the numerical simulation of the mean circulation and relevant thermal-salinity fields in June with a three-dimensional ocean model (ECOM-si), the model outputs are used as first guess of initial fields for numerical integration of the model equations and the numerical results are applied to investigate the dynamical responses of the Huanghai Sea and East China Sea (HECS) during the course of a weak land-to-sea cyclones' passage over the Huanghai Sea on 15-16 June 1999 (see Qin et al., 2005). Their major results were as follows (see Qin et al., 2005). The response of oceanic currents to the wind stresses driven by the cyclone and its southern subtropical high were strongly characterized by the wind drift with its extent of equivalent scale of cyclone in the horizontal and of Ekman layer in the vertical. The sea response at a given site was closely related to the transient local wind speed and direction, especially was sensitive to the local wind direction, which is demonstrated at three points locating at the southern and western Huanghai Sea and the northern East China Sea. So the sea response at the locations differed considerably from one another. The current responded to the wind stress in a simple way**:** directly to the wind-driven current and subsequent gradient current and slope current etc., whereas sea temperature responded to the wind stress in the following two ways: directly to the cyclone-induced cooling and indirectly to water movements both in the horizontal and the vertical by the cyclone's wind stress. So the sea temperature variation under the influence of cyclone was more complicate than the current. The HSEC in response to the cyclone and its ambient weather system was likely to be a

fast process and such a response could last at least for more than one day. The currents increased with duration of wind stress exerted on the surface and decreased with increase of depth. Affected by the cyclone, the maximum sea surface temperature decreased by almost 1.6℃ during the 24 h cyclone.

Xu et al. (2003) studied to understand the roles of bottom boundary mixing and the topographic Heat Accumulation Effect (THAE) in the Yellow Sea Cold Water Mass (YSCWM) circulation using a theoretic solution of one-dimensional heat transfer equation and a numerical simulation of 3D baroclinic circulation by MOM2. Their results display the following feature:: 1) The time scale of heat transfer changes from days to weeks and from shallow to deep water column. The strong bottom boundary mixing makes the thermocline domed. 2) The YSCWM circulation has a two-layer structure. The upper layer is cyclonic, while the lower layer is anticyclonic, and the lower layer is thinner (about 10—20 m) and weaker than the upper layer. The depth-integrated (net) circulation is cyclonic. 3) The strength of the bottom boundary mixing influences the temperature structures greatly but has less effect on the velocity structure.

The accumulated in situ hydrographic survey as well as the satellite observed sea surface temperature (SST) displayed a consistent westward shifting of the Yellow Sea Warm Salty Tongue (YSWST) in winter (see Huang et al. 2005). Their results showed the westward shifting of the YSWST due to cooling and advection using the 2-D thermal model. The MITgcm was applied to simulate the circulation in the Yellow and East China Seas (see Huang et al. 2005). Results showed that under the northern monsoon wind in winter, the sea surface height (SSH) was adjusted to have a ridge in the channel and a trough in the 50–70 m isobath in the Yellow Sea. The barotropic transport of SSH and baroclinic transport of horizontal density gradient played the major role in the shifting of the YSWST, while the Ekman wind drift plays a minor role.

1.2 Variability of volume transport (VT) of the Kuroshio in the East China Sea and the meso-scale eddies near the Kuroshio

On variability of VT of the Kuroshio in the East China Sea, there were some works to be made by the Chinese scientists during July of 2002- July of 2006. Yuan et al. (2003a) pointed out that the net northward volume transport (VT) of the Kuroshio and the offshore branch of Taiwan Warm Current (TWCOB) through Section PN was about $26.2\times10^6 m^3/s$ in June 1999.The VT of inshore branch of Taiwan Warm Current (TWCIB) through the investigated region was about $0.4\times10^6 m^3/s$. From the model results, which had a resolution of 1/6° for the China seas and a resolution of 3° for the global ocean, Fang et al. (2003) showed that as conventionally recognized, the computed Kuroshio enters the ECS mainly through the Taiwan-Iriomote passage and flows out through the Tokara Strait. The volume transport of the Kuroshio in the ECS was $25.6\times10^6 m^3/s$, in which a little TV of less than 1/4 passed through the Iriomote-Okinawa passage.

On the basis of hydrographic data obtained in the period of 5 cruises of 2000 onboad the R/V *Chofu Maru* and the QuikSCAT wind data during the period, Yuan et al. (2006a) pointed out by using the modified inverse method the following result that 1) The net northeastward volume transport (VT) through Section PN was maximal ($28.1\times10^6 m^3/s$) in November, and is next to it in July, and was minimal ($24.6\times10^6 m^3/s$) in October during the period. The annual average of its net northeastward VT was $26.4\times10^6 m^3/s$ in 2000. 2) The weak cyclonic eddy occurred only in November and in the area east of the Kuroshio at Section PN. But an anticyclonic and warm eddy occurred in the area east of the Kuroshio at Section PN in other months, especially, was the

strongest in October. When an anticyclonic and warm eddy east of the Kuroshio strengthened, the VT of Kuroshio seemed to decrease, such as in October. Inversely, when an anticyclonic and warm eddy east of the Kuroshioi was weak, such as in July, or when the cyclonic eddy occurred east of the Kuroshioi, the VT of Kuroshio seems to increase, such as in November. In comparison of the current patterns of the circulation in October and November in the ECS, the variations of the circulation were greater in the ECS. This shows also that the interaction between the Kuroshio and its adjacent meso-scale eddies near the Kuroshio is important. 3) The net eastward VT through Section TK (at the Tokara strait) was maximal also in November among 5 cruises of 2000, and was next to it in July, and was minimal in October and January-February during the period. Its annual average net eastward VT through Section TK was $21.9\times10^{6}m^{3}/s$ in 2000.

Lin et al. (2004) discussed the intraseasonal long Rossby wave in Subtropical Ocean and its effect on the Kuroshio in the East China Sea. They pointed out that there existed markedly intraseasonal signals associated with the intraseasonal long Rossby wave in the region east of Taiwan. The intrusion of the intraseasonal long Rossby wave may result in the intraseasonal variation of the Kuroshio transport and axis position in the upper reaches of the Kuroshio in the ECS.

Yuan et al. (2004b) explained on the air-sea interaction process of cyclone outbreak over the southern Yellow and East China seas, of which the joint investigation was carried out by the cooperative studies between Chinese (inclusive of Chinese Taiwan), Japanese and Korean Scientists. Their results indicated the variations of circulations in the southern Yellow and East China seas in two cruises.

1.3 Variability of structure of the Kuroshio and their formation mechanism

A lot of work about the path and structure of the Kuroshio has been done by Chinese scientists. Recently, on the basis of the hydrographic data obtained in the period of 5 cruises of 2000 onboad the R/V Chofu Maru and the QuikSCAT wind data during the period, Yuan et al. (2006a) accomplished the following results by using the modified inverse method: 1) the Kuroshio at Section PN had two current cores in January-February, October and November, and only one current core in April and July, respectively. The main axis of Kuroshio is located at the computated point 9 of Section PN in January-February, and at the computated point 8 of Section PN, which moves toward the shelf in the other months, respectively. 2) The Kuroshio through Section TK had multi-current cores during the 2000 cruises. The main current core of Kuroshio occurred only at the computated point 8, whose water depth is greater than 1200 m in November, and occured at the computational point 2 or 4, whose water depth is less than the 400 m in the other months, respectively. Lou and Yuan (2004) pointed out that the Kuroshio in summer of 1996 was stronger than that in summer of 1995.

On the basis of hydrographic data since 1978, Chen Hongxia and Yuan Ye-li (2003) analysed the current field structure of Kuroshio at Section PN in the East China Sea, which showed the existence of the two-cores and multi-cores structure in each season. Recently Chen et al. (2006a) calculated the geostrophic current using dynamic height method at the transect of the Kuroshio on the basis of hydrographic temperature and salinity data at section G-PN in the East China Sea from June 1955 to November 2001. Their main results show as follows: 1) the single-core structure, double-core structure and multi-core structure are the basic patterns in the axial part of the Kuroshio; 2) The current structure of the East China Sea Kuroshio has obviously temporal

variety. There is a close relation between different seasons and different current structures. The number of cores of current profiles comes up to the maximum in autumn and the minimum in winter, ranges from 1 to 5, and it has not only seasonal, but also inter-annual variations. 3) The number of current-cores being up to its maximum in fall may be related with relatively low transport of the Kuroshio.

On the formation mechanism of multi-core structure of the Kuroshio, Yuan Yeli et al. (2003) presented a motion instability formation mechanism of the multi-core structure of Kuroshio in the East China Sea. This theoretical work includes presentation of the simplified model, derivation of the existence condition of the instable solution and some scaling estimation of the multi-core structure. When the condition derived by them was satisfied, the instable perturbation would grow exponentially as a type of standing wave and the motion would have a sort of orderedness. The perturbation with a wave length satisfying some conditions would grow fastest , which should correspond to the observed multi-core structure in the current field. The theoretical results are in consistent with the observations.

Another important feature for the current structure of the Kuroshio is that there always exists the countercurrent or an anticyclonic and warm eddy east of the Kuroshio (see Yuan et al., 2006a, Lou and Yuan, 2004). Recently, Chen et al. (2006b) suggested a physical pattern of subcirculation system in the main part of the Kuroshio in the East China Sea by analyzing different survey data, which was a double-loop circulation structure consisting of a relatively stable main stream of the Kuroshio, a countercurrent frequently occuring on its right side and a outer shelf countercurrent conditionally occurring. A part of the Kuroshio water from the north part of the Kuroshio main stream flowed into the shelf area to form the outer shelf countercurrent, or turned to flow into the sea area east of t he Kuroshio to form the right side countercurrent ; a part of shelf water coming from the outer shelf countercurrent flowed into the Kuroshio from the south part of the Kuroshio main stream to close the outer shelf branch of double-loop structure, and most of the Kuroshio right side countercurrent water formed anticyclonic flow and returned to the Kuroshio main stream to close the east branch of double-loop structure. Chen et al. (2003) made a geostrophic velocity calculation of the Kuroshio in the East China Sea by using the nonlinear conjugate gradient method.

On the basis of a vast amount of satellite tracked drifter data Yu et al. (2002) analyzed the distributions of the Kuroshio in the East China Sea and the upper layer circulation in the shelf area. Their results show that the Tsushima Warm Current is not only the extension of Kuroshio, but also the confluence of several currents. There might be a countercurrent flowing counter to the Kuroshio direction at the 100 m isobaths west of the Kuroshio in the East China Sea in autumn, and the seasonal variations and dynamic mechanism of the countercurrent remain to be further studied.

Based on the hydrographic data collected from October to December 2000, and using the inverse method Zhu et al. (2006) pointed out that the Kuroshio flowing from the ECS through the Tokara Strait (TK) with a subsurface maximum velocity of 89 cm/s at 460 dbar. In section TI southeast of Kyushu, a subsurface maximum velocity of 92 cm /s at 250 dbar is found.

1.4 The circulation on the continental shelf of the East China Sea

Lin and Tang (2002) analyzed the observed surface and upper layer currents in the Yellow and East China seas and pointed out that the Tsushima Warm Current flowed away from the Kuroshio

and had multiple origins in the warm half year and came only from the Kuroshio surface water in the cold half year. Ge et al. (2005) made the FFT analysis of the observed current data (ADCP) in the southeastern shelf edge area of the East China Sea in water and summer.

Guo et al.(2003) analyzed the main processes of interaction between the coastal water, shelf water and Kuroshio water in the Huanghai Sea (HS) and East China Sea based on the observation and study results in recent years. These processes include the intrusion of the Kuroshio water into the shelf area of the ECS, the entrainment of the shelf water into the Kuroshio, the seasonal process in the southern area of the ECS controlled alternatively by the Taiwan Strait water and the Kruoshio water intruding into the shelf area, and so on.

Based on the improved ECOM-si (Estuarine Coastal Ocean Model with semi-implicit scheme), the extension of the Changjiang diluted water was studied by Zhu et al. (2004). Their numerical results showed that the tide has an obvious impact on the circulation and extension of the Changjiang diluted water as compared to the results without the tide effect. The Changjiang river runoff empting into the sea is branched into three parts in the Changjiang estuary, a northward one flows along the Jiangsu coast, another southward one flows along the Zhejiang coast and the major one first flows eastward near the estuary, then turn its direction to the northeast off the estuary. Moreover, there exists a westward return current to the south of the major runoff. The northward flowing runoff along the Subei coast and the southward flowing runoff along Zhejiang coast are stronger. However, the eastward flowing runoff would be weaker if the tide effect was removed in the model. The tongue of the Changjiang diluted water would obviously extend northeastward, which is more consistent with the observation pattern, if the effect of tide was included in the model. Compared with the observation data along the east-west transect 32°N in August 2000, the vertical distribution of salinity and temperature are more in keeping with the data. So, the tide impact should be considered in the study of the extension of Changjiang diluted water.

Bai and Wang (2003) investigated the behavior and mechanism of the expansion of the Changjiang River diluted water on the shelf of the East China Sea on the basis of a series of numerical experiments using POM. Their results showed that the bottom topography with variable depths was an essential prerequisite in determining the northeastward turning of the Changjiang River diluted water in summer. The turning of the outflowof the Changjiang River in summer is due to the combined effects of the upwelling-favorable wind stress ,baroclinicity and bottom topography ,whereas the interaction between the wind stress and topography is the main cause. On the contrary, in the case of flat bottom, neither the upwelling-favorable wind nor the buoyancy forcing induced by the outflow freshwater could make the diluted water turn northeastward. Further ,without wind forcing ,the inflow freshwater could induce an anticyclonic eddy near the estuary and a southward coastal current; the former is due to the buoyancy forcing ,while the latter is produced by the mass input from the Changjiang River. In the case of flat bottom, the anticyclonic eddy would be located in the east of the river mouth. When the bottom with variable depths was included in the model, the anticyclonic eddy would stretch northward, and a part of the discharged water flows northward. The inflow freshwater can produce a closed vertical circulation cell in the estuary.

Zhou et al. (2005) discussed some small-scale processes over shelf break in the East China Sea on the basis of the in situ data from March 7 to 9, 2004. The spatially averaged mixing rate over the whole observed section is $2.3\times10^{-3}m^2\cdot s^{-1}$, which is much larger than $1\times10^{-5}m^2\cdot s^{-1}$ of the

background diapycnal mixing rate in the open ocean.

Ⅱ. CIRCULATION AND THE KUROSHIO EAST OF TAIWAN

2.1 Variability of current structure and volume transport (VT) of the Kuroshio east of Taiwan Island and the meso-scale eddies around the Kuroshio

On the basis of hydrographic data obtained in July of 1997 the three dimensional and nonlinear diagnostic, semidiagnostic and prognostic models in the σ coordinate are used to compute the circulation east of Taiwan (see Yuan et al., 2002). Their computed results from these three models can be summed up as follows: 1) The Kuroshio east of Taiwan first flowed northeastward, then turned to the northward after making a cyclonic meander. Its maximum velocities in the above order were 147.4, 164.9 and 164.6 cm/s at the surface, respectively. This means that the Kuroshio east of Taiwan is strengthened for the semidiagnostic and prognostic models. 2) There would exist an anticyclonic eddy W_1 east of the Kuroshio and a cyclonic cold eddy C_1 from these three models. These two eddies constituted a dipole. However the positions of both eddies southward from the semidiagnostic and prognostic computations, are situated more southward than that from diagnostic calculation. 3) There was a southward flow between the above two eddies. 4) An anticyclonic recirculating eddy appeared in the northeastern part of computed region. 5) There was a southward countercurrent below the Kuroshio. 6) The upwelling appeared in the upper and deep layers near the area southeast of Taiwan Island. There were the upwelling and downwelling at Section K_4, which are located at the western and eastern parts of Section K_4, respectively.

Drifting buoys, satellite altimetry and satellite-derived sea surface thermal images were used to identify the existence of a large cold-core, cyclonic Kuroshio frontal eddy between Hengchun Peninsula and Lanyu Island to the southeast of Taiwan Island around March 1996 (see Jing and Li, 2003). Their results are as follows. The cold eddy accompanied an offshore meander of the Kuroshio near Lanyu Island, with about 70 km and 100 km in the zonal and meridional scales, respectively. The cold eddy was different from the normal Kuroshio frontal eddies for its persistence of about 2 months near Lanyu Island. The present evidence suggested that the Kuroshio intruded into the South China Sea (SCS, hereafter) forming a loop-like structure during the persistence period of the cold eddy and that the similar eddies occur occasionally in the same location. Compared with the corresponding studies in the Gulf of Mexico, it is suggested that the Lanyu cold eddies be in the SCS analogue to the Tortugas eddies found in the southern Straits of Florida. The overshooting of the meandering Kuroshio when it left the SCS and the effect due to the conservation of potential vorticity would be the possible mechanism of eddy genesis.

Guan and Yuan (2006) made an overview of research in some cyclonic and anti–cyclonic eddies in the region east of Taiwan Island,where meso–scale eddies (MSE) always occurred in the both sides of Kuroshio，and their variabilities were large and complicated. They discussed mainly the following two cyclonic cold eddies: the Lanyu cold eddy and the cyclonic cold eddy northeast of Taiwan Island.

2.2 Volume transport (VT) of the Kuroshio and ocean-atmosphere interaction in the area around Taiwan Island

Through the regression analysis between the sea level records and the Kuroshio volume

transport, sea level records, Jia et al. (2004) calculated the Kuroshio volume transport from 1980 to 1997 along the WOCE PCM21 section day by day based on the Keelung and Ishigaki in WOCE dataset. From their Kuroshio volume transport anomaly time serial (also called SLDKV), it is shown that the maximum Kuroshio volume transport occurred in 1980 —1983, 1986, 1988 and 1991 (positive anomaly , exceeds 0.5Sv) , and the minimum Kuroshio transport in 1984 ,1990 ,1993 —1995 (positive anomaly exceeds - 0. 5 Sv) , which indicated a trend of reduction of the Kuroshio transport east of Taiwan after 1991. Their wavelet analysis suggested the 2 —5 years significant variations in the Kuroshio transport to the east of Taiwan with a few peaks of 2 and 5 years. The 2 —3 years fluctuations were stronger in the 1980s and the 1990s and the 5 years fluctuations stronger in the following 8 years. The wavelet analysis showed that the primary period of the WDKV was 2 —7years with maximum of 3 and 6 years. From 1980 to 1994, the 6 —7 years period was dominant while the 2 —3years period was dominant from 1980 to 1990. Before 1991, the interannual variation of the Kuroshio transport agreed well with that of the Sverdrup transport. Since 1991 there was a great differeace in the variation between the Kuroshio transport and the Sverdrup transport. During the years when the Kuroshio large meander frequently occurred (such as 1980 —1991), the Kuroshio transport was large and the 2 —5 year variation was distinct. Beside, there was close relationship between the Kuroshio transport and the wind stress curl. In the years of no Kuroshio large meander (such as 1991 —1995), the Kuroshio transport became small and the close relationship with wind stress curl disappeared.

Using the NCAR /NCEP reanalysis (1958—1999), the COADS monthly data (1945—1993) and the Kuroshio transport field data from various sources from 1980 to 1997, Wen and Liu (2006) studied mainly the relationship between Kuroshio transport and ocean-atmosphere interaction in the area northeast of Taiwan in Northwest Pacific (NWP) in winter. Their results showed that the year of strong air-sea interaction in NWP largely corresponds to the year of large Kuroshio transport. Having formed a relation of the Kuroshio flux to the first principle component obtained with SVD using lead or lag correlations, they discovered that when Kuroshio transport lead by two months, it could best match the air-sea interaction in NWP in winter. In conclusion, they considered that the Kuroshio played an important role in the wintertime air-sea interactions in NWP for transporting heat. In other words, the warm advection of the Kuroshio in late fall sustained the wintertime air-sea interaction in NWP.

A study of the comparison of the output of the Flexible Global Climate Model Version 1．0 (FGCM—1．0) and the observed data was performed by Liu et al. (2006). Their results showed that on the interannual timescale，the strong (weak) Kuroshio transports to the east of Taiwan led to the increasing (decreasing) net heat flux，which was centered over the Kuroshio Extension region，by 1—2 months，with low (high) pressure anomaly responses appearing at 500 hPa over the North Pacific(north of 25ºN)in winter．The northward heat transport of the Kuroshio was one of the important heat sources to support the warming of the atmosphere by the ocean and the formation of the low pressure anomaly at 500 hPa over the North Pacific in winter．

Gu et al. (2004) discussed the anomalous Kuroshio transport and its relationship with large scale atmosphere-sea interaction. Their results by singular spectrum analysis (SSA) showed that the interdecadal variation accounts for 45% on the total variance, and the interannual variation accounts for 13. 6% on the Kuroshio transport. The anomalous Kuroshio transport had a close relationship with Pacific Interdecadal Oscillation (PDO) and ENSO. On an interdecadal scale, a possible process would be that PDO lead the anomalous Kuroshio transport, and the anomalous

Kuroshio transport modulate the variation of ENSO through ocean-atmosphere interaction induced by the changed gradient of SST in the central North Pacific. On an interannual scale, the anomalous Kuroshio transport lags behind the variations of PDO and ENSO, and is negatively correlated with them.

Ⅲ. THE CURRENTS EAST OF THE RYUKYU ISLANDS

3.1 Variability of current structure and meso-scale eddies east of the Ryukyu Islands

Lou and Yuan (2004) pointed out that there was a northeastward current (the Ryukyu Current) east of the Ryukyu Islands in summer of 1995. There existed a weaker southwestward countercurrent under the Ryukyu Current. There was a meso-scale anticyclonic eddy east of Ryukyu Current, which was the warm waters from the surface to the lower layer and located at 128°30′-129°10′E, 25°-25°30′N with average speed of about 15cm/s. A southward current appeared in the surface layer east of the Ryukyu Islands in summer of 1996 when the Ryukyu Current didn't appear obviously. The Ryukyu Current existed in the layer below depth 200m. Its core located in the subsurface layer, with its maximum velocity of about 14cm/s at depth 300m. A southward current also exists under the Ryukyu Current. There is also an anticyclonic warm eddy east of the Ryukyu Current. There are an anticyclonic warm and a cyclonic cold eddies in the region southeast of the Okinawa Island, respectively. These two eddies make up a dipole, which is found for the first time in this region. There is a southward current between the above two eddies with the maximum velocity of 36cm/s at the surface.

On the basis of the hydrographic data obtained in the period of 5 cruises of 2000 onboad the R/V Chofu Maru and the QuikSCAT wind data during the period, the modified inverse method is used to compute the current structure and meso-scale eddies east of the Ryukyu Islands (see Yuan et al., 2006b). Their main computed results can be summed up as follows: 1) The Ryukyu Current is a northeastward and western boundary current east of Ryukyu Islands. The maximum velocities of Ryukyu Current are more than 40 , 15, 20, 20 and 55 cm/ s in January-February，April, July, October and November respectively, which means that its maximum velocity is the largest in January-February and November, and is the smallest in April during the period. The Ryukyu Current extends a depth of 1200m and below in the vertical during the period, and its current core is located at the subsurface layer. There is a week southwestward current under the Ryukyu Current. 2) There are some anticyclonic warm eddies and cyclonic cold eddies with different scales east of the Ryukyu Current in the computed region. For example, in January-February there are anticyclonic warm eddies W1 and W2, and cyclonic cold eddies C1 and C2 in the middle and eastern parts of computed region respectively. In April there are a stronger anticyclonic warm eddy having larger scale and a cyclonic cold eddy, which composes dipole, and there is a southward flow between them. This shows that the variability of various strength and scales warm and cold eddies are very large east of Ryukyu Islands during the period.

3.2 Variability of volume transport (VT) and its interaction with the meso-scale eddies east of the Ryukyu Islands

From the hydrographic data obtained in the period of the 5 cruises of 2000, by using the modified inverse method Yuan et al. (2006) pointed out the following results.1) The net northeastward volume transport (VT) of the Ryukyu Current was maximum in January-February

and the next to it in November, and its VT was 20 and 14.5×10 ^{6}m ^{3}/s, respectively, and was minimum in April with its VT of 3.1×10 ^{6}m ^{3}/s. This means that its variability of VT is very large. 2) The volume transport (VT) of the Ryukyu Current is strongly influenced by eddies, for example, it decreases probably, when the strength of eddies strengthened. 3) There was a southward current east of Ryukyu Islands, and its maximum VT was greater than 15×10 ^{6}m ^{3}/s in November and more than 10×10 ^{6}m ^{3}/s in January-February , and its minimum VT was 3×10 ^{6}m ^{3}/s in April . From the above, the tendency of seasonal variation of the southward current agrees basically with that of the Ryukyu Current.

On the basis of the hydrographic section data collected from October to December 2000, Zhu et al. (2006) pointed out by using the inverse method that the Ryukyu Current (RC) southeast of the Ryukyu Islands flowed over the continental slope from the region southeast of Okinawa (OS) to the region east of Amami-Ohshima (AE) with a subsurface maximum velocity of 67 cm /s at 400 dbar, before joining in the Kuroshio southeast of Kyushu (TI). The volume transport around the subsurface velocity maximum southeast of Kyushu (TI) balanced well with the sum of those in TK and AE. The temperature-salinity relationships found around these velocity cores were very similar, indicating that the same water mass was involved. These results helped demonstrate the joining of the RC with the Kuroshio southeast of Kyushu. The net volume transport of the Kuroshio south of central Japan is estimated to be 64~79 Sv (1 Sv ≡ 10^6 m^3s^{-1}), of which 27 Sv were supplied by the Kuroshio from the ECS and 13 Sv were supplied by the RC from OS. The rest of VT (about 24~39 Sv) was presumably supplied by the Kuroshio recirculation south of Shikoku, Japan.

REFERENCES

Bai Xue-Zhi , Wang Fan (2003), Numerical study on the mechanism of the expansion of the Changjiang river diluted water in summer, OCEANOLOGIA ET L IMNOLOGIA SINICA, 34(6): 593-603

Chen Hongxia, Yuan Ye-li, Liu Na,Qu Yuan-yuan (2003), Application of nonlinear conjugate gradient method in geostrophic velocity calculation of Kuroshio in the East China Sea, Acta Oceanologica Sinica, 25(6): 31-38 (in Chinese with English Abstract)

Chen Hongxia and Yuan Ye-li (2003) The current structure analysis of PN Section in the East China Sea, Proceedings of 12th PAMS/JECSS Workshop, Hangzhou, 2-17-1—2-17-4

Chen Hongxia, Yuan Yeli and Hua Feng (2006a) Multi-core structure of the main part of the Kuroshio at G-PN section in the East China Sea, Chinese Science Bulletin. Vol. 51 No. 6 738—746

Chen Hongxia, Yuan Yeli and Hua Feng , Xiong Xue-jun1 , Guo Bing-huo (2006b),Study on Circulation Substructure in the Main Part of the Kuroshio in the East China Sea, Advance in Marine Science, 24 (2), 137-145(in Chinese with English Abstract)

Fang Guohong, Wei Zexun, Choi Byung-Ho, Wang Kai (2003)；Interbasin freshwater, heat and salt transport through the boundaries of the East and South China Seas from a variable-grid global ocean circulation model, Science in China,Ser.D, 46 (2): 149-161

Ge Reb-feng, Guo Bing –huo, Qiao Fang-li, et al.(2004), FFT Analysis of the Observed Current Data in the Southeastern Shelf Edge Area of the East China Sea in Winter an Summer, Advance in Marine Science, 22(4): 429-43 (in Chinese with English Abstract)

Gu De-jun , WANG Dong-xiao ,YUAN Jin-nan (2004), Anomalous transport of Kuroshio and its relationship with large scale atmosphere-sea interaction, Journal of tropical oceanography , 23(6): 30-39 (in Chinese with

English Abstract)

Guan Bing-xian and Yuan Yao-chu (2006), Overview of studies on some eddies in the China Seas and their adjacent seas Ⅰ—the South China Sea and the region east of Taiwan, Acta Oceanologica Sinica, 28(3), 1-16 (in Chinese with English Abstract)

Guo Binghuo; Xiaomin Hu; Xuejun Xiong; Renfeng Ge (2003), Study on interaction between the coastal water, shelf water and Kuroshio water in the Huanghai Sea and East China Sea，Acta Oceanologica Sinica, 22(3): 351-367

Guo Jing-song, Hu Xiao-min, Yuan Ye-li (2005), A Diagnostic Analysis of Variations in Volume Transport Through the Taiwan Strait Using Satellite Altimeter Data, Advance in Marine Science, 23 (1), 20-26 (in Chinese with English Abstract)

Huang Daji, Fan Xiaopeng, Xu Dongfeng, Tong Yuanzheng, and Su Jilan (2005), Westward shift of the Yellow Sea warm salty tongue, GEOPHYSICAL RESEARCH LETTERS, VOL. 32, L24613, doi:10.1029/2005GL024749

Jia Ying-Lai ,Liu Qin-Yu ,Liu Wei ,Lin Xiao-Pei (2004), The interannual Variation of the Kuroshio transport east of Taiwan, OCEANOLOGIA ET L IMNOLOGIA SINICA,35(6):507-512 (in Chinese with English Abstract)

Jing Chunsheng and LI Li (2003) An initial note on quasi-stationary, cold-core Lanyu eddies southeast off Taiwan Island. Chinese Science Bulletin, 48 No. 19 2101—2107

Lin Kui, Binghuo and Yuxiang Tang (2002), An analysis on observational surface and upper layer current in the Yellow Sea and the East China Sea, Journal of the Korean Society of Oceanography, 37(3): 187-195

Lin Xiaopei Wu Dexing Lan Jian（2004）, The intraseasonal long Rossby wave in Subtropical Ocean and its effect to the Kuroshio in the East China Sea (2004). In: Proceeding of the Second International Symposium on Program of the East Asian Cooperative Experiments (PEACE), Nov.25-26, 2004, Kasuga, Japan, 61-64.

Liu Qinyu, Wen Na and Yu Yongqiang (2006), The role of the Kuroshio in the winter North Pacific ocean-atmosphere interaction: Comparison of a coupled model and observations. Advances in Atmospheric Sciences DOI: 10.1007/s00376-006-0181-4, Volume 23, 2, 181 – 189.

Liu Yong-gang, Yuan Yao-chu , Liu Cho-Teng , Hong Chen（2004）Measurement of the current and spectra analysis on the continental shelf in the East China Sea, Acta Oceanologica Sinica, Vol.23 (2), 201-212

Lou Ruyun, Yuan Yaochu (2004), The Circulation on the both sides of the Ryukyu Islands during the summer of 1995 and 1996, Acta Oceanologica Sinica, 26 (3) 1-10 22. (in Chinese with English Abstract)

Qin Zenghao, Li Yongping, Yuan Yaochu, Yu Runling(2005) A three-dimensional model study on ocean dynamic response to traveling cyclone over the Huanghai Sea, Acta Oceanologica Sinica, vol.24 (1), 60-75

Wang Huiqun, Yuan Yaochu, Liu Yonggang, Zhou Mingyu (2003) Three-Dimensional calculations of the currents in the Huanghai Sea and China Sea during June of 1999, Acta Oceanologica Sinica,Vol. 22 (3), 333-349.

Wen Na, and Liu Qin-Yu (2006), Winter ocean-atmosphere interaction in the northwest pacific, OCEANOLOGIA ET L IMNOLOGIA SINICA, 37(3): 264-270 (in Chinese with English Abstract)

Xu Dongfeng , Yuan Yaochu, Liu Yuan (2003) The baroclinic circulation structure of Yellow Sea Cold Water Mass, Science in China (series D) , 46 (2), 117-126.

Yu Fei, Zang Jia-ye, Guo Bing-hou, Hu Xiao-min (2002) Some Phenomena of the Kuroshio In trusion In to Shelf Area and the Shelf Circulation of the East China Sea, Advance in Marine Science, 20 (3), 21-28 (in Chinese with English Abstract)

Yuan Yaochu, Huiqun Wang, Yonggang Liu， Jilan Su, Arata Kaneko (2002) Three Dimensional Diagnostic, Semidiagnostic and Prognostic Calculation of Circulation east of Taiwan during July of 1997 Marine .Environment :The Past ,Present and Future, edited by Chen-Tung Arthur Chen. The Fuwen Press, Kaohsiung, Taiwan, 356-382.

Yuan Yaochu, Yongang Liu, Mingyu Zhou, Arata Kaneko, Zhou Yuan, Noriaki Gohda (2003) The circulation in the southern Huanghai Sea and northern East China Sea in June 1999,Acta Oceanologica Sinica,Vol. 22 (3), 321-332.

Yuan Yaochu , Yonggang Liu , Heung-jae Lie，Ruyun Lou （2004a） Variability of the circulation in the southern Huanghai Sea and East China Sea during two investigative cruises of June 1999, Acta Oceanologica Sinica, Acta Oceanologica Sinica,Vol.23 (1), 1-10

Yuan Yaochu , Arata Kaneko and Heung-Jae Lie (2004b) the circulation in the East China and the southern Huanghai Seas. In: Proceeding of the Second International Symposium on Program of the East Asian Cooperative Experiments (PEACE), Nov.25-26, 2004, Kasuga, Japan, 55-60.

Yuan Yaochu, Yang Cheng-hao, Wang Zhang-gui（2006a）,Variability of the Kuroshio in the East China Sea and the Currents east of Ryukyu IslandsⅠ. Variability of the Kuroshio in the East China Sea and the meso-scale eddies near the Kuroshio, Acta Oceanologica Sinica, 28(2),1-13 (in Chinese with English Abstract)

Yuan Yaochu, Yang Cheng-hao, Wang Zhang-gui（2006b）,Variability of the Kuroshio in the East China Sea and the Currents east of Ryukyu IslandsⅡ.Variability of the currents and the meso-scale eddies in the region southeast of Okinawa Island, Acta Oceanologica Sinica, 28(3), 17-28 (in Chinese with English Abstract)

Yuan Yeli, WAN Zhenwen, ZHANG Qinghua (2003); A motion instability formation mechanism of the multi-core structure of the East China Sea Kuroshio; Science in China,Ser.D , 46 (2): 182-192.

Zhu Jianrong, Takeshi Matsuno and Jae Hak Lee (2004), The impact of tide on the extension of the Changjiang diluted water. In: Proceeding of the Second International Symposium on Program of the East Asian Cooperative Experiments (PEACE), Nov.25-26, 2004, Kasuga, Japan, 17-22.

Zhou Lei; TIAN Jiwei & ZHANG Xiaoqian (2005), Observation of small-scale processes over shelf break in the East China Sea，Chinese Science Bulletin, 50(24): 2885-2990.

Zhu,Xiao-Hua Jae-Hun Park and Ikuo Kaneko (2006) Velocity Structures and Transports of the Kuroshio and the Ryukyu Current during Fall of 2000 Estimated by an Inverse Technique , Journal of Oceanography, Vol. 62, 587 -596.

RESEARCH PROGRESS IN THE SOUTH CHINA SEA CIRCULATION AND LOCAL AIR-SEA INTERACTION IN 2003~2006

WANG Dongxiao, DENG Yi, WANG Weiwen

Key Laboratory of Tropical Marine Environmental Dynamic, South China Sea Institute of Oceanology, Chinese Academy of Sciences, Guangzhou 510301, China

Abstract: The research progress of the South China Sea (SCS) physical oceanography and air-sea interaction achieved by Chinese scholars from 2003 to 2006 is reviewed in this paper. This overview is mainly concerned with the development in dynamic interpretation of the basic circulation, mesoscale eddies, coastal upwelling, internal wave and tide, dynamic mechanism and adjustment of the basin circulation, strait water exchange, relationship between the SCS circulation and ENSO, barrier layers and warm waters, local air-sea interaction in the SCS.

Under the background of global climatic variation and regional sustainable development, more and more researchers focus on the physical and climatic situations of marginal seas (Wang et al., 2002). The South China Sea (SCS) is the largest marginal sea of the western Pacific Ocean with several straits connecting the outer waters and open oceans, and it is an important channel between the western Pacific and the Indian Ocean in term of the so-called throughflow. Straits and complex topography make the water exchanges between the SCS and the outer oceans possible, and complicate the SCS circulation. The 3D structure and annual variation of the SCS circulation are deeply affected by the Kuroshio and deep water exchange through straits.

The multiple space-time scales of SCS circulation are based on a regional air-sea interaction. The formation of SCS circulation scales has inevitable relationship with external force and air-sea heat exchange. Numerous researches in recent years point out that the SCS monsoon has its unique features, i. e., there is a tropical sub-system of East Asian Monsoon in the SCS which was named the SCS Monsoon. Short-term climate and weather phenomenon, such as typhoon, bring strong mesoscale eddies in the ocean, which are combined with straight cooling by wind, and set up upper ocean stratification evidently. In addition, the sea surface net heat and fresh water fluxes due to monsoon fluctuation would affect the upper layer thermodynamics and dynamics in the SCS (Wang et al., 2003).

This paper attempts to review the oceanographic research progress of SCS achieved by Chinese scholars from 2003 to 2006 related with the circulation dynamic and local air-sea interaction.

1. Regional Oceanography of the SCS

The upper layer circulation of the SCS is driven mainly by the monsoon, with additional influence from the Kuroshio in its northern part. In winter there is a basin-wide cyclonic gyre, while in summer the circulation splits into a weakened cyclonic gyre north of about 12°N and a strong anticyclonic gyre south of it. Associated with these gyres are strong western boundary currents. This prominent seasonal variability of the SCS basin-scale circulation has been

researched maturely, and was validated by many numerical studies and observations (Su et al., 1999; Qu, 2000; Wang et al., 2000; Cai et al., 2002; Yang et al., 2002; Chern and Wang, 2003; Xue et al., 2004).

1.1 Dynamic Interpretation of Basic Circulation

SU (2006) reviewed the progress in the SCS current dynamic mechanism research and pointed out that three major factors contributing to a generally cyclonic gyre in the upper ocean of the northern SCS are identified as: (1) monsoonal wind forcing; (2) net water transport into the SCS through the Luzon Strait; (3) vorticity advection from the Kuroshio. The intensified western boundary current of the cyclonic gyre, called the "Dongsha Current" in this paper, flows southwestward next to the shelf south of China. It extends all the way south in winter and reaches central Vietnam in summer. Every year around 10 mesoscale eddies are present in the SCS. Strong wind-stress curl from orographic effects is likely responsible for their generation. Vorticity advection from the Kuroshio can also induce mesoscale eddies. The available hydrographic data do not support the notion that the Kuroshio water enters the SCS as a "branch", nor primarily as mesoscale eddies. More likely, the Kuroshio water enters the SCS principally during the winter monsoon through sub-mesoscale processes confined in the surface layer.

Due to the various factors, the upper layer circulation in the SCS varies greatly in different seasons. The route of circulation and the shape, location and strength of eddies are always in a consecutive movement. The seasonal variations of circulation in the SCS are primary due to monsoon. In summer, the circulation pattern is quite opposite to that in winter. There are transitional pattern which appear in spring and autumn (Bao et al. 2005). The anticyclonic circulation in the southern SCS is mostly driven by the southwest monsoon, and its intensity is strengthened by baroclinic effect; the Kuroshio forcing and the bottom topographic effect are the main factors for producing the SCS Warm Current and the current flowing northeastward through the Taiwan Strait; baroclinic and bottom topographic effects are the main factors for forming the current flowing in right hand of the SCS Warm Current in summer; and the cyclonic eddy in the northern SCS is formed due to the combined actions of Kuroshio forcing, bottom topographic effect and baroclinic effect. On the basis of the hydrographic data obtained in cruise, Liao et al. (2005) computed the three dimensional structure of circulation in the SCS by using three dimensional diagnostic model. On the circulation systems in the SCS during the winter of 1998, it is found that in the northern SCS, there is a cold and cyclonic eddy northwest of Luzon, and there is an anticyclonic eddy near the Dongsha Islands; in the centra1 SCS, a coastal southward jet is present at the western boundary near the coast of Vietnam; there is a stronger cyclonic circulation east of Vietnam, and there is a weaker anticyclonic circulation east of this cyclonic circulation: in the southern SCS, there is an anticyclonic circulation in the area west of 112°E, and there is a cyclonic circulation northwest of Borneo Island.

1.2 Oceanography of Southern SCS

The circulation in the southern SCS has its own features due to the existence of the Nansha Islands. Based on the observational data from two investigation cruises in the Nansha Islands sea area in spring, Cai et al. (2004) employed the P-vector method to calculate the current field. Computational results show that, in spring, it is basically anticyclonic meander (eddy) in the upper current field west of the adjacent sea area from Borneo to Palawan Island, while the flow in the

deep layer is eastward by and large in the northern Nansha Islands sea area. The evident distinction of the spatial distributions of temperature, salinity and current fields between these two cruises may be related to the difference of wind fields during the investigation periods. According to the observational results of the two cruises, the water exchange via the Balabake Strait is much less in spring.

Based on the CTD data collected in the Nansha Islands waters during the cruise period from May 9 to May 22, 2002, the hydrographic features of Nansha Islands sea area during the spring to summer monsoon transition were analyzed and the temperature and salinity distributions in different regions were compared (Mao et al., 2005). The SST was generally higher than 30°C, and the vertical temperature stratification was stable. There were significant differences on vertical distributions of temperature and salinity between the northwestern and southeastern sea areas. In the northwestern area, the temperature was higher and a salinity inversion existed; while in the southeastern area, the temperature was lower and there was a double halocline in the vertical salinity structure. These differences are closely related to the monsoon pattern and local circulation. By analyzing the spatial-temporal distribution of temperature and salinity at a mooring station, it can be seen that the mixed semi-diurnal inner-tide had a significant impact on the distribution of temperature and salinity below the halocline.

2. Mesoscale Phenomenon

Mesoscale phenomenon in the ocean happens from several days to several months in time scale and tens to hundreds of kilometers in space scale (Li, 2002). They are neither short cycle phenomenon as tide and wave nor large-scale phenomenon as the ocean circulation for long period, like interannual or interdecadal process. In fact, meandering, mesoscale eddies, coastal upwelling, fronts and frontal eddies, coastal trapped waves and some mesoscale gyres all can be classified as mesoscale phenomenon.

The SCS is a semi-enclosed basin with complex topography. Forced by the East Asian Monsoon and the Kuroshio, the SCS shows unique features of mesoscale variability. Strengths of some mesosca1e signals are comparable with or even greater than strengths of the general circulation. Their dynamical significances are very important to research and exploitation of the SCS.

2.1. Mesoscale Eddies

The mesoscale eddy has been studied by oceanographers since it was discovered and many unique features have been revealed. The study on mesoscale eddies is more active than before with the applications of satellite altimeters and the development of numerical models. Many observations and satellite altimeters data show that mesoscale eddies are common in the SCS, whose variations in time and space reflect the variational properties of SCS circulation, and have significant influence on the distributions of temperature and chlorophyll in the SCS.

Wang et al. (2004) analyzed hydrological data in the SCS collected in marine investigation cruises during mid-summer 2000. It shows that during the survey period in the southern SCS, a cyclonic circulatory pattern presented at the lower layer, while an anti-cyclonic circulatory pattern revealed in the upper layer. In fact, a multi-eddy structure was found comprising of several mesoscale eddies including anti-cyclonic eddies of the Vietnam coast, near Zhongsha Islands and

in the NE region of Nansha Islands. Vertical sheer of velocity occurs in these eddies, especially those off the coast of Vietnam, which are typical examples of baroclinic eddies. The circulation and eddy patterns well reflect the geostrophic effect in the areas. There is a multi-eddy structure in the southern SCS, and there are obvious seasonal variations in the multi-eddy structure (Lan et al. 2005). A composite time series (1993-2000) of the sea surface height anomaly from several satellites is used to identify eddies in the SCS (Wang et al., 2003). The eddy lifetime, radius, strength, and straight-line travel distance are estimated. Altogether 58 anticyclonic eddies and 28 cyclonic eddies are identified for this period. They are grouped into four geographical zones according to the known eddy generation mechanisms, and their statistics are discussed accordingly. This geographical classification is a useful first step in gaining an overview of their generation. Warm eddies start to occur and become fully grown in spring in the central SCS. In summer, warm eddies become frequent in the SCS. In autumn, cold eddies distribute along the coast of Vietnam, while warm eddies appear in the northern SCS. In winter, cold eddies mostly distribute in the waters northwest of Luzon and southeast of Vietnam, while warm eddies to the north of 18°N. Chen et al. (2005) used the 11-yr (1993--2003) TOPEX/Poseidon, Janson and ERS1/2 altimeter data to acquire the temporal and spatial distribution characteristics of mesoscale eddies in the SCS. The seasonal and interannual variabilities as well as the forming mechanism of mesoscale eddy in the SCS were studied. The results shows that the mesoscale eddies in the SCS have obvious seasonal and interannual variabilities and the monsoon is the main driving factor.

Most studies of dynamic adjustment mechanism about mesoscale eddies in the SCS are based on numerical model at present. Metzger (2003) pointed out that wind fields treated by different methods may lead to the different driven effect on the SCS circulation and mesoscale eddies. Yang et al. (2003) pointed out that the winter Luzon Cold Eddy, which has been found from field observations, could be identified as a forced Rossby wave with a negative SSH anomaly in winter. In fact, the ocean gains potential energy from Ekman pumping of large-scale wind stress, which is transformed into kinetic energy of mesoscale eddies in the static condition. Based on numerical simulation, as pointed out by Wang (2004) , the strong sea surface wind stress curl formed by monsoon and coastal mountain orographic effect is an important factor resulting in the generation of mesoscale eddies in the SCS. Wang et al. (2005) discussed the statistical characteristics of mesoscale eddies in different monsoon conditions and pointed out that wind stress curl formed by wind and topography of land interaction might be an important generation mechanism of SCS mesoscale eddies. Su (2005) reviewed the progress on the SCS circulation mechanism research and pointed out that strong wind stress curl from orographic effects was likely responsible for the generation of mesoscale eddies. According to the current studies (Cai, et al., 2005), most of the mesoscale eddies in the SCS are formed near the major islands in the east. These eddies, after being formed, move westward by the β effect and then dissipate in the western boundary; Generally speaking, the associated fluctuation propagates westward by way of Rossby waves. Thus, there exist some relationships between the multi-eddy structure of the SCS circulation and mesoscale fluctuation. In the northern SCS, the mesoscale eddies are mainly induced by the intrusion of Kuroshio and wind stress curl, whilst in the southern SCS they are induced by the wind stress curl. A linear dynamic model is applied to study and analyze the characteristics and rule of the wind. To drive mesoscale fluctuation in the southern SCS, a corresponding numerical model is set up based on the above results to reveal the dynamic and thermodynamic mechanisms of the circulation in the sea, so that the internal relationship between the seasonal variation of the current field and mesoscale fluctuation in the southern SCS could be understood.

Based on the observation, simulation and review studies in the SCS mesoscale eddies at present (Wang, et al., 2005; Guan et al., 2006), we can find that, mesoscale eddies are rather active in the SCS. However, how is the physical processes of the eddies in the western Philippine Sea and the SCS across the Luzon Strait? Could the Kuroshio form a loop current west of the Luzon Strait inside the SCS when the Kuroshio intrudes into the SCS? Up to now these questions remain untouched, especially the studies about their dynamic mechanism. To solve the above questions, it is necessary to get the long-term observed current and hydrographic data and the long-term satellite remote data from the cooperative program in the Luzon Strait in the future.

2.2. Coastal Upwelling

Upwelling is an important phenomenon in the ocean. It's an upward movement of water. It brings the water from the sub-surface layer to the surface layer and pushes it out of the upward movement region. General speaking, upwelling is generated by the surface divergence, and the upwelled water is often from deep sea of hundreds of meters. The most frequent upwelling is coastal upwelling. Coastal upwelling is common in the SCS, and it's an important component of the complex circulation system of the SCS.

Wu and Li (2003) summarized the studies on upwelling system in the SCS in recent 40 years and especially introduced the results of temporal and spatial distribution and evolution of upwelling over the northern shelf of the SCS. It is shown that the upwelling is a common phenomenon in the area with its scale of being comparable to the scale of the SCS basin. Dynamical factor of upwelling in the area is the strong southwest monsoon. It appears that the upwelling is not well-distributed either in space or in time. There are some upwelling centers to the northeast of the Hainan Island and the edge area between Provinces Fujian and Guangdong. In the southern part of Taiwan Strait, the upwelling shows multi-cell structure around the Taiwan Shoals. Each upwelling water mass has its own physical and chemical characters. In the eastern Guangdong coast, the influence of upwelling may reach inner part of coastal bay and dominates hydrographic condition of these bays in summer. In the SCS, besides upwelling over the northern shelf in summer, there are an upwelling along the eastern coast of Vietnam in summer and an upwelling along the coast of Luzon Island in winter respectively.

Based on the hydrology investigation off the eastern Guangdong carried out from July 22 to August 2, 2002, the upwelled cold water and ocean front along the eastern Guangdong coast have been discussed by Xu et al. (2003). It is shown that the upwelled cold water exists along the eastern Guangdong coast, which is much stronger than that of the areas off Daya Bay and Huilai. The high dense isotherms in this area indicate the upwelled front. The front expands outwards with the depth. Besides, signs of the upwelling cold water appear in the south part of Taiwan Bank and continental shelf break east and southwest of Dongsha Islands. Two warm centers which maybe come from coastal waters and sink a certain distance away from the Coast are found in the area north and west of Dongsha Islands, Based on the CTD data from the two cruises off the Zhujiang River Estuary in the northern SCS in July, 2000 and in May, 2001, the meteorological data in the corresponding period and historical observations and modeling results in this area, Zeng et al. (2005) found upwelling and downwelling when the southwest monsoon was strong enough. The southwest monsoon plays the most important role in leading to the appearance of upwelling, which transports water across the shelf due to the Ekman effect; the topography of the investigated section may enhance the intensity of the upwelling, but can not result in upwelling when the

monsoon is weak. The upwelling and downwelling areas coexist in the area when the southwest monsoon is strong. There may be two explanations on the appearance of downwelling. One explanation is weak anticyclonic eddy resulted from the flows in opposite flowing directions along the slope and along the continent, and the other explanation is that the upwelling and downwelling coexist in need of the water complement.

The development in numerical simulation is a new opportunity for the SCS upwelling research. From the numerical modeling results by Chao et al. (2003), it is shown that the distributions of the upwelling (downwelling), coastal jet and temperature front zone well consist with the observations. On the vertical component of current velocity (VCCV) distribution of SCS in winter (Liao et al., 2005), it is found that: (1) in the surface layer, there is a upwelling region northwest of Luzon, and some downwelling areas near the Dongsha Islands and to the south and southeast of Hainan Island; the downwelling exists in the region east of Vietnam, which is ca11ed DWEV, and the upwelling exists in the region east of DWEV; there is also the downwelling northwest of Palawan Island; the upwelling dominates in the southern SCS; (2) there are some differences in the VCCV between the surface layer and the sub-surface layer; for example, there is the upwelling southeast of Hainan Island in the sub-surface layer; (3) the VCCV distribution in the middle and deep layers is similar to that in the sub-surface layer. The VCCV is mainly driven by the curl wind stress in the surface layer. In the sub-surface layer, the joint effect of β effect and baroclinicity (JEβBC) is the main dynamical factor; secondly, the wind stress curl and the joint effect of β effect and barotropicity (JEβBT) are all important in the some area as well; in the middle layer of the southern SCS and the deep lavers of the SCS, the JEβBC and the JEβBT are both the main dynamical mechanism which causes the VCCV distribution in winter.

2.3 Thermal fronts

There are many water masses in the northern SCS continental shelf region, where thermal fronts often appear. Based on the seven years' (1993~1999) monthly mean SST satellite data, the features of monthly variations for the thermal fronts in the northern SCS is analyzed (Wang et al., 2004). The Results show that the intraseasonal variations of the thermal fronts are significant. By analying the wind satellite data and the above SST data, they shows that the increase of the wind velocity of the northeast monsoon can strengthen the intensity of the thermal fronts. Through the contrast of SST features in February 1998 when the Kuroshio intrusion was weak and in February 1999 when the Kuroshio intrusion was strong, it is bound that the Strong Kuroshio intrusion can increase the intensity of the thermal front and affect the direction of the thermal front. The thermal infrared images from the NOAA AVHRR between 1989 and 2001 have been used to study the sea surface thermal front in the Taiwan Strait and its adjacent seas (Huang et al., 2006), and the location, length, width and strength of the front has been retrieved from the thermal infrared images. The Satellite data have revealed that the front exists all year round and has a length of 470 km. The frontal location coincides approximately with the 50 m offshore depth contour. The frontal width and strength vary with time, which have average values of about 15.15 km and 0.147°C/km respectively. The front is instable and characterized as the edges of eddies, which have a time scale of 1-7 d and a length of 25-70 km.

3. Internal Wave and Tide

Wu et al. (2003) assimilated the data, which is obtained from TOPEX/Poseidon satellite altimeter data (248 periods lasting six years) in the SCS by use of the orthogonal response method,

into tides model by using ad joint method. Optimal open boundary conditions and bottom friction coefficient were given, and so were the co-tidal charts for m1 and M2. Their results of the numerical simulation coincide with the data form tide gauges. Wu et al. (2004) used a three dimensional numerical model (POM) to simulate the tidal movement in the SCS, in which four main constituents were included and into which the T/P altimeter data were assimilated as the open boundary. Their computational results coincide with the observed data.

Du et al. (2004) used harmonic analysis, singular value decomposition and wavelet transformation to analyze the continuous current records observed above the continental shelf nearby the southwestern SCS. Harmonic analysis of barotropic current shows that the diurnal tidal current is the main part of tidal current. The tidal ellipses rotate with depth. The current has a distinct vertical structure. The residual currents obtained by using singular value decomposition consist of different vertical modes. The first mode matches the averaged current very wel1. The second mode matches the trend component. The time series of all modes show a period of two days. Wavelet transformation further reveals the feature of the vertical structure. The main frequency of the observed current changes in the vertical direction and drafts from time to time. Zhang et al. (2005) used the mooring ADCP current observations from August to November to study the barotropic tides, baroclinic tides and near-inertial motions in the upper 450 m layer of the northern SCS. The barotropic and baroclinic tides at the mooring station are all dominated by M2, K1, O1, P1, with the barotropic amplitudes being 7.8 cm/s, 7.0 cm/s, 5.4 cm/s and 3.5 cm/s respectively. The amplitudes of M2, K1, O1, P1, and internal tides vary greatly, which are 12~15 cm/s in the thermocline, and then decrease with increasing depth. The amplitude of the barotropic nearinertial motions is less than 1 cm/s, contributing little to the barotropic currents, and that of the baroclinic near-inertial motions can be as large as 5 cm/s. The inclination of tidal ellipse tends to increase with increasing depth, implying the upward propagation of energy, while that of the near-inertial ellipse tends to decrease with increasing depth, implying the downward propagation of energy.

Based on the observed current, tide and wind data at the Yongshu Reef by Multidisciplinary Oceanographic Expedition to the Nansha Islands in May 2002 and over the past decade, the characteristics of tide and current at the Yongshu Reef have been discussed and the combined extreme current has been estimated by Zhu et al. (2005). Their results show that the tide at the Yongshu Reef is of irregular diurnal tide, the main diurnal constituents are larger than the main semi-diurnal constituents and the maximum tidal range is theoretically large relatively. The range of the observed velocity variation is large. The observed maximum velocity is 75cm/s. The mixed tidal current is dominant among the tidal current features. With the increase of water depth, the diurnal tidal current features decrease. At the Yongshu Reef, the major axis of K1 diurnal constituent current ellipse is more obvious and located along the directions of NW and SE. The major diurnal constituent currents rotate clock-wisely, but the major semi-diurnal constituent currents rotate counter-clock-wisely. The residual current is not so large with both speed and direction being relatively stable in spring. The combined extreme currents in different orientations are different, and the monsoon currents are prevailing in the orientations NE and SSW.

4. Dynamic Mechanism and Adjustment of Basin Circulation

On the basis of the recently obtained hydrographic data in the SCS, Wang et al. (2004) used the improved Princeton Ocean Model with a generalized topography-following coordinate system to study the circulation in the region during summer of 2000 and pointed out that the dynamical

mechanisms of the circulation pattern in the SCS were the interaction between the wind stress and bottom topography and the joint effect of baroclinicity and relief. A three-dimensional ocean model has been utilized to study circulation and its variability in the SCS in response to the forcing of the Asian monsoon and the Kuroshio intrusion (Gan et al., 2006). The results show that the seasonal circulation in the SCS is driven by the monsoonal wind stress with a great influence by the inflow from the Kuroshio intrusion. The examination of the momentum balances indicate that a large negative ageostrophic pressure gradient in the Kuroshio north of the Luzon Strait leads to the eastward turning of the Kuroshio. The Kuroshio intrusion in different depths along the continental slope is governed by the ageostrophic flows.

The SCS warm current is an intensified western boundary current of the cyclonic gyre in the northern SCS, flowing southwestward next to the shelf south of China, called the Dongsha Current (Su, 2004). It extends all the way south in winter and reaches central Vietnam in summer. Available hydrographic data do not support the notion that the Kuroshio water enters the SCS as a "branch" current, nor primarily as mesoscale eddies. More likely, the Kuroshio water enters the SCS principally during the winter monsoon through sub-mesoscale processes confined in the surface layer. Hsueh and Zhong (2004) suggest that the SCS Branch of Kuroshio should be feeding the SCS Warm Current all along the shelf break through a weak onshore flow driven by the gradual drop in pressure in the SCS Branch of Kuroshio due to bottom friction.

Chu et al. (2003) identified the first baroclinic Rossby wave with a phase speed around 3-5 cm/s in the northern SCS using 1994-2001 daily SSH data. They also found that there was no evident Rossby wave signal in the southern SCS. The time-longitude diagrams of monthly anomalies of TOPEX/Poseidon sea surface height (SSH),the Levitus steric height, the COADS wind stress curl and the meridional surface wind averaged over the northern SCS from 18° to 22°N (Yang and Liu, 2003) exhibit a coherent westward phase propagation, with a westward propagation speed of about 5 cm/s. The consistency between oceanic and atmospheric variables indicates that there is a forced Rossby wave in the northern SCS. The horizontal patterns of monthly SSH anomalies from observations and model sensitivity experiments show that the forced Rossby wave, originating to the northwest off Luzon Island, actually propagates west-northwestward towards the Guangdong coast because of zonal migration of the meridional surface wind.

Except for the basin-scale circulation character of the SCS mentioned above, the large-scale upper circulations and meridional overturning in the upper layer of the SCS with the idealized bottom topography in winter and summer are investigated (Wang et al., 2004). Simulations with the GFDL general circulation model are carried out under the conditions of open or enclosed boundary regarding transport in the Luzon Strait. The impact of the Kuroshio intrusion area on the meridional overturning in the upper layer of the SCS and seasonal characteristics of this impact are explored, respectively. The resultant meridional overturning is non-enclosed, with transporting from north to south in the surface and returning to north in the depth of about 500 m in winter, about 200 m in summer, with amplitudes of 105 m3/s. It shows the transporting path of intermediate water of the SCS and offers an idealized reference for further study on dynamics of the wind-driven and thermohaline circulation of the SCS.

5. Water Exchange through straits

The SCS is connected with the western Pacific Ocean and the eastern Indian Ocean via a lot of narrow and shallow sea straits, and it is a significant channel between the western Pacific and

the Indian Ocean. The Luzon Strait is one of the most important straits that influence the SCS with the maximum sill depth of over 2500m and make the water exchange between the SCS and the western Pacific possible. The dynamic process of SCS circulation is really complex due to the water exchange through strait between the SCS and the oceans, which impacts the SCS circulation and is a significant problem for research of the SCS circulation.

5.1 Kuroshio Intrusion through Upper Luzon Strait

The Kuroshio is one of the western boundary currents in the North Pacific Ocean, with character of high temperature and salinity. It has great influence on the northern SCS circulation through the Luzon Strait. The focus of studying the upper layer water exchange through the Luzon Strait is mainly on the dynamic mechanism of Kuroshio intrusion.The velocity data near the surface obtiained by Argos satellite-tracked drifters between 1989 and 2002 provide evidence of seasonal currents entering the SCS from the Philippine Sea through the Luzon Strait (Centurioni et al., 2004). The drifters cross the strait and reach the interior of the SCS only between October and January, with ensemble mean speeds of 0.7 ± 0.4 m s^{-1} and daily mean westward speeds that can exceed 1.65 m s^{-1}. Following the westward currents located at 20°N and crossing the prevailing northward Kuroshio path, the majority of the drifters enter the SCS. The TOPEX/POSEDIENT-ERS satellite altimeter data and the mean state from the Parallel Ocean Climate Model results have been used to investigate the variation of Kuroshio intrusion and eddy shedding in the Luzon Strait during 1992–2001 (Jia and Liu, 2004). The Kuroshio enters the SCS and forms a loop. The Kuroshio loop varies with time, periodically shedding anticyclonic eddies. The most frequent eddy shedding intervals are 70, 80 and 90 days. Satellite ocean color, sea surface temperature, and altimeter data are used to study the surface Kuroshio path in the Luzon Strait area by Yuan et al. (2006). The results suggest that the dominant path of surface Kuroshio intrusion in winter be a direct route from the northeast of Luzon to the southwest of Taiwan and then goes westward along the continental slope of the northern SCS. Winter is the most favorable season for the formation of the anti-cyclonic intrusions. The loop currents of the Kuroshio, which feature prominent inflow-outflow currents in the Luzon Strait during the anti-cyclonic intrusions, are observed only occasionally, with more episodes in summer than in winter.

From the above study, we can see that the way how the Kuroshio intrudes in the SCS is not so clear at present. We can not form an integrated cognition since our study on water exchange through the Luzon Strait is not enough. Interaction between the Kuroshio and the SCS through the Luzon Strait is still a disputable problem, and understanding of its dynamic mechanism needs further observations and studies.

5.2 Vertical Structure of Water Exchange in Luzon Strait

The data observed from March 29, 2002 to June 6, 2002 with regard to the water masses in the northern SCS and Bashi Channel were analyzed with the quadrangle method by Tian et al. (2005). The waters in this area can be divided into four water masses: the Surface Water Mass, Subsurface Water Mass, Intermediate Water Mass and Deep Water Mass. They are located respectively in the depths from 0m to 50m, 50m to 300m, 500m to 1000m and below 1000m.The Kuroshio water intruded into the SCS, but no Kuroshio water passed 119.5°E in the investigation period. Using recently collected current and hydrographic data; Tian et al. (2006) provided a high resolution picture of the sub-inertial flow and estimated the volume transport through the Luzon Strait. The distribution of the sub-inertial flow shows a strong westward flow around 100 m in the northern part of the Luzon Strait, while the eastward flow is confined to the deeper layers, mostly

in a depth of around 1000 m. The total volume transport is estimated to be 6 ± 3 Sv during the period of observations from October 4 to 16, 2005. The observations also confirm that the Luzon Strait transport has a sandwiched vertical structure. The net westward volume transport in the deep (>1500 m) layer of the Luzon Strait reaches 2 Sv. On the basis of the current measurements at 200, 500 and 800 m from the moored current meters with the time series data from March 17 to April 15 at the mooring station (20°49′57″N, 120°48′12″E) and the hydrographic data obtained on the both sides of Luzon Strait in the spring cruise of 2002, the circulation in the investigated area is computed by using the modified inverse method (Yuan et al., 2005). The results show that the Kuroshio intrudes in the SCS to flow northwestward through the Luzon Strait in the 200 and 500 m layers. The flow condition in the 800 m layer differs from that at the 200 and 500 m layers.

At present, we are not able to study the deep layer water (especially deeper than 1000m) intrusion into the SCS through the Luzon Strait because of the observation instruments, and can not know much about its influence on the SCS upper layer circulation.

6. Relationship between SCS and ENSO

There is not only seasonal , but also interannual variations in the SCS circulation which has high ENSO-associated correlation patterns. The variability of sea surface temperature in the region of the Kuroshio intrusion into the SCS through the Luzon Strait was studied using SST derived from AVHRR from 1985 to 2002 (Ho et al., 2004). The covariance empirical orthogonal function (CEOF) method was applied for analyzing the temporal and spatial variability in the study area. The results show that the Kuroshio intrusion in the El Niño period is weaker than that in the La Niña period. The surface layer heat in the Kuroshio intrusion region is in response to the El Niño-La Niña events. The results from a high-resolution ocean general circulation model reveal the Luzon Strait transport (LST) from the Pacific into the SCS (Qu et al., 2004). On the interannual time scale, the LST tends to be higher in El Niño years and lower in La Niña years. The interannual variations of LST appear to have the opposite phase with the Kuroshio transport east of the Luzon Strait, indicating a possible nonlinear hysteresis of the Kuroshio as a driving mechanism of the LST. An oceanic connection is revealed, in which the LST seems to be a key process conveying the impact of the Pacific ENSO into the SCS. An analysis of wind data over the past 40 years and the results from a high-resolution general circulation model have revealed the existence of a previously undescribed circulation that connects the tropical Pacific with the Indian Ocean (Qu et al., 2005). As a direct response to the Pacific wind, water of the Pacific origin enters the SCS through the Luzon Strait, and from there part of the water continues southward into the Java Sea and returns to the Pacific through the Makassar Strait. This circulation contains a strong signal of El Niño and Southern Oscillation and appears to have a notable impact on the Indonesian Throughflow heat transport. The interannual variability of the LST is studied (Wang et al., 2006), using the Island Rule theory and the assimilated data from an ocean general circulation model. The assessment of contribution from each integral segment involved in the Island Rule indicates that wind stress in the western and central equatorial Pacific is the key factor regulating the interannual variability of the LST, whereas the effect of local wind stress in the vicinity of the Luzon Strait is secondary. The analysis also shows that when the westerly (easterly) wind anomalies in the tropical Pacific break out, the Luzon Strait transport increases (decreases), which is consistent with the variations in the North Equatorial Current during El Niño (La Niña) events.

Fang et al. (2006) indicated that, the sea level rising rate and sea surface warming rate of the SCS were significantly higher than the corresponding global rates. By using the EOF analysis, the

ENSO-associated correlation patterns of the SW, SSH, and SST are presented. Based on the COADS and OISST data, the relationship between the interannual variability of SSTA in the SCS and the ENSO events is studied, and the contribution of Ekman pumping to the variability is further discussed (Zhu et al., 2003). Their results show that the SSTA in the SCS correlates well with the Nino 3 SSTA, with a lag time of 5 months. And three typical periods of 42.7 months, 25.6 months and 36.6 months are recognized according to the variance contribution. The three modes can approximately describe the interannual variability of SSTA in the SCS, which proves that the regional response does exist in the SCS in the large-scale ENSO background.

7. Barrier Layer and Warm Waters

A number of studies have reported that there are some regions in the world ocean where the base of the surface isothermal layer is substantially deeper than the base of the surface mixed layer. The layer between the bases of the mixed layer and the isothermal layer has been referred to as the barrier layer. When a barrier layer is present, the kinetic energy transferred from the wind momentum to the ocean is trapped above the barrier layer, thus accelerating the flow in the mixed layer. On the other hand, the presence of a barrier layer reduces the entrainment cooling or may even cause the entrainment heating in the mixed layer. Therefore, the barrier layer is an important factor influencing the SST and complicates air-sea interaction.

The SCS is a large tropical marginal sea, as a part of the Indo-Pacific warm pool that plays a significant role in the formation and development of the Southeast Asian monsoon, warm water over the SCS has a large variation. The seasonal variation of warm water in the SCS has been previously studied by using both observations and numerical models.

7.1 Mechanism of Barrier Layer

An analysis of the climatological temperature and salinity shows the evidence of the barrier layer in the southern SCS in the summer (Du et al., 2004). The net fresh water flux is a key factor to determine the occurrence of the barrier layer. The structure and distribution of the barrier layer is dominated by the wind fields, and adjusted by the development of the mixed layer and isothermal layer. In summer, the SCS boundaries restrict the easterly Ekman transport, and the Ekman pumping is negative in the eastern SCS. Those two effects result in the fresher water pile up in the southeastern SCS. The high temperature waters detrain from the mixed layer and retain in the isothermal layer, which cause the deepest and thickest barrier layer in the southeastern SCS, where its maximum reaches 30 m. The thickest BI occurs where the SCS Warm Water occurs, so the “heat barrier effect” facilitates the development of the SCS Warm Water.

The robust evidence for the barrier layer in the northeastern SCS (16°–25°N, 112°–124°E) is presented (Pan et al., 2006). The occurrence rate of the barrier layer peaks in autumn (45.7%), then summer (31.1%) and spring (23.3%), sequently. It is estimated that the annual occurrence rate of the barrier layer reaches about 40.0% in the central northeastern SCS (18°–22°N, 112°–120°E) and the Luzon Strait. The Stratification-formed (Rain-formed) mechanism is the major factor responsible for the occurrence of the barrier layer in the northeastern SCS in the spring (the summer and autumn), respectively. The rainfall observation from TRMM provides reliable evidence for the latter.

7.2 SCS Warm Waters

The climatology monthly mean sea temperature from the Levitus and Comprehensive Ocean-Atmosphere Data Set (COADS) and sea surface flux from COADS were used by Wang et

al. (2005) to study the formation and decay of spring warm pool in the SCS. In May, SST is rapidly increased, and a large area of warm water (greater than 29.5°C) of the so-called spring warm pool appears in the central SCS with its thickness of about 15 m. At that time, the northeast monsoon is gradually weakened and disappears. As a result, the mixed layer depth becomes shallow, which means that the upper layer water is easier warmed than before. The spring warm pool decays in June when the south-west monsoon prevails in the SCS and disappears in July. From the above, the spring warm pool is a transient phenomenon in response to the atmosphere change, which influences SST variation by ocean dynamics. According to the upper mixed layer dynamical equation, the formation and the decay of spring warm pool are investigated. It shows that the formation is due to increasing surface net heat flux and the downwelling caused by Ekman pumping , which effectively restrain the cold water upwelling and maintain the water warming .The decay of spring warm pool is due to the local strengthening upwelling and the southeast Ekman currents. All of that indicates that the ocean dynamics plays a determinant role in this process.

The SCS warm water has a large seasonal cycle and interannual fluctuations. Meng and Wang (2005) analyzes the annual variation of the SCS warm water and its relation with the net heat flux as well as atmospheric circulation associated with the warm water, using the COADS and NCEP datasets. The analysis suggests that the net heat flux be the most important factor in the annual cycle of the warm water; the largest upward motion region of the atmosphere is located south to the of the equator and over Indonesia in winter (There is no warm water in the SCS), and it moves northward to the SCS region in summer (The SCS warm water is strongest). The SCS warm water becomes a convective center of the atmosphere in summer.

The formation and decay of the warm water with SST higher than 30℃ in the upper SCS west of the Philippines was investigated by Jiang et al. (2006) using a set of new satellite measurements and the NCEP/NCAR reanalysis data. It is found that the appearance and rapid expansion of this warm water can be utilized to objectively predict the SCS summer monsoon (SCSSM) onset. Their hypothesis suggests an air-sea feedback scenario that may explain the development of the SCSSM. The warm water exhibits considerable year-to-year variations. There are close relations between the warm water area and its strength and the onset date of the SCSSM.

As far as the Nansha Warm Water (NWW) in the southern SCS is concerned, Cai et al. (2004) used a reduced vertically integrated upper mixed model to study the dynamic and thermodynamic process of formation of it. Their results can be outlined as follows: (1) In spring, the formation of the NWW is mainly due to the sea surface net heat flux, and the contribution of the thermal advection and the entered warm water from the Su1u Sea or the area south of the Sunda Shelf are small. (2) In winter, the strength of the current field in the Nansha Islands sea area increases, and the contribution of the thermal advection is greater than or equal to that of the sea surface net heat flux, so the drop in sea temperature is greater than that of the other deep sea areas。but the sea temperature in the sea area still keeps high because the initial sea temperature field in the preceding season is higher. (3) The mechanism of formation and maintenance of high temperature of the NWW varies with season.

8. Air-Sea Interaction

Situated the pathway of East Asian monsoon system, the SCS circulation is largely influenced by the seasonal reversal of the monsoonal winds, northeasterly in winter and southwesterly in summer. The observations show that this region is characterized by active local

air-sea interaction, which may affect the local ocean circulation, water cycle, etc., and is unique compared with many other ocean basins. Therefore, enhancing the SCS local air-sea interaction research is significant to gain a deep insight into the circulation structure and mesoscale oceanic process of the SCS and the SCS climate change, to improve the abilities of weather forecast and to reduce casualties and economic losses in disastrous event caused by the ocean.

8.1 Air-sea Flux

In order to explore the interaction between the sea and monsoon in the SCS, Wu et al. (2006) calculated the heat exchanges at air-sea interface in the monsoon period in 1986 using observational data. It shows that when the summer monsoon bursts and prevails over the SCS, the air-sea interface heat exchange is strong and the latent heat rises rapidly in the intertropical convergence zone and the tropic cyclone system near 20.49°N, 114.14°E. On May 24, 1986, the sensible heat became positive in the typhoon system, and heat, mainly from the latent heat, is transported from the ocean to atmosphere. When the summer monsoon prevails over the SCS, and the weather is fine, and even SST is high, but the sensible heat appears to be negative, this heat is transported from atmosphere to the ocean, to which the short-wave radiation absorbed by sea surface and sensible heat have the major contribution. When the summer monsoon is over and the northeast monsoon prevails over the SCS, the heat exchange at air-sea interface is very strong, and the ocean heats the atmosphere due to the major contribution of latent heat when cold air arrives, and the sensible heat rises rapidly and become positive. Therefore it can be concluded that the heat exchange at air-sea interface is different from the SST in the SCS.

From 24 April to 22 June 2002, before and after the SCS monsoon onset, the 3rd experiment of air-sea flux observation was carried out in the region of Xisha Islands(16°50′N, 112°20′E). A series of high quality and high frequency (1 time/min) data were gained in the experiment (Chen et al., 2005). The three main results from the experiment are shown as follows. (1) The mean momentum flux was 0. 0458 W · m^-2, the mean latent heat flux was 94.06 W · m^-2, and the mean sensible heat flux was 4.07 W · m^-2. The three fluxes were smaller than those in the western Pacific. (2) In the northern part of the SCS, the air-sea fluxes and their correlated factors were remarkably the different before and after the SCS monsoon onset, and they also varied greatly under different weather conditions. Every factor evolved stably besides the daily variation before the monsoon onset. But after the monsoon onset, the daily variation enhanced, the high frequency turbulence increased, and every flux varied greatly in a short time, especially in the raining phase, which reflected that the mesoscale and microscale strong turbulence occurred in the acute weather background after the monsoon onset. (3) The northern part of the SCS had the oceanic common characteristics as well as the western Pacific. Its sensible heat flux is much smaller than its latent heat flux. But the northern part of the SCS might play a less important role in the global air-sea interaction than the western Pacific. The air-sea fluxes in the northern part of the SCS changed little from May to June according to the average of the three experiments. Moreover, there was a stable ratio of the sensible heat flux to the latent heat flux. The latent heat flux was about twenty times as much as the sensible heat flux, in other words, the Bowen ratio was about 0.05.

Based on the three ATLAS Mooring buoy data provided by the SCSMEX project (SCS Monsoon Experiment), the harmonic analysis method was applied to determine amplitudes and phases for the annual and semi-annual cycles of temperatures in the upper layer (1~ 250 m) of the SCS. At stations SCS1 (18°05′54″N, 115°35′48″E) and SCS3 (12°58′30″N, 114°24′30″E), the

temperature variances of annual and semi-annual cycle in the surface layer (surface to 50 m) are out-of-phase with those in the sub-surface layer (50 m through 250 m). However, the corresponding temperature variations at Station SCS2 (15°20′36″N, 114°57′18″E) are vertically in phase. The further studies suggest that temperature variations at SCS2 be controlled by the advection term, while temperature variations at the other two sites are dominated by the convection term induced by Ekman pumping. As far as the annual cycle is concerned, the maximum amplitude appears in the sub-surface at Sts. SCS2 and SCS3, but in the surface at St.SCS1.The maximum amplitude for the semi-annual cycle appears in the sub-surface similarly at the three sites. Nevertheless, the amplitudes for the annual cycle at Sts. SCS1 and SCS3 decrease with depth beneath the mixed layer, which results in contribution of the semi-annual cycle comparable that of annual cycle, especially at St. SCS3.

8.2 Tropical Cyclones

The SCS is an area with frequent tropic cyclone activities, some of them come from the western Pacific, and the others generate locally. Tropic cyclones generate in the western Pacific in summer, most of which grow into typhoon or tropic hurricane, which will attack this sea area. The moving tracks of tropic cyclones in the SCS are often complex, and their intensities are different.

A three-dimensional baroclinic model with a free surface has been employed to calculate the response of upper current field to the Frankic (9606) severe tropical storm in the SCS. Li et al. (2003) pointed out that the response of surface currents field to the Frankic wind field only had one day, and the deeper the ocean, the slower the response of it. The type of the Frankic-driven currents was much similar to that of cyclonic wind field, and the sea surface elevations rose to some extent when the Frankic passed. Numerical experiments were performed on a strong tropical cyclone Vongfong (No. 0214) in the SCS by a Mesoscale Coupled Model (Wang et al., 2006). The quantitative effects of mesoscale air-sea interaction on the cyclone process made the tracks and intensity of the cyclone influenced significantly, and made the atmospheric temperature of lower level (925hPa) decrease by more than 1℃. The upward heat flux is decreased by the SST reduction induced by air-sea interaction and the latent heat flux is more sensitive to the SST reduction.

Understanding the interaction of ocean eddies with tropical cyclones is critical for improving the understanding and prediction of the tropical cyclone intensity. Lin et al.(2003) studied the interaction between Super Typhoon Maemi (2003) and a warm ocean eddy in the western North Pacific. Based on the Coupled Hurricane Intensity Prediction System and satellite microwave sea surface temperature observations, it is suggested that the warm eddies act as an effective insulator between typhoons and the deeper ocean cold water. This study can serve as a starting point in the largely speculative and unexplored field of the typhoon-warm ocean eddy interaction in the western North Pacific. Given the abundance of ocean eddies and intense typhoons in the western North Pacific, these results highlight the importance of a systematic and in-depth investigation of the interaction between typhoons and western North Pacific eddies. A case study on the cyclonic eddy generated by the tropical cyclone looping over the northern SCS is presented (Hu et al., 2004). Three cases relating to the tropical cyclone events over the northern SCS have been analyzed. For each looping tropical cyclone case, the cyclonic eddy with an obvious sea level depression appears in the sea area where the tropical cyclone takes a loop form, and lasts for about 2 weeks with a slight variation in location. The cold core with the SST difference greater than 2℃ against its surrounding areas is also observed by the satellite-derived SST data.

It has long been recognized that the evolution of the western Pacific typhoons may be strongly affected by large-scale circulations, asymmetric structure of typhoons themselves and terrain, etc. However, the roles of flux transfer processes at the air-sea interface have remained unclear. Li et al. (2004) pointed out that high winds of typhoons could generate large amounts of spray. They simulated typhoon "Sinlaku", a recent western Pacific typhoon in 2002, by using a coupled atmosphere-sea spray modeling system. It is found that (1) sea spray can cause a significant latent heat flux increase up to 50% of the interfacial fluxes in typhoon "Sinlaku"; (2) taking into account the effects of sea spray, the intensity of a modeled typhoon can increase significantly, by 30% in wind speed at 10m, which may much improve the estimate of maximum storm intensity in the atmospheric model; and (3) the effects of sea spray mainly focus on the high wind regions around the storm center and are mainly felt in the lower part of troposphere.

Huang and Lin (2004) analyzed thirteen tropical cyclones tracking westward at high speed into the SCS. It is shown that the major characteristics of the westerlies is that from the Middle Asia to the East Asia it was covered by a ridge or by zonal circulation, and westerly troughs were at higher latitudes. Their results also show that a constantly intense zonal spreading subtropical high dominated from the west North Pacific to the central and southern China, or a continually strengthening subtropical ridge extending westward gradually built up the gradient between the ridge and tropical cyclone and strengthened the easterly steering flows. Moreover, the easterly environmental flows prevailing in both of the southern and northern sides of tropical cyclone would drive it to travel more quickly.

8.3 Sea Fog

Sea fog is kind of disaster weather in the sea and coastal region. Observation and forecast of sea fog is significant. A synoptic forecasting method was developed and 37 sea fog examples were analyzed (Sun et al., 2006), based on meteorological observation data, NOAA- 17 and EOS/MODIS satellite remote sensing image data. The statistical characteristics of sea fog, atmospheric and oceanic background conditions which were helpful for sea fog formation were revealed.

The relative humidity equation and numerical model are used to study the advection, turbulence and radiation effects in the sea fog formation process (Hu, et al., 2006). It is shown from their study that the main driving force of sea fog formation is the longwave radiation cooling, the turbulence cooling of the lower layer atmosphere occurs only at the initial stage of advection process, and the turbulence effect on the lower layer atmosphere quickly turns to heating effect with the elapse of time so as to be unfavorable to the sea fog formation. The turbulence and radiation effects in the lower layer atmosphere have signs opposite to each other (have the same sign only at the initial stage of sea fog formation process), and are of the same order; the turbulence and radiation effects in the upper layer atmosphere have the same sign, but the radiation effect is predominant. The turbulence and radiation effects are the main factors affecting the sea fog formation, and the direct effect of advection is relatively small. The effects of advection, turbulence, radiation and sum of them all decrease with the elapse of time.

9. Conclusions

The physical oceanographic research into the SCS achieved by Chinese Scholars from 2003 to 2006 has reached a new level in both depth and breadth of the scientific problems concerned. New oceanographic phenomena have been discovered by carrying out some of the SCS projects as the SCS Monsoon Experiment, the Nansha Islands Synthetical Investigation, and the Northern

SCS Opening Cruise of South China Sea Institute. Application of the high precision and resolution satellite remote sensing data brings a new opportunity to the oceanographic research. Great deals of numerical studies provide a mathematical method for understanding the formation and variation of the SCS circulation dynamic mechanism and its perdition and forecast. We can not cover all of the SCS oceanographic achievements in this period because the limit of the paper length and un-entire relative information has been collected by the author, but the results summarized above are enough for attract us to pay attention on the SCS issues. We believe that more abundant and distinctive achievements will be presented not long for the future, and promote the development of marine science continuously.

Acknowledgements: This paper was supported by the National Science Foundation of China (Grant 40625017); the Chinese Academy of Sciences (Grant KZCX3-227) and the National 863 Project of China (Grant 2006AA09Z156).

References:

1. BAO Li-Feng, LU Yang, WANG Yong, HSU Hou-ze, Seasonal variation of upper ocean circulation over the South China Sea from satellite altimetry data of many years. Chinese Journal of Geophysics, 48(3): 543-550, 2005.
2. CAI Shu-qun, DONG Dan-peng, WANG Sheng-an, LONG Xiao-min, HUANG Qi-zhou, Progress of The Study on The Mesoscale fluctuation Phenomenan The South China Sea. Advance in Earth Sciences, 20(2): 180-184, 2005.
3. CAI Shu-qun, GAN Zi-jun, LI Chi-wei, LONG Xiao-rain, DONG Dan-peng, Preliminary Numerical Study on the Dynamic and Thermodynamic Process of Nansha W arm Water. Advances in Marine Science, 22(2): 137-146, 2004.
4. CAI Shu-qun, LONG Xiao-min, CHEN Rong-yu, HUANG Qi-zhou, A Study On Circulation Structure In Spring In Nansha Islands Sea Area, South China Sea. Journal of Tropical Oceanography, 23(2): 37-44, 2004.
5. Caruso, M., G. Gawarkiewica, and R. Beardsley, Interannual variability of the Kuroshio intrusion in the South China Sea, J. Oceanogr., 62, 559-575, 2006.
6. CENTURIONI L.R., NILLER P, LEE D.K., Observations of Inflow of Philippine Sea Surface Water into the South China Sea through the Luzon Strait. Journal of Physical Oceanography, 34(1)：113-121, 2004.
7. CHAO Jiping, CHEN Xianyao, A Semi-Analytical Theory of Coastal Upwelling and Jet. Chinese Journal of Geophysics, 2003, 46(1): 26-30.
8. CHEN Xuhua, QI Yiquan, WANG Weiqiang, Seasonal and Interannual Variabilities of Mesoscale Eddies in South China Sea. Journal of Tropical Oceanography, 24(4): 51-59, 2005.
9. CHEN Yi-De, JIANG Guo-Rong, ZHANG Ren, YAN Jun-Yue, YAO Hua-Dong, and TANG Zhi-Yi, Analysis and Comparison of Air-Sea Flux in the Northern South China Sea. Chinese Journal of Atmospheric Sciences, 29(5): 761-770, 2005.
10. CHERN, CS, WANG J. Numerical study of the upper-layer circulation in the South China Sea. J. Oceanogr., 59 (1): 11-24, 2003.
11. CHU, P., and C., Fang, Observed Rossby waves in the South China Sea from satellite altimetry data, Proceedings of SPIE conference on remote sensing of the ocean and sea ice, Barcelona, Spain, 8-12, 2003.
12. DU, Yan, WANG Dong-xiao, CHEN Ju, QI Yi-quan, SHI Ping, Structure Of Abnormal Saline Water Under Mixed Layer In Southern South China Sea. Journal of Tropical Oceanography, 23(6): 52-59, 2004.
13. DU, Yan, WANG Dong-xiao, CHEN Ju, WANG Wei-qiang, XIE Qiang, Advance On Observation And Simulation of Oceanic Dynamics In South China Sea. Journal of Tropical Oceanography, 23(6): 82-92, 2004.
14. DU, Yan, WANG Dong-xiao, CHEN Rong-yu, MAO Qing-wen, QI Yi-quan, Vertical structure of ADCP observed current in the western boundary of the South China Sea. Chinese Ocean Engineering, 22(2): 31-38, 2004.
15. DU, Yan, WANG Dongxiao, SHI Ping, GUO Peifang, and CHEN Ju, Seasonal Variation of the Barrier Layer in the South China Sea and Its Relationship to the Sea Surface Flux. Chinese Journal of Atmospheric Sciences, 28(1): 101-111, 2004.

16. FANG, G., H. CHEN, Z. WEI, Y. WANG, X. WANG, and C. LI, Trends and interannual variability of the South China Sea surface winds, surface height, and surface temperature in the recent decade, J. Geophys. Res., 111, C11S16, 2006.
17. GAN, J., H. LI, E. N. CURCHITSER, and D. B. HAIDVOGEL, Modeling South China Sea circulation: Response to seasonal forcing regimes, J. Geophys. Res., 111, C06034, 2006.
18. GAO Rongzhen, WANG Dongxiao, WANG Weiqiang, ZHOU Faxiu, and XIE Qiang, Annual and Semi-Annual Cycles of the Upper Thermal Structure in the South China Sea. Chinese Journal of Atmospheric Sciences, 27(3): 345-353, 2003.
19. GAWARKIEWICA, G., J. WANG, M. CARUSO, S. RAMP, K. BRINK, and F. BAHR, Shelfbreak circulation and thermohaline structure in the northern South China Sea—contrasting spring conditions in 2000 and 2001, IEEE J. Ocean. Eng., 29, 1131–1143, 2004.
20. GUAN Bing-xian , YUAN Yao-chu, Overview of studies on some eddies in the China seas and their adjacent seas Ⅰ. The South China Sea and the region east of Taiwan. Acta Oceanologica Sinica, 28(3): 1-16, 2006.
21. HE Zhigsng, WANG Dongxiao, CHEN Ju, HU Jianyu, Eddy structure in South China Sea from satellite-tracked surface drifting buoys and satellite-remote sensing sea surface height. Journal of Tropical Oceanography, 20(1): 27-35, 2001.
22. HO, C., Q. ZHENG, N. KUO, C. TSA, and N. HUANG, Observation of the Kuroshio intrusion region in the South China Sea from AVHRR data, Int. J. Remote sensing, 25, 4583-4591, 2004.
23. HSUEH Y., and ZHONG L.J. A pressure-driven South China Sea Warm Current. J. Geophy. Res., 109, C09014, 2004.
24. HU J., KAWAMURA H. Detection of cyclonic eddy generated by looping tropical cyclone in the northern South China Sea: a case study. Oceanologica Acta Sinica, 23(2): 213-224, 2004.
25. HU Rui-jin, DONG Ke-hui, ZHOU Fa-xiu, Numerical experiments with the advection, turbulence and radiation effects in the seafog formation. Advances in Marine Science, 24(2): 156-165, 2006.
26. HUANG Wei-gen, LIN Chuan-lan, LOU Xiu-lin, XIAO Qing-mei, SHI Ai-qin, JIN Wei-min, Satellite observations of the thermal front in the Taiwan Strait and its adjacent seas . Acta Oceanologica Sinica, 28(4): 49-55, 2006.
27. HUANG Zhong LIN Liangxun, Statistical characteristics of tracking westward typhoons at high speed into the South China Sea. Meteorological Monthly, 30(9): 14-18, 2004.
28. JIA, Y., and Q. LIU, Eddy shedding from the Kuroshio bend at Luzon Strait. J. Oceanogr., 60, 1063-1069, 2004.
29. JIANG, Xia, LIU, Qin-Yu, WANG, Qi, Effects of warm water west of the Philippines on the South China Sea summer monsoon onset. Periodical of Ocean University of China, 36(3): 349-354, 2006.
30. LAN Jian , YU Fei , BAO Ying, Multi-eddy structure in the southern South China Sea. Advances in Marine Science, 23(4): 408-413, 2005.
31. LI Chao, ZHANG Yan, WANG Dongxiao, Impact of cold surges on sea surface temperature in South China Sea in autumn of 2004. Journal of Tropical Oceanography, 25(2): 6-11, 2006.
32. LI Dong-hui, YOU Xiao-bao, ZHANG Ming, A Study on Circulation Mechanism of South China Sea in Summer by Numerical Experiment. Journal of Tropical Oceanography, 22(6): 54-63, 2003.
33. LI Dong-hui, ZHANG Ming, Numerical Calculation Of The Response Of Upper Currents Field Of South China Sea To Frankic (9606) Severe Tropical Storm. Marine Forecasts, 20(4): 56-63, 2003.
34. LI Li, A review on mesoscale oceanographic phenomena in the South China Sea. Journal of Oceanography in Taiwan Strait, 21(2): 265-274, 2002.
35. LI Wei-Biao, HE Xi-Cheng, TANG Jie, Numerical simulation of Typhoon “Sinlaku ”: roles of sea spray. Journal of Tropical Oceanography, 23(3): 58-65, 2004.
36. LIANG, Xinfeng, ZHANG, Xiaoqian, TIAN, Jiwei, Observation of internal tides and near-inertial motions in the upper 450 m layer of the northern South China Sea. Chinese Science Bulletin, 50(24): 2890-2895, 2005.
37. LIAO Guang-hong, YUAN Yao-chu, XU Xiao-hua, The three dimensional structure of the circulation in the South China Sea during the winter of 1998. ACTA OCEANOLOGICA SINICA, 27(2): 8-17, 2005.
38. LIN, I. I., C. C. WU, K. A. EMANUEL, I. H. LEE, C. R. WU, and I. F. PUN. The interaction of Supertyphoon Maemi (2003) with a warm ocean eddy. Mon. Weather Rev., 133 (9), 2635–2649, 2005.
39. LIN. I. I., LIU W. T., WU C. C., et al. New evidence for enhanced ocean primary production triggered by tropical cyclone. Geophysical Reseach Letters, 30(13): 1718-1722, 2003.
40. LIN. I.I., LIU W.T., WU C.C., et al. Satellite observations of modulation of surface winds bu typhoon-induced

upper ocean cooling. Geophysical Reseach Letters, 30(3): 1131-1134, 2003.
41. MAO Qin-wen, WANG Wei-qiang, QI Yi-quan, CHEN Rong-yu, Analyses On Temperature And Salinity Distributions In Nansha Islands W Aters During Spring To Sum Mer Monsoon Transition. Journal of Tropical Oceanography, 24(1): 28-36, 2005.
42. MENG Xiang-Xin, WANG Qi, A Preliminary Study of the Seasonal and Interannual Variations of the South China Sea Warm Water. Periodical of Ocean University of China, 36(2): 187-192, 2006.
43. METZGER E. J., Upper Ocean Sensitivity to wind forcing in the South China Sea. Journal of Oceanography, 59: 783-798, 2003.
44. PAN Aijun, WAN Xiaofang, XU Jindian, GUO Xiao-gang, WU Ri-sheng, Barrier layer in the central South China Sea and its formation mechanism. Acta Oceanologica Sinica, 28(5): 35-43, 2006.
45. PAN Aijun, WAN Xiaofang, XU Jindian, GUO Xiaogang and LI Li, Barrier layer in the northeastern South China Sea and its formation mechanism. Chinese Science Bulletin, 5(8): 951-957, 2006.
46. CHU, Peter, Qinyu LIU, Yinglai JIA et al. Evidence of a barrier in the Sulu and Celebes Seas. Journal of Physical Oceanography, 32: 3299-3309, 2002.
47. QU, T., Y. DU, G. MEYERS, A. ISHIDA, and D. WANG , Connecting the tropical Pacific with Indian Ocean through South China Sea, Geophys. Res. Lett., 32, L24609, 2005.
48. QU, T., Y. KIM, M. YAREMCHUK, T. TOZUKA, A. ISHIDA, T. YAMAGATA, Can Luzon strait transport play a role in conveying the impact of ENSO to the South China Sea? J. Clim., 17, 3644-3657, 2004.
49. SU, Ji-lan, Overview of the South China Sea Circulation and its Influence on the Coastal Physical Oceanography near the Pearl River Estuary, Continental Shelf Research, 24:1745–1760, 2004.
50. SU, Ji-lan, Overview of the South China Sea circulation and its dynamics. Acta Oceanologica Sinica, 27(6): 1-8, 2005.
51. SUN Lianqiang, LIU Shuping, GAO Songying, CAO Shimin, WANG Wenwu, FAN Xibin, Conditions for sea fog formation in Dandong coast and its synoptic forecasting method. Journal of Meteorology and Environment, 22(1): 25-28, 2006.
52. TIAN Tian, W EI Hao, Analysis of W ater Masses in the Northern South China Sea and Bashi Channel. PERIODICAI OF OCEAN UNIVERSITY OF CHINA, 35(1): 9-12, 2005.
53. TIAN, J., Q., YANG, X., LIANG, L., XIE, D., HU, F., WANG, and T. QU, Observation of Luzon Strait transport, Geophys. Res. Lett., 33, L19607, 2006.
54. WANG Dong-Xiao, CHEN Ju, CHEN Rong-Yu, ZHU Bo-Cheng, GUO Xiao-Gang, XU Jin-Dian, WU Ri-Shen, Hydrographic and Circulation Characteristics in Middle and Southern South China Sea in Summer, 2000. OCEANOLOGIA ET LIMNOLOGIA SINICA, 35(2): 97-109, 2004.
55. WANG Dongxiao, LIU Xiongbin, WANG Wenzhi, DU Yan and ZHOU Weidong, Simulation of meridional overturning in the upper layer of the South China Sea with an idealized bottom topograhpy. Chinese Science Bulletin, 49(7): 740-747, 2004.
56. WANG G H, SU J L, LI R F. Mesoscale eddies in the South China Sea and their impact on temperature profiles. Acta Oceanologic Sinica, 24(1), 39-45, 2005.
57. WANG G H, SU J L, CHU P C. Mesoscale eddies in the South China Sea observed with altimeter. Geophysical Research Letters, 30(21): 2121, 2003.
58. WANG G H, SU J L, QI Yiquan, Advances In Studying Mesoscale Eddies In South China Sea. Advance in Earth Sciences, 20(7): 744-747, 2005.
59. WANG Lei, WANG Li-ya, WEI Hao, An Analysis of the Sea-Surface Thermal Fronts in the Northern Shelf Region of the South China Sea with Satellite Data. PERIODICAL OF OCEAN UNIVERSITY 0F CHINA, 34(3): 351-357, 2004.
60. WANG Si-si, HUANG Li-wenl, WANG Li-jun, Numerical simulation of effects of cyclone-sea interaction on a strong tropical cyclone process in South China Sea. Journal of Tropical Oceanography, 25(3): 14-20, 2006.
61. WANG Weiqiang, WANG Chunzai, Formation and decay of the spring warm pool in the South China Sea. GEOPHYSICAL RESEARCH LETTERS, 33 (L02615), 2006.
62. WANG Wei-Qiang, ZHU Xiu-Hua and HOU Yi-Jun, The Role of Ocean Dynamics in Spring Warm Pool of the South China Sea. Chinese Journal of Atmospheric Sciences, 29(4): 565-572, 2005.
63. WANG, D., Q. LIU, R. HUANG, D. YAN, and T. QU, Interannual variability of the South China Sea throughflow inferred from wind data and an ocean data assimilation product, Res. Lett., 33, L14605, 2006.
64. WANG, H., Y. YUAN, W. GUAN, R. LOU, and K. WANG, Circulation in the South China Sea during summer 2000 as obtained from observations and a generalized topography-following ocean model, J. Geophys. Res.,

109, C07007, 2004.

65. WU Disheng, FENG Weizhong, XU Jianping, YAN Jinghua, ZHAO Xue, ZHOU Shuihua, ZHANG Jiwei, QIAO Guanyu, LIN Fu, LU Boming, Heat exchange at air-sea interface in the South China Sea during monsoon periods in 1986. Chinese Science Bulletin, 51(19): 2413-2420, 2006.
66. WU Lisheng, LI Li, Summarization of study on upwelling system in the South China Sea. Journal of Oceanography In Taiwan Strait, 22(2): 269-277, 2003.
67. WU Zi-fu, TIAN Ji-wei, LU Xian-qing, WONG Lai-Ah, A Numerical Model of Tides in The South China Sea by Adjoint Method. OCEANOLOGIA ET LIMNOLOGIA SINICA, 34(1): 101-108, 2003.
68. WU Zi-ku, TIAN ji-wei, ZHAO qian, 3-D numerical simulation of the South China Sea tidal waves with assimilation method. JOURNAL OF HYDRODYNAMICS, 19(4): 501-506, 2004.
69. Xie S.P., Xie Q., Wang D.X., Liu W.T., Summer upwelling in the South China Sea and its role in regional climate variations. Journal of Geophysical Research, 108(c8):3261, 2003.
70. XU Jin-dian, GUO Xiao-gang, LI Li, WU Ri-sheng, J ING Chun-sheng, Hydrology features in outer sea of eastern Guangdong in summer 2002. Journal of Oceanography In Taiwan Strait, 22(2): 218-228, 2003.
71. XUE HJ, CHAI F, PETTIGREW N, et al. Kuroshio intrusion and the circulation in the South China Sea. J. Geophys. Res., 109 (C2): Art. No. C02017, 2004.
72. YANG H., LIU Q., Forced Rossby wave in the northern South China Sea, Deep Sea Research, Part I, 50: 917-926, 2003.
73. YUAN Yao-chu, LOU Ru-yun, Liu Yong-gang, SU Ji-lan, WANG Kang-shan, Currents in the Luzon Strait during spring of 2002: observation and computation by modified inverse model. ACTA OCEANOLOGICA SINICA, 27(3): 1-10, 2005.
74. YUAN, D., W. HAN, and D. HU , Surface Kuroshio path in the Luzon Strait area derived from satellite remote sensing data, J. Geophys. Res., 111, C11007, 2006.
75. ZENG Ganning, HU Jianyu, HONG Huasheng, CHEN Zhaozhang, Analysis of hydrologic section off Zhujiang River estuary in northern South China Sea during various southwest monsoon phases. Journal of Tropical Oceanography, 24(3): 10-17, 2005.
76. ZHAO Hui , QI Yi-quan ,WANG Dong-xiao ,WANG Wen-zhi, Study on the Features of Chlorophyll-a Derived From SeaWiFS in the South China Sea. Acta Oceanologica Sinica, 27(4): 45-52, 2005.
77. ZHAO Hui, TANG Dan-ling, WANG Su-fen, Spatial distribution of chlorophyll a concentration in summer in western south china sea and its response to oceanographic environmental factors. Journal of Tropical Oceanography, 24(6): 31-37, 2005.
78. ZHU Jia, HU Jianyu, CHEN Zhaozhang et al., Analysis on Sectional Characteristics of Temperature and Salinity off the Zhujiang River Estuary-During the Cruises of May 2001 and November 2002. Journal of Xiamen University (Natural Science), 44(5): 680-683, 2005.
79. ZHU Liang-sheng, CHEN Xiuhua, QIU Zhang, Characteristics Analysis of Tide and Current at Yongshu Reef. Marine Science Bulletin, 24(4): 1-7, 2005.
80. ZHU Xiuhua, WANG Weiqiang, et al., Interannual Mode of Sea Surface Temperature In Relation to Monsoon Forcing in South China Sea. Journal of Tropical Oceanography, 22(4): 42-50, 2003.
81. ZHUANG Wei, HU Jianyu, HE Zhigang, ZENG Ganning, CHEN Zhaozhang, An analysis on surface temperature and salinity from southern Taiwan Strait to Zhujiang River Estuary during July-August. Journal of Tropical Oceanography, 22(4): 68-76, 2003.
82. ZHUANG Wei, WSNG Dongxiao, WU Risheng, and HU Jianyu, Coastal upwelling off eastern Fujian-Guangdong detected by remote sensing. Chinese Journal of Atmospheric Sciences, 29(3): 438-444, 2005.

A REVIEW OF OCEAN-ATMOSPHERE INTERACTION STUDIES IN CHINA

LIU Qinyu[*]*, YANG Jianling, WU Shu, HU Haibo, HU Ruijin and LI Lijuan*

Physical Oceanography Lab. & Ocean-Atmosphere Interaction and Climate Lab., Ocean University of China，

Qingdao，266003，China

Abstract： A large number of papers have been published and great efforts have been made in the past 4 years (2002-2006) by the Chinese oceanographic and meteorological scientists in the Ocean-Atmosphere interaction studies. The present paper is an overview of the major achievements made by Chinese scientists and their collaborators in the studies of large scale Ocean-Atmosphere interaction in the following oceans: the South China Sea, the Tropical Pacific, the Indian Ocean and the North Pacific. Many interesting phenomena and dynamic mechanisms have been discovered and studied in these papers. These achievements have improved our understanding of climate variability and have great implications in climate prediction, and thus highly relevant to the ongoing international CLIVAR efforts.

Key Words: Ocean-Atmosphere interaction, Pacific, Indian Ocean, South China Sea, Chinese scientist

Key words: Ocean-Atmosphere interaction, Pacific, Indian Ocean, South China Sea, Chinese scientist

1. Introduction

The Ocean-Atmosphere interaction is important in the climate variability. In the past 4 years, Chinese scientists have been interested in the Ocean-Atmosphere interaction and have participated in international projects related with the Ocean-Atmosphere interaction, such as the Climate Variability and Predictability (CLIVAR) and others. Chinese scientists organized an international project, “South China Sea Monsoon Experiment (SCSMEX)”, which is operated by the Ministry of Science and Technology of China during the period of 1996–2001. The SCSMEX aims to better understand the onset, maintenance, and variability of the summer monsoon over the South China Sea (SCS) and is a large-scale international effort with many participating countries and regions cooperatively involved in this experiment. There are other programs and projects about the Ocean-Atmosphere Interaction, which have been organized and funded by the National Natural Science Foundation of China, the Ministry of Science and Technology of China, the Chinese Academy of Sciences, the China Meteorological Administration, the State Oceanic Administration of China, the Ministry of Education of the People’s Republic of China and other agencies.

In this report, the main progresses made in the Ocean-Atmosphere interaction studies by the mainland Chinese scientists (excluding those of Hong Kang and Taiwan) since July of 2002, will be briefly stated. In order to avoid overlapping with some climate and ocean dynamic researches, this review will be limited to the interaction between upper layer ocean and lower layer atmosphere in larger scale. In the second section some researches about the Ocean-Atmosphere

[*] E-mail:liuqy@ouc.edu.cn

interaction in the South China Sea (SCS) will be reviewed. The research progress on El Nino and South Oscillation (ENSO) will be summarized in section 3; other new tropical Pacific researches related to ENSO will be introduced in section 3, too. The progress of studies of the Ocean-Atmosphere interaction in the Indian Ocean and its relation with ENSO will be introduced in section 4. In section 5 some studies on the Ocean-Atmosphere interaction in the extra-tropical North Pacific will be summarized. The paper has a summary as ending.

2. Ocean-Atmosphere interaction in the South China Sea (SCS)

In SCS, the most significant feature of the Ocean-Atmosphere interaction is the seasonal variations of the upper layer ocean as oceanic response to monsoon forcing, which have been described by some Chinese scientists, large amounts of researches about the Ocean-Atmosphere interaction and ocean circulation have been carried out (Su, 2005).

Based on a simple and unified dynamic frame of the SCS seasonal variability of the upper ocean, the seasonal variations of the Sea Surface Height (SSH) is controlled by the monsoon (Yang et al. 2002) and Luzon Cold Eddy (LCE) characterized by a negative SSH anomaly center associated with strong upwelling by the forcing of positive wind curl to the northwest of the Philippines (Yang and Liu . 2003).

In addition to the sea surface wind forcing, the heat flux is very important for the sea surface temperature (SST) variability in spring and summer (Liu et al. 2002). Through the international collaboration between Chinese and USA Scientists, new climate features have been found in the SCS, including summer cold filament (Xie et al. 2003) and winter cold tongue (Liu et al. 2004). The summer cold filament originates from the open ocean upwelling that helps cool the ocean surface, while the winter cold tongue is attributed to the cold advection of the ocean west boundary current. The Indo-Pacific warm water pool in boreal winter shows a conspicuous gap over the SCS where SST is considerably lower than that of the oceans at the west and east sides, because of the winter cold tongue, which displays considerable interannual variability that is highly correlated with the eastern equatorial SST (Liu et al. 2004). This research first discovered that the west boundary current plays an important role in the SCS climate variability except heat flux and the setting up of the relation between the upper ocean circulation in the SCS, Tropical Pacific and Indian Ocean.

The intraseasonal variations of SST and thermocline in the SCS have been first found and some mechanisms have been described, respectively (Zhou and Gao 2002, Gao and Zhou 2002). Some interesting phenomena and new problems have been found in the SCSMEX, which have been reviewed (Ding et al. 2004). Except some studies about Warm Water (>28℃) in the SCS, the formation and decay of the warm water with SST higher than 30℃ in the upper SCS west of the Philippines is found using a suite of new satellite measurements and the NCEP/NCAR reanalysis data and it is detected that the appearance and rapid expansion of this warm water is related with the SCSSM onset (Jiang et al. 2006).

The South China Sea circulation, in particular, is strongly affected by orographic-induced wind curl; under the northeast monsoon in winter, the wind wake lee of Luzon Island is important for the formation of the Luzon cold eddy (Wang 2004) while in summer, a wind jet observed off Ho Chih Ming city at the southern corner of the Annam range drives a double gyre circulation and an offshore cold upwelling filament (Xie et al. 2003; Wang et al. 2006).

The above researches have shown clearly the response of the SCS to monsoon forcing in winter and summer, but the ocean-atmosphere interaction in synoptic scale is not clear and the

response process and feedback effect of ocean on the monsoon transition have been poorly understood.

3. Ocean-Atmosphere interaction in the Tropical Pacific

The largest source of climate interannual variability is El Nino – Southern Oscillation (ENSO) in the tropical Pacific. Within the past 4 years great progress in the study of ENSO phenomenon and mechanism has been achieved.

Chao (2002), Chao et al.(2003) gradually revealed the propagation path of the sub-surface temperature anomaly signal and its relation with ENSO cycle. Using a coupled ocean-atmosphere general circulation model, Wu et al. (2005a) first described that the tropical north Atlantic SST variability can influence the tropical Pacific through its effect on seasonal migration of the ITCZ and Wind-Evaporation-SST feedback mechanism. Zhao and Yang (2004) used an intermediate tropical atmospheric and oceanic coupled models to study the interaction between the tropical Pacific and the Indian Ocean through the wind-stress ”bridge” and their results suggested a negative feedback role of the tropical Indian Ocean on the tropical Pacific SSTA, which is more obvious on the interdecadal time scale. Ju et al. (2004) have analyzed the variations of the SST of the Indian Ocean and the Pacific Ocean by the EOF method and found a stable pattern with SSTA in the mid-western part of the Indian Ocean and the mid-eastern part of the equatorial Pacific and an inverse case in the western Pacific during the four seasons of the year. They named it as a coupled Pacific-Indian Ocean SSTA mode and defined an index of this mode.

Sun et al (2004) found that direction of EUC (Equatorial Undercurrent) in the Pacific is westwards beginning from the eastern equatorial Pacific in the boreal spring. The meridional cell south of the equator plays an important role in this seasonal change of EUC, and mainly controls the seasonal temperature change in the central Pacific. The meridional cell north of equator is most responsible to the seasonal temperature variations in the eastern equatorial Pacific.

Sun et al. (2006) first point out that the second “baroclinic mode” is halted in the central equatorial Pacific corresponding to a positive SST anomaly while the first “baroclinic mode” propagates eastwards in the eastern equatorial Pacific and describe a new mechanism in the formation of El Ni˜no: the westerly bursts in boreal winter over the western equatorial Pacific generate the halted second “baroclinic mode” in the central equatorial Pacific, leading to the increase of heat content and temperature in the upper layer of the central Pacific which induces the shift of convection from over the western equatorial Pacific to the central equatorial Pacific; another wider, westerly anomaly burst is induced over the western region of convection above the central equatorial Pacific and the westerly anomaly burst generates the first “baroclinic mode” propagating to the eastern equatorial Pacific, resulting in a warm event in the eastern equatorial Pacific. The mechanism presented reveals that the central equatorial Pacific is a key region in detecting the possibility of ENSO by analyzing TAO observation data of ocean currents and temperature in the central equatorial Pacific, in predicting the coming of an El Ni˜no several months ahead (Sun et al.2006).

The above research results showing the ocean dynamic process, such as Kelvin wave Rossby wave and meridional cell are very important in tropical Pacific ocean-atmosphere interaction system.

In the tropical Pacific region, El Niño/Southern Oscillation (ENSO) and the Quasi-Biennial Oscillation in far west equatorial Pacific(QBOWP) are two kinds of the most prominent interannual variation phenomena. The former time scale dependeds on the oceanic wave time

while the latter time scale depended on the coupled feedback between monsoon and SST in the far west equatorial Pacific. In order to understand the interaction between ENSO and QBOWP, a combined ENSO-QBOWP system conceptual model is constructed first by Liu et al. (2006b). It is found that through the interaction between ENSO and QBOWP, a free ENSO oscillation with a period of 3－5 years could be substituted by a oscillation with the quasi-biennial period, and the dominant period of SST anomaly and wind anomaly in the far west equatorial Pacific tends to be prolonged the enhanced ENSO forcing. Generally, the multi-period variability in the coupled Atmosphere-Ocean System in the Tropical Pacific can be achieved through the interaction between ENSO and QBOWP (Liu et al. 2006b)

4. **Ocean-Atmosphere interaction in the Indian Ocean**

In contrast to the Pacific, the variability of the coupled ocean-atmosphere in the Indian Ocean is overwhelmed by monsoon, and it is closely related to the tropical Pacific by Walker Circulation and the Indonesian Through flow (ITF). As the summer monsoon takes a lot of moisture from the Indian Ocean to China and impacts on precipitation in China, more researches about ocean-atmosphere interaction in the Indian Ocean have been achieved during past 4 years.

Zhou and Zhang (2002) found that SSTA was closely related to the net sea surface heat flux in the tropical Indian Ocean, especially in the wintertime in the central-eastern Indian Ocean and in the summertime in the western and northern Indian Ocean. Wang D. et al.(2003) studied the correlation between the upper ocean heat content of the Indian Ocean and the Western Pacific Ocean during the period of El Nino from 1997 to 1998 and found that the anomaly change of the tropical Indian Ocean from 1997 to 1998 was partly influenced by the western Pacific through ITF.

Chao et al. (2003, 2005) showed that there existed a dipole mode on the thermocline in the Indian Ocean, with opposite sign in the eastern and western parts. Qian et al. (2005) suggested that the subsurface temperature anomaly propagating westward in the off-equator region of the Indian Ocean should be one of the pre-signals of the Indian Ocean Dipole (IOD) development. Yu et al. (2005) first pointed out that the atmospheric forcing patterns led to the fact that the oceanic thermocline variations associated with IOD were confined to the region north of 10°S, while the ENSO-induced thermocline variations were dominant in south of 10°S This result means that the thermocline dynamics is different between both sides of 10°S.

Tan et al. (2003, 2004) investigated the interannual variations of the tropical Indian Ocean SST anomaly and its relation with the equatorial mid-eastern Pacific Ocean SSTA. They found that the SSTA in Nino3 region are closely related to the monopole and dipole modes in the tropical Indian Ocean, i.e., the El Nino from its developing phase to its decaying phase corresponds to SST anomaly in the tropical Indian Ocean changing from the dipole mode to the monopole mode. In general, the El Nino lags behind the dipole mode by 4 months and leads the monopole mode by 6 months.

Hu et al. (2005a, b) investigated the mechanism of seasonal and interannual variations of SST in the tropical Indian Ocean, using a new heat budget equation linked to an OGCM (MOM2) with 10-year integration (1987-1996). They point out the time-varying and spatial-varying relative importance on the seasonal and interannual variability of SST. Hu et. al (2005c) also studied the shallow meridional overturning circulation in the northern Indian Ocean and its interannual variability, based on the same model outputs. They first revealed a good relationship between the variability of this shallow meridian circulation and that of surface wind stress and proposed several indices to describe the anomaly of this circulation. The interanuual and decadal variability

of shallow meridian circulation is very important in SST variation.

Liu et al. (2005) investigated the sea level pressure anomalies in the high latitudes of southern hemisphere associated with the IOD. Their results suggest that the IOD signal exist in the high latitudes of southern hemisphere and it should be enhanced in boreal autumn, an active season of IOD.

Li et al. (2005) revealed the features of ISO of the tropical Indian Ocean using the observational data. It is shown that the major period is about 20-30 days at the equatorial region, about 30-50 days at $10^oN/10^oS$ latitudes and 60-90 days at $20^oN/20^oS$ latitudes. The intensity of ISO increases with latitude, but the speed of westward propagation of ISO decreases with latitude. The intensity and propagating speed of ISO have clear interannual variation features. The atmospheric ISO over the tropical Indian Ocean is also very obvious, but it has many different characters to that of oceanic ISO (Li et al., 2005).

5. Ocean-Atmosphere interaction in the extra-tropical North Pacific

The ocean response to stochastic wind forcing is the free Rossby wave, which has been studied by using the TOPEX/POSEIDON (T/P) data. The quasi 90-day oscillation is evident in the zonal belts of about 20ºN and 20ºS, and is more apparent in the western Pacific Ocean of the 20ºN belt. The signal for the quasi 60-day oscillation is distributed in the 10ºN zone. It is weaker in the 20ºS zone than the quasi 90-day signal (Hu and Liu 2002). These oscillations are the oceanic Rossby waves in the Subtropical Countercurrent and in the North Equatorial Current, and the baroclinic stability of the Rossby wave was studied by using a 2.5-layer model (Liu et al. 2003a). The zonal band feature of the space distribution of the free Rossby wave in the global oceans have been discovered by Qiao et al. (2004). Lin et al. (2004, 2005) studied the amplification mechanism of the Rossby wave and its effect on the Kuroshio in the East China Sea.

A unique feature of the coupled ocean-atmosphere system off the tropics has been discovered, which includes a wake extending westward behind the Hawaiian Islands (Liu et al. 2003b). The wind wake drives an eastward oceanic current and draws warm water from the Asian coast, affecting remarkable changes in surface and sub-surface temperatures. Located in the steady trade wind zone, Hawaii triggers a kind of ocean-atmosphere interaction, which provides the feedback to sustain the influence of these small islands over a long stretch of the North Pacific (Liu et al. 2003b). It is particularly interesting because the effects of meteorology, topography and ocean circulation can be seen to interact dynamically in creating this incredibly long wake leeward of the Hawaiian Islands. Following the discovery of the coupled island wake of Hawaii, some similar orographic-induced coupled air-sea phenomena were reported elsewhere including it in the South China Sea (Xie et al. 2003; Wang et al. 2006). All these studies of orographic-induced air-sea interactions were made possible by the advent of all-weather, high-resolution microwave remote sensing of the oceans and atmosphere from satellite in the 1990s.

In the extratropical Pacific, the Ocean plays an important role in seasonal, interannual and decadal-interdecadal variability. The heat advection effect of the West Boundary current is dominant in the heat balance of the upper mixed layer in winter (Liu et al., 2005). Such interannual and decadal-interdecadal variability propagated westward from the central North Pacific. It is found that the thermal anomalies subducted from the central North Pacific to the east of the dateline can only reach 18^oN in the western tropical ocean. There has been no further southward propagation across 18^oN due to a certain barrier (ITCZ). However the origin of the interdecadal oceanic signal in the western tropical Pacific can be traced to the southern tropical Pacific. The oceanic interdecadal variations are mainly confined to the mid-to-high latitudes of

Pacific, the off-equator Pacific and Atlantic (Yang et al. 2005). Zhu et al. (2002) studied the coupled pattern of the middle and low latitude atmosphere/ocean interaction and its decadal variation. They found that the abrupt changes of the coupled system happened in the middle 1970s, with the significant SST increase in the central and eastern tropical Pacific Ocean and decrease in the middle part of the North Pacific Ocean. These research results describes some physical process in ocean controlled by atmosphere. Wu et al. (2005c) studied the coupled ocean-atmosphere system over the western North Pacific, which may regulate global climate in the tropical Indian Ocean, the western subtropical south Pacific and the tropical and North Atlantic through potential atmospheric teleconnections of the Asian winter monsoon and the Arctic Oscillation/North Atlantic Oscillation (AO/NAO). The study suggests that the North Pacific Ocean-atmosphere interaction may be an important regulator of global decadal climate variability.

As a result of air–sea interaction, the Subtropical Mode Water (STMW) often keeps the long memory of the external atmosphere forcing, and the deduction process is the main process of STMW formation. Based on the SODA (Simple Ocean Data Assimilation) and LICOM1.0 (a high-resolution general circulation model), Liu et al. (2006a), Hu et al. (2006) calculated the annual subduction rate in the North Pacific, especially in the three mode water formation areas. They found obvious annual and decadal variations of subduction rate, and the characteristics and the mechanism of the variations are different from each other in the three formation areas.

More details of the inter-decadal variability of the ocean-atmosphere system in the Pacific region can be found in Li et al. (2001a).

By using the AGRO float data of the Kuroshio recirculation area, SST data of TRMM and the SSH data of T/P-ERS, Pan and Liu (2005) analyze the influence of eddies on the mixed layer in winter, which is a good test to prove first how the eddy effects on the ocean stratification.

More recently, Wu et al. (2005b) has proposed a new mechanism for about the middle of the 70s' North Pacific regime shift. Using the "Modeling Surgery" approach, they found that the delayed adjustment of the subtropical North Pacific ocean circulation in response to the wind stress can induce SST changes first in the western subtropical Pacific, and that can subsequently induce a shift of the atmospheric circulation to produce SST in the central Pacific and then in the Kuroshio-Oyashio Extension (KOE) region. This new hypothesis appears to unify the current disputes on the role of ocean circulation and the ocean-atmosphere feedbacks in North Pacific decadal climate changes. Furthermore, Wu et al. (2006) suggests that the extra-tropical North Pacific decadal climate shift can exert significant control over the recent tropical Pacific decadal climate variability through an ocean-atmosphere relay teleconnection.

Based on some correlation analyses of the NCEP data, Zhu and Sun (2006) derived a positive feedback physical process: when there was a deeper Aleutian Low accompanied by a stronger north wind in the western part of the Aleutian low, the subpolar gyre is strengthened. When colder air moved to the south, SST in the region of the Oyashio decreases and meridional SST gradient between the Kuroshio and Oyashio regions increaseds, which will enhance the westerly jet in the upper layer according to the thermal-wind equation.

The other recent researches about heat flux in North Pacific have been reviewed in the paper (Pu et al. 2004). For Ocean-Atmosphere interaction in the extra-tropical North Pacific, the most difficult problem is to found out when and where the ocean anomaly can impact on atmosphere by feedback mechanism. Recently Liu et al.(2006c) first showed that there was a very close statistic relation between summer atmosphere and the preceding winter SST over the North Pacific. Based on their statistic analysis a "horseshoe" SSTA in winter, with a positive SSTA loading over the

central-western North Pacific surrounded by a negative SSTA, appears to persist into the spring and summer, eventually could lead to an atmospheric response in summer with a wave-train over the mid-latitude North Pacific(Liu et al. 2006c). But It is still not clear why there is the close statistic relation.

6. Summary

During the past 4 years, studies of the Ocean-Atmosphere interaction in China have been developed unprecedentedly, and a lot of important achievements have been made. Some achievements play important roles in understanding the climate variability and the physical mechanism of the interaction. In the SCS, the theories of monsoon oceanography have been developed. The main dynamic mechanisms of ENSO have been understood, knowledge about the interaction between the Monsoon and ENSO has been accumulated. Some features of the SST and the current in the Indian Ocean have been discovered. Although Chinese scientists have made great progress in almost all aspects of this research field, there are still some important problems left for future study, especially in observational and coupled numerical model research.

Acknowledgement: The authors take this chance to thank Dr. Wu Lixin , Dr. Wang Fan and Dr. Yu Weidong for their kindly providing of the relevant information. This paper is supported by the NSFC 40333030.

References

Chao Jiping, 2002: ENSO: the harmonic Ocean-atmosphere interaction in tropics. *Advance in Marine Science*, 20(3), 1-8

Chao Jiping., Yuan Shaoyu, Chao Qingchen, and Tian Jiwei, 2003: The origin of warm water mass in “warm pool” subsurface of the western tropical pacific-the analysis of the 1997~1998 El Nino. *Chinese J. Atmos. Sci*, 27(2), 145-151(in Chinese).

Chao Jiping and Yuan Shaoyu, 2003: Relationship of air-sea interaction in the tropical Pacific and Indian Ocean. *Progress in Natural Science*, 13(12), 1280-1285 (in Chinese)

Chao Jiping and Liu Lin, 2005: The ENSO events in the tropical pacific and dipole events in the Indian Ocean. *Acta Meteor. Sinica*, 594-602 (in Chinese).

Ding Yihui, Li Chongyin and Liu Yanju, 2004: Overview of the South China Sea Monsoon Experiment. *Advances in Atmospheric Science*, 21(3) 343-360.

Gao Rongzhen and Zhou Faxiu, 2002: Monsoonal Characteristic revealed by intraseasonal variability of sea surface temperature, *Geophysical Research. Letter,*29(8), 10.1029/2001GL014225.

Hu Haibo, Liu Qinyu and Liu Wei, 2006: Interannual and decadal variation of the seduction rate in the Subtropical Mode Water formation regions in the North Pacific. *Acta Oceanologica Sinica*, 28 (2), 22-28 (in Chinese).

Hu Ruijin and Liu Qinyu, 2002: Annual and interannual variations in sea surface height over the tropical Pacific. *Oceanologoa et Limnologia Sinica*, 33（3），303－313.

Hu Ruijin., Liu Qingyu., Meng Xingfeng and J.S. Godfrey, 2005a: On the mechanism of the seasonal variability of SST in the Tropical Indian Ocean. *Advances in Atmospheric Science*, 22(3), 451-462.

Hu Ruijin and Liu Qinyu, 2005b. A heat budget study on the mechanism of SST variations in the Indian Ocean dipole regions. *Journal of Ocean University of China*, 4(4), 334-342.

Hu Ruijin., Liu Qinyu., Wang Qi., J. S. Godfrey and Meng Xiangfeng, 2005c: The shallow meridianal overturning circulation in the northern Indian Ocean and its interannual variability. *Advances in Atmospheric Science*, 22(2), 220-229.

Jiang Xia, Liu Qinyu, Wang Qi, 2006, Effects of Warm Water West of the Philippines on the South China Sea

Summer Monsoon Onset, *Periodical of Ocean University of China*, **26(3) 349-355. (in Chinese)**

Ju Jianhua., Chen Linling, and Li Chongyin, 2004: The preliminary research of Pacific-Indian Ocean sea surface temperature anomaly mode and the defintion of its index. *J. Tropical Meteorology,* 20(6): 617-624(in Chinese).

Li Chongyin, Hu Ruijin and Yang Hui, 2005: Intraseasonal oscillation in the tropical Indian Ocean. *Advances in Atmospheric Science*, 22 (5), 617-624.

Lin Xiaopei, Wu Dexing and Lan Jan, 2004: The intrusion and influences of intraseasonal long Rossby waves in the East China Sea. *Journal of Hydrodynamics*, 16,621-632.

Lin Xiaopei, Wu Dexing, Li Qiang and Lan Jian. 2005: An Amplification Mechanism of Intraseasonal Long Rossby Wave in Subtropical Ocean. *Journal of Oceanography*, 61, 369-378.

Liu Qinyu，Wang Dongxiao，Jia Yinglai，Yang Haijun，Sun Jilin and Du Yan, 2002: Seasonal variation and formation mechanism of the South China Sea warm water. *Acta oceanologica Sinica*，VOL.21，NO.3，331-343

Liu Qinyu, Pan Aaijun and Liu Zhengyu, 2003a: Intraseasonal Oscillation and baroclinic instability of upper layer ocean in North Equatoral Current of Pacific. *Joumal of Oceanology and Limnology*, 34(1), 94-100 (in Chinese).

Liu Q., S. Wang, Q. Wang and W. Wang, 2003b: On the Formation of Subtropical Countercurrent in the west to Hawaiian Islands. *J. Geophys．Res．* 108, C5, 3167~3175

Liu, Q., X. Jiang, S.-P. Xie and W. T. Liu, 2004: A gap in the Indo-Pacific warm pool over the South China Sea in boreal winter: Seasonal development and interannual variability. *J. Geophys. Res.*, 109, C07012, doi:10.1029/2003JC002179.

Liu Q.，S.-P. Xie，L. Li，and Nikolai A. Maximenko, 2005: Ocean Thermal Advective Effect on the Annual Range of Sea Surface Temperature. *Geophysical Research Letters*，32, L24604.

Liu Qinyu, Hu Haibo and Liu Wei, 2006a: Effect of Sea Surface Wind on Subduction Rate and its variability in North Pacific. *Oceanologoa et Limnologia Sinica*,.37(2),184-192 (in Chinese)

Liu Q Y, Liu Z Y and Pan A J, 2006b, Conceptual model about the interaction between El Niño/Southern Oscillation and Quasi-Biennial Oscillation in far west equatorial Pacific, Science in China Series D-Earth Sciences, Vol.49 No. 8 889-896

Liu Qinyu, Wen Na and Zhengyu Liu, 2006c, An observational study of the impact of the North Pacific SST on the atmosphere, *Geophys. Res. Lett* 33(18), 2006GL026082 (in Press)

Pan Aijun and Liu Qinyu，2005: Mesoscale eddy effects on the wintertime vertical mixing in the formation region of the North Pacific Subtropical Mode Water. *Chinese Science Bulletin*，50（17），P.1949-1956

Pu Suzheng. Zhao Jingping, Yu Weidong, Zhao Yongping. and Yang Bo, 2004: Progress of Large-Scale Air-Sea Interaction Studies in China. *Advances in Atmospheric Sciences*, 21, 383 – 398.

Qiao Fangli, Tal Ezer and Yeli Yuan, 2004: On the zonal structure of high freguency oscillations in the global ocean derived from altimeter data. *Acta Oceanologica Sinica*, 23 (1) 91-96

Qian Weihong and Hu Haoran, 2005: Propagate and correlation of the subsurface sea temperature anomaly signals between the tropical Pacific and Indian Ocean. *Progress in Natural Science*, 15(5), 957-963. (in Chinese)

Su Jilan, 2005: Overview of the South China Sea circulation and its dynamics. *Acta Oceanologica Sinic*,27 (6) ,1-8 (in Chinese)

Sun Jilin, Peter Chu and Qinyu Liu, The seasonal variation of undercurrent and temperature in the Equatorial Pacific jointly derived from buoy measurement and assimilation analysis。2004, Acta Oceanologica Sinica. No.1, 51 – 60

Sun Jilin Chu Pete and Liu Qinyu,2006, The role of the halted baroclinic mode in the central equatorial Pacific in

an El Nino event, 2006, Advances In Atmospheric Sciences. Vol. 23, No. 1.45-53

Tan Yanke, Zhang Renhe and He Jinhai, 2003: Features of the interannual variation of sea surface temperature anomalies and the air-sea interaction in tropical Indian Ocean. *Chinese J. Atmos. Sci*., 27 (1), 53-66. (in Chinese)

Tan Yanke, Zhang Renhe and He Jinhai, 2004: Relationship of the Interannual variations of sea surface temperature in tropical Indian Ocean to ENSO. *Chinese J. Atmos. Sci*., 62(6), 831-840 (in Chinese).

Wang Dongxiao, Xie Qiang, Du Yan, Wang Weiqiang and Chen Ju, 2002: 1997/1998 Warm Event in the South China Sea. *Chinese Science Bulletin*，47（14）.

Wang, Dongxiao, Weiqiang Wang, Ping Shi, Peifang Guo and Zijun Gan, 2003: Establishment and adjustment of monsoon-driven circulation in the South China Sea. *Science in China* (Ser. D), 46(2), 173-181.

Wang, G, D. Chen, and J. Su, 2006: Generation and Life Cycle of the Dipole in the South China Sea Summer Circulation. *J. Geophys. Res.*, doi: 10.1029/2005JC003314

Wang Shaowu, Zhu Jinhong, Cai Jingning and Wen Xinyu, 2003: Irregularities in ENSO variability. *Acta Scientiarum Naturalium Universitatis Pekinensis*, 39,125-133

Wu, L., F. He, and Z. Liu, 2005a: Coupled ocean-atmosphere response to north tropical Atlantic SST: Tropical Atlantic dipole and ENSO. *Geophys. Res. Lett.*, 32, L21712, doi:10.1029/2005GL024222

Wu，L., D. Lee and Z. Liu. 2005b: The 1976/77 North Pacific Climate Regime Shift: The Role of Subtropical Ocean Adjustment and Coupled Ocean-Atmosphere Feedbacks. *J. Climat*e, 18, 5125-5140

Wu, L., Z. Liu, Y. Liu, Q. Liu, and X. Liu, 2005c: Potential global climatic impacts of the North Pacific Ocean. *Geophys. Res. Lett.*, 32, L24710, doi:10.1029/2005GL024812

Wu Shu, Liu Qinyu and Hu Ruijin, 2005: The main coupled mode of SSW and SST in the tropical Pacific-South China Sea-Tropical Indian Ocean on interannual time scale. *Periodical J. of Ocean University of China*, 35(4),521-526. (in Chinese)

Xie, S.-P., Q. Xie, D. Wang and W. T. Liu, 2003: Summer upwelling in the South China Sea and its role in regional climate variations. *J. Geophys. Res.*, 108(C8), 3261, doi:10.1029/2003JC001867

Xie, S.-P., H. Xu, W.S. Kessler, and M. Nonaka, 2005: Air-sea interaction over the eastern Pacific warm pool: Gap winds, thermocline dome, and atmospheric convection. *J. Climate*, 18, 5-25.

Yang Haijin, Qinyu Liu, Zhengyu Liu, Dongxiao Wang and Xiongbin Liu，2002: A general circulation model study of the dynamics of the upper ocean circulation of the South China Sea．*J. of Geophysical Research*，107(C7)，10．1029－1043．

Yang Haijun and Qinyu Liu, 2003: Forced Rossby wave in the northern South China Sea, *Deep Sea Research I* 50 , 917-926.

Yang, H., Q. Zhang, Y. Zhong, S. Vavrus, and Z. Liu, 2005: How does Extratropical Warming Affect ENSO. *Geophys. Res. Lett.*, 32, L01702, doi: 10.1029/2004GL021624

Yu Weidong and Chao Jiping, 2004: Analysis on the ocean-atmosphere interaction during ENSO cycle ---- the interannual variations of the rotational and divergent components of the atmosphere circulation. *Adv. Nat. Sci.*, Vol.14 (No.8) 917-924 (in Chinese).

Yu W., B. Xiang, L. Liu and N. Liu, 2005: Understanding the origins of interannual thermocline variations in the tropical Indian Ocean, *Geophy. Research Letter* VOL. 32, L24706, doi:10.1029/2005GL024327,

Zhao Shanshan and Yang Xiuqun, 2004: Numerical experiment on interaction between the tropical Pacific and the Indian Ocean through the wind-stress "bridge". *Acta Oeanologica Sinica*,26(4),33-48.(in Chinese)

Zhou Tianjun and Zhang Xuehong, 2002: The air-sea heat exchange in the Indian Ocean. *Chinese J. Atmos. Sci.*,

26(2), 161-170. (in Chinese)

Zhou Faxiu and Gao Rongzhen, 2002: Intraseasonal variability of the South China Sea, *Chinese Science Bulletin*, 47, 337-342.

Zhu X. J. and Sun Jilin, 2006, Positive feedback of winter ocean-atmosphere interaction in Northwest Pacific). 2006, *Chinese Science Bulletin* 51(9), 1097-1102 (in chinese)

ADVANCES IN TIDE AND SEA LEVEL RESEARCH IN CHINA FROM 2002 TO 2006

ZUO Juncheng[1], *DU Ling*[2], *LI Lei*[2] *and LI Peiliang*[2]

[1] College of Oceanography, Hohai University, Nanjing, 210098, P.R.China

[2] Department of Oceanography, Ocean University of China, Qingdao, 266100, P.R.China

ABSTRACT

The ocean tide is considerably prominent phenomenon in the China Seas, which mostly appears on the continental shelf, and as a result it is one of the focuses of physical oceanography community in China. Sea level variation is an important component of global change with significant application value. In this paper, the latest development of the research in tide and sea level variation in the last 4 years in China is reviewed comprehensively. Numerical assimilation which is applied to tidal wave simulation gives more precise solutions in regional tide wave. The study on internal tide, internal wave, tidal mixing and tidal front also made some progress in the last several years and particularly, tidal mixing is becoming an important scientific issue in tide research. Meanwhile, loading tide was also studied, ocean tide is a kind of loading in the earth gravitational field, which should be modified in the research of earth gravitational field of high precision.

Both the trends of global and regional sea level and the spatial distribution of steric effect on different time scale were studied. The influence of sea level variation on tide wave in continental shelf was simulated, and the effect of seasonal and long term variability of sea level on the calculation of engineering water level was analyzed.

KEY WORDS: tide, sea level, steric effect

Ⅰ. INTRODUCTION

1. Tide

Tide research is an important part in physical oceanography study. As tide is one of the fundamental motions in the ocean, especially in continental shelf, tide is an important component of dynamic oceanography, and the research on tide has direct effect on the research of many oceanographic issues such as ocean circulation, storm surge, wave, water mass, material transport and water exchange, etc. From the TOPEX/Poseidon altimetry data, a steady sea level was obtained through a series of geophysical and physical modification in which the contribution of ocean tide can be up to 82% (Ray et al., 1994). Tidal wave on continent shelf is the dominant part in the whole water motion.

Ocean tide plays an important role in geophysics and geodesy. The westward propagation of tidal wave and energy dissipation caused by friction decelerate the rotation of the earth. Based on the TOPEX/Poseidon data, the global tidal models suggested that the ocean tides dissipate the energy of 3.5*TW* (1*TW*=1×10^{12}*W*, Kantha, 1998), which is generated by the tide generating force in the earth-moon system, and as a result, the earth rotation slow down and day be longer. The

deformation of the earth caused by the load of ocean tide affects the measurement and analysis of earth tide and the earth's crust structure calculated from Love's number. The other related geophysical issues include flexible earth deformation caused by ocean tide load and the variation of moon orbit induced by tidal friction. The earth deformation caused by the ocean tidal load is one of the major problems in geodesy. Xu (1988) studied the influence of global ocean tide on coastal measurement, which can reach 80% of the total earth tide, and discussed the effect of the coastal ocean tide in the China Seas when he calculated the correction of ocean load tide. Computation of the deformation caused by ocean tidal load needs a high-precision ocean tidal model.

Tide is one of the most prominent phenomena in the coastal region and estuary, and it has important effect on production and life activities such as agricultural drainage and irrigation, fishery and aquiculture in the coastal area and navigation, port construction, transportation and oil and gas exploitation. Tide research also has a considerable importance of economy and military. Tidal wave and the induced internal tide and internal waves can greatly affect the activity of submarine.

2 Sea Level Variation

As the impact of activities of human beings on the earth system is extending quickly, sea level rise has become one of the greatest global environment problems.

As sea level rises, most of the sedimentary coast is confronted with serious erosion, and coastal people have to deal with the ensuing coastal management. The most vulnerable regions are the low arenaceous or slimy coasts, where a little sea level rise can submerge large quantity of land and intensify seawater erosion, such as the Bohai Bay，the Yellow River Delta, the Changjiang River Delta and the Pearl River Delta in China.

Global, regional and local factors affect sea level variation together. Global mean sea level variation is mainly caused by the thermal expansion of the ocean, the melting and vanishing of the mountain glacier, and variation of ice sheet volume in Greenland and Antarctica. In some cases, regional and local factors like vertical movement of the earth crust and drainage of the surface water may induce a greater sea level change with a rate of 10 or 100 times larger than the current evaluated one.

Furthermore, some new methods and research fields are developed and a lot of achievements of tide and sea level are gained in the last 4 years.

Ⅱ. SUMMARY OF THE TIDE RESEARCH

1 Analysis and Computation of Ocean Tides

Fang Guohong developed a method of 'Quasi-harmonic Constituent' to analyse the short-term data in 1960 (Fang, 1974, 1976, 1981). A nodal tide and perigee tide correction (j,v) model for tide analysis was given in 1990 (Chen,1990). Huang (Huang et al., 1997) analyzed the data of 19 years at several stations, and discussed the stability of tidal analysis caused by astronomical, nonlinear, topographic factors and so on. The tidal harmonic analysis method on the

basis of the high and low water level data was introduced by Li et al. (2004).

2 Numerical Simulation of Tidal Wave

The tidal wave numerical model includes mainly two types, two and three dimension, which can conduct the simple and complex physical processes respectively. Most of the early numerical models are two-dimensional, because the tidal motion is mainly barotropic, whose process can be simulated by the two-dimensional model. However, in many applications (such as coastal engineering), the three-dimensional model is necessary to meet the need for the vertical structure of tidal current. Running the there-dimensional model needs longer computation time but give more accurate spatial structure of tidal currents and tidal waves. So the three-dimensional model dominates the simulation at present (Sha, 2000).

There have been many numerical simulation results in the Bohai Sea, the Yellow Sea and the East China Sea (Zhao et al., 1994; Ye and Mei, 1995; Wan et al., 1998; Wang et al., 1999; Lin et al., 2000; Fang et al., 2000; Bao et al., 2001; and Li et al., 2003).

Li et al. (2003) used a 3-dimensional finite element model (QUODDY) in Cartesian coordinate to study the tidal waves in the Bohai Sea, the Yellow Sea, and the East China Sea. The co-tidal charts of the five major constituents, M_2, S_2, K_1, O_1 and M_4, are presented, which show that the phase-lag of M_2varies little in the Laizhou Bay, there exists an area with a large amplitude of M_4 near 32.8°N, 124.8°E; it is found that the amphidromic point of M_2 tidal wave in the Liaodong Bay vanishes when drag coefficient of the bottom stress increases to 0.0028. Li et al. (2005) simulated the semi-diurnal constituents with the TOPEX/Poseidon assimilation data.

Lin et al. (2000, 2001) solved the linear shallow-water equation with a two-dimensional finite element model, in which the rotary effect of the earth was ignored and the non-reflect condition at open boundary was used. Their results agree well with the observed data, and show that the reason, why the amplitude of semi-diurnal constituents is amplified in the west bank of the Taiwan Strait, is mainly due to resonance, while the bottom topography and water depth play an important role on tidal propagation. Wang et al. (2003) analyzed the mounted-ADCP data from 1999 to 2001 and obtained the characteristics of tidal currents in the Taiwan Strait with the spatial least square method, based on the tidal model in which the open boundary water level at the north and south sides of the strait is used as the equation constraint. Sen et al. (2002, 2004) developed a three-dimensional shallow-water model of high resolution with the initial condition at the two open boundaries being taken as the tidal water level, which is obtained by the four-dimensional variational assimilation method, and the sensitivity of the vertical structure of tidal current to bottom friction coefficients was discussed in detail. Du et al. (2005) simulated the tidal waves in the Taiwan Strait by a finite element model, which showed that the diurnal tidal wave mainly propagated southward, which was different from that of the semi-diurnal tidal wave. There was a southward Kelvin wave in the west of Taiwan Strait, and a stand wave in the east of the Strait, which disappeared quickly around the shoal south of the strait.

3 Tide Retrieval from TOPEX/Poseidon Altimeter Data

The harmonic constants of 12 constituents are obtained from the TOPEX/Poseidon altimeter data during 1993-1999. The results agree well with the observed data, but there are large deviations in the coastal area because of the error in satellite altimeter data in this area (Dong et al., 2002).

The orthogonalized convolution method was used to analyze the TOPEX/Poseidon satellite altimeter data in the South China Sea (Li et al. 2002), which are more accurate than that of Mazzega and Bergé(1994).

4 Assimilation Method

Open boundary condition and bottom friction coefficient are two important factors affecting tide and tidal current simulation. The precision of tide and tidal current simulations will be improved if the open boundary condition and bottom friction coefficient are optimized well. By using the adjoint assimilation method developed in the recent years, this problem was been resolved successfully. The main approach is to solve an equation of minimum restriction. The model is converted to a dynamical restriction so as to make the observation and simulation results agree well in some sense (usually the least square method). It is essentially an inverse problem of the differential equation.

In the past ten years, a lot of work has been done in simulating tide and tidal current with adjoint assimilation method. Zhu (1997) estimated the open boundary conditions in the coastal model by using tide gauge data. Han et al. (2001) assimilated the TOPEX/POSEIDON data into the tidal model using the adjoint assimilation method, and simulated the M_2 tidal constituent in the Yellow Sea and the East China Sea.

A lot of researches about tidal waves in the East China Sea have been done. The open boundary condition in the Bohai Sea is retrieved from the harmonic tidal constants at 19 tide gauges in the Bohai Sea with the adjoint method, in order to simulate the tidal waves in the Bohai Sea (Lv and Fang, 2002). The TOPEX/Poseidon altimeter data were assimilated by the adjoint assimilation method to simulate four main tidal constituents in the Yellow Sea and Bohai Sea (Qiu et al., 2005). Li et al. (2005) simulated the distribution of semi-diurnal tide constituents in the Bohai Sea, the Yellow Sea and East China Sea by assimilating the TOPEX/Poseidon altimeter data. The precisions of these results are more satisfactory than that of the former published numerical models.

There are also some researches on tidal simulation in the South China Sea by using assimilation method. Wu et al. (2003b) assimilated the TOPEX/Poseidon altimeter data (248 periods lasting 6 years) in the South China Sea into a tidal model with the adjoint method, the optimal open boundary conditions and the bottom friction coefficient were given, the similar research was also done for the simulation of tidal waves in the Beibu Gulf (Wu et al., 2003a).

5 Internal tide and Internal Wave

By underlying the ADCP data of two and a half months, Zhang et al. (2005) discussed the

characteristics of the barotropic tide, internal tide and the wind-driven inertial internal waves in the upper 450m of the northern South China Sea. The amplitude of the internal tidal current varies considerably spatially, and decreases with depth. The contribution of the near-inertial motion to the barotropic current is very small, but the amplitude of the near-inertial baroclinic current is large. The internal tide energy propagates from the deeper layer to the surface, but the energy of the near-inertial internal wave propagates from the sea surface to the deeper layer.

6 Tide Mixing and Tidal Front

Simpson (1974) first put forward the parameterization method of stratification caused by tidal mixing, and after that many researchers discussed the distribution of tidal front and its variations by this parameterization method.

Li et al. (2005) discussed the tidal energy fluxes and dissipation in the Bohai Sea, the Yellow Sea and the East China Sea. The M_2 tidal energy in the Bohai Sea, the Yellow Sea and East China Sea is 122. 5GW coming from the Pacific Ocean, which accounts for 79% of the total energy of the four major constituents. Most of the tidal energy of semidiurnal constituents is dissipated in the Yellow Sea, while that of diurnal constituents is dissipated mostly in the East China Sea. A part of the diurnal tidal energy coming from the Pacific Ocean spreads west-southward along the Tokara Strait because of the block of continental slope, and the another part tracks back to the Pacific Ocean, in which 44 % of the total O_1 tidal energy entering from the Pacific Ocean at his section east off Taiwan is reflected back into the Pacific Ocean.

There are some reports and researches on the tidal fronts (Zhao, 1987; Huang et al., 1996). Zhao (1987) showed some tidal fronts in the Bohai Strait and the Yellow Sea. Huang et al. (1996) also pointed out some tidal fronts in the Bohai Sea through the numerical simulation. A numerical study of circulation in summer in the Yellow Sea shows the upwelling appearing near a tidal front (Liu, 2003).

7 Interactions among Tide，Storm Surge, Wave, Run-Off and Other Ocean Factors

By using a coupled high resolution numerical model consisting of the nonlinear interaction among wave, tide, and storm surge, it is shown that, the coupled model including radiation stress gave the results closer to the observation (Lin et al., 2002). The thermocline in the Bohai Sea is influenced largely by tidal waves.

Ou and Yang (2004) discussed the interaction between the run-off and the tidal currents in the river-net area of the Pearl River Delta and concluded that the water level contained some typical tidal periods as semidiurnal, diurnal and semi-monthly periods, and the runoff period. The negative correlation between tidal amplitude and river discharges is significant, the more the river discharge the less the tidal range. It is indicated that the tidal effect decreases rapidly up the river because of the dissipation of tidal energy for overcoming the resistance of river discharge.

8 Loading Tides and its Influence on the Gravitational Field

The effect of Ocean tide on the earth gravitational field can be recognized as a load on the earth surface. The loading effect of ocean tide on the gravitational field must be taken into account

in the high resolution numerical model of gravity field because it may be over than μgal at some islands in the ocean or coastal stations. Zhang et al. (2004) studied the influences of loading tide on the gravitational field theoretically. He did not use the spherical function to develop the density field, but introduced the potential of ocean loading tide into the gravitational field model directly.

Sun et al. (2005) calculated the gravitational loading effect using the loading theory and a numerical integral convolution technique, which was based on several global ocean tidal models with the altimetry data, tide gauge data and finite element method, and carried out the loading corrections to tidal gravity parameters in diurnal and semidiurnal frequency.

Ⅲ. MEAN SEA LEVEL (MSL) VARIATION

The recent studies on the MSL variations in China pay much attention to the causes and mechanism of global and regional sea level variations, meanwhile the study of the steric and dynamic effect on sea level variations are also carried out.

Yu (2004) reviewed the recent development on studying the MSL variations in the coastal areas of the China Seas and summarized the causes of the MSL variations, the development of the investigation technique, the analysis methods, and the representative studies on the MSL rise.

1 Global and Regional Sea Level Rise

Shen et al. (2003) analyzed the TOPEX/Poseidon altimeter data during 1993-2001 and found that global MSL showed a distinct trend of rise with a velocity of +1.2mm/a. Sea temperature variation plays an important role on the global MSL variation, but its contribution to the global MSL rise is less than 50%. The spatial distribution of sea level variation is mainly affected by the wind stress anomaly, especially the zonal wind stress anomaly.

Jiao et al. (2004) used the tide gauge data and the high precision GPS to monitor the absolute sea level change and obtained the rate of vertical land movements from GPS data at 3 tide gauge stations.

Zhong (2003) built a chronology of the eustatic sea level variations for the past 42 million years, and established a link between the interface of layers of continental margins and the eustatic sea level descent by analyzing the collected data from more than 10 legs of ocean drillings, and made a better estimation of the amplitudes of sea level changes. However, there are fundamental uncertainties in the rates, amplitudes, and mechanisms for the eustatic sea level change and its stratigraphic response.

2 Sea Level Variation

Hu and Liu (2002) analyzed the sea surface height data in the tropical Pacific Ocean and pointed out that there were variations with periods of one year, 58-139 days and 29-35 days. An annual variation appeared in 0°-15°N, 135°E-95°W, but there was no obvious propagation. The oscillation with the period of 58-139 days is remarkable in two subtropical regions with its central latitude of 20°N and 20°S, it propagated westward with the wave speed decreasing with latitude. The wave speed and wavelength in 20°N are around 10cm/s and 800km, respectively. The oscillation of 90 days or so reveals an annual variability and has a good correlation with ENSO.

The variation of 29-35 days appears mainly in two latitude bands in the central and eastern Pacific centered at 5°N and 5°S, without the obvious propagation.

Zuo et al. (2005) analyzed the sea level variations in the Bering Sea and found that there was a trend of sea level rise of about -2.47mm/yr during 1992-2002, and the MSL descend in the central basin and the northeast part of the Bering Sea. During the 1998/1999 El Niño event, the sea level exhibits a significant descent in the deep basin where the SST falls in the same location. The maximal MSL descent is about 10cm in the southwestern part of the Bering Sea, where the maximal SST falls of about 2℃. His results also show that the seasonal amplitude of the steric height is about 35% of the observed TOPEX/Poseidon amplitude, which is much smaller than the 83% in the mid-latitude (Zuo et al., submitted). The TOPEX/Poseidon data varies with a range of about 7.5cm and the thermal contribution with a range of about 2.5cm, whose systematic difference is about 5cm. This indicates that the thermal effect on the sea level is not as important as the case in the mid-latitude area. In the Bering Sea, the phase of the thermosteric height leads the observed sea level by about 3 months (Zuo et al., 2005).

There exists a strong seasonal sea level variation, especially in the northern hemisphere. In the mid-latitude region near 30°N-50°N, a typical range of the seasonal variations is about 10 cm, while in the southern mid-latitude region near 20°S-50°S, it is only about 5cm.

An analysis from the TOPEX/Poseidon data shows that the region of the extreme sea-level rise exists in the western tropic Pacific, where the warm pool locates. Another region of the extreme sea-level rise with a rate of 30mm/a situated near 30°N from the east of Japan to 220ºE. The sea-level in the eastern Pacific descend at a rate of -20mm/a. Another descending region is located in the northwest of the Indian Ocean with a rate of -10mm/a. The sea-level in the rest region of the Indian Ocean almost rises with a rate of 5mm/a. In the Atlantic Ocean, the sea-level in the latitude zone of 0ºS-50ºS decreases at a rate of -2mm/a and rises at a rate of 5mm/a in the rest part. The global-averaged MSL rises at a rate of 2.2mm/a.

3 Cause of Sea-level Variation

Yang et al. (2004) analyzed the sea surface height anomaly (SSHA) data in the China Seas. The five typical areas, the Bohai Sea, the Luzon Strait and its adjacent seas, the Yellow Sea, the East China Sea, and the northern South China Sea, were chosen carefully for calculating the anomaly index. The correlation analysis was carried out among SSHA, SST and wind-speed. Their results show that the positive correlation between the anomaly index and wind speed appears mainly in the low-middle latitude region of the west Pacific Ocean, and the negative correlation areas are in the South Asia and the northern India Ocean. The positive correlation between SST and SSHA appears in the south of Africa mainland, the south of America mainland and the south of Australia. The negative areas are mainly in the eastern Pacific and northern India Ocean.

The seasonal steric sea-level variation accounts for about 86% of the total sea-level variation in the mid-latitude area in the northern hemisphere, and 73% in the mid-latitude area in the southern hemisphere. The systematic difference between the observed TOPEX/Poseidon

amplitude and the steric sea-level is about 1-2cm. The cause for the difference might include: the deviations in the estimate of the water exchange among atmosphere, land and ocean, the steric sea-level, and the inaccurate physical correction which is applied to the TOPEX/Poseidon data.

The steric sea-level variation and the TOPEX/Poseidon altimeter data are out of phase. In the high-latitude area of 50°~60°N or 50°~60°S, the phase of steric height leads the TOPEX/Poseidon sea level by about 4 months. In the middle-latitude area, they are basically in phase. In the equator area and the Antarctic circumpolar current area, they aren't uniform, and their phase relations aren't regular either (Zuo et al., submitted).

4 Sea-level Effect on the Calculation of Engineering Water Level

The long-term and seasonal variations of sea level have some effects on the calculation of engineering water level.

Zuo et al. (2001) pointed out that the seasonal and long-term sea level variations had a notable effect on the calculation of engineering water level in the China Seas. The maximal amplitude of inter-annual anomaly of the monthly MSL along the China coast is larger than 60 cm. Both storm surges and cold waves often cause the main seasonal disasters in some regions, so the water level is expected to be designed with its seasonal variations. For example, the difference between them reaches maximum in June, July and August for the northern part of the China Seas, and maximum in September, October and November for the southern part of the China Seas. Two kinds of the distributions corresponding to the astronomical tide and storm surge are obtained according to whether the astronomical tide and storm surge correlate or not. The maximal difference between the two water levels is more than 30 cm. Both of the two check water levels have disadvantages in the use of observation data, so the mean value is supposed as the final check water level. A comparison between the check water levels indicates that the effect of the sea level variations upon the design water level and the check water level is larger than 80 cm at some stations.

Yu and Yu (2003a) discussed the effect of long-term MSL variations on the calculation of the extreme water levels of multiyear return periods by using 24 years' data of the yearly extreme high (low) water levels and yearly MSLs at station Rushan. The extreme high water levels of multiyear return periods calculated from the original data is larger than that calculated from the data of which the long-term sea level had been removed, and vice versa for the extreme low water levels. Du (2005) studied the effect of sea level rise on the calculation of engineering water levels in the Jiaozhou bay by a finite element numerical model.

5 Effect of Sea Level Variation upon Tide

Yu et al.(2003b) first studied the effect of long-term sea level variation on the tidal wave propagation in the East China Sea by using the numerical model and the data analysis in detail. The variation of bottom friction and lateral friction in shallow sea caused by MSL variation results in the change of tidal wave propagation, the tidal amplitude variation and the amphidromic point movement to some extent. Generally, the tidal amplitude increases when the mean sea level rises,

but this relationship may inverse for some sea areas. The maximal variation of tidal amplitude takes place in the zones near the Fujian and the Zhejiang coast, rather than the shallowest Bohai Sea. The maximum increase of M_2 amplitude can exceed about 15cm corresponding to the 60cm rise of the mean sea level along the Fujian coast. The other regions with large variations of tidal amplitude are those along the Jiangsu coast, the southeast coast of Shandong, and the southeast coast of Dalian. The propagation of tidal waves is also related to the mean sea level variation, and the tidal phase-lag decreases generally when the mean sea level rises. The tidal phase-lag increases with the rising mean sea level are almost near the amphidromic points, whose area is limited.

6 Effect of Sea Level Rise upon Circulation and Saltwater Intrusion in Estuary

The land-ward density-induced current around the channel mouth increases with sea level rising, the stagnation point moves up stream, and the speed of offshore current becomes larger in the surface layer. The salinity intrusion increases within the river mouth, and the area of the diluted water reduces outside the mouth. Sea level rise has an obvious impact on the salinity intrusion, especially in the bottom layer (Hu et al, 2003).

7 Effect of Sea Level Variation upon the Estuarine Turbidity Maximum Zone

The effect of sea level variation upon the estuarine turbidity maximum zone has been analyzed by Zhu et al. (2004). The estuarine turbidity maximum zone locates around the stagnation point. The residual currents both from the upper-stream and the down-stream in the low layers convey sediments to the stagnation point, so as to induce the convergence of sediments, and the upwelling induced by the convergence makes sediment difficult to settle down near the stagnation point. In the case of sea level rise, the land-ward density-induced currents near the channel mouth bar increase, and the stagnation point moves upstream, which makes the turbidity maximum zone move upstream. The sand concentration in the turbidity maximum zone tends to be higher, but the sand concentration in the channel mouth bar tends to be lower. The variations of river discharge and sea level have obvious impact on the turbidity maximum zone.

8 Measures to Prevent the Effect of Sea Level Rise along the Coast of China

In the 21st century, sea level rise will speed up, which will make it heavier for the land submergence, storm surge and flooding disasters, shortage of water resources along the coast of China (Wu et al., 2002). Cui (2005) used Geographical Information System to evaluate the risk of the sea level rise in the Liao River Delta. The risk assessment model includes several factors as the hazards of sea level rise, vulnerability of land system, socio-economic and ecological vulnerability, and the capability of precautions against the hazards. The risk assessment pattern of sea level rise in city Panjin was drawn by the above model.

IV. CONCLUSION

The China seas are one of the prominent tidal regions along the continent shelf in the world, which is studied comprehensively by the physical oceanographers in China. As an important part of global change, the sea level variation is a significant contributor in the global ocean circulation evolvement affected by climate change.

In the last 4 years, Chinese physical oceanographers focus on the tidal waves by the numerical simulation, with a series of progress in internal tide, internal wave and tidal front. In particular, tidal mixing is one of the extensively concerned issues on tide study. Ocean tide is a kind of load in the earth gravitational field which needs to be improved in the research of the high-precision earth gravitational field.

The steric effect on the sea level variations can be different on the different time scales. Sea level variations greatly influence the tidal wave in shallow water, and the seasonal and long term variations should be considered in engineering water levels calculation.

Reference

BAO Xiawen, GAO Guoping, YAN Ju. Three dimensional simulation of tide and tidal current characteristics in the East China Sea. Oceanologica Acta, 2001, 24(2): 135-149.

Chen Zongyong, Huang Zuke et al.. A j, v model for tidal harmonic analysis and prediction. Acta Oceanologica Sinica, 1990, 12(6): 693-703. (In Chinese)

Cui Hongyan. Risk Assessment of Potential Sea-level-rise of Liao River Delta Region Based on GIS, Journal of Liaoning Normal University (Natural Science Edition), 2005, 28(1): 107-111. (In Chinese)

Dong Xiaojun, Ma Jirui et al.. Tidal information of the yellow and east China seas from Topex/Poseidon satellite altimetric data, Oceanologia Et Limnologia Sinica,, 2002, 33(4): 387-392. (In Chinese)

Du Ling, Zuo Juncheng et al.. Simulation of tide and current in the Taiwan strait by finite element method, Transactions of Oceanology and Limnology, 2005, 4: 1-9. (In Chinese)

Du Ling, Zuo Juncheng, et al.. The Response of Tidal Wave and Engineering Water Level to Long-Term Sea Level Variation in the Jiaozhou Bay，15th ISOPE symposium, 2005.

Fang Guohong. Quasi-harmonic constituent method for analysis and prediction of tides. Studia Marinea Sinica. 1974, 9, 1-16; 1976, 11, 33-56; 1981, 18, 19-40. (In Chinese)

Fang, G., K. Yu and B. H, Choi. A three-dimensional numerical model for tides in the Bohai, Yellow and East China Seas. Proceedings of International Workshop on Tides in the East Asian Marginal Seas. Korean Society of Coastal and Ocean Engineers, 2000, 41-52

Han Guijun, Fang Guohong et al.. Optimizing open boundary conditions of nonlinear tidal model using adjoint method. II. Assimilation experiment for tide in the Yellow Sea and the East China Sea. Acta Oceanologica Sinica, 2001, 23(2): 25-31. (In Chinese)

Huang Daji, Shu Jilan and Chen Zongyong. The application of 3-D shallow water model in the Bohai SeaII. The seasonal variation of temperature, Acta Oceanologia Sinica, 1996, 18(6): 8-17. (In Chinese)

Huang Zuke, Chen Zongyong et al.. Analysis of 19-year tidal data. Science in China Series D, 1997, 40(4), 352-360.

Hu Ruijin and Liu Qinyu. Annual and intraseasonal variations in sea surface height over the tropical pacific, Oceanologia Et Limnologia Sinica, 2002, 33(3): 303-313. (In Chinese)

Hu Song, Zhu Jianrong et al.. Estuarine Circulation and Saltwater Intrusion Ⅱ: Impacts of River Discharge and Rise of Sea Level, Journal of Ocean University of Qingdao, 2003, 33(3): 337-342. (In Chinese)

Jiao Wenhai, Guo Haironget al.. Absolute Change Monitoring of Sea Level with High Precision GPS Data and Tide Gauge Data, Hydrographic Surveying and Charting, 2004, 24(3): 5-8. (In Chinese)

Kantha L.H.. Tides--A modern perspective. Marine Geodesy, 1998, 21: 275–297.

Li Lei, Zuo Juncheng, Li Peiliang. Tidal Simulation in the Yellow Sea and Bohai Sea with Finite Element Method. 13th ISOPE symposium, 2003, pp.802-808.

Li Peiliang, Zuo Juncheng et al.. An Orthogonalized Convolution Method of Tidal Analyses in South China

Sea from TOPEX/POSEIDON, Oceanologia Et Limnologia Sinica, 2002, 33(3): 288-295. (In Chinese)

Li Peiliang, Zhao Wei et al.. A numerical study of the wave, current and tide interactions by a coupling model in Bohai Sea during a winter storm. 13th ISOPE symposium, 2003, pp.270-276.

Li Peiliang, Li Lei et al.. Tidal analysis from data on high and low time. Journal of Ocean University of China. 2004, 3(1): 10-16. (In Chinese)

Li Peiliang, Li Lei et al.. Tidal Energy Fluxes and Dissipation in the Bohai Sea, the Yellow Sea and the East China Sea, Journal of Ocean University of Qingdao, 2005, 35(5): 713-718. (In Chinese)

Li Peiliang, Zuo Juncheng et al.. Numerical simulation of semidiurnal constituents in the Bohai Sea, the Yellow Sea and the East China Sea with assimilation TOPEX/POSEIDON data, Oceanologia Et Limnologia Sinica, 2005, 36(1): 24-30. (In Chinese)

Lin Hui, Lv Guonian, Song Zhiyao. Simulation and research on tidal waves and coast evolution in the Bohai Sea, the Yellow Sea and the East China Sea. China Science Press, 2000, pp266. (In Chinese)

Lin Ming-Cung, Juang Wen-Jye, Tsay Ting-Kuei. Applications of the mild-slope equations to tidal computations in the Taiwan Strait. Journal of Oceanography, 2000, 56, 625-642.

Lin Ming-Chung, Juang Wen-Jye, Tsay Ting-Kuei. Anomalous amplifications of semidiurnal tides along the western coast of Taiwan. Ocean Engineering, 2001, 28, 1171-1198.

Lin Xiang, Yin Baoshu et al.. Effects of radiantion stress in the interaction of coupled wave-tide-surge in the coastal area of Huanghai delta, Oceanologia Et Limnologia Sinica, 2002, 33(6): 615-621. (In Chinese)

Liu Guimei, Wang Hui et al.. Numerical study on the velocity structure around tidal fronts in the Yellow Sea. Advances in Atmospheric Science, 2003, 20(1):453-460.

Lv XianQing, Fang Guohong. Inversion of the tides on the open boundary of the Bohai Sea by adjoint method. Oceanologia et Limnologia Sinica, 2002, 33(2), 113-120.

Mazzega, P. and M. Bergé. Ocean tides in the Asian Semienclosed from TOPEX/POSEIDON, *J. Geophys. Res.,* 1994，99, 24867-24881.

Ou Suying and Yang Qingshu. Interaction of fluctuating river flow with a barotropic tide in river network of the Zhujiang Delta, Acta Oceanologia Sinica, 2004, 26(1): 125-131. (In Chinese)

Qiu Zhongfeng, He Yijun and Lv Xianqing. Tidal adjoint assimilation with the TOPEX/Poseidon altimetry data in the Yellow Sea and Bohai Seas, Acta Oceanologia Sinica, 2005, 27(4): 11-18. (In Chinese)

Ray. R., B. Sanchez, and D. Cartwright. Some extensions to the response method of tidal analysis applied to TOPEX/POSEIDON altimetry(abstract). EoS Trans. AGU. 75(16), Spring Meet. Suppl. 1994, 108.

Sen Jan, Ching-Sheng Chern, Joe Wang. Transition of tidal waves from the east to South China Sea over the Taiwan Strait: influence of the abrupt step in the topography. *Journal of Oceanography*, 2002, 58, 837-850

Sen Jan, Wang Yu-Huai et al.. Incremental inference of boundary forcing for a three-dimensional tidal model: tides in the Taiwan Strait. Continental Shelf Research, 2004, 24, 337-351

Sha Wenyu. Advance in tide research in the China Seas. Marine Forecasts, 2000, 17(2), 73-77. (In Chinese)

Shen Hui, Guo Peifang et al.. Sea surface level variations during 1993-2001, Oceanologia Et Limnologia Sinica, 2003, 34(2): 169-178. (In Chinese)

Simpson J.H., Hunter, J.R., Fronts in the Irish Sea. Nature, 1974, 250-404-406.

Sun Heping; Xu Houze et al.. Latest observation results from superconducting gravimeter at station Wuhan and investigation of the ocean tide models, Chinese Journal of Sinica, 2005, 48(2): 299-306. (In Chinese)

Wan Zhenwen, Qiao Fang li, Yuan Yeli. Numerical simulation of Three-dimensional tidal waves in the Bohai Sea, the Yellow Sea and the East China Sea. Oceanologia et Limnologia Sinica. 1998, 29(6), 611-616. (In Chinese)

Wang Kai, Fang guohong, Feng Shizuo. A 3-D numerical simulation of M2 tides and tidal currents in the Bohai Sea, the Yellow Sea and the East China Sea. Act Oceanologica sinica, 1999, 21(4), 1-13. (In Chinese)

Wang Y.H., S. Jan, Wang D.P.. Transports and tidal current estimates in the Taiwan Strait from shipboard

ADCP observations (1999-2001). Estuarine, Coastal and Shelf Science, 2003, 57, 193-199.

Wu Qiang, Zheng Xianxin et al.. Relative Sea-level Rising and Strategies of Control in Coastal Region of China in 21 Century, Science in China, Ser.D, 2002, 32(9): 760-766. (In Chinese)

WU Ziku, Tian Jiwei et al.. A numerical model of tides in the South China Sea by adjoint method. Oceanologia et Limnologia Sinica, 2003a, 34(1): 101-108. (In Chinese)

WU Ziku, Wang Liya et al.. A numerical model of tides in the Beibu Gulf by adjoint method. Acta Oceanologia Sinica, 2003b, 25(2): 129-135. (In Chinese)

Xu Houze. A correction model of ocean loading tide in the China Seas. Science in China Series B, 1988, 9, 984-994. (In Chinese)

Yang Jian, Lu Junzhi et al.. The related analysis of the sea surfacd height abnormality (SSHA) near the China Sea., Marine Forecasts, 2004, 21(2): 29-36. (In Chinese)

Ye Anle and Mei Liming. Numerical modeling of tidal waves in the Bohai Sea, the Yellow Sea and the East china Sea. Oceanologia et Limnologia Sinica. 1995, 26(1): 63-70. (In Chinese)

Yu Yifa. Advance of the Researches on the Variations of Mean-Sea-Level (MSL) in the Coastal Waters of China, Journal of Ocean Universtiy of Qingdao, 2004, 34(5): 713-719. (In Chinese)

Yu Yifa and Yu Yuxiu. The effect of long-term sea-level variation on calculating the extreme water levels of multiyear return periods, Acta Oceanologia Sinica, 2003a, 25(3): 1-7. (In Chinese).

Yu Yifa, Yu Yuxiu et al.. Effect of Sea Level Variation upon the Tidal Characteristic Values in the Eastern China Seas. China Ocean Engineering. 2003b, 17(3): 369-382.

Zhang Han-wei, Xu Hou-ze, and Zhou Xu-hua. A Theoretical Research of the Influence of Ocean Loading Tide on the Time Variation of Gravitational Field. Chinese Astronomy and Astrophysics, 2004, 28: 348-355.

Zhang Xiaoqian, Liang Xinfeng and Tian Jiwei. The study of internal tide and near inertial motion in the upper 450m in the north of the South China Sea, Chinese Science Bulletin, 2005, 50(18): 2027-2031. (In Chinese)

Zhao Baoren. The primary study of the circulation structure around continental front and cold water front in west of the South Yellow Sea. Oceanologia Et Limnologia Sinica, 1987, 18(3): 217-226. (In Chinese)

Zhao Baoren, Fang Guohong, Cao Deming. Numerical simulation of tide and tidal current in the Bohai Sea, the Yellow Sea and the East China Sea. Acta Oceanologica Sinica, 1994, 16(5), 1-10. (In Chinese)

Zhong Guangfa. Causes and effects of sea-level change, Advance in Earth Sciences, 2003, 18(5): 706-711. (In Chinese)

Zhou Xiaobing, Zhang Yanting and Zeng Qingcun. The interface waves of thermocline excited by the principal tidal constituents in the Bohai Sea, Acta Oceanologia Sinica, 2002, 24(2): 21-29. (In Chinese)

Zhu Jiang, Zeng Qing-chun et al.. Estimation of the open boundary conditions of tidal model from coastal tidal observations by the adjoint method. Science in China Series D, 1997, 27(5), 462-468. (In Chinese)

Zhu Jianrong, Qi Dingman et al.. Impacts of change of river discharge and sea level on estuarine turbidity maximum zone, Acta Oceanologia Sinica, 2004, 26(5): 14-22. (In Chinese)

Zuo Juncheng, Yu Yifa et al.. Effect of Sea Level Variation upon Calculation of Engineering Water Level. China Ocean Engineering, 2001, 15(3): 383-394.

Zuo Juncheng, Zhang Jianli et al.. Sea-level variation/change and thermal contribution in the Bering Sea. Acta Oceanologica Sinica, 2005, Vol. 24, No. 6, p. 36-45.

Zuo Juncheng, Zhang Jianli et al. Global sea level variation/change and thermal contribution. Acta Oceanologica Sinica. (submitted)

RESEARCH PROGRESS IN INTERNAL WAVES IN CHINA DURING 2002-2006*

FAN Conghui[a, b], *LI Shuang*[a, b] *and SONG Jinbao*[a]

(a. Institute of Oceanology, Chinese Academy of Sciences, Qingdao, 266071, China;

b. Graduate University of the Chinese Academy of Sciences, Beijing, 100049, China.)

Key words: internal waves; internal tide; internal solitary waves; China

ABSTRACT

The research progress in internal waves in China based on the past four years (2002-2006) is reviewed. Through analysis of the papers published by Chinese scholars in national or international journals, we review the progress mainly from the following three aspects: the development of the internal wave theories, the numerical studies, and the observational data including the measurements in situ, in lab and by remote sensing. Furthermore, researches in the future are discussed in the end.

INTRODUCTION

The internal waves (IWs) is generated in a density stratified fluid, it is ubiquitous in the world ocean in situ measurements and by remote sensing. IWs plays an important role in the ocean. For example, it is one of the main mechanisms of tidal energy dissipation and ocean mixing. The development of the research of IWs would greatly promote the development of maine acoustics, ocean sediments, military oceanography and so on. Besides, it is also very important for the safety of ocean facilities, marine exploitation, and marine traffic etc.

Therefore IWs has been paid more attention to by many marine scientists and countries (Li 2005; Jiang et al. 2005). Based on the papers published in national or international journals by Chinese scholars during past four years (2002-2006), IWs research carried out mainly by three major ways: theory, numerical method, observations and data analysis.

* This research is supported by Knowledge Innovation Programs of the Chinese Academy of Sciences (No. KZCX3-SW-222).

THE DEVELOPMENTS OF THE IWS THEORIES

The two-layer fluid model of IWs is commonly used by many researchers for a long time, since this kind of model is simple and practical. Until recently, a great many researchers still use the two-layer model to study the behaviors of IWs. Based on the potential flow theory of water waves, Wei et al. (2003) studied the interaction mechanism between the free-surface waves and internal waves which is generated by a moving point source in the lower layer of a two-layer fluid. They found that the coupling interaction between the surface-wave mode and internal-wave mode must be taken into account for the case of the large density difference between two layers. Wei et al. (2005) analyzed the waves induced by a submerged moving dipole in a two-layer fluid of finite depth analytically and experimentally. The qualitative consistency between their theory and laboratory result was examined and confirmed. Afterwards, Wei and Dai (2006) reviewed the research work on both the Kelvin-wake and the non-Kelvin-wake generated by a submerged moving body, in continuous and discontinuous density stratification systems, respectively. The general governing equation for the non-Kelvin-wake in continuously stratified fluid and the potential-flow analysis for the Kelvin-wake in the discontinuously stratified fluid were analyzed. The complicated dynamical characteristics in the internal wave generation due to a moving body in a linearly-distributed density fluid were summarized, including the space-time structures at near and far fields of wakes, the coupled configurations between vortex and turbulence, and the interactions between internal wave and turbulence. Song (2004) deduced the second-order random wave solutions for IWs in a two-layer fluid. It is shown that the first-order solutions represent a linear superposition of many waves with different amplitudes, wave numbers and frequencies, and the second-order solutions describe the second-order wave-wave interactions. Afterwards Song and Sun (2006) extended their previous study to a more general case of the two-layer fluid with a top free surface.

Some theories for IWs in two-layer fluid have also been extended to the three-layer or n-layer cases by some scholars. Chen and Song (2005) obtained the second-order Stokes solutions for IWs in the three-layer density-stratified fluid. For the first time, Chen et al. (2006) gained the second-order random wave solutions for interfacial IWs in the n-layer density-stratified fluid, and deduced both the first-order and second-order solutions depending on the density and depth of

each layer, from which the above Song's (2004) solutions for IWs in a two-layer fluid can be obtained as a particular case.

Gao et al. (2002) predicted some two-dimensional and non-travelling-wave observable effects of the shallow-water waves, which might be found in the coming fluid experiments. They investigated the approximately concentric Korteweg-de Vries equation, and found out some exact solitonic solutions by an auto-Backlund transformation. To further study the split principle of initial internal solitons on the continental shelf, Xu et al. (2005) corrected the 2D KdV equation of Djordjevic and Redekopp for the exponentially stratified fluid (or ocean) with two-dimensional topography. Through a combination of theoretical study and numerical experiments, they showed that solitons in the odd vertical modes could be split. The even modes cannot be split unless the initial internal solitons propagate from shallow sea to deep sea. At the same time, Li and Du (2005) deduced a dispersive relation of internal solitary wave from a two-layer model of K-dV equation by perturbation expansion individually. Afterwards, Xu et al. (2006) analyzed the surface characters of internal waves generated by Rankine ovoid. It is shown that IWs is a sort of trapped wave which propagates in a wave guide, and its waveform is a kind of Mach front-type internal wave in pycnocline. At the same time, it is also shown that under the hypothesis of inviscid fluid, the synchronism between the surface velocity gradient fields at the free surface and the internal wave fields in the fluid is retained.

There are some other developments as well. Shen and Xiang (2002) analyzed the similarity for the internal wave load and wave-making generated by the submarine in the stratified ocean. Ye and Shen (2004) strictly deduced a subsection solution to the vertical structure of internal waves. Su et al. (2005) studied the two-dimensional algebraic solitary wave and its associated eigenvalue problem in the deep stratified fluid with free surface. Besides, an exact solution for the derived 2D Benjamin-Ono equation was obtained, and its physical explanation was given with the corresponding dispersion relation.

The general governing equations for IWs was derived by Yuan et al. (2003) from the basic laws of physics: law of mass conservation, law of salt conservation, law of momentum conservation, equation of entropy evolution and equation of state, and the emphasis is placed on the mathematic and physical implications of various approximation forms of the governing equations in their derivation process, which will enable us to strictly and accurately use these

equations.

In addition, the monograph “Fundamentals of oceanic internal waves and internal waves in the China seas” came out in 2005. This monograph was written by Fang Xinghua and Du Tao. It expatiates on the basic knowledge of the oceanic internal waves through the basic theory. The book contains: basic concepts and equations of internal waves; propagating properties of linear internal waves that both vertical profile with all kinds of buoyant frequencies and ocean with shear flow; linear and nonlinear tide-generated internal waves; laboratory experiments of internal waves; measurements and data analysis of internal waves; probability distribution and spectral expression of random internal wave fields; the mechanism of generation, interaction and dissipation of internal waves; internal waves in the China seas etc. Another monograph “Research fundamentals of ocean interior mixing ” written by Fan Zhisong was published in 2002. Considering the important relations between IWs and ocean interior mixing, it is accounted for nearly one-third of the content to describe the basic concepts and equations of IWs, the oceanic IWs and the shallow sea IWs in this book.

THE DEVELOPMENTS OF THE NUMERICAL STUDIES

The IWs theoretical model is often too simplistic, for example, many models are two-dimensional, even linear, and this is not accorded with three-dimensional and non-linear characteristics of IWs. In order to predict IWs, many scholars devoted to researching numerical models.

Cai et al. (2002) studied the generation and propagation of internal solitary waves in the Luzon Strait by a numerical model, and developed a new composite model, which consists of a generation model of the internal tides and a regularized long wave propagation model. The generation and propagation of internal solitary waves in the Luzon Strait were simulated. And the reasons for the asymmetry of their propagation are also explained. Since internal solitons can bring about strong force on the oil drilling platform and pipeline at sea, which causes severe threat to the ocean engineering, Cai et al. (2003) adopted a method to estimate the forces exerted by internal solitons on cylindrical piles. In their paper, Morison's empirical method, modal separation and regression analysis are introduced to estimate the forces and torques exerted by internal soliton on cylindrical piles. Afterwards, Cai et al. (2006) obtain a more practical estimation of the

force exerted by internal solitons on cylindrical piles. They concluded that the force by the first internal wave mode dominated most part of the global force. Thus, a simple estimation method of the force based on only the first internal wave mode was put forward.

Other scholars have also done a lot of researches in this area. Some work on the generation, others dedicate on propagation, and still others focus on evolution and breaking of IWs.

Bai and Song (2005) simulated the effects of lateral boundary on the propagation of internal long waves. Using a nonlinear, horizontal two dimensional modified Lynett-Liu model for internal long waves, they simulated the propagation process of small amplitude solitary waves going into and out of the tank outlet, and the diffraction through the narrow tank. By analyzing the variances of the vertical profiles of solitary waves and the form of two dimensional horizontal wave patterns with the shape of the tank outlet and the width of the open fluid area, they investigated the lateral boundary effects on the propagation of solitary waves. Afterwards, Shen and He (2006) deduced a new two-dimensional horizontal internal wave propagation model with rotation effect based on the research of Lynett and Liu. it can be used to simulate the characteristics of internal waves in a horizontal fully two-dimensional plane. The case studies were performed in South China Sea (SCS). A very good consistency was found between the simulation results and satellite images. Xu et al. (2005) simulated the disturbed movement of slender submerged body in the stratified ocean internal wave.

As for internal tides, Wu et al. (2005) simulated barotropic and baroclinic tides in the SCS. The four major tidal constituents M_2, S_2, K_1 and O_1 in the SCS are simulated by using the POM. The model is forced with tide-generating potential and four major tidal constituents at the open boundary. In order to simulate more exactly, TOPEX/Poseidon (T/P) altimeter data were assimilated into the model and the open boundary was optimized. The computed co-tidal charts for constituents M_2 and K_1 were generally consistent with the previous results in this region. The numerical simulation showed that the energetic internal tides were generated over the bottom topography like the Dongsha Islands etc.

Based on Reynolds averaged Navier-Stokes (RANS) equations and volume of fluid (VOF) method, Chang et al. (2006) used an unsteady viscous numerical method, simulated the wake characteristics of a moving submarine in a two-layer fluid. The surface wave and internal wave generated by a submarine were obtained successfully. Numerical results were in good agreement

with theoretical analysis and results from literatures.

Furthermore, Li et al. (2006) directly made a numerical simulation of the evolution and breaking of a propagating internal wave in a stratified ocean using the pseudo-spectral method. The mechanism of PSI (parametric sub-harmonic instability) involved in the evolution is testified clearly. With the growth of the wave packet, wave breaking occurs and causes strong nonlinear regime, i.e. stratified turbulence. The strong mixing and intermittent of the turbulence can be learned from the evolution of the total energy and kurtosis of vorticity vs. time. Some statistic properties of the stratified turbulence were analyzed.

To sum up, numerical models achieved great development on generation, propagation, evolution and breaking of IWs. However, most of the numerical results need to be further verified by observational data.

OBSERVATIONS AND DATA ANALYSIS

1. Measurements in Situ and in Lab

Direct measurements are a good way to study IWs. However, the equipments to directly measure IWs are rare in our country now. Although some scholars started studying measurement technique for IWs (Yang et al. 2004), most scholars mainly used CTD (Conductivity Temperature Depth) or ADCP (Acoustic Doppler Current Profiler) data from in situ measurements to analyze IWs.

Cai et al. (2002) obtained some characteristics of the internal soliton based on the observational data of an internal soliton in the SCS on June 14, 1998. The possible origin of internal soliton and characteristics of currents induced by internal wave were analyzed. The observed environmental parameters were used as initial conditions to simulate the propagation and evolution of the internal soliton in the continental shelf of the northern SCS.

Fan et al. (2003) found infragravity waves with internal wave characteristics in the southern Bohai Sea of China. By using ADCP and CTD the measurements were made during August 2000 in the southern Bohai Sea. The data of horizontal velocity with a sampling interval of 2 min in 7 layers were obtained. It is speculated that the instability processes of sheared stratified tidal flow owing to the effect of sea-floor slope in the coastal area might be the main mechanism generating these infragravity waves. And Du et al. (2003) analyzed the continuous current data by ADCP at

the observation station in the East China Sea (ECS).

Yang et al. (2004) showed the internal wave characteristics at the ASIAEX (Asian Sea International Acoustics Experiment) site of the ECS in 2001. Temperature data from a thermistor chain exhibit clear IW features in shallow water. Both semi-diurnal internal tides and high-frequency IWs were analyzed. Comparison of it with their other data from SWARM95, the Barents Sea and the Gulf of Mexico, they display some common characteristics of shallow-water IWs.

Liang et al. (2005) observed the internal tides and near-inertial motions in the upper 450m layer of the northern SCS. The current observations by mooring ADCP from August to November were used to study the barotropic tides, baroclinic tides and near-inertial motions. The study showed that the inclination of tidal ellipse tended to increase with increasing depth, implying upward propagation of energy, while that of the near-inertial ellipse tended to decrease with increasing depth, implying downward propagation of energy. Fang et al. (2005) demonstrated the characteristics of strong internal solitons at the southern edge of Dongsha Islands in the northern SCS during May-June 1998. They obtained the characteristics using in situ time series data from CTD, ADCP and thermistor chain. Zhang et al. (2005) designed a shadowgraph system for the IWs visualization. The system improved visualizing sensitivity. A CCD direct imaging approach was introduced to reduce the system noise and realize full automation. The experimental results show that this system can visualize small variations in density gradient, and can be used to visualize IWs in study of IWs dynamics.

Bao et al. (2006) analyzed the slanting property of semi-diurnal internal tide propagation in the Pacific Ocean. By analyzing the data collected using a moored instrument array and CTD during TOGA-COARE , it is found that there exist remarkable internal tides in the western equatorial Pacific Ocean, the waveform propagates downwards slantingly. Moreover, the propagating direction rotates statistically.

Some scholars studied IWs from the laboratory experiments. Xu et al. (2002) presented the experimental results on drag increment caused by internal waves, which are generated by a Rankine ovoid towed horizontally at a constant velocity in a two-layer stratified water with strong pycnocline initially at rest. The drag increment due to stratification is obtained experimentally as a function of internal Froude number and Reynolds number.

2. Remote Sensing

Remote sensing is a promising approach to study IWs. The data mainly came from SAR (synthetic aperture radar) and T/P altimeter data. These data are used by a large number of scholars to study IWs in China's coastal areas.

Yang (2003) retrieved the nonlinear internal wave amplitude from SAR imagery. It is assumed that the observed groups of nonlinear internal wave packets on SAR imagery are generated by local semidiurnal tides. The mean distance between the two leading successive wave packets have been used to retrieve the group velocity of the nonlinear internal waves. The amplitudes of nonlinear internal waves were retrieved from a model consisting of the KdV equation. And then Yang et al. (2005) obtained the oceanic pycnocline depth retrieved from SAR imagery in the existence of solitary internal waves. A numerical model is presented for retrieving the pycnocline depth from SAR images, where the solitary internal waves are visible. A case study in the ECS shows a good agreement with in situ CTD data. Based on tens of satellite images, Shen and He (2005) analyzed oceanic internal waves in the northwest part of SCS. Satellite images captured in different time are compiled in a schematic plot, which shows internal waves are widely spread in the northwestern SCS. They summarized the characteristics of IWs in this area. The two-layer Kdv equation was applied to study the dynamical process of internal waves in the northwestern SCS. The mixing-layer depth of the studied area is retrieved. According to the theory of polarity conversion of oceanic internal waves, the mixing-layer depth is equal to the half of the water depth of the polarity conversion point. Therefore, for satellite images to capture the polarity conversion process of internal waves, the mixing-layer depth can directly be obtained. The depths of the mixing-layer retrieved by the two methods showed a good consistency.

Tian et al. (2003) estimated the M_2 internal tide energy fluxes along the margin of the Northwest Pacific using T/P altimeter data. The data were used to compute the energy flux of internal tide M_2 along the margin of the Northwest Pacific. They extracted baroclinic tides, which yielded energy transmission, from temporarily coherent internal tide signals in the altimeter data. A good consistency was found between the M_2 tide derived from satellite and that measured in situ. The computed results indicated that the maximum energy flux of internal tide M_2, 3 kW /m, appears in the Ryukyu Trench. The total energy flux of the M_2 internal tides along the margin of

the Northwest Pacific is about 15GW. Recently, Tian et al. (2006) studied latitudinal distribution of mixing rate caused by the M_2 internal tide. Ten years of Ocean Topography Experiment T/P tidal data and an energy balance relation are used to estimate the mixing rate caused by the M_2 internal tides in the upper ocean. The results indicated that latitudinal distribution of the mixing rate had a generally symmetrical structure with respect to the equator. Tian obtained the distribution of some locations of the maximum values. The minimum is located near the equator. The data imply that midlatitudes are the key regions for internal tide mixing.

Fan (2005) studied the simulation model of SAR remote sensing of turbulent wake of semi-elliptical submerged body. They built up a 2-dimensional simulation model of SAR remote sensing of this semi-elliptical submerged body to apply in the SCS. Satisfactory results were obtained through simulation of the delay time and delay distance of turbulent surface wake of this semi-elliptical submerged body, as well as the minimum submerged depth at which this submerged body cannot be discovered by SAR.

Dong et al. (2002) analyzed the SCS internal wave using radar imagery. It is shown that the internal wave can affect the sea wind-generated wave crucially. Backscattering coefficients were retrieved from sea surface of the SCS using some existing models and the results were compared with the calculations of the SIR-C/X-SAR data. The different results among the radar bands exist and are affected by sea surface roughness. Then the ocean wave spectrum was derived from the X-SAR image. Finally, they pointed out that the main factor causing the internal waves was the tidal current.

RESEARCHES IN THE FUTURE

The energy of oceanic internal solitary waves and internal tide are mainly concentrated in the shallow water. Moreover, there have high incidence of internal solitary waves and internal tide in the ECS and SCS. So the internal solitary wave and internal tide researches are the preferred direction for the future of IWs research in China.

Direct in-site observation is the best way to study IWs, however, this method is limited to a certain area only. But remote sensing research by SAR or new sensors to be developed is a very promising development prospects.

References

[1]. Bai, Ye-fei and Song, Jin-bao, (2005), Numerical simulation of effects of lateral boundary on the propagation of internal long waves(in Chinese), MARINE SCIENCES, 29(9): 42-50,55

[2]. Bao, XW et al. (2006), The slanting property of semi-diurnal internal tide propagation in the Pacific Ocean at 1 degrees 45 ' S, 156 degrees E,ACTA OCEANOLOGICA SINICA,25(4):143-145.

[3]. Cai, SQ et al. (2002), Some characteristics and evolution of the internal soliton in the northern South China Sea,CHINESE SCIENCE BULLETIN,47(1):21-27.

[4]. Cai, SQ et al. (2003), A method to estimate the forces exerted by internal solitons on cylindrical piles,OCEAN ENGINEERING,30(5):673-689.

[5]. Cai, SQ et al. (2002), A numerical study of the generation and propagation of internal solitary waves in the Luzon Strait,OCEANOLOGICA ACTA,25(2):51-60.

[6]. Cai, SQ et al. (2006), A simple estimation of the force exerted by internal solitons on cylindrical piles,OCEAN ENGINEERING,33(7):974-980.

[7]. Chang, Yu and Hong, Fang-wen, (2006), Numerical simulation submarine in a of wakes for moving two-layer fluid(in Chinese), Journal of Hydrodynamics, 21(1): 76-83

[8]. Chen, XG and Song, JB, (2006), Second-order random wave solutions for interfacial internal waves in N-layer density-stratified fluid,CHINESE PHYSICS, ,15(4):756-766.

[9]. Chen, XG et al. (2005), Second-order Stokes solutions for internal waves in three-layer density-stratified fluid,ACTA PHYSICA SINICA,54(12):5699-5706.

[10]. Dong, Qing et al. (2002), South-China sea internal wave analysis using radar imagery , International Geoscience and Remote Sensing Symposium (IGARSS), (5): 3008-3010

[11]. Du Yan et al. (2003), Current analysis at a continuous observation station in the East China Sea (in Chinese), Ocean Engineering.21(1):94-100

[12]. Fan, ZS, (2005), Simulation model of SAR remote sensing of turbulent wake of semi-elliptical submerged body, ACTA OCEANOLOGICA SINICA,24(5):50-60.

[13]. Fan, ZS et al. (2003), Infragravity waves with internal wave characteristics in the south of the Bohai Sea of China,ACTA OCEANOLOGICA SINICA,22(2):171-177.

[14]. Fan, ZS, (2002), Research Fundamentals of Ocean Interior Mixing (in Chinese)[M]. China Ocean Press, Beijing

[15]. Fang, WD et al. (2005), Internal solitons in the northern South China Sea from insitu observations(in Chinese),CHINESE SCIENCE BULLETIN,50(15):1627-1631.

[16]. Fang, Xinhua and Du Tao. (2005).Fundamentals of Oceanic Internal Waves and Internal Waves in the China Seas (in Chinese)[M]. Qingdao:China Ocean University Press.

[17]. Gao, YT and Tian, B, (2002), Some two-dimensional and non-travelling-wave observable effects of the shallow-water waves, PHYSICS LETTERS A,301(1-2):74-82.

[18]. Gao, YT et al. (2006), Macropterons, micropterons and similarity reductions for the regularized Ostrovsky-Grimshaw model for fluids and plasmas with symbolic computation,ACTA MECHANICA,182(1-2):17-29.

[19]. Han, CM et al. (2002), Extraction of internal tidal currents from a portion of sea current profile,CHINA OCEAN ENGINEERING,16(2):249-256.

[20]. Huang, XD et al. (2004), Effects of the internal waves on the time correlation of the acoustic fields in the East China Sea,PROGRESS IN NATURAL SCIENCE,14(11):945.

[21]. Jiang, G et al. (2005), THE DEVELOPMENT OF INTERNAL WAVES RESEACH AT HO ME AND ABROAD(in Chinese), MARINE FORECASTS,22 (z1) :176-182

[22]. Li, BR et al. (2006), Evolution and breaking of a propagating internal wave in stratified ocean,CHINESE JOURNAL OF GEOPHYSICS-CHINESE EDITION,49(2):360-366.

[23]. Li, HY and Du, T, (2005), Dispersive relation of internal solitary waves of the two layers model K-dv function(in Chinese), Journal of Hydrodynamics.20(5):673-679

[24]. Li, JC, (2005), billow under the sea surface — internal waves in the ocean (in Chinese), Mechanics and Engineering.27(2):1-6

[25]. Liang, XF et al. ,(2005),Observation of internal tides and near-inertial motions in the upper 450 m layer of the northern South China Sea,CHINESE SCIENCE BULLETIN,50(24):2890-2895.

[26]. Shen, Guoguang and Xiang, Weizheng, (2002), Similarity Analyses of Ocean Internal Wave Research(in Chinese), JOURNAL OF TIANJIN UNIVERSITY.35(6):691-695

[27]. Shen, Hui and He, Yi-Jun, (2006),SAR imaging simulation of horizontal fully two-dimensional internal waves, Journal of Hydrodynamics,18(3):294-302.

[28]. Shen, Hui and He, Yi-Jun, (2005),Study internal waves in north west of South China Sea by satellite images,International Geoscience and Remote Sensing Symposium (IGARSS),4(25):2539-2542.

[29]. Song, JB, (2004),,Second-order random wave solutions for internal waves in a two-layer fluid,GEOPHYSICAL RESEARCH LETTERS31(15).

[30]. Song, JB and Sun, Q,(2006),Second-order random interfacial wave solutions for two-layer fluid with a free

surface, ACTA OCEANOLOGICA SINICA,25(1):15-20.

[31]. Su, XB et al., (2005),Two-dimensional algebraic solitary wave and its vertical structure in stratified fluid,APPLIED MATHEMATICS AND MECHANICS-ENGLISH EDITION,26(10):1255-1265.

[32]. Tian, B and Gao, YT, (2004),Computerized symbolic computation, nonintegrable Ostrovsky's model for the oceanic or plasma environment and similarity solutions,NUOVO CIMENTO DELLA SOCIETA ITALIANA DI FISICA B-GENERAL PHYSICS RELATIVITY ASTRONOMY AND MATHEMATICAL PHYSICS AND METHODS,119(6):539-546.

[33]. Tian, JW et al., (2006), Latitudinal distribution of mixing rate caused by the M-2 internal tide,JOURNAL OF PHYSICAL OCEANOGRAPHY,36(1):35-42.

[34]. Tian, JW et al.,(2003),Estimates of M-2 internal tide energy fluxes along the margin of Northwestern Pacific using TOPEX/POSEIDON altimeter data,GEOPHYSICAL RESEARCH LETTERS,30(17).

[35]. Wang, SQ et al., (2004),Observations on fluctuations of sound transmission and temperature field from the ASIAEX 2001 South China Sea experiment and inversion of the characterizations of internal tides (waves),PROGRESS IN NATURAL SCIENCE,14(9):793-799.

[36]. Wei, Gang et al., (2003),Surface effects of internal wave generated by a moving source in a two-layer fluid of finite depth, APPLIED MATHEMATICS AND MECHANICS-ENGLISH EDITION,24(9):1025-1040

[37]. Wei Gang et al., (2005),Waves induced by a submerged moving dipole in a two-layer fluid of finite depth,ACTA MECHANICA SINICA,21(1):24-31.

[38]. Wei Gang and DAI Shiqiang, (2006), ADVANCES IN INTERNAL WAVES DUE TO MOVING BODY IN STRATIFIED FLUID SYSTEMS(in Chinese), Advances in Mechanics, 36(1):111-124

[39]. Wu, ZK et al., (2005),Simulation of barotropic and baroclinic tides in the South China Sea,ACTA OCEANOLOGICA SINICA,24(2):1-8.

[40]. Xu YF et al., (2005), Modeling and Simulation of Disturbed Movement of Slender Submerged Body in Stratified Ocean Internal Wave(in Chinese), Journal of System Simulation,18(7): 1797-1799,1829

[41]. Xu, ZT et al., (2006), Surface characters of internal waves generated by Rankine ovoid,ACTA MECHANICA SINICA,22(5):417-423.

[42]. Xu, ZT et al., (2005), A correction of the 2D KdV equation of Djordjevic Redekopp in exponentially stratified fluid, ACTA MECHANICA SINICA,21(4):346-352.

[43]. Xu, ZT et al., (2002),Drag increment due to internal waves generated by Rankine ovoid,PROGRESS IN NATURAL SCIENCE,12(11):849-853.

[44]. Yang, J et al., (2004), Internal wave characteristics at the ASIAEX site in the East China Sea,IEEE JOURNAL OF OCEANIC ENGINEERING,29(4):1054-1060.

[45]. Yang, JS, (2003),Nonlinear internal wave amplitude remote sensing from SAR imagery,Proceedings of SPIE - The International Society for Optical Engineering,4892:450-454.

[46]. Yang, JS et al., (2005), Oceanic pycnocline depth retrieval from SAR imagery in the existence of solitary internal waves,ACTA OCEANOLOGICA SINICA,24(5):46-49.

[47]. Yang L et al. (2004), A Study on the Measurement Technique for Marine Internal Wave, Meteorological(in Chinese), Hydrological and Marine Instruments, (2):7-10

[48]. Ye Chunsheng and Shen Guoguang, (2004), A Subsection Solution to the Vertical Structure of Internal Waves(in Chinese), Journal of Tianjin Universit.37(12).-1041-1045

[49]. Yuan Yeli et al., (2003) ,Governing Equations for Marine Internal Wave(in Chinese), ADVANCES IN MARINE SCIENCE, 21(3):243-250

[50]. Zhang, Mingzhao et al., (2005), Design of high sensitive shadowgraph system for internal wave visualization, Optics and Precision Engineering, 13(6): 664-667

SEA FOG RESEARCH OF CHINA: A REVIEW

ZHANG Suping[1*] *BAO Xianwen*[1] *YANG Yuqiang*[2] *REN Zhaopeng*[1]

1 Physical Oceanography Lab. & Ocean –Atmosphere Interaction and Climate Lab.
Ocean University of China, Qingdao, China, 266100
2 Qingdao Meteorological Bureau, Qingdao, China, 266003

Abstract

The Chinese east coast and marginal seas are foggy regions. Sea fog is one of the most important events that can lead to low visibility thus causing casualties and property losses. Development of effective forecasting methods is rested upon comprehensive knowledge of the phenomena. This review covers the main advances in the sea fog research during the past ten years in China, including the sea fog synoptic and climatological study, the interannual variations of sea fog frequency, the numerical simulations, and the fog watching and detection techniques by satellites and microphysics of sea fog. This paper can provide a general image of sea fog research in China.

Key words: Sea fog, review, coast, marginal sea, China

1 Introduction

Sea fog is a kind of condensation phenomenon occurring in the lower layer of the atmosphere over seas or coastal areas. It is dangerous because the huge amount of suspending water droplets and ice crystals can weaken the visibility, thus severely disturbing voyage, seaport operations and other activities at sea. Fog can be classified as dense, moderate, or light according to whether the range of visibility is 0 to <1km, 1 to <5km, or 5 to <11km. The Chinese marginal seas, especially the Yellow Sea, are foggy areas. About half of the collision accidents near Qingdao port, which faces the Yellow Sea, are related to sea fog in the past two years according to the statistics of Qingdao Maritime Safety Administration.

There are different kinds of sea fogs, such as advection cooling fog, advection evaporating fog, mixing fog, radiation fog and topographic fog (Wang, 1983). The most common one along the Chinese coast is the advection cooling fog, which is formed when warm air flows over cold sea surface leading to condensation. Therefore，American meteorological society gives the following definition: sea fog is a type of advection fog formed when air that has been lying over a warm water surface is transported over a colder water surface, resulting in cooling of the lower layer of

* email: zsping@ouc.edu.cn, Tele:0532-66781528

air below its dewpoint. The sea fog mentioned in this present paper primarily means the advection cooling fog, but other types of fog, which sometimes occur in or intrude into the coastal areas, may be included because the observations can not distinguish the advection cooling fog from the other fogs.

The beginning of the organized study on fog can be traced back to 1960-1970s in China. Shandong Oceanography College (nowadays Ocean University of China) carried out some special programs to investigate the Yellow Sea fog in 1965-1968 and 1971-1973 respectively. In 1983, Wang Binhua, a professor of the college, published his book Sea Fog (its English version was published in 1985), which was the first monograph on sea fog at that time and is still the unique one in the world so far. This book, summing up the main achievements made by Prof. Wang in his almost 40 years of teaching and researching and the main achievements made by other scientists，provided us a rather comprehensive knowledge of sea fog, such as the global distributions, the classification, the characteristics, the forming conditions and the forecasting methods of sea fogs. Another remarkable work is the Numerical Forecasting Methods on the East China Sea Fog finished by the Institute of Oceanology, Chinese Academy of Sciences and Ocean University of Qingdao (nowadays Ocean University of China) from 1991 to 1995 (the 8th Five-year Plan) supported by the National Ministry of Science and Technology of China. This program, focusing on the atmospheric and marine background of sea fog formation, conditions of the atmospheric boundary layer (ABL), microphysics, numerical model, numerical forecast and etc.[1], is the first time for China to investigate sea fog systematically after Wang's historic book. Though some researches had been kept doing after the program, no important project supporting such a study until the end of the 20th century. During the 10th Five-year Plan of China (from 2001 to 2005), the satellite remote sensing techniques developed quickly. The Modularized Heavy Sea Fog Detection Technique by Remote Sensing, supported by the National High-tech R&D Program (the 863 program), marked the beginning of sea fog detection by weather satellites[2]. This paper provides a comprehensive review on the sea fog research in the past 10 years or so in China and gives discussions on some problems. Figures in the present paper are drawn by the authors and some of the latest work produced by the authors is included too.

2 Synoptic and climatological researches of sea fog

The meteorological and climatological studies of sea fog have a long history. In the 1970's and 1980's, majority of papers focused on the synoptic conditions and patterns in favor of the fog formation. In the recent ten years, the obvious progresses have been made in the following three aspects: (a) the sea fog statistics, e.g. the monthly frequency of fog occurrence; (b) the elementary

[1] Scientific Reports on the Study of Numerical Forecasting Methods on East China Sea, 1995. Program No.85-903-08-08

[2] Scientific Reports on the Modularized Heavy Sea Fog Detection Technique by Remote Sensing, 2005. Program No. 2001AA633040

marine and atmospheric factors relating to sea fog, e.g. sea surface temperature and water vapor content; and (c) the stratification of atmospheric boundary layer, e.g. the temperature inversion.

2.1 Sea fog statistic features

More statistic research on sea fog have been made in recent years using the China 30-year (1971-2000) re-compiled datasets (CRCD-30) which were produced under the leadership of the CMA (China Meteorological Administration).. Individual authors from different areas usually show their interests closely related to their surroundings, and thus the statistic results are strongly local (Fig.1). In Changshan Islands of the Bohai Sea, for instance, fog mainly occurs from May to July. Fog season in the Yellow Sea, which is the most remarkable foggy region, usually lasts 4 months from April to July. In the region of Zhoushan Islands in the East China Sea， fog happens mostly from April to June (Hou and Wang 2004). Fog is primarily in March, April and May in the Taiwan Strait (Su,1998)， and in winter—spring, from December to next April along the Guangxi autonomous region coast (Kong 1997) (Fig.2).

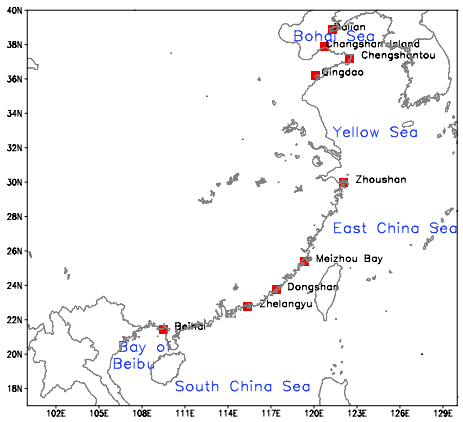

Fig.1 The geographic positions of the places listed in Fig.2 and Fig.3.

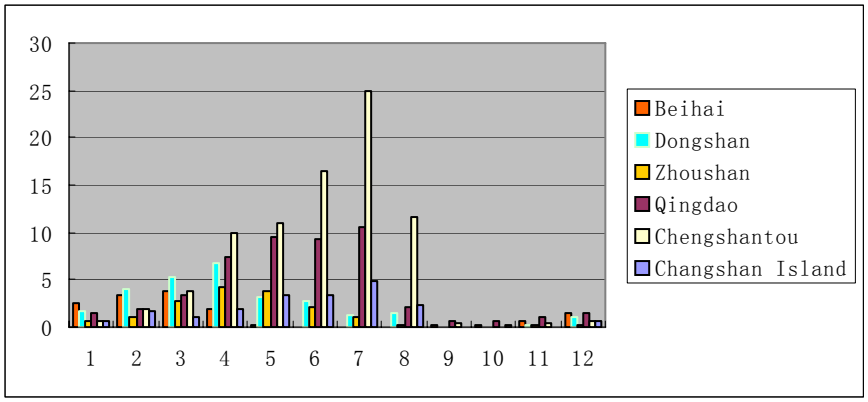

Fig.2 Monthly sea fog frequency along the east coast of China（data is from CRCD-30 and after Hou and Wang 2004, Su 1998, Kong 1997, Xu et al. 2002, Lang and Li 2002, Chen and Huang 1999）.

The annual sea fog frequency along east coast of China can be found in Fig.3. The highest frequency is found in the Yellow Sea, for instance, 83 foggy days in Chengshantou, and 48 days in Qingdao annually. Dalian, Changshan Islands and Yantai are all situated along coast of the Bohai Sea, and the foggy days are 37, 20 and 19 respectively. The frequency is lower around the East China Sea coastal areas; Zhoushan Islands and Meizhou Bay both have 16 foggy days annually. Foggy days are even less in the South China Sea; Shantou, Guangdong province experiences about 2 days of sea fog annually. Sea fog is very rare from the east of Taiwan Islands to the vicinity of Ryukyu Islands. The lasting time of sea fog varies greatly. For example, sea fog primarily lasts 4-6 hours on average, with the longest 25 hours according to the observations by the visibility sensor in Qingdao from 2005 to 2006 .

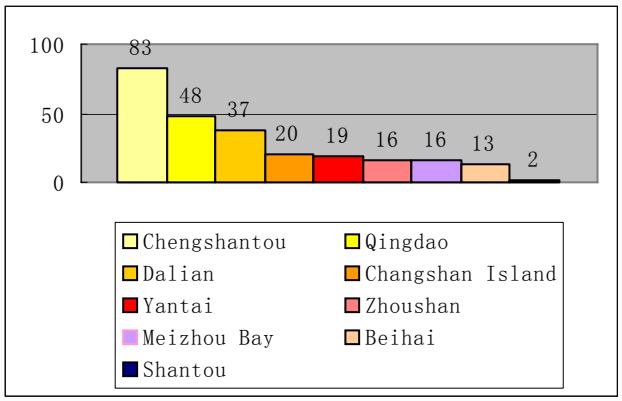

Fig.3 Annual sea fog frequency along the east coast of China (data sources are the same as in Fig.2)

2.2 Marine and atmospheric conditions

Wang (1983) summarizes the marine and atmospheric factors in favor of the fog formation such as $0.5℃\leq(t_a—t_w)\leq3.0℃$, where t_a is the air temperature at 10m above sea surface and t_w is the sea surface temperature (SST). If t_w or SST>25°C or wind speed≥10.8-13.8m/s, there will be no fog. During the past ten years, though no remarkable breakthrough had been made, scientists had been able to figure out fog conditions with greater specifications and certainties thanks to the more and more accurate observations. For instance, the temperature differences between air and sea water are 3.3°C and 2.4°C, and SST is 21.8°C and 24.7°C in June and July respectively in Yantai according to statistics of 40-year data (Xu 1997). The latest 10-year data show that if t_a-t_w is about 0.6～2.6℃ and SST is about 12.6 ～23.6°C, fog will be very likely to appear in the Zhoushan area (Xu et al.2002). The favorable conditions for sea fog in Qingdao is $(t_a—t_w)\leq3.5℃$, yet about 22% of fog occurs under the conditions of $(t_a—t_w)>3.5℃$(Wang and Qu,1997). Wind speeds and wind directions contributing to fog formation vary from place to place. NE-E-SE

winds and wind speed < 8m/s are common in foggy days in Yantai (Xu 1997)，while fog occurs with nearly no winds (still wind) along the Guangxi coast (Kong 1997).

The different wind conditions substantially reflect different weather patterns which are very helpful and useful for fog forecasting and therefore have never been overlooked by meteorologists. For example, the main synoptic systems for fog formation are stationary front, cold front, southeast low pressure pattern and transformed high pressure pattern in the Beibu Bay near the Guangxi coastal areas (Kong 1997). While the primary weather patterns of the Yellow Sea fog are the western part of a high pressure having moved into the sea and the eastern part of Jianghuai cyclonic systems. It should be pointed out that sea fog does not always occur whenever these weather patterns happened, and that the favorable synoptic system actually means the favorable weather factors, e.g. the stable stratification of the ABL, the proper atmospheric turbulences and the sensible and latent heat flux in the air-sea interface. Fog is likely to occur if the favorable weather elements appeared no matter what kinds of weather patterns.

2.3 Atmospheric boundary layer

Two conditions are required theoretically for fog formation: (a) there must be a huge amount of particles as the nuclei for the condensation; and (b) the fog droplets must be able to suspend over the sea surface for a period of time, thus leading to a poor visibility (<1km) near the surface. So a stable ABL is required.

In the past, we could only obtain the standard isobaric chart, e.g. 1000hPa, 925hPa, 850hPa, 700hPa, etc., from the routine radio soundings, which were obviously not enough in terms of vertical resolution for the ABL study. The detailed detections of ABL were generally supported by some research programs, during which about 10-20 successive days of field observations were made, just like the observations implemented in the program mentioned in the first section of the present paper. During the implementation period of the program, the special ABL detections were made using captive balloon soundings in the Yellow Sea near Qingdao from June to July in 1994. The results showed that the Yellow Sea fog always occurred in the stable ABL with temperature inversions.

In the recent years, with the development of the atmospheric detection modernization, progresses have been made in the ABL research relating to sea fog by using digital soundings. In the marine boundary layer (MBL) (atmospheric boundary layer over the oceans) turbulent mixing deriving from wind vertical shear produces a rather homogenous potential temperature or virtual potential temperature. Therefore, this layer can also be called mixing layer in which the vertical variations in temperature and humidity are weak because of mixing. The turbulent mixing tends to stop when it meets the temperature inversion that acts as a barrier prohibiting the further upward

mixing. Thus the mixing layer top is formed. The potential temperature variations with the increasing height peak around the mixing layer top. Therefore, the vertical gradients of potential temperature can be used to locate the mixing layer top. The digital sounding and the associated L-band radar, which is just put into routine operation years ago in Qingdao Observatory, can provide very high vertical resolution data. Fig.4 depicts the daily variations in the height of the mixing layer top and the sea fog events in Qingdao in 2005. The two lines of time-series tend to be out of phase year round. The time-lagged correlation coefficient is –0.33 if no time lagged, and –0.34 with the height leading one day; both cases are far beyond the 99% significant confidence (Zhang et al.2006). The relative lower mixing layer top benefits the occurrence of sea fog for the fog droplets, once it forms, are readily confined in a shallow layer of MBL to produce poor visibility.

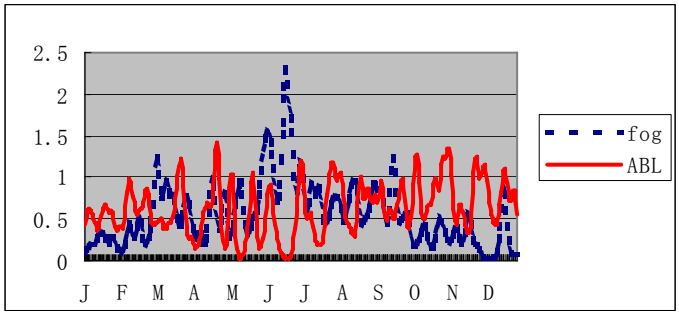

Fig.4 The height of the ABL (solid line) and the sea fog frequency (dashed line) with 2-10 days filtering (data is normalized).

Some previous studies fail to find the stable boundary layer or temperature inversion. For example, only 36 of 93 fog events accompanied by temperature inversion according to Xu et al.(2002). Such situations are probably due to the low resolution of the conventional radiosonde. Fig.5 is a profile given by digital sounding in a fog event. It is quite clear that the temperature inversion, which is in between 700-900 meters high, is unlikely to be found if only the standard isobaric data were used.

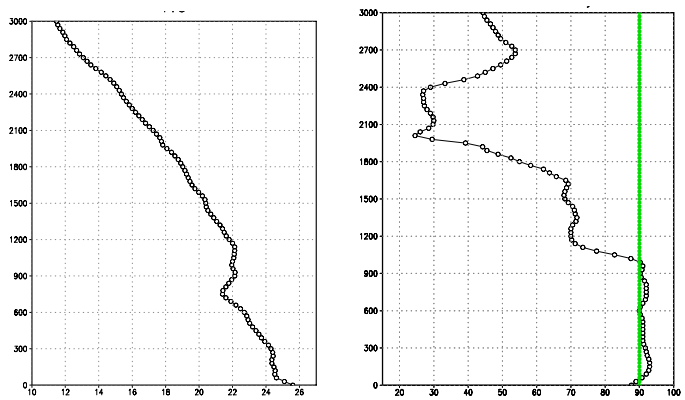

Fig. 5 Sounding profiles by L-band radar in Qingdao weather observatory at 07:00 September 9, 2005. a. Virtual temperature/°C，b. Relative humidity/%. The solid straight line represents the 90% of relative humidity（in fog）. Y-axis：height/m.

A recent research figured out the average wind speed profiles in both fog days and non-fog days in Qingdao during the fog season of 2005 (Fig.6). It shows that the wind is stronger in fog days than in non-fog days below 1000m, and the opposite situation is found above 1000m, i.e. the wind is weaker in fog days than in non-fog days. That could be the most significant feature differing from the radiation fog. As found from Fig.6, the wind speed shear in fog days is stronger than non-fog days in the frictional layer (below 300m), and the shear becomes nearly zero or even negative from about 300m to 3000m in altitude. In non-fog days the wind speed keeps increasing with height very coincident to the traditional logarithmic velocity profile. Such detailed structures were hardly found before the L-band radar came into operation. Yet the dynamics and thermodynamics involved in the phenomena are currently under study.

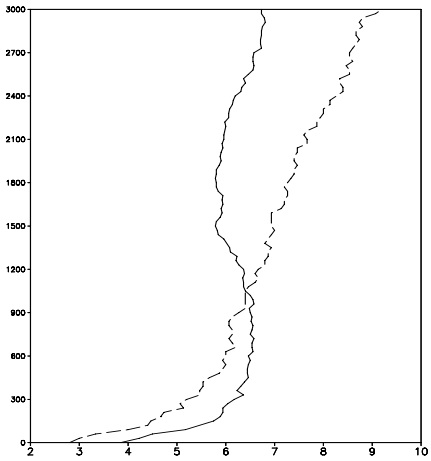

Fig. 6 The daily mean (June to August, 2005) wind speed-height profiles. Solid line is the average for fog days, and the dashed line is the average for non-fog days.

Another progress is about the seasonal variations in the height of ABL top and sea fog frequency (Zhang et al. 2006). The latest research shows that the height of the ABL top goes higher in winter and lower in summer (Fig.7). The lower ABL top can lead to the thinner mixing layer in summer, contributing to the fog season in Qingdao in later spring and summer as shown in Fig.2. It should be pointed out that figures 4-7 are derived from the L-band radar detections in Qingdao Observatory, so these results just stand for the situations above Qingdao.

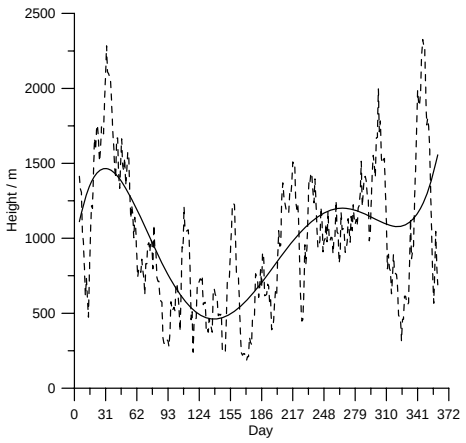

Fig.7 Daily variations of the height of the ABL top in 2005. The dashed line is 9-days smoothing and the solid line is orthogonal polynomial of 5 degree fit.

3 Interannual variations

The study on the interannual variations in the sea fog frequency began in the early 1990s. Most authors were concerned about the statistic relations between ENSO and the sea fog frequency, e.g. Zhao et al.(1990), yet few literatures made discussions about the relevant physical processes. During the past ten years, more attentions have been paid to the mechanism of interannual variations. Factors like the anomalous atmospheric circulation, humidity transport, atmospheric stratification and sea surface longwave radiation have been taken into consideration, and the obvious progresses have been made so far.

According to Zhang et al. (2005), there could be more fog days in May if the atmospheric circulations became more zonal over the Eurasia in the previous winter. In such a case the anomalies of southerly winds could transport more moisture into the Yellow Sea, and the stable stratification occurred more often in the lower and middle layer of atmosphere. Zhou et al. (2004) pointed out further that if the winter atmospheric circulations were stable and strong (meridional), the Yellow Sea area would be primarily still under the control of winter winds in spring. In such circumstances the warm and humid air could hardly approach the Yellow Sea, and the air above the sea was unlikely to reach its dew-point to produce fog even though the SST was very favorable for the formation of sea fog. On the other hand, if the winter circulation was weaker, the westerlies might retreat northward readily, and the weather systems in low latitude would be more active, thus transporting rich moisture to the Yellow Sea. They also found that the moisture, from which the Yellow Sea fog was produced, did not originate from the local sea water but came from tropical ocean. The atmospheric circulations played a role as a conveyor that brought tropical warm and moist air into the Yellow Sea, and the wet air condensed over the cold Yellow Sea water. So the Yellow Sea fog was of monsoonal characteristics in a sense.

Wang et al.(2006) investigated the interannual variations in summer fog in the Yellow Sea

and found that the stronger summer monsoon was in favor of more fog days, while less fog days were found with weaker summer monsoon. The strong summer winds take huge amount of warm and humid air from tropical regions into the Yellow Sea in favor of fog occurrence. A strong low-level jet, deriving from the convergence of the southwest summer monsoon, which comes from the South China Sea and the Bay of Bengal, and the southeast summer monsoon linking to the western Pacific subtropical high, is the most important feature in terms of atmospheric circulation in years of more fog. While in years of less fog the circulation pattern is just the opposite, and that reflects the importance of the low-level jet in the transportation of moisture in the ABL. Another key factor contributing to summer fog formation is SST, which is not important in the occurrence of sea fog in springs. In summer, the sea fog is more common when the SST in the Yellow Sea is higher than usual, leading to a rather small temperature difference between air and sea water. These results deepen our understanding of the interannual variations of sea fog and are very helpful for the short-term climatic prediction of sea fog frequency.

4 Numerical study

4.1 Mechanism of sea fog

Two physical processes are involved in the formation of fog: increasing the humidity and lowering the temperature. Moisture comes merely from the evaporation of the sea surface, but several processes are involved in the cooling, among which the turbulent transport and longwave radiation are the most important. The air in contact with the cold sea surface becomes colder and the cooling effect moves upward by means of wind shear and turbulence. And the air at the top of the fog is cooling by longwave radiation, thus leading to instability in the fog and then the cooling of the lower air. Numerical experiment is the main access to the understanding of these mechanisms. Zhong et al.(1995) develops a two dimensional ABL model, in which several physical processes are considered such as advection, turbulence, longwave radiation, gravitational sinking of the fog droplets, condensation and evaporation. The output of the model emphasizes the longwave radiation cooling in the formation of sea fog. Hu et al.(1997,1998) obtained the similar results by using a deduced formula of relative humidity and pointed out further that the primary mechanism for the occurrence of fog was the longwave radiation cooling, and the turbulent mixing plays a part in the very beginning of fog formation and is just confined to the lower level. They also found that SST contributed to the formation of sea fog but its effect was getting weaker when fog had formed, and that moderate strong wind was unfavorable to the formation of fog but favorable to the advection of fog. Another output of a three dimensional ABL model demonstrates that the temperature and humidity at the lower level upstream can affect the formation of fog downstream (Lian et al. 1995).

4.2 Numerical simulation

It is possible to make numerical fog forecast if the numerical model could simulate the actual fog events successfully. The numerical simulations started just years ago in China and some progresses have been achieved. Fu et al. (2002) simulated a Yellow Sea fog event by means of a three dimensional ABL model, and analyzed the liquid water content, the other physical factors in the processes of the formation, the development and the dissipation of sea fog. The output depicts the development of an advection cooling fog: under the favorable synoptic conditions, the sea fog at first forms just above the sea surface and then develops gradually upward, and the stable ABL is both essential and is exited throughout the process of the fog. Another numerical run indicates that the simulated fog area is coincident with the observations and with the satellite images (Fu et al.2002).

5 Sea fog detecting and monitoring by satellites

China is one of the rare countries possessing their own geostationary and polar orbit satellites. Besides, several satellite service stations in China make it possible to obtain data from NOAA, TERRA and AQUA satellites. During the 10th Five-year Plan of China, the project Modularized Heavy Sea Fog Detection Technique by Remote Sensing supported by the National High-tech R&D Program (863 program) is implemented. It is the first step in China toward the sea fog remote sensing detection by using satellites. The target of the project is to distinguish fog from clouds automatically. For this purpose, different methods, e.g. multi-channel analysis, texture analysis and threshold technique, are used to investigate the spectrum features from satellites FY-2B, GMS5 and NOAA 12-14. Though some problems, especially the discrimination of fog from the lower stratus, remain to be solved, the fog detection techniques developed in the project can provide fog areas based on the satellite observations to a certain extent (Bao, et al. 2005).

In recent years, the satellite-borne radiometer, spectrometer and other high-tech equipments develop rapidly. The Moderate Resolution Imaging Spectroradiometer (MODIS) on AQUA and TERRA have 36 channels, among which channels 1-7 can reflect aerosol information，channels 8-16 can retrieve sea water color, channels 20-30 and channels 31-32 can show surface (cloud top) temperature, channels 17-19 can expose water vapor and channel 24-25 can tell atmospheric temperature. So these data are able to supply information relevant to sea fog from different aspects. Qian et al. (2004) found that the radiance and reflectivity from MODIS channels 1, 3, 4, 8, 16, 24, 25, and 29-36 were well correlated to the visibility with the significant confidence >90% after clouds were filtered. A case study shows that relatively obvious differences exist in radiation and reflection between days with high visibility and poor visibility. Further experiments in the coastal area of South China demonstrate some functional relations between long and successive time

series of visibilities and quantitative retrievals of the MODIS albedo (Qian et al,2006). Based on these relations the classified retrieval models are established and horizontal visibilities are retrieved. The comparison between the conventional observations and the retrievals shows that the visibility can be retrieved well in clear days or in precipitable cumulus situations (correlation coefficients are 0.6 and 0.9 respectively, far beyond 95% confidence), whereas the accuracy lowers under the conditions of fog and low clouds with the correlation coefficient 0.5. Therefore, there is still long way to go to the target of sea fog detection by satellites.

6 Microphysics of sea fog

The microphysics of sea fog is helpful both for the improvement of sea fog model and for the data validation in the process of fog retrieval. The microphysical study of sea fog was rarely found in China before 1980s. During the 8th Five-year Plan, several special field observations were carried out to investigate the microstructure of sea fog and the air-sea interface turbulent flux in the Yellow Sea near the Qingdao coast. Large amount of the first-hand data were collected during that period of time.

6.1 The sea fog droplet spectrum

Fog droplet samples are collected 9 times in Xiaomaidao, a small island very close to Qingdao, from the end of June to the beginning of July, 1993. It is found that (a) the size of sea fog droplets are quite small with the mean radius of about 2.2μm, and about 90% of the droplets are less than 5μm; (b) the concentration of the droplets varies from less than 10/cm^3 in light fog to nearly 250/cm^3 in dense fog; (c) generally no nucleus are found in the droplets less than 10μm (possibly the resolvable nucleus), the droplets of 10-20μm have nucleus obviously, about 20-30％ dry nucleus can be found in strong winds, and opaque salty crystal bigger than 20μm exist sometimes; (d) the droplet spectra appear bimodal patterns and are widened in thick fog, and become narrowed and non-bimodal gradually when fog began scattering. The first peak value is always near the minimum droplets (r=2μm), while the second peak generally appears near bigger droplets of r=8-10μm; and (e) the water content in fog is about 0.207-0.023g/m^3. Based on the above analysis, linear relations between the sea fog water content and the visibility are obtained, and relations between the extinction coefficient and the water content are also established for the Yellow Sea fog near Qingdao in spring-summer period (Xu et al. 1994).

6.2 The turbulent flux at the air-sea interface

The results gained from the field observations indicate that the turbulent exchange in the lower level of atmosphere contribute much to the sea fog appearance and disappearance. In the summer of 1992, a 10m pole with equipments fixed on it was set up in order to obtain wind and temperature gradients near Qingdao offshore. The momentum flux and sensible heat flux close to

the sea surface are calculated from the observed wind and temperature profiles. The results indicate that the stratification of the marine boundary layer (atmospheric boundary layer close to the sea surface) is neutral or stable, and the sensible heat flux is downward i.e. from atmosphere to ocean in the summer. The mean heat flux is 2.5W/m^2 and the maximum is 28.9W/m^2 without obvious daily variations. The turbulent momentum flux is quite weak with the average wind-stress of 0.012N/m^2, and the maximum of 0.042N/m^2.

6.3 Microphysical conceptual model of sea fog

The microphysical conceptual model of sea fog is derived from the analysis of the elementary factors in the marine boundary layer (MBL) during the whole process of a sea fog event that lasts 26 hours. Before the occurrence of the advection fog, there is a strong warm advection in the MBL, thus forming a strong temperature inversion and humidity inversion above the sea surface with the air-sea temperature difference of about 2°C. After the formation of fog, the air-sea temperature inversion is getting weaker gradually due to the molecular exchange at the air-sea interface. At the same time, a rather homogenous layer of air appears because of the effect of dynamic turbulent mixing of the higher level. The stratification turns to neutral instead of the previous stable, and the densest fog occurs. Fog could persist if the winds, and the supplies of the water vapor and the energy remained. The dissipation of fog starts once the winds tapered off, the unbalanced heat energy was used up, and the supplies of water vapor by advection were insufficient to maintain the dense fog.

It is worth mentioning that the microphysical structures and characteristics of sea fog may vary greatly in different droplet samples even though the location, the season and the types of fogs are the same. This reflects the unorganized and chaotic natures of sea fog, and represents the very necessity of further investigations of microphysics of sea fog on the other hand.

7 Conclusions and discussions

Though obvious progresses have been made in the aspects of the meteorological and climatological research, numerical simulation, sea fog detection and etc., great difficulties still exist in respect of the prediction of sea fog occurrence and dissipation, and the real time watching. That is because of the lack of observations and detections over the seas and the lack of understanding the mechanisms involved in the whole progression of sea fog events. The present accesses to the sea fog data are still relied primarily on the surface-based observation systems that are confined to the coastal areas of the continent or to the sparsely distributed islands. The conventional radiosonde is unable to provide data with the resolutions high enough to study the MBL. Great efforts must be made in the microphysical studies in order to improve the sea fog models. The numerical simulations are only for case studies so far, and there is a long way to go to

the operational applications. The techniques of detecting and monitoring sea fog by satellite are still under study, and tremendous and painstaking efforts must be made in order to achieve the goal of sea fog/low stratus discrimination.

China is a developing country with expansive marginal seas. The sea fog happens frequently in the coastal areas and over the seas. No doubt, studies of sea fog are of significant importance to the development of economics and security of society. The central government and the governments of the coastal provinces nowadays pay more and more attention to the sea fog research. The Chinese Meteorological Administration (CMA) has been taking measures to establish the new L-band radar network along the coastal areas. The new generation of L-band radar along with the digital sounding can provide information of the atmospheric boundary layer in a much more detailed way compared with the old ones. Besides, other high-tech equipments, like wind profilers, GPS receivers, visibility sensors, automatic weather stations, and buoy observations have come into use in the marine weather observatories in the coastal provinces. Days ago the new weather satellite FY-2D is successfully launched. More accurate satellite-borne radiometers, sensors, and imagers will supply us with large amount of data over the seas. How to use these unconventional data is a new challenge the meteorologists must face. It could be a big step towards our final target of sea fog forecasting and auto watching, if these data can be fully used.

Acknowledgements

This paper is a section of the Chinese Report especially prepared for IUGG, 2007. The authors wish to thank Dr. Hu Ruijin, Prof. Zhou Faxiu, Prof. Zhao Jinping and Prof. Liu Qinyu for their helpful comments and suggestions. The authors thank Qingdao meteorological bureau and Qingdao weather observatory for providing L-band data. This work is supported by the Scientific and Technological R&D Program of Shandong Province No.2004G G2208111, and the Scientific and Technological R&D Program of Qingdao No. 05-2-NS-35.

References

Bao Xianwen, Wang Xin, Sun Litan, Zhou Faxiu, 2005. The weatherproof detection system of sea fog by remote sensing and its applications. High Technology Letters, 15(1): 101-106.

Chen Yuzhen and Huang Yuzao, 1999. A preliminary analysis of maritime fog in Meizhou Bay. Journal of Oceanography in Taiwan Strait, 18 (1): 49-54.

Fu Gang, Zhang Tao and Zhou Faxiu, 2002. Three-dimensional numerical simulation of real sea fog event over the yellow sea. Journal of Ocean University of Qingdao, 32(6): 859-867.

Fu Gang; Wang Jing-qian; Zhang Mei-gen; Guo Jing-tian; Guo Ming-ke and Guo Ke-cai, 2004. An observational and numerical study of a sea fog event over the Yellow Sea on 11 April, 2004. Journal of Ocean University of Qingdao, 34(5): 720-726.

Hou Wei-fen and Wang Jia-hong, 2004. Analyze zhejiang inshore fog's law and cause. Donghai Marine Science, 22(2): 9-12.

Hu Ruijin and Zhou Faxiu, 1997. A numerical study on the effects of air sea conditions on the process of seafog. Journal of Ocean University of Qingdao, 27(3): 283-290.

Hu Rui-jin; Dong Ke-hui and Zhou Fa-xiu, 2006. Numerical experiments with the advection, turbulence and radiation effects in the seafog formation process. Advances in Marine Science, 20 (1):25-32.

Kong Ningqian, 1997. Characteristic analyzes of sea fog along Guangxi coast. Journal of Guangxi Meteorology, 18(2): 41-45

Lian Jun and Li Yan, 2000. Analyze of sea fog in Dalian sea area. Liaoning Meteorological Quarterly, 1: 5-8.

Qian Jun-ping, Huang Fei, Cui Zu-qing, Zheng Zhi-hong and Wu Zhi-jun，2004. Marine meteorological visibility remote sensing spectral analysis and statistical inversion based on MODIS data. Advances in Marine Sience, 22(10B): 58-64.

Qian Jun-ping, Huang Fei, Wang Guo-fu, Liu Wan-xi, Cui Zu-qiang and Zheng Zhi-hong, 2006. Empirical models for retrieval of atmospheric horizontal visibility over the sea based on MODIS data. Periodical of Ocean University of China, 36(3): 355-360.

Su Hongming, 1998. Climatic analysis of fog in Taiwan Strait. Journal of Oceanography in Taiwan Strait, 17(1): 25-28.

Wang Binhua, 1983. Sea Fog . Oceanography Press, Beijing, pp352.

Wang Houguang and Qu Weizheng, 1997. Sea fog forecasts in Qingdao area. Marine Forecasts, 14(3): 52-57.

Wang Xin; Huang Fei and Zhou Fa-xiu, 2006. Climatic characteristics of sea fog formation of the Huanghai sea in summer. Acta Oceanologica Sinica, 28(1): 26-34.

Xu Jingqi, Zhang Zheng and Wei Hao, 1994. Measurement and analysis of droplet spectrum and liquid water content of sea fog. Transaction of Oceanology and Limnology, 2: 174-178.

Xu Xuran, 1997. Characteristics and the causes of sea fog in the northern part of Jiaodong Peninsula. Marine Forecasts, 14(2): 58-63.

Xu Yanfeng, Chen Shuqin, Dai Qunying and Ye Junwu, 2002. Regularity and formation cause analyses of fog in Zhoushan sea area in spring. Marine Forecasts, 19 (3): 60-64.

Zhang Chaofeng, 2002. The climate characteristic analyzes of sea fog in Guangdong sea area. Journal of Guangdong Meteorology, 2: 20-21.

Zhang Suping, Ren Zhaopeng and Yu Xiaolong, 2006. The seasonal variations in physical characteristics of the atmospheric boundary layer and the influence on sea fog. Submitted.

Zhang Hong-yan; Zhou Fa-xiu and Zhang Xiao-hui, 2005. Interannual change of sea fog over the Yellow sea in spring. Oceanologia et Limnologia Sinica, 36(1): 36-42.

Zhao Xukong, Ban Huizhou, Zhang Yujun and You Baochuan, 1990. ENSO and sea fog in north Yellow Sea. Journal of Oceanography of Huanghai &Bohai Seas. 8(3): 16-20.

Zhou Fa-xiu; Wang Xin and Bao Xian-wen, 2004. Climatic characteristics of sea fog formation of the Huanghai sea in spring. Acta Oceanologica Sinica, 26(3): 28-37.

MARINE SEDIMENT DYNAMICS AND RELATED RESEARCH IN CHINA, 2002-2006

Shu Gao[1], Ai-jun Wang[1,2]

(1. Ministry of Education Key Laboratory for Coast and Island Development, Nanjing University, Nanjing 210093, China；2. Open Lab of Coast and Ocean Environmental Geology, Third Institute of Oceanography, State Oceanic Administration, Xiamen 361005, China)

Abstract: Research in marine sediment dynamics and related disciplines has been carried out by the coastal engineers, physical oceanographers and marine geologists in mainland China. Some progress in this research field has been made over the last four years, in terms of sediment transport and deposition processes, new methods and techniques, coastal morphodynamics, and marine sediment records for global change studies. Further development of marine sediment dynamics in the near future is anticipated in the basic research about the formation of sediment systems, such as the processes of benthic boundary layer, sediment resuspension and transport. It is also anticipated that the science of marine sediment dynamics will be involved more deeply in the earth system and global change sciences, especially in the study of the sediment sequence formation, continuity of sedimentary record, the requirement of information completeness for the past climate and environment changes, coastal morphodynamic simulation and marine ecosystem dynamics.

Keywords: Marine sediment dynamics, methods and techniques, coastal morphodynamics, marine sediment record and global change, China seas

1. Introduction

Research in marine sediment dynamics and related disciplines has been carried out by the coastal engineers, physical oceanographers and marine geologists in mainland China. A number of research groups, belonging to government institutions and universities, are working actively in this field. Such a situation is related to the natural characteristics of China: there are large rivers discharging into the sea with extremely heavy sediment load, wide continental shelf seas with strong tidal currents and complex ocean current systems, and numerous estuaries and coastal embayments that are characterized by active sediment movement. Solution to the engineering problems associated with harbour siltation and maintenance of navigational channels were once of

priority. Today, new problems associated with global changes, sustainable uses of the marine resources and management of the environment become the focus for the research. In this report, we intend to summarize the progress in this field made by the scientists of mainland China over the last four years i.e. between July 2002 and June 2006, on the basis of a literature review of the refereed academic journals mainly in the Chinese language. Additional information can be found by the reader in international journals. The review is presented under the headings of sediment transport and accumulation processes, new methods and techniques, coastal morphodynamics, and marine sediment records and global changes.

2. Sediment Transport and Accumulation Processes in Marine Environments

2.1 Deep sea and continental shelf processes

Because of the different hydrodynamic conditions, the processes of sediment transport and deposition on continental shelves and in deep seas are different. On the continental shelf, the influence of tides is strong, and the patterns of sediment transport and deposition vary with location and spring and neap tidal cycles. The mobility and resuspension of bed sediment are intense in areas where tidal currents are strong. For example, in the Jingtang Channel, in northern Zhejiang Province, where maximum tidal current speed reaches up to 3 m/s on springs, intense resuspension occurs, and the suspended sediment concentration itself becomes an important factor that affect resuspension (Li Z H *et al*., 2006). Studies for the Laizhou Bay in the Bohai Sea show that the grain size distributions can be modified when the settled suspended sediment is mixed with bed sediment (Jiang & Wang, 2005). In the areas where settling and resuspension effects are significant, the mobile layer on small time scales can be much larger than the value of the long-term averaged net accumulation rate and, therefore, the vertical distribution of mean grain size in a sediment core may represent different types of depositional records in the same sedimentary environment (Zhou & Gao, 2004).

In the shelf waters near the Changjiang River estuary and the upwelling areas along the Zhejiang coast, flocculation results in large size aggregates, with more significant influence of near-bottom advection on the suspended sediment flux than on the outer continental shelf; the settling of the suspended matter results in burial of carbon derived from land (Zhang Y S *et al*., 2006). The transport of suspended matter on open continental shelf is controlled by shelf circulation patterns. Generally, little suspended matter can be transported to the east of 126º30´ E both in winter and summer along the 32º N transaction, but along the PN transaction (which has been established for long-term monitoring of material fluxes), the suspended matter can be preserved in summer while transported to the Okinawa Trough in winter (Guo *et al*. 2002). Over the Yellow Sea region, it has been observed that the settling flux varies in different layers in the

water column, with maximum fluxes occurring in the middle layer, and the burial rate of carbon is controlled by settling flux of suspended matter. (Zhang Y S *et al*., 2004). The suspended sediment concentration in the bottom layer is influenced by resuspension processes.

Over China's marginal seas, sediments transport from continental shelf to deep sea is mainly in the form of slumping and gravity induced debris flow (Liu B H *et al*., 2005). Analyses of seismic reflection profiles and sediment cores indicate that the continental slope of the western Okinawa Trough has received abundant sedimentary materials that are derived from the continental shelf of the East China Sea (Li X S *et al*., 2004). In the South China Sea, sediment transport on the continental slope is related to turbidity currents, as indicated by analyses of Sr isotope, grain size and mineralogy; the terrigenous sediments from the northern shelf are spreads southward to about 17º N, with the western Luzon Strait being a major passage for the terrigenous material from the Asian continent, specially China's mainland, to enter the eastern South China Sea (Zhang F Y *et al*., 2005). The region is characterized by highly varied bathymetry, together with complex material sources, seabed features, volcanic eruptions, organism activities and hydraulic conditions. As a result, the sediment transport and deposition processes vary, causing distinct patterns of seabed sediment partitioning (Zhang F Y *et al*., 2004).

2.2 Tidal flat sedimentary processes

In the tidal flat environment in China, time-velocity asymmetry during a flood-ebb tidal cycle is significant, resulting in differences of suspended sediment concentration between the flood and the ebb phases of the tide and net sediment transport. Further, the pattern of sediment transport is affected strongly by tidal creeks and salt-marsh vegetations. On the lower inter-tidal flat, the bed is subjected to wave action, where tidal creeks are rare and vegetation cover is absent, and the mobility of bed sediment is enhanced to such an extent that the normal sequence is severely modified (Fan *et al*., 2004) and the bed-load transport rate is large (Jia et al. 2006; Wang Y P *et al*. 2006a). From the middle to the upper parts of the inter-tidal flat, the density of the tidal creeks shows a tendency of increase. Different sediment transport patterns are found between the flat surface and tidal creeks: net sediment transport is directed towards the land on the flat surface (Li Z H *et al*., 2005), whilst it is towards the sea in tidal creeks (Yang Y *et al*., 2003; Li Z H *et al*., 2005; Wang A J *et al*., 2006). During the ebb, the water mass from the marsh surface discharging into the creek systems causes significant time-velocity asymmetry in the creeks (Li Z H *et al*., 2005). The tidal creek connects the upper flat with the open sea during the flood-ebb cycle, transporting sediment towards the land during the flood and towards the sea during the ebb; this is a major form of material exchange between the sea and the flat surface.

Spartina alterniflora is an exotic plant introduced to China in the 1980s, which has a higher

net primary productivity than that of the native salt-marsh plants (Chen Y N *et al*., 2005). At the same time, the sedimentary and morphological evolution of tidal salt-marshes has been influenced significantly by *Spartina alterniflora*. For example, the presence of *Spartina alterniflora* can enhance the deposition rate and change the morphological evolution processes, which can be related to the processes that fine-grained sediment is trapped by *Spartina alterniflora* within the marsh (Wang A J *et al*., 2006). Moreover, the existence of *Spartina alterniflora* can also change the cross-sectional shape of tidal creeks (Wang A J *et al*., op cit.).

2.3 Estuarine sedimentary processes

Sediment transport and deposition in China's estuaries are influenced by freshwater and sediment discharges. In response to the spatial variations in water and sediment movement and in the conditions of sedimentary environments (Wang Y P *et al*., 2006b), there exist significant spatial differences of geomorphic characteristics, erosion and deposition patterns, distribution of suspended matter in the estuarine waters (Li J *et al*., 2003; Cheng H Q *et al*., 2004; Liu G F *et al*., 2005a, b; Wang Y P *et al*., 2005). Under the action of normal tidal currents, the bed sediment within the estuary is resuspended to generate relatively high suspended sediment concentrations (SSCs) in the water column, but the SSC decreases in coastal waters that are far from the estuarine mouth because of reduced resuspension of bed sediment (Jiang & Wang, 2005). The sediment dynamic environment of China's estuaries is controlled by both the river discharge and the marine forces, and resuspension of bed sediment by strong tidal currents tends to be responsible for the formation of turbidity maxima in the estuaries (Gao J H *et al*., 2004a). Further, fluid mud tends to form during the slack water periods (Jiang & Yao, 2006).

The processes of suspended sediment transport are complicated and changeable because of the river-sea interaction. An analysis of periodic changes in suspended sediment flux on the basis of a fractional model shows that the transport mechanisms of residual fluxes are dominated by Lagrangian transport and tidal pumping (Wu *et al*., 2002). The water temperature and salinity vary with the river discharges, which influence the estuarine mixing. As a result, the flocculation processes for suspended sediment are affected. *In situ* observations have indicated that the main factors affecting flocculation include water temperature, the length of period of time, salinity, particle size of suspended matter, SSC and current speed, the listing of the factors being in an order of reduced correlation with the flocculation intensity (Jiang *et al*., 2002).

Under the influences of human activities, freshwater and suspended sediment fluxes from the rivers are reduced, resulting in reduction of the quantity of sediment that is accumulated and the deposition rate in the estuarine and deltaic areas (Yang S L *et al*., 2003; Chen X Q *et al*., 2005). Likewise, the suspended sediment transport processes in estuaries are also modified by localized

human activities such as sediment disposal associated with harbor and navigation channel dredging (Wu J X *et al*., 2003, 2005).

2.4 Sediment grain size trend analysis

The purpose of grain size trends analysis (GSTA) is to define net sediment transport pathways. Since this method was proposed, improvements to the analytical procedure have been made and it has been applied widely to sediment dynamic area in China in recent years. On the basis of GSTA for the Bohai Strait and the continental shelf of the northern Yellow Sea, Cheng P *et al*. (2004) analyzed the sediment dynamic environment in combination with the information on sediment supply and shelf circulation. Because the natural environment of the coastal zone is highly dynamic, it is necessary to take the environmental conditions into account in interpreting any results of GSTA. For example, the sediment transport trend may be masked by short-term transport induced by localized anthropogenic processes like port construction and salt-marsh vegetation planting (Wang A J *et al*., 2004a), and the sediment transport patterns can become very complicated where the tidal current is influenced by geomorphic features such as tidal creeks (Jia *et al*., 2006).

The processes and mechanisms for the formation grain size trends still represent a scientific problem for which improved solutions are required. Based on *in-situ* observations of tidal current and suspended sediment, Jia *et al*. (2006) calculated the bed-load transport rate and compared the results with the quantitative information on sediment transport derived from GSTA; they have attempted to explain the observed grain size trends using sediment dynamic principles.

3. Methods, techniques and applications

3.1 Numerical modeling techniques

Numerical modelling is an important approach for the study of sediment dynamic processes, and has been used extensively to investigate into the coastal and estuarine sediment dynamics in China. For instance, Jiang D H *et al.* (2002) studied the sediment transport processes of Bohai Strait using a numerical model, Gao & Jia (2003) simulated the distribution patterns and deposition processes of suspended matter at the upwelling and downwelling area on the continental shelf, and Zhu & Zhang (2005) simulated the characteristics of the paleo-estuary of the Changjiang River and the paleo-current off the northern Jiangsu coast and analyzed the evolution of the radial sand ridges of the southern Yellow Sea.

Achievements have been obtained on the simulation of current and suspended sediment transport in coastal and estuarine waters. With a modification to the sediment erosion function, Xu & Liu (2003) established a 2-D numerical model for the sediment transport in the Lingdingyang

area in the Zhujiang River estuary. Ding *et al*. (2003) developed a 2-D numerical model for total sediment transport; they used this model to simulate suspended sediment and bed-load transport under combined waves and currents with an improved precision of the calculations, and to calculate the bed erosion and deposition rates in response to typhoon events. Hu *et al*. (2004) used the SWAN model to simulate typhoon waves, with certain success.

For 3-D numerical models, Li M G *et al*. (2003) developed a mathematical model for suspended sediment movement caused by tidal current, using a vertical coordinate transformation technique and a finite difference scheme; in the model, the advective terms of the advection-diffusion equation of suspended sediment were treated with a third-order upwind scheme in order to enhance the model stability and reduce the numerical diffusion. By taking into account the river sediment discharge, flocculation of suspended sediment and spatial variations of bed erosion and deposition, Chen X H *et al*. (2005) developed a 3-D transport model for suspended sediment transport under non-equilibrium conditions in the Pearl River estuary by coupling with a 3-D baroclinic hydrodynamic model; the simulated results represent the general pattern of the estuary and agree well with the *in-situ* observations.

3.2 Remote sensing techniques

Remote sensing techniques have been applied extensively in sediment dynamics and related research areas. It has been a focus to study sea surface suspended sediment concentration by remote sensing models. Statistical modeling is the most frequently used method to establish the relationship between the remote sensing data and *in-situ* suspended sediment concentration observations. For example, a remote sensing algorithm to retrieve suspended sediment concentrations from the reflectance of NOAA/AVHRR Channels 1 and 2 has been applied to the Pearl River estuarine waters (Deng *et al*., 2002). In this algorithm, the atmosphere effect is removed on the basis of a study on the correlation curve between the two channels. The results indicate that the concentration data derived from remote sensing by the slope method has a high stability. Another approach is to determine the suspended sediment parameters, the sensitive wave bands and the various combinations of suitable wave bands on the basis of an analysis of the spectrum characteristics of suspended sediment and the data sets derived from *in-situ* experiments (Song *et al*., 2004; Liao *et al*., 2005; Li H L *et al*., 2006).

Patterns of shoreline changes can be detected using a series of remote sensing images of different times. Thus, Han and Yun (2003) applied the technique of reverse algorithm for shoreline elevation determination to analyze the evolution of the coastline of the Dachan Bay, Guangdong Province. Subsequently, other researchers began to study coastal changes using the similar method (Huang & Fan, 2004a, b; Fan & Huang, 2004). Furthermore, this multi-period image analysis has

been also used to monitor the changes of bio-geomorphology characteristics in the coastal zone, such as the evolution patterns of mangrove wetlands in estuaries (Li & Han, 2002; Li X *et al*., 2006) and the expansion of *Spartina alterniflora* on the Jiangsu coast (Zhang R S *et al*., 2004).

3.3 Observations of sediment dynamic processes

In-situ observations form a basis for marine sediment dynamic studies and for the verification of any numerical models. Recently, it has become one of the research topics to obtain the information on suspended sediment concentrations using acoustic measurements. Based on theoretical and experimental studies of acoustic attenuation in suspended sediment, new ultra-sonic instruments for real-time measurements of suspended sediment concentrations have been developed, which can be used to determine the concentration in very turbid environments (Zhang & Qian, 2003). Progress has been made in the study of deriving suspended sediment concentration data from ADCP acoustic signature (Wu J *et al*., 2003a, b; Gao J H *et al*., 2004b; Wang Y P *et al*., 2005; Wang Y P *et al*., 2006b). In analyzing the single-channel acoustic backscatter data in relation to suspended sediment concentrations, caution should be taken to discriminate the effects of the concentration and the grain size. Detailed knowledge of the characteristics of the suspended sediment, therefore, is essential for obtaining an accurate measurement. Based on the Rayleigh Scattering Theory, the equivalent particle radius as well as the calibration equation has been derived for grain size correction obtained by *in-situ* observation using a LISST-100, and data analysis of these field tests has shown considerable improvements following the application of the grain size correction formula (Lan *et al*., 2004). Finally, a method using flow structure to interpolate the current speed within the blind layers associated with ADCP measurements has been proposed to obtain a complete current velocity profile in an estuarine environment (Wang A J *et al*., 2004b).

In the mudflat environment associated with small water depth, high current speed and rapid erosion and accretion, the water depth tends to be smaller than the tidal boundary layers in deep waters. In order to understand the boundary layer process in extremely shallow water areas, Wang Y P *et al*. (2004) observed the boundary layer characteristics using a self-made system for water level, current speed and turbidity monitoring on an inter-tidal flat in northern Jiangsu Province. They found that around 90% of the velocity profiles were in agreement with the logarithmic distribution, and the boundary layer parameters calculated by the logarithmic profile revealed some of the processes at the water-sediment interface. However, limitation of this system exists in terms of its ability to dealing with wave data on the mid-lower inter-tidal flat; here, wave action represents an important hydrodynamic forcing (Fan *et al*., 2004, 2006). In order to obtain high resolution sediment dynamic data, a MIDAS-400 Customized Data Acquisition System was

deployed to obtain current velocity and suspended sediment concentration profiles on the inter-tidal flat of the Jiangsu coast (Wang Y P *et al*., 2006a). The results show that the apparent bed roughness length has a magnitude close to the height of ripples, much larger than the grain size diameter. The bottom shear stress associated with current-wave interaction is higher than the tidally-induced stress, enhancing the turbulent mixing and resuspension processes. Furthermore, several suspended sediment concentration peaks occurred during a tidal cycle, which can be related to strong turbulence near the bed caused by frontal tidal currents and the enhanced resuspension. This study demonstrates that the MIDAS-400 is a suitable tool for high-resolution data collection for the situations of combined current-wave action over inter-tidal flats (Wang Y P *et al*., 2006a).

3.4 Application of isotope dating techniques

Research in sedimentation rates has been active in recent years due to the application of isotope techniques of ^{210}Pb and ^{137}Cs in coastal and continental shelf environments. The content of ^{210}Pb enriched in fine-grained sediment (Wang A J *et al*., 2005). Therefore, the feasibility of dating analysis is limited by sediment types. Sedimentation rates of the continental shelf mud patches have been shown to be relatively stable (Li F Y *et al*., 2002). Apparently, the technique of ^{137}Cs is not influenced by sediment type, and the average sedimentation rate can be calculated on the basis of the measurement of the ^{137}Cs background value (Meng W *et al*., 2005). However, the calculated value of sedimentation rates may be exaggerated if the diffusion of ^{137}Cs within the stratum is ignored. Further, in the area with high sedimentation rates, the sediment cores may be too short to define the ^{137}Cs background value. In this case, sedimentation rates may be calculated using some assumption about the peak of ^{137}Cs, but it must be calibrated using other sedimentation rate data (Wang A J *et al*., 2005). A requirement for ^{210}Pb and ^{137}Cs dating is that the deposited sediment will not change. In reality, however, disturbances occur; for example, the roots of salt-marsh plants may penetrate into the stratum by 1 m to cause sediment exchange between the different layers. Such processes may reduce the accuracy of the dating analysis (Wang A J *et al*., 2006). Further studies are needed to provide solutions to such problems.

3.5 Tracer methods in marine sediment dynamics

Tracing is an important method in marine sediment dynamic studies. There are qualitative and quantitative approaches. In qualitative research, based on analyses of heavy minerals components and compounding characteristics of surfacial sediment samples from the Xinghua Bay, Fujian Province, silty materials are shown to be derived mainly comes from fluvial input and bedrock erosion of the nearby coast and the islands within the Xinghua Bay (Xu M Q *et al*., 2004).

Based on analysis of the samples collected from the eastern South China Sea, the material sources for the different areas of the South China Sea are determined using the tracing method (Zhang F Y *et al*., 2005).

Quantitative tracing is dependent upon mixing models (Gao, 2003). These models require a sufficiently large number of fingerprints that remain stable during transport. If this condition is not satisfied, then some of the less stable fingerprints may be added, the premise being that the changes of these fingerprints during transport must be defined. Clay minerals are often used for quantitative tracing. Preliminary studies indicate that the relative contents of illite, montmorillonite and kaolinite are stable during transport and, therefore, these clay minerals are suitable for the purpose of quantitative tracing (Zhou *et al*., 2003; Gao *et al*., 2004). Generally, further studies are required with regard to the changes in the physical and chemical properties of clay minerals after leaving the river mouth, especially those associated with flocculation for cohesive sediment, differential settling of clay particles, biogeochemical processes and early diagenesis.

4. Research of coastal morphodynamics

4.1 Morphodynamics of tidal inlet systems

Tidal inlets are common geomorphic features on the coast. Within the entrance channel, time-velocity asymmetry is often observed (Jia *et al*., 2003a, b). The bed-load transport rate is adaptive to the time-velocity asymmetry pattern (Xue *et al*., 2002), forming a morphodynamic system that results from the sediment dynamic conditions. Recent studies have revealed some interesting time-velocity asymmetry patterns associated with small inlet systems (Jia *et al*., 2003a): any of the four combinations of the flood-ebb durations and the flood-ebb velocities will occur in a small inlet, although the frequency of occurrence differs. Such a phenomenon is due to the geomorphological adjustment of the cross-section shape at the entrance of small tidal inlets.

The relationship between tidal prism on spring tide (P) and the cross-sectional area at the entrance channel (A) represents the equilibrium condition of tidal inlets, which can be expressed mathematically as a power-law function. Jia *et al*. (2005) have proposed a sediment dynamic approach to the P-A relationship for a tidal inlet. According to this method, the tidal inlet system is related to a number of hydrodynamic and sediment dynamic factors including flood and ebb durations, cross-sectional mean current velocity, the cross-sectional shape of the entrance channel, freshwater discharge, longshore sediment transport rate and sediment property. An equilibrium P-A relationship for the tidal inlet varies with changes in any of these factors. An example from the Yuehu Inlet, a small inlet-lagoon system in Shandong Peninsula, shows that the value of parameter *n* in the P-A relationship is around 1.15 under equilibrium conditions.

4.2 Shoreline morphodynamics

The evolution of coastal geomorphology results from comprehensive interaction between endogenic and exogenic forces. The endogenic force controls the large scale patterns of coastal geomorphology, whilst the exogenic force mainly affects the processes of sediment erosion, transport and deposition. In the shoreline environment, the combined action of waves and currents plays an important role in the threshold for initial sediment motion (Cao *et al*., 2003), and such processes shape the intermediate to small scale geomorphological features (Cai F *et al*., 2005). The shoreline geomorphology may reach a dynamic equilibrium status under normal conditions, but equilibrium is disturbed by natural or antropogenic events such as typhoon events (Cai F *et al*., 2006) and sand mining activities (Li F L *et al*., 2004). Moreover, the evolution of shoreline geomorphology is related to sediment supply and spatial variations in dynamic factors, resulting in a high diversity in terms of the processes of shoreline evolution and coastal profile stability (Zhang & Zhang, 2004).

4.3 Morphodynamics of catchment-coast systems

In recent years the study of the morphodynamics of catchment-coast systems has been focused on the dynamic evolution of estuarine and coastal geomorphology in response to changes in freshwater and sediment discharges from the rivers due to anthropogenic activities in the catchment. For example, based on the observations undertaken in the Changjiang River estuary, Cheng H Q *et al*. (2004) have revealed that the ebb and flood tidal currents, bed sediment particle size and sandwave morphology are controlled by the seasonal variations in runoff; they have proposed a new transition boundary between ripples and dunes in the estuarine channel floored with very fine sand. Observations in flood and dry seasons of the Changjiang River enabled Liu G F *et al*. (2005a) to find that the sedimentary environment differs significantly in both flood and ebb channels. Comparison of the charts of different periods shows that the Xinqiao Channel in the Changjiang estuary has been already in its dynamic equilibrium status for the last 50 years after a long period of adjustment and, if the basic conditions of the Changjiang catchment remain unchanged, then this channel will maintain its equilibrium (Wang Y H *et al*., 2005). Because the river discharges are decreasing due to the catchment human activities (e.g. dam building and sand mining in the river channel) (Chen X Q *et al*., 2005), changes in the geomorphology of the estuarine and adjoining areas are taking place, such as shift of the main channel in the estuarine area (Wang H J *et al*., 2005), decrease in sand bar size (Yang Z S *et al*., 2005), migration patterns of tidal creek systems in the estuarine delta (Huang & Fan, 2004b), and changing patterns of sea bed erosion (Wang H *et al*., 2004). In the Pearl River estuary, the “gate” is a special morphological

feature, and its existence has to a large extent changed the relationship between marine and river dynamics, which plays an important role in the long-term evolution of the river channel network and the geomorphologic characteristics of the Pearl River delta (Wu C Y *et al*., 2006).

5. Marine sedimentary record and global change

The study of marine sediment record is an important aspect in the "past global change" research. Grain size parameters represent an indication of the processes of sediment transport and accumulation and are therefore useful in establishing the indices of environmental changes. Based on grain size analysis for two sediment cores collected from the Okinawa Trough and Ryukyu Trench, Sun *et al.* (2003) have compared the sediment sources and environmental characteristics at the two sites and proposed the rate and cyclicity of environmental changes. Xiang *et al.* (2003) have utilized the combined data of sediment grain size, sedimentation rate, geochemistry, minerals and micropaleontology, to analyze the environmental changes of the Okinawa Trough and to establish a relationship with the intensity of the Kuroshio since the beginning of the Holocene. Different methods for particle size analysis and grain size parameter calculation exists, which may cause problems in the comparison of the parameters. In order to overcome this difficulty in the interpretation of grain size data, Jia *et al.* (2002) have established a relationship between the parameters obtained using graphic and moment methods.

Recently, shallow seismic survey has been undertaken frequently in studying the marine sediment record. Thus, high resolution seismic profiles have analyzed by Wu & Wong (2002) to study the Quaternary sedimentary sequences, crust movement, sedimentary processes and environmental changes; they revealed the sediment composition, the age of the deposits and evolution of paleo-river channels in the area off the southern Guangdong coast. Based on seismic survey, Liu A C *et al.* (2005) analyzed the characteristics of paleo-river channels that had been filled and buried by continental shelf sediment during Holocene sea level rise. Finally, seismic profiles from the sub-aqueous delta of the Yellow River have been analyzed to identify environmental evolution patterns during the Holocene in relation to sea level change (Wang G Z *et al*., 2003; Liu J P *et al*., 2004).

Another main approach to the study of the sedimentary and environmental changes is analysis of sediment cores. In this research area, Liu B Z *et al.* (2005) have studied the characteristics of paleo-currents over the Changjiang River delta areas, using magnetic, established the chronology of the sequences and reconstructed the sedimentary paleo-environments of the region. Based on the analysis of clay mineralogy for the samples collected from the southern Changjiang River delta, four sedimentary environment zones have been identified using the mineral suits (Wang Z H *et al*., 2006). Using the dating data of sediment

cores from the Bohai Bay, Meng G L *et al*. (2005) analyzed the patterns of climate and sea level changes on the northern China coast, and identified a warm stage of the Holocene before 6 ka with sea level being 1.3 m higher than the present. Based upon the data from 500 bore holes, Lin C M *et al*. (2005) analyzed the evolution of the Qiantangjiang Estuary infilling processes since the late Quaternary, in relation to sea level rise.

6. Future research directions

The further development of marine sediment dynamic will depends on the deep basic researches in the subject and the involvement in the research of earth system process and global change. For the former aspect, contemporary processes for the formation of sediment systems, such as the processes of benthic boundary layer, resuspension and transport, are still the main focus. Generally, quantitative description of these processes has not yet been achieved. For the latter aspect, i.e. earth system process and global change, the science of marine sediment dynamics can make significant contributions in the study of the processes of the sediment sequence formation, continuity of sedimentary record, the requirement of information completeness for the past climate and environment changes, simulation of coastal morphodynamics and the processes of marine ecosystem dynamics.

Acknowledgements: This study is supported financially by the Natural Science Foundation of China (Grant Number 40231010). During the study Shu Gao was supported also by the APN funded project “Climate variability and human activities in relation to Northeast Asian land-ocean interactions and their implications for coastal zone management” (M2003-17SG and 2005-18-CMY).

References

Cai F，Lei G，Su X Z，et al.. Study on process response of Fujian beach geomorphology to typhoon Aere. The Ocean Engineering，2006，24（1）：98-109. (in Chinese with English abstract)

Cai F，Su X Z，Cao H M，et al.. Analysis on morphodynamics of sandy beaches in South China. Acta Oceanologica Sinica，2005，27（2）：106-114. (in Chinese with English abstract)

Cao Z D，Kong L S & Jiao G Y. Initiation of sediment movement for a wave－current coexistent system. Acta Oceanologica Sinica，2003，25（3）：113-119. (in Chinese with English abstract)

Chen X H，Chen Y Q & Lai G Y. Modeling transportation of suspended solid in Zhujiang River estuary，South China. Chinese Journal of Oceanology & Limnology，2005，23（1）：1-10.

Chen X Q，Zhang E F，Mu H Q，et al.. A preliminary analysis of human impacts on sediment discharges from the

Yangtze，China，into the sea. Journal of Coastal Research，2005，21：515-521.

Chen Y N，Gao S，Jia J J，et al.. Tidalflat ecological changes by transplanting Spartina anglica and Spartina alterniflora，northern Jiangsu Coast. Oceanologia et Limnologia Sinica，2005，36（5）：394-403. (in Chinese with English abstract)

Cheng H Q，Shi Z，Ray K，et al.. Stability field for sand bedforms at the south Branch and the South Channel in the Changjiang (Yangtze) estuary. Oceanologia et Limnologia Sinica，2004，35（3）：214-220. (in Chinese with English abstract)

Cheng P，Gao S & Bokuniewicz H. Net sediment transport patterns over the Bohai Straight based on grain size trend analysis. Estuarine，Coastal and Shelf Science，2004，60（2）：203-212.

Deng M，Huang W & Li Y. Data collection of remote sensing derived suspended sediment concentration in Zhujiang River estuary. Oceanologia et Limnologia Sinica，2002，33（4）：341-348. (in Chinese with English abstract)

Ding P X，Hu K L，Kong Y Z，et al.. Numerical simulation of total sediment under waves and currents in the Changjiang Estuary. Acta Oceanologica Sinica，2003，25（5）：113-124. (in Chinese with English abstract)

Fan D D，Guo Y，Wang P，et al.. Cross-shore variations in morphodynamic processes of an open-coast mudflat in the Changjiang Delta，China：with an emphasis on storm impacts. Continental Shelf Research，2006，26：517-538.

Fan D D，Li C X，Wang D J，et al.. Morphology and sedimentation on open-coast intertidal flats of the Changjiang delta. Journal of Coastal Research，2004，SI（43）：23-35.

Fan H & Huang H J. Changes in Huanghe (Yellow) River estuary since artificial re-routing in 1996. Chinese Journal of Oceanography and Liminology，2005，23：299-305.

Gao J H，Gao S，Cheng Y，et al.. Suspended sediment movement and the formation of turbidity maxima in Yalu River Estuary. Journal of Coastal Research，2004a，SI43：134-146.

Gao J H，Wang Y P，Wang A J，et al.. Suspended sediment behavior and transport in Changjiang River Estuary. Geographical Research，2004b，23（4）：455-462. (in Chinese with English abstract)

Gao S. Tracer methods in marine sediment dynamics. Acta Sedimentologica Sinica，2003，21（1）：61-65. (in Chinese with English abstract)

Gao S & Jia J J. Modeling suspended sediment distribution in continental shelf upwelling / downwelling settings. Geo-Marine Letters，2003，22（3）：218-226.

Gao S，Zhou X J & Jia J J. Clay mineral suites of the coastal mud belt associated with the Changjiang River. Revista de la Asociación Argentina de Sedimentología，2004，11（1）： 1-8.

Guo Z G，Yang Z S，Zhang D Q，et al.. Seasonal distribution of suspended matter in the northern East China Sea and barrier effect of current circulation on its transport. Acta Oceanologica Sinica，2002，24（5）：71-80. (in Chinese with English abstract).

Han Z & Yun C X. Deposition and erosion remote-sensing reverse of Dachan Bay beach in Lingdingyang estuary.

Acta Oceanologica Sinica，2003，25（5）：58-64. (in Chinese with English abstract)

Hu K L，Ding P X，Zhu S X，et al.. Numerical simulation of typhoon waves around the waters of the Changjiang Estuary. Acta Oceanologica Sinica，2004，23（5）：23-33. (in Chinese with English abstract)

Huang H J & Fan H. Monitoring changes of nearshore zones in the Huanghe (Yellow) River delta since 1976. Oceanologia Et Limnologia Sinica，2004a，35（4）：306-314. (in Chinese with English abstract)

Huang H J & Fan H. Change Detection of Tidal Flats and Tidal Creeks in the Yellow River Delta Using Landsat TM/ETM +Images. Acta Geographica Sinica，2004b，59（5）：723-730. (in Chinese with English abstract)

Jia J J & Gao S. Sediment dynamic approach to the establishment of P-A relationship for tidal inlet systems. Oceanologia et Limnologia，2005，36（3）：268-276. (in Chinese with English abstract)

Jia J J，Gao S & Xue Y C. Grain-size parameters derived from graphic and moment methods：a comparative study. Oceanologia et Limnologia Sinica，2002，33（6）：577-582. (in Chinese with English abstract)

Jia J J，Gao S & Xue Y C. Patterns of time-velocity asymmetry at the Yuehu Inlet，Shandong Peninsula，China. Acta Oceanologica Sinica，2003a，25（3）：68-76. (in Chinese with English abstract)

Jia J J，Gao S & Xue Y C. Sediment dynamics of small tidal inlets：an example from Yuehu Inlet，Shandong Peninsula，China. Estuarine，Coastal and Shelf Science，2003b，57：783-801.

Jia J J，Wang Y P，Gao S，et al.. Interpreting grain-size trends associated with bedload transport on the intertidal flats at Dafeng，Central Jiangsu Coast. Chinese Science Bulletin，2006，51（3）：341-351.

Jiang D H，Gao S & Cheng P. Modeling sediment transport in the Bohai Straight. Oceanologia et Limnologia Sinica，2002，33（5）：553-561. (in Chinese with English abstract)

Jiang G J & Yao Y M. Periodical changes of mud fluid in the Northern Channel of Changjiang Estuary in China. Acta Oceanologica Sinica，2006，28（2）：135-139. (in Chinese with English abstract)

Jiang G J，Yao Y M & Tang Z W. The analysis for influencing factors of fine sediment flocculation in the Changjiang Estuary. Acta Oceanologica Sinica，2002，24（4）：51-57. (in Chinese with English abstract)

Jiang W S & Wang H J. Distribution of suspended matter and its relationship with sediment particle size in Laizhou Bay. Oceanologia et Limnologia Sinica，2005，36（2）：97-103. (in Chinese with English abstract)

Lan Z G，Gong D J，Yu X S，et al.. Particle size correction of suspended sediment concentration measured by ADCP with in-situ particle size analyzer. Oceanologia et Limnologia Sinica，2004，35（5）：385-392. (in Chinese with English abstract)

Li F L，Xia D X，Wang W H，et al.. Discussion on the evolution causes and its recovery for the Dengzhou Shoal，China. Acta Oceanologica Sinica，2004，26（6）：65-73. (in Chinese with English abstract)

Li F Y，Gao S，Jia J J，et al.. Contemporary deposition rates of fine-grained sediment in the Bohai and Yellow Seas. Oceanologia et Limnologia Sinica，2002，33（4）：364-369. (in Chinese with English abstract)

Li H L，Zhang Y & Jiang J. Study on the inversion model for the suspended sediment concentration in remote sensing technology. Advances in Water Science，2006，17（2）：242-245. (in Chinese with English abstract)

Li J，Gao S，Zeng Z G，et al.. Particle size characteristics and seasonal variability of suspended particulate

materials in the Changjiang River estuary. Oceanologia et Limnologia Sinica，2003，34（5）：499-510. (in Chinese with English abstract)

Li M G，Shi Z & Qin C R. Three-dimensional suspended sediment movement simulation of the Lingdingyang Bay. Journal of Hydraulic Engineering，2003，（4）：51-57. (in Chinese with English abstract)

Li T H & Han P. Detection and analysis of mangrove changes with multi-temporal remote sensed imagery in the Shenzhen River estuary. Journal of Remote Sensing，2002，6（5）：364-360. (in Chinese with English abstract)

Li X，Liu K & Wang S G. Mangrove Wetland Changes in the Pearl River Estuary Using Remote Sensing. Acta Geographica Sinica，2006，61（1）：26-34. (in Chinese with English abstract)

Li X S，Liu B H，Wu J L，et al.. Seismic reflection facies and deposit systems in the west slope of the Okinawa Trough. Oceanologia et Limnologia Sinica，2004，35（2）：120-129. (in Chinese with English abstract)

Li Z H，Gao S，Ke X K，et al.. Sediment dynamic processes of a salt marsh creek and adjacent tidal flats on the Dafeng Coast, Jiangsu, China. Acta Oceanologica Sinica，2005，27（6）：75-82. (in Chinese with English abstract)

Li Z H，Gao S & Shen H T. Processes of suspended sediment transport and resuspension in Jintang Channel. Journal of Sediment Research，2006，（3）：55-62. (in Chinese with English abstract)

Liao Y D，Zhang W & Deschamps P Y. Remote sensing of suspended sediments in China east coastal waters from SeaWiFS data. Journal of Hydrodynamics，2005，25（5）：558-564. (in Chinese with English abstract)

Lin C M，Zhuo H C & Gao S. Sedimentary facies and evolution in the Qiantang River incised valley，eastern China. Marine Geology，2005，219：235-259.

Liu A C，Lü W Y & Cai F. A buried meandering river of Late Quaternary off Shantou City，Guangdong Province. Oceanologia et Limnologia Sinica，2005，36（2）：104-110. (in Chinese with English abstract)

Liu B H，Li X S，Zhao Y X，et al.. Debris transport on the western continental slope of the Okinawa Trough：slumping and gravity flowing. Oceanologia et Limnologia Sinica, 2005，36（1）：1-9. (in Chinese with English abstract)

Liu B Z，Saito Y，Yamazaki T，et al.. Anisotropy magnetic susceptibility (AMS) characteristics of tide-influenced sediments in the Late Pleistocene-Holocene Changjiang incised-valley fill，China. Journal of Coastal Research，2005，21（5）：1031-1041.

Liu G F，Shen H T，Wu J X，et al.. The study of hydrodynamic characteristics of flood and ebb channels and channel type judgment. Acta Oceanologica Sinica，2005a，27（5）：151-156. (in Chinese with English abstract)

Liu G F，Zhu J R，Shen H T，et al.. Study on mechanism of water and suspended sediment transport in flood and ebb channels. Journal of Sediment Research，2005b，（5）：51-57. (in Chinese with English abstract)

Liu J P，Milliman J D，Gao S，et al.. Holocene development of the Yellow River's subaqueous delta，North Yellow Sea. Marine Geology，2004，45-67.

Meng G L，Han Y S & Wang S Q. Middle-Holocene warm period and sea level high in coastal areas，North China. Chinese Journal of Oceanology and Limnology，2005，23（2）：252-258.

Meng W，Lei K，Zheng B H，et al.. Modern sedimentation rates in the intertidal zone on the west coastal zone of the Bohai Gulf. Acta Oceanologica Sinica，2005，27（3）：67-72. (in Chinese with English abstract)

Song L S，Chen W，Xiang W H，et al.. Remote sensing model for sediment information of Hangzhou Bay based on rough sets. Journal of Hydraulic Engineering，2004，（5）：58-63. (in Chinese with English abstract)

Sun Y B，Gao S & Li J. Preliminary analysis of the grain-size populations with environmentally sensitive terrigenous constituents in a marginal sea setting. Chinese Science Bulletin，2003，48（2）：184-187.

Wang A J，Gao S，Jia J J，et al.. Contemporary sedimentation rates on salt marshes at Wanggang，Jiangsu，China. Acta Geographica Sinica，2005，60（1）：61-70. (in Chinese with English abstract)

Wang A J，Gao S & Jia J J. Impacts of Spartina alterniflora on sedimentary and morphology evolution of Wanggang tidalflat，Jiangsu，China. Acta Oceanologica Sinica，2006，28（1）：92-99. (in Chinese with English abstract)

Wang A J，Wang Y P & Gao S. Determination of current velocity in blank layer of ADCP. Journal of Hydraulic Engineering，2004b，（10）：77-82. (in Chinese with English abstract)

Wang A J，Wang Y P & Yang Y. Surface sediment characteristics and transport trends on the Wanggang intertidal flat，Jiangsu Province. Acta Sedimentologica Sinica，2004a，22（1）：124-129. (in Chinese with English abstract)

Wang G Z，Gao S & Li F Y. Holocene mud deposits in the northwestern Yellow Sea. Acta Oceanologica Sinica，2003，25（4）：125-134. (in Chinese with English abstract)

Wang H，Fan W & Yun C X. Indicators and impact analysis of sediment from the Changjiang Estuary and East China Sea to the Hangzhou Bay. Acta Oceanologica Sinica，2004，23（2）：297-308.

Wang H J，Yang Z S，Bi N S，et al.. Huanghe River, water-sediment regulation scheme，river plume，rapid shifts，cluster of mouth bars. Chinese Science Bulletin， 2005，50（24）：2878-2884.

Wang Y H，Shen H T，Li G X，et al.. Calculation of the amount of siltation and erosion in the Xinqiao Channel of the South Branch of the Chan iang Estuary in China. Acta Oceanologica Sinica，2005，27（5）：145-150. (in Chinese with English abstract)

Wang Y P，Chu Y S，Lee H J，et al.. Estimation of suspended sediment flux from acoustic Doppler current profiling along the Jiuhae Bay entrance. Acta Oceanologica Sinica，2005，24（2）：16-27.

Wang Y P，Gao S & Jia J J. High-resolution data collection for analysis of sediment dynamic processes associated with combined current-wave action over intertidal flats. Chinese Science Bulletin，2006a，51（7）：866-877.

Wang Y P，Gao S & Ke X K. Observations of boundary layer parameters and suspended sediment transport over the intertidal flats of northern Jiangsu，China. Acta Oceanologica Sinica，2004，23（3）：437-448.

Wang Y P，Pan S M，Wang H V，et al.. Measurements and analysis of water discharges and suspended sediment fluxes in Changjiang Estuary. Acta Geographica Sinica，2006b，61（1）：35-46. (in Chinese with English abstract)

Wang Z H，Chen Z Y & Tao J. Clay mineral analysis of sediments in the Changjiang delta plain and its application

to the late Quaternary variations of sea level and sediment provenance. Journal of Coastal Research，2006，22：683-691.

Wu C Y，Ren J，Bao Y，et al.. A Preliminary Study on the M orphodynami c Evolution of the ‘Gate’of the Pearl River Delta，China. Acta Geographica Sinica，2006，61（5）：537-548. (in Chinese with English abstract)

Wu J X，Shen H T & Wu H L. Fractional model of cross-sectional suspended sediment flux and its application in the Changjiang (Yangtze) Estuary. Acta Oceanologica Sinica，2002，24（6）：49-58. (in Chinese with English abstract)

Wu J X，Zhang S Y & Ren L F. Field observations of current and suspended sediment concentration during sediment disposal in the Changjiang (Yangtze) Estuary. Acta Oceanologica Sinica，2003a，25（4）：91-103. (in Chinese with English abstract)

Wu J X，Zhang S Y & Ren L F. Suspended sediment concentration profiles and dispersion patterns under sediment disposal conditions in the Changjiang River Estuary. Oceanologia et Limnologia Sinica，2003b，34（1）：83-93. (in Chinese with English abstract)

Xiang R，Li T G，Yang Z S，et al.. Geological records of marine environmental changes in the southern. Chinese Science Bulletin，2003，48（2）：194-199.

Xu F J & Liu J Y. 2D numerical modeling on sediment transport of Lingdingyang sea area in Zhujiang River estuary. Journal of Hydraulic Engineering，2003，（7）：16-21，29. (in Chinese with English abstract)

Xu M Q，Xu W B，Sun M Q，et al.. The characteristics of heavy minerals composition and distribution in surface sediment from the Xinghua Bay of Fujian. Acta Oceanologica Sinica，2004，26（5）：74-82. (in Chinese with English abstract)

Xue Y C，Gao S & Jia J J. Bedload transport within the ebb channel of a tidal inlet system，Swan Lake，Shandong Peninsula，China. Oceanologia et Limnologia Sinica，2002，33（4）：356-363. (in Chinese with English abstract)

Yang S L，Zhu J & Zhao Q Y. A Preliminary study on the influence of Changjiang River sediment supply of subaqueous delta. Acta Oceanologica Sinica，2003，25（5）：83-91. (in Chinese with English abstract)

Yang Y，Wang Y P & Gao S. Hydrodynamic processes and suspended sediment transport in the salt-marsh creeks，Wanggang，Jiangsu. Marine Geology & Quaternary Geology，2003，23（4）：23-28. (in Chinese with English abstract)

Yang Z S，Zhang Y，Liu Z，et al.. Temporal and spatial variations of the Huanghe River mouth bars [J]. Acta Oceanologica Sinica，2005，24（2）：43-56.

Zhang F Y，Zhang W Y，Zhang D Y，et al.. Research on surface sediment types and distributions from the eastern South China Sea，China. Acta Oceanologica Sinica，2004，26（5）：94-105. (in Chinese with English abstract)

Zhang F Y，Zhang X Y，Yang Q H，et al.. Research on sedimentations and material sources in the eastern South China Sea. Acta Oceanologica Sinica，2005，27（2）：79-90. (in Chinese with English abstract)

Zhang L P & Zhang M X. Spatial and temporal evolution of eroding coast in Hangzhou Bay，China. Journal of

Coastal Research，2004, SI43：67-74.

Zhang R S，Shen Y M，Lu L Y，et al.. Formation of Spartina alterniflora salt marshes on the coast of Jiangsu Province，China. Ecological Engineering，2004，23：95-105.

Zhang S Y & Qian B X. Acoustic observation of thick suspended sediments. Acta Oceanologica Sinica，2003，25（6）：54-60. (in Chinese with English abstract)

Zhang Y S，Zhang F J，Guo X W，et al.. Vertical flux of the settling particulate matter in the water column of the Yellow Sea in summer. Oceanologia et Limnologia Sinica，2004，35（3）：230-238. (in Chinese with English abstract)

Zhang Y S，Zhang F J，Guo X W，et al.. Autumn flux of particle settling observed at three representative stations in East China Sea. Oceanologia et Limnologia Sinica，2006，37（1）：28-37. (in Chinese with English abstract)

Zhou X J & Gao S. Spatial variability and representation of seabed sediment grain sizes：an example from the Zhoushan-Jinshanwei transect，Hangzhou Bay，China. Chinese Science Bulletin，2004，49（23）：2503-2507.

Zhou X J，Gao S & Jia J J. Preliminary evaluation of the stability of Changjiang clay minerals as fingerprints for material source tracing. Oceanologia et Limnologia Sinica，2003，34（6）：683-692. (in Chinese with English abstract)

Zhu Y R & Zhang Q Q. On the origin of the radial sand ridges in the southern Yellow Sea：results from the modeling of the paleoradial tidal current fields off the Paleo-Yangtze Estuary and northern Jiangsu coast. Journal of Coastal Research，2005，21（6）：1245-1256.

Wu X G & Wong H K. Late Quaternary seismic sequences and sedimentation along the coast off Taishan, Guangdong，as revealed by high resolution seismic data. Chinese Journal of Oceanology and Limnology，2002，20（3）：270-276.

PROGRESS OF CHEMICAL OCEANOGRAPHY IN CHINA (2002-2006)

Li Xuegang Song Jinming Dai Jicui Yuan Huamao Zhang Peng

（Institute of Oceanology，Chinese Academy of Science，qingdao266071）

Abstract Since 2002, Chinese chemical oceanography have been achieved a remarkable development due to its interdiscipline. This paper reviews the main progress made in the biogeochemical process of marine carbon cycling, dynamical process of nutrients, persistent organic pollutants (POPs), improvement and innovation of analysis method and so on in China during the last 4 years.

Key words chemical oceanography, marine carbon cycling, nutrient dynamics, persistent organic pollutants

Chemical oceanography is the study of the mechanisms that control the distributions of elements and compounds in the ocean. It has predominant regional characteristics because it studies the chemical problems about the distribution, transfer and transforms processes of chemical materials in the ocean. Now, chemical oceanography is focused on the changes between such inhomogeneous interfaces as seawater-air interface, bottom-seawater interface, suspended solid-seawater interface, organism-seawater interface and fresh water-sea water interface.

In recent years, Chinese Chemical oceanographer mainly focused on the frontier of the marine sciences，such as marine carbon cycle, the key geochemical process of biogenic elements in sediments and the behaviors of refractory degradation organic pollutant in marine environment. The significant progresses made in these fields are as follow.

1 Biogeochemical process in marine carbon cycling

In the oceans CO_2 is a crucial link for global carbon cycle, and plays a predominant role in the exchange and transfer of carbon among the atmosphere, hydrosphere, ecosphere and lithosphere. The marginal sea and continental slope, especially the estuary and bay impacted

greatly by human activities, play a significant role in marine carbon cycle. Recent years, the research into these regions has made great progress, which focus mainly on CO_2 exchange between sea water and atmosphere, colorful dissolved organic matter (CDOM), inorganic carbon in sediments in such typical regions as the Jiaozhou Bay, the Pearl River Estuary and the Changjiang River Estuary.

The research into the Jiaozhou Bay showed that the average DIC of surface water was 2066μmol/L in June and 2075μmol/L in July, 2003. Outside the bay, the average DIC of surface water was 1949μmol/L and 2147μmol/L of bottom water. In June, the DIC values of the inner bay were higher than that of outside the bay, but the case was opposite in July. The concentration was the maximum in the northeastern bay and decreased to the minimum toward the west of the bay. The total trend of vertical distributions was to increase gradually from surface to bottom, which had some relation with the particulate N and P. The average CO_2 seawater-atmosphere flux in the Jiaozhou Bay was 0.55mol/ (m^2·a) and 0.725mol/ (m^2·a) in June and July, respectively. The total CO_2 flux from seawater into atmosphere was 62t and 81t in June and July, respectively（Li et al，2004a）.The northern South China Sea is the source of atmosphere CO_2, and the average seawater-atmosphere flux in summer is 7mmol CO_2 $m^{-2}d^{-1}$ and 1~3 mmol CO_2 $m^{-2}d^{-1}$ in spring and autumn. The PCO_2 of surface seawater is influenced greatly by seawater temperature (Zhai et al., 2005).

Colorful dissolved organic matter (CDOM) is the substance with distinctive optical characteristics and plays an important role in marine material cycle. In the Jiaozhou Bay, the total fatty is 86.90% of CDOM, total sugar is 5.82%, free amino acids is 7.22% and glucidamin is 0.06%.The percentages of the carotene and phenol are lower by several orders than the total fatty, amino acids and total sugar. The CDOM in the Jiaozhou Bay is mainly land-derived (Wu et al, 2004). Based on CDOM and DOC of the Pear River Estuary in 1999, Chen et al. (2004) revealed that the CDOM contents was the highest in freshwater and was the lowest in seawater, which indicated that the river water was the primary source of the CDOM in the Estuary. However, the CODM in the estuary was lower than that in the other estuaries of the world. Hong et al (2005) revealed that the CODM adsorption coefficient at 355nm of the Pearl River Estuary was lower than that of the America and Europe estuaries due to great impact by human activities. The CODM

produced by human activities was apparently more than that of natural plant degradation. Additionally, the location of CODM fluorophore varies with its source, which can be used to determine the constitute characteristics and to trace the sources.

In marine sediments carbon plays a very important role in carbon cycle, which includes mainly organic carbon and inorganic carbon. The organic carbon in sediments is mainly land-derived and autogenetic, but their percentage is not the same in the different sea areas. According to the spatial distribution of OC、TN、$\delta^{13}C$ and $\delta^{15}N$ in sediments, Hu et al (2005) found that the land-derived particulate organic matter accumulation was faster than that of marine organism debris in the Pearl River Estuary and its adjacent South China Sea sediments, and the contribution of marine organic matter was 67%~31%. As far from the estuary, the contribution of marine organic matter was higher. The organic carbon derived from algae was less than 0.06% in the estuary, but more than 0.57% in the inner shelf (Hu et al., 2006).

Carbonate is an important composition of inorganic carbon in marine sediments. Up to now, the research into inorganic carbon concentrates mainly on source, distribution, dissolution and precipitation of carbonate in sediments. In the western South China Sea, the contents of carbonate in its northern and mid-southern part are high but low in its middle and southeastern part. Its distribution is controlled by terrigenous material supply. The contents of carbonate are highest in the area between 400m and 600m in depth. The average content is as high as 44.37% in the area between 500m and 600m in depth. The dissolution of carbonate increased below the depth of 1300m, and the contents decreased distinctly. Carbonate concentration become stable near the depth of 3500m, which suggested that 3500m should be a CCD of the western South China Sea (Li et al., 2004e).

In order to evaluate the contribution to marine carbon cycle, Li et al (2004c) divided the inorganic carbon in sediments into several forms and studied them in detail in the Jiaozhou Bay and the Changjiang River Estuary. The characteristics of different inorganic carbon in sediments is NaCl form < $NH_3 \cdot H_2O$ form <NaOH form < $NH_2OH \cdot HCl$ form <HCl form. In the Changjiang River surface sediments the average content of IC was 0.33mg/g in the NaCl form, 0.58mg/g in the $NH_3 \cdot H_2O$ form, 0.68mg/g in the NaOH form, 3.89mg/g in the $NH_2OH \cdot HCl$ form and 5.13mg/g in the HCl form. Different forms of IC could be transformed into each other, and it should be paid

more attention to the transformation from the NaCl form, $NH_3 \cdot H_2O$ form, NaOH form and $NH_2OH \cdot HCl$ form to the HCl form. The NaCl, $NH_3 \cdot H_2O$, NaOH and $NH_2OH \cdot HCl$ forms of IC could be released into water to take part in carbon recycle, however, the HCl form of IC would be buried for long time and not to participate in carbon recycle, which might be one of the ultimate sink of atmosphere CO_2.（Li et al，2006）.

2 The biogeochemical cycle of biogenic elements

2.1 The biogeochemical cycle of nitrogen

In the ocean the nitrogen forms include organic and inorganic forms (NH_4^+-N、NO_3^--N和 NO_2-N). In general, the organic nitrogen concentration is higher than that of inorganic nitrogen in sediments (Lü, 2005c). However, only the inorganic nitrogen can be utilized directly by phytoplankton, so most researches focus on inorganic nitrogen.

In the Bohai Sea surface sediments, the adsorbed inorganic nitrogen accounted for only 3.28% of total nitrogen，which was mainly NO_3^--N accounting for 83.7%. The NH_4^+-N adsorbed in surface sediments was primarily derived from the organic matter anoxic mineralization, and its distribution was controlled by the content of organism and Es. pH and the characteristics of clay had an important influence too. The adsorbed NO_3^--N was from the overlying water and controlled by the NO_3^- concentration and distribution in the overlying water. The content of NO_3^--N was higher than that of NH_4^+-N, NO_3^--N was the predominant species of adsorbed nitrogen，which showed that the mineralization of organisms was weak and couldn't provide much nutrient for primary productivity，and the terrestrial input of NO_3^--N was the dominating nutrient source (Song et al., 2004b). The variations of NH_4^+-N in sediments had some relations with organic matter variations. However, the high organic matter contents did not mean the high NH_4^+-N contents. The organic matter contents, nitrogen contents in sediments and degradation degree would influence the NH_4^+-N contents (Liu et al, 2004). Additionally, the slim variation of salinity may affect greatly on the NH_4^+-N adsorption (Liu et al., 2005d).

Besides the distributions and sources of nitrogen in sediments, scientist's studies focused mainly on the sediment-seawater exchange flux and their controlling factors in different regions. In the abyssal equatorial northeastern Pacific, the benthic fluxes of silicate, phosphate and nitrate

are -886.45~42.62 μmol/ (m^2·d), -3.04~5.83 μmol/ (m^2·d) and -189.43~21.05 μmol/ (m^2·d), respectively (Ni et al, 2005). In the Changjiang River Estuary, nitrous oxide (N_2O) production is very low in water, the intertidal flat sediments is the source of the water N_2O during the submerging period and N_2O comes from several process such as nitrification and denitrification of nitrogen cycle. The natural production rate of N_2O in sediment is between 0.10~8.50 μmol/(m^2·h), and the denitrification rate changes between 21.91~35.87 μmol / (m^2·h). During the ebb tide, the middle tidal flat is the source of atmosphere N_2O with the exchange flux between -11.03~13.17 μmol/(m^2·h). The ground temperature at the depth of 5~10 cm is the significant effect factors controlling the emission flux. The N_2O emission in the low tidal flat-atmosphere interface is -5.75~0.49 μmol/ (m^2·h). Overall, the middle tidal flat is the source of air N_2O, while the low tidal flat adsorbs air N_2O obviously. The N_2O emission and absorption through the intertidal flat-atmosphere interface has a significant positive correlation to the emission and adsorption of CO_2 (Wang et al., 2006). There are complicated spatial distributions and seasonal variations for inorganic nitrogen exchange between sediment and water interface. The measured fluxes of NO_3^--N and NH_4^+-N could change in a large range from -32.82 to 24.13 mmo1·m^{-2}·d^{-1} and from -l8.45 to l0.65mmo1·m^{-2}·d^{-1}, respectively. However, the fluxes of NO_2-N were very low with a range of -1.15 to 2.82 mmo1·m^{-2}·d^{-1}. It had been recognized that the NH_4^+-N exchange behavior was mainly controlled by the salinity, whereas the NO_3^--N exchange behavior was influenced by the sediment grain size, nitrate concentration in overlying water, organic matter content, water temperature and dissolved oxygen concentration (Chen et al, 2005d). Additionally, benthos-burrowing activities could increase NH_4^+ release and NO_3^- efflux from sediments to overlying water. (Chen et al, 2005c).

In the Pearl River Estuary sediments, the average of nitrification, denitrification and nitrate reduction rates ranged from 0.32 to 2.43 mmol·m^{-2}·h^{-1}, 0.03 to 0.84 mmol·m^{-2}·$h^{-1}$and 4.17 to 13.06 mmol·m^{-2}·h^{-1}, respectively. The vertical profiles of the sediments showed that the nitrification and denitrification processed mainly took place in the depths between 0 and 4cm. The rate of nitrification and denitrification and nitrate reduction were dominated by Eh, nitrate and ammonium concentrations in sediments and DO in overlying water (Xu et al, 2005).

The research into the NO_3^-、NO_2^-、NH_4^+、P、Si in the pore water and their exchange between

the sediment-water interface in the Yellow Sea and East China Sea sediments revealed that their distribution was controlled by sedimentary environment, and NH_4-N was the main inorganic nitrogen in pore water. The exchange fluxes of ammonium, dissolved inorganic nitrogen, phosphorus, silicon were 299.3~2214.8, 404.4~2159.5, 5.5~18.8 and 541.3~l781.6 μmol/(m^2·d), respectively. The sediments in the central Yellow Sea provides a large amount of nitrate to the sea water，which contributes 56% of nitrogen for the new production (Tian et al, 2003). In the Yellow Sea and East China Sea, the exchange fluxes were negative, which showed that sediments would absorb the dissolved inorganic nitrogen from water (Ni et al, 2006; Qi et al, 2006).

In the Jiaozhou Bay, Jiang et al (2004) measured the benthic exchange rates across sediment-seawater interface, which ranged from -0.5 to 1.6 mmol/(m^2·d) for NH_4^+-N , from 0.005 to 0.67 mmol/(m^2·d) for NO_2^--N，from -2.0 to 2.8 mmol/(m^2·d) for NO_3^--N, respectively. The NH_4^+-N diffusion was the dominant process of DIN exchange between pore water and overlying water. The exchange flux of DIN between sediments and seawater was estimated as 9.68×l0^8 mmol/d, which was about 50% of river input DIN, and could provide 52% of nitrogen required by phytoplankton growth in the bay. In the Sanggou Bay, the diffusion fluxes across sediments-water interface were 376.33, 33.02, 6.41 and 10.08 (μmol/m^2·d) for NH_4^+, NO_3^-, NO_2^- and PO_4^{3-}, respectively. The total inorganic nitrogen from sediments to overlying water was estimated as 281.7t, which could supply 28.73% of nitrogen requirement for the phytoplankton primary production (Cai et al. 2004).

In order to synthetically evaluate the contribution of nitrogen to marine nitrogen cycle, nitrogen in natural grain size sediments from the Bohai Sea were divided into transferable and nontransferable nitrogen by sequential extraction technique. The transferable nitrogen include four forms: exchangeable form (IEF-N), carbonate form (CF-N), iron-manganese oxides form (IMOF-N)and organic matter-sulfide form (OSF-N). Transferable nitrogen accounts for 30.85% for TN in the Bohai Sea sediments and nontransferable nitrogen was 69.15%. Thereinto, IEF-N, CF-N, IMOF-N and OSF-N account for 3.67%, 0.31%, 0.43% and 26.45% for TN, respectively. The absolute contribution on marine nitrogen cycle is decided by their content in sediments，which has the sequence of OSF-N (84.6%)> IEF-N (1.30%)> IMOF-N (1.4%)> CF-N(1.0%) (Ma et al,

2003).

The transferable nitrogen in the southern Yellow Sea sediments was divided into four forms by Lü et al, which were ion exchangeable nitrogen (IEF-N), weak acid extractable nitrogen (WAEF-N), strong alkaline extractable nitrogen (SAEF-N) and strong oxidant extractable nitrogen (SOEF-N). The content of the SOEF-N was the highest in all transferable nitrogen. The IEF-N was the predominant form of transferable inorganic nitrogen, which could take part in cycling more easily. If all the transferable nitrogen in the same grain size sediments could take part in cycling, their relative contributions to cycling might decrease according to the order of SOEF-N, IEF-N, SAEF-N, WAEF-N. For different grain size sediments, the absolute contents of every transferable forms of nitrogen were the highest in the fine sediments and the lowest in the coarse sediments. If the proportions of each grain in sediments were the same, the contents of the transferable nitrogen in the fine sediments could occupy 60% of the total transferable nitrogen, which was two times that in the medium size sediments and almost seven times that in the coarse sediments. Namely, the fine sediments had the most potential contribution to nitrogen cycling. In addition, the relative contents of organic transferable nitrogen increased with grain size getting finer, while those of inorganic nitrogen decreased (Lü et al, 2004b). The finer the sediments are, the smaller the decomposition rate of organic nitrogen will be. (Lü et al, 2005a). The nitrogen released from sediments could supply 6.54% nitrogen for the new primary productivity of the southern Yellow Sea (Lü et al, 2005b). However, the ecological function of different form of nitrogen in different grain sizes is different. Generally, the transferable nitrogen in the fine grain size sediments had close relationship with phytoplankton and benthos, and the transferable nitrogen of the medium and coarse sediments was mainly correlated with zooplankton. In the four transferable forms of nitrogen of different grain size in the southern Yellow Sea surface sediments, the SOEF-N and SAEF-N had a close relationship with the growth and breed of phytoplankton and the promotion of productivity. Chlorophyll a, the total phytoplankton abundance and the primary productivity had positive relationship with the contents of the two inorganic existence forms of nitrogen (NH_4-N and NO_3-N), which indicated that the transferable NH_4-N and NO_3-N could accelerate the phytop1ankton growth and promote the primary productivity. No matter what

form of nitrogen was，its ecological role was easily realized when these nitrogen are transformed into inorganic form (Lü et al, 2004a).

2.2 The biogeochemical cycle of phosphorus

Phosphorus in sediments includes mainly organic phosphorus (OP) and inorganic phosphorus (IP), and IP is the primary forms. However, the percentage of IP in different regions is different. For example, The IP percentage of total phosphorus (TP) in the Jiaozhou Bay sediments was more than 60% (Li et al., 2005c) and over 50% for the Bohai Bay sediments (Zhao et al., 2005b). It cannot fully reflect the biogeochemical behavior of phosphorus in sediments if phosphorus were only divided into inorganic and organic phosphorus. Therefore, phosphorus in sediments was generally divided into 5 forms: adsorption-phosphorus (Ad-P), iron-phosphorus (Fe-P), calcium-phosphorus (Ca-P), detrital-phosphorus (De-P) and organic- phosphorus (OP). The contents of total phosphorus (TP), organic phosphorus (OP) and the iron-bound phosphorus (Fe-P) were primarily controlled by the matter source. Ad-P, Fe-P and OP belonged to bioavailable phosphorus and the cycle of them in sediments were dependent on iron-oxides. Calcium-bound phosphorus (Ca-P) in sediments was mainly come from marine plankton (Zheng et al., 2003a). Song et al divided the transferable phosphorus in natural grain size sediments into ion-exchange form, carbon-bound form, iron-manganese oxide form, organic matter-sulphide form. In the Bohai Sea sediments, the transferable phosphorus accounted for 19.2% of total phosphorus, and organic matter-sulphide form was the primary form of transferable accounting for 10.7% (Song et al, 2003).

The spatial distribution of phosphorus in sediments is primarily controlled by matter source and hydrodynamic conditions, which have clear regional characteristics. In the Changjiang River estuary and its adjacent area, the P distribution have clear spatial and seasonal variation，which is dominated by the sources of P input，sediment texture and a number of biogeochemical processes in different hydrodynamic and environmental conditions (Gao et al., 2003b). In the Nansha Islands area, the apatite combined phosphorus and inorganic phosphorus in sediments can mostly return to the biogeochemical phosphorus cycle through biological utilization. So, their contents were mainly controlled by biological action. (Wang et al, 2005a). In the Pearl River Estuary sediments,

the total phosphorus increased from bottom to surface, and the maxima mostly emerged at surface or below the surface about 10cm. The vertical profiles of organic phosphorus were similar to that of total phosphorus with the maxima mostly emerged at the depth of 5~10cm. The contents of the Fe-P and Al-P were higher and had a trend of decreasing downward. TP, OP, Fe-P and Al-P have distinct synchronous effect on their sedimentation process, especially on total phosphorus and organic phosphorus (Yue and huang, 2005).

In the Yellow Sea and East China Sea，sediments absorbed dissolved phosphorus from water and was a sink of PO_4^{3-}(Qi, et al, 2006). The PO_4^{3-} absorbed from water every year accounts for 67% of the Changjiang River inputs in these regions (Qi, et al., 2003). In the Jiaozhou Bay, PO_4^{3-}-P was transferred from sediments to seawater with the exchange rate ranging from 0.1 to 90μmol·m^{-2}·d^{-1}. The exchange flux of PO_4^{3-}-P from sediments to seawater was estimated as 9.76×10^6mmol·d^{-1}, which occupied 24％ of the river input, and could provide 9%±3% of phosphate required by phytoplankton in the Jiaozhou Bay (Jiang et al., 2003). In the Laizhou Bay of the Bohai Sea, the PO_4^{3-} exchange flux were 6.7~6.8μmol·m^{-2}·d^{-1}, which influenced greatly by biology activity (Chen, et al., 2003).

In order to understand the phosphorus release behavior in sediments, a lot of simulations in lab and investigations in field have been done. Li et al (2005b) showed that the phosphorus adsorption capacities for different sediments had a “stable pH scope” with a range of 6.5 and 9.5. The maximum phosphorus adsorption capacity for different sediments occurs at salinity 6 with the range of 5~7. The phosphate adsorption capacity for most sediments increases with temperature increasing，showing endothermic reactions, while some sediments is exothermic reactions. Under static environment, phosphorus released from sediments reaches its extreme value after being thoroughly mixed with seawater for about 10 minutes, then tend to stable 3h later. Adsorption kinetics could be both fitted to the Elovich equation and two-constant rate equation. The Fe-P is the most active one，whose release ratio was higher than the other forms of phosphorus，then followed by Ad-P and OP (Zheng et al., 2003b). The variations of dissolved inorganic phosphate (DIP) and dissolved organic phosphate (DOP) are similar under the static conditions. In the lower vibration frequency (60 times/min)，DOP and DIP have the similar trend to that in the static

conditions．However, in the higher vibration frequency (120 times/min，150 times/min)，the variation of DOP has an opposite trend to that of DIP. (Wang et al, 2005b). The phosphorus adsorption quantity can exceed the percentage of 85% of balanced adsorption quantity 4h later. The adsorption quantity almost did not increase with time 12h later. (Li et al, 2004b).

Xu et al (2006) studied the phosphorus adsorption in the Changjiang River Estuary sediments and revealed that the sediments was buffers to phosphate, and the balance time of phosphorus adsorption (desorption) was about 6h. The saturated adsorption quantity of phosphorus was about 600μg/g, and the saturated desorption was about 126.37μg/g. The apparent adsorption heat of fine sediments (△H) was 47.59 kJ/mol. The adsorption of phosphate could be described by the Ferundlich Adsorption Isotherm , which was an endothermic reaction. The contents of sand and mud in sediments could influence phosphorus adsorption and the adsorption would decrease with the increase of sand or mud content. The Changjiang River estuary sediments tended to release phosphorus to overlying water (Li and Yang, 2004).

In addition, paleoenvironment can be traced by sediments phosphorus. The data about environment and biogeochemistry of phosphorus extracted from the South China Sea shelf sediments showed that the supply of terrigenous phosphorus was steady. The variation of phosphorus contents in different depths was resulted in by climate and environment change. The decrease of phosphorus and the increase of calcium carbonate in sediments might be one of key factors for leading to the atmosphere CO_2 decrease in ice age (Wong, 2005).

2.3 The characteristics of biogenic silicate

The accumulation of biogenic silica in sediments can reflect the influence of the nutrients changes on the growth of diatom and other phytoplankton; moreover, it also records the occurrence and development of eutrophication process. In the East China Sea and Yellow Sea surface sediments, the BSi contents ranged from 0.21％ to 0.70％, which distribution was in accordance with that of the primary productivity. The variation of the BSi content in the sediments recorded the annual variation of the nutrients flux of N, P, Si transported by the Changjiang River (Ye et al, 2006).

Song et al (2003) divided silica in natural grain size sediments into ion-exchange form, carbonate- bound form, iron-manganese oxides form and organic matter-sulfide form, and thought

that only these form silica can take part in biogeochemical cycle. In the Bohai Sea sediments, the content of transferable form of silicon accounted for 0.12% of total silica, and the carbonate-bound silica was the primary form occupied 0.05% of total silica. In the East China Sea and Yellow Sea, SiO_3^{2-} may transform from sediment to seawater, and the contribution of SiO_3^{2-} released from sediments to the primary productivity were 13%, 10~18%, respectively. Compared with river input and atmospheric deposition, the SiO_3^{2-} contribution of sediments to the Yellow Sea and East China Sea were 90% and 86%, which indicated that sediments was the main source of SiO_3^{2-} (Qi et al., 2006).

The regeneration of silica in sediments is the main supply source for the ocean, and the silica supplied to the world ocean from biogenic silica dissolution in sediments is four times that from rivers. However, in marginal sea, the sediment silica behavior is different from ocean due to shallow water depth, high primary productivity and considerable terrigenous inputs. Long-term research into the Jiaozhou Bay nutrients showed that the nutrients were characteristic of high nitrogen, low phosphorus and silica. In the past four decades, the nitrogen has increased unceasingly but the silica contents decreased continually, and as a result, silica may have become the primary limiting factor for the phytoplankton growth in the Jiaozhou Bay (Liu et al., 2005a). It is showed that the biogenic silica in three surface sediments samples of the Jiaozhou bay are 1.58%, 1.44% and 1.48%, respectively, which are higher than that of the East China Sea and Yellow Sea (biogenic silica contents are lower than 1%, Zhao et al., 2005a). The sediments BSi:TN ratios were much greater than 1 and BSi:TP ratios were >16 too, which were opposite to the water ratios of Si:TN<1, BSi:16P<1 in the Jiaozhou Bay. At the same time, the OC: BSi ratios in sediments were lower than Redfield ratio (106:16). These indicated that the decomposition rate of OC was much higher than that of BSi and the biogenic silicate decomposition rate was very slow. In addition, during the course of deposition, only 15.5% biogenic silicate formed by diatom was decomposed into water, thus approximate 84.5% of biogenic silicate was buried and entered into sediments. The rate of silica returning to water across sediment-seawater was lower than the biogenic silica sedimentation rate in the Jiaozhou Bay sediments. All these indicated that silica in seawater was transported into sediments, and as a result, the silica in water kept low concentration. This is the key reason for silicate limiting to phytoplankton growth in the Jiaozhou Bay (Li et al.,

2005d).

3 Environment chemical process of the persistent organic pollutants (POPs)

The most of POPs are anthropogenic origin productions and enter environment by two main ways. One is that POPs transfer from the atmospheric environment to the aquatic environment by dry or wet sedimentation; the other way is that POPs enter the aquatic environment via surface effluent release. In the coastal areas, the primary routine that POPs enter marine environment is the surface riverine input. In the different coastal areas, the flux and species of POPs schlepped by rivers are quite different. In the Humen tidal channel of the Pearl River, the total PAHs flux (dissolved and particulate phase) is 4.38×10^5 kg/a, thereinto, the particulate phase flux is 5.25×10^4 kg/a, and the flux of 16 prior controlling PAHs is 2.48×10^5 kg/a. Among them, the PAHs with less rings, such as naphthalene and acenaphtylene, are transported mainly in dissolved phase, while the PAHs with more rings, such as benzo (a) pyrene, are transported mainly by particles, whose proportion exceed 92%. The total flux of OCPs is 2.6×10^3 kg/a with the equal proportions of dissolved and particulate phase. The fluxes of Hexachlorocyclohexane and DDT are 1.1×10^3 kg/a and 0.3×10^3 kg/a respectively, and the flux of the rest of OCPs is 1.2×10^3 kg/a (Yang et al, 2004a). However, in the polar coastal areas, POPs came from atmospheric deposition mainly by the volatilization of global distillation effect in tropic and subtropic Zone and the deposition of the condensation effect in the high latitude Frigid Zone (Lu et al, 2005).

In the aquatic environment, POPs are mainly adsorbed in the suspended particles, and then enter the sediments environment through deposition, which cause the POPs concentration in sediments higher by one or two orders than that in seawater. Whereas, the spatial distributions in sea water agree well with that in sediments, namely, the POPs concentrations decrease continuously with increase of the distance from coast to open sea. In the surface water and sediments of the Pearl River Estuary and its adjacent northern South China Sea, a continuous down tendency of the alkyphenols concentrations is shown from the river down to the estuary and then to the open sea (Chen et al, 2006). Moreover, the concentration of PAHs and OCPs in sediments decreased in turn from the Pearl River Estuary to the South China Sea too (Luo et al, 2005a; 2005b). Even so, the components and variation of POPs in the above overlying sea water do not agree with that in the sediments well. Firstly, the components of POPs in the sediments may

be different from that in the sea water. For instance, in the Daya Bay, the PAHs components is 3 rings mainly in sea water, while the majority of PAHs had 4 rings in the sediments (Qiu et al, 2005b). Secondly, the composition and species of POPs displays significant seasonal variation in water. Yang et al (2004b) studied the distribution and seasonal variation of polycyclic aromatic hydrocarbons (PAHs) in surface water from the Humen tidal channel, and found that the PAHs in the dry season existed in the dissolved phase with 2 rings exceeded 95%, and the PAH concentration was by one order higher than that in monsoon season, when the PAHs transported in the particulate phase mainly and its concentration increased obviously.

The POPs concentration in suspended particle is likely higher than that in surface sediments. The PCBs distribution near the Changjiang River Estuary showed that the PCBs concentration in the suspended particles was higher than that in the corresponding sediments. Furthermore, no significant relationship between PCBs and TOC is found, but the source of organic matter and the composition of the inorganic mineral matter may affect PCBs distribution to some extent. The low chlorinated level PCBs (3～5 Cl) account for more than 70%, whereas, the predominant PCBs congeners in the suspended particle is 2 chlorinated substituted compounds (Cheng et al 2006). The distribution of OCPs is quite similar to that (Liu et al, 2005c).

The POPs concentration in the pore water is much higher than that in the overlying seawater (Maskaoui et al，2005). However, the POPs concentrations in sediments are higher than that in pore water and overlying water. POPs transfers from sediments to the overlying water by re-suspending (Zhang et al, 2003). Consequently, it is vital to confirm the POPs sources, compositions and controlling factors for evaluating bioavailability, environmental toxicity and constitute remediation technology. Hao et al (2006) investigated the concentrations and distributions of free and bound PAHs in sediments from Nam Van artificial Lake of Macao under the natural circumstances, which showed that the free PAHs were predominated by 4-ring，6，7-ring，and 5-ring PAHs，with the percentages of 28.7~40.6%, 17.6~29.6%, and 13.2~28.2%, respectively, and the main components of bound PAHs were 4-ring，3-ring，and 2-ring ones, with the percentages of 42.3~55.8%, 20.2~35.8% and 7.8~l8.8%, respectively, which suggested that PAHs with low molecular weight were more prone to entering the micro-pores of organic matters.

Vertical profile of free PAHs concentrations in core sediments, on a certain extent, was correlated with the regional economy development and the proceeding of environmental management. The bound PAHs concentrations in the core sediments were controlled by the total PAHs input to the sediments and the structure (especially the polymerization) of organic mater. Wu et al (2003) studied the sorption behaviors of phenol in marine sediments of the South China Sea systemically. The sorption behavior of phenol in the sediments was extremely complex, which could be described by Freundlich, Langmuir and linear models. The sorption behaviors of phenol in the sediments were affected by some factors such as organic carbon content of sediments, salinity, temperature and acidity of medium. The saturated sorption amount of phenol increased with increase of organic carbon content, salinity and acidity, but decreased with increase of temperature. Wu and Jia (2005) used wet sieving method to separate the sediments into five size fractions and further separated them into low and high density fractions with cesium chloride solutions. They found that OCPs enrichment in different type of fraction was influenced by many factors, especially, the sources and structures of pollutant play important role. The low density organic fraction revealed higher enrichment capacity on OCPs than that of high density fraction (inorganic mineral matter and amorphous organic matter), and adsorption capacity of organic matter on Hydrophobic Organic Pollutants (HOPs) was much larger than that of inorganic mineral matter and amorphous organic matter. However, it was hard to explain the horizontal distribution of OCPs in different grain size sediments in terms of the Total Organic Carbon (TOC) and Black Carbon (BC) contents, because the distribution of OCPs in the different grain size sediments had close relationship with the species and structures of the organic matter in sediments.

Taking typical POPs of HCHs, DDTs and PCBs as the indexes of environmental pollution, we can trace the history of OCPs and analyze the pollution process of the OCPs to the marine environment. The analysis of the PAHs vertical distribution of the core sediments reconstructed the sediment history of the PAHs in the last hundred years in the Lingdingyang Sea. An initial increase in PAH concentration was found around the 1860s, followed with the first maximum in the 1950s, then slightly decreased in the 1960s and 1970s. A sharp increase was observed from the 1980s and an extreme value was found in the1990s. PAH in the core sediments are mainly of pyrolytic origin, and its flux were found to correlate positively with the Gross Domestic

Production, vehicle numbers and power generation in the surrounding regions (Liu et al, 2005b). In the Nam Van artificial lake of Macao，the nonylphenols (NPs) concentrations in sediments ranged from 2.17 to 5.91μg/g with the mean value of 3.66μg/g, which belongs the estuarine sedimentary environment from the 1970s to the 1980s, and from 0.69 to 3.04μg/g with the mean value of 2.08μg/g, which belongs lagoon sedimentary environment in the 1990s. During the initial stages of lagoon environment in the early 1990s, the concentrations of octylpheno (OP) were similar to that in the estuarine environment, and ranged from 14.33 to 39.1μg/g. Subsequently, the concentration of OP rapidly decreased to the range of 6.52 ~ 2.58μg/g (Hao et al, 2004).

4 Major and minor elements in marine environments

According to the combination of major and minor elements in sediments, we can trace their source (Jiang et al, 2006; Chen et al, 2005a) and analyze paleoenvironmental changes (Wang et al, 2004; Du et al, 2004). However, the heavy metals are still drawn comprehensive attention to because their accumulation could affect the growth and reproduction of aquatic animals and plants. Moreover, they can enter the human body through the food chains to threat human's health. In recent years, Chinese researchers continued to study the contents, distributions and sources of heavy metals in the typical region of the China seas and deeply studied their forms and bioavailability (Hong et al, 2003; Qiu et al, 2005a).

In general, the heavy metals could be divided into exchangeable form, carbonate bond form, Fe-Mn oxidate form, organic matter form and residue form. The results in sediments near the Bailong River sewage outlet in the Changjiang River Estuary showed that Cu, Pb, Zn, Fe and Cr were mainly in residual form, while Mn was mainly in carbonate form with the percentage concentration reaching 50%. The concentrations of exchangeable and organic heavy metals showed less distinct seasonal variation, however carbonate form might transform to Fe-Mn oxidate form in autumn. Cu, Pb, Fe, and Mn in carbonate form and Fe-Mn oxidate forms behaved similarly in the transporting and converting process. Nevertheless, the circulation of Fe and Mn was one of the major mechanisms controlling the behavior of heavy metals. (Bi et al, 2003). Yuan et al (2004) used the sequential extraction protocol to obtain four extraction fractions of sediments, named acid soluble form (include exchangeable ions and carbonates), reducible form (iron–manganese oxides), oxidable form (sulfide-organics) and residual form (metals bound in

lithogenic minerals). In the East China Sea sediments, more than 90% of the total concentrations of V, Cr, Mo and Sn existed in the residual fraction. Fe, Co, Ni, Cu and Zn mainly (more than 60%) occurred in the residual fraction. While Mn, Pb and Cd dominantly presented in the non-residual fractions in the top sediments. For most heavy metal except Fe, the concentration of element in the acid soluble form and reducible form in surface sediments was higher than that in deep sediments. The total contents of four familiar heavy metals (Cu, Zn, Pb and Cd) in rhizosphere sediments around Suaeda heteroptera showed the similar phenomenon (Zhu et al, 2005). Cu and Pb transformed from the active form to the residuals, which led to the bioavailability reduction.

In the every form of heavy metals, the acid soluble fraction is most active. It controls the distribution of heavy metals in sediments-pore waters and their availability. The difference between acid-volatile sulfide and simultaneous extracted metals (SEM-AVS) was investigated to explain the biological toxicity of zinc in the sediments to benthic organisms. When the molar difference between SEM and AVS (i. e., SEM_{Zn}- AVS) was <0 μmol/g, the concentration of zinc in the sediment interstitial water was low and few toxic effects were observed. Conversely, when SEMzn-AVS exceeded 0μmol/g，a dose-dependent increase in the relative concentration of zinc in the pore water was detected and apparent organisms toxic effects were observed (Han et al, 2003). Due to the different aeration time in high tideland and low tideland, the depth of oxidative layer decreased from high tideland to low tideland. In tideland sediments, the layer, in which the maximal value of acid extracted metals (AEM) appeared, shoaled from high tideland to low tideland and AEM enriched in the oxide-reduce interface layer. The heavy metals were easy to be released to overlaying water in the medium tideland (Zhang et al, 2004).

The factors influencing the distribution of different form of heavy metals are mainly oxidative- reductive conditions and pH besides sediments themselves. In the oxidative environment, heavy metals are mainly adsorbed by Fe-Mn oxidate. In the reductive environment, they are combined with organic matter and S^{2-}. Therefore, the study on the activity of heavy metals is focused on the changes of oxidative-reductive conditions and pH. In the surface sediments, the oxygen content determines the oxidative-reductive capability. The changes of Fe-Mn oxidate below the subsurface sediments influence the oxidative-reductive conditions. The vertical distributions of Fe and Mn are controlled by the reduction, diffusion and re-precipitation

of Fe-Mn oxidate and hydroxid. The concentration of Fe and Mn in the upper sediments was the highest, which is related with the diffusion depth of oxygen and the diffusion flux of Mn^{2+} and Fe^{2+}. The Mn bacteria play an important role in the cycle of Fe and Mn in solid. They can oxidate dissolved Mn^{2+} and Fe^{2+} to Mn^{4+} and Fe^{3+} in oxidative condition and can reduce Mn^{4+} and Fe^{3+} to Mn^{2+} and Fe^{2+} when oxygen is deficient (Zhou et al 2003). Active iron and Fe^{3+}/Fe^{2+} were usually used to estimate the oxidative-reductive conditions in sediments (Li et al, 2003; 2004d).

Except for heavy elements, rare earth elements, radionuclide, Te, I, and Al were also studied as the typical elements.

Rare earth elements (REE) have the similar chemical characteristics and low dissolubility. They are not easy to migrate in weathering, erosion, transportation, deposition and early diagenetic processes and have little fractional distillation in transportation process. Therefore, rare earth elements are usually used to trace matter source of marine sediments and geochemical characteristics of matter source area. For examples, the abundance of the REE in the Chukchi Sea is very similar to that in fine-grained sediments in the East China Sea shelf, which indicated the REE in sediments are mainly originated from the terrene (Huo et al, 2003). The distribution of rare earth elements (REE) in water, suspend particle and pore water in the intertidalite of the Tianjin City are similar with that in natural rivers, which are quite different from that in the ocean. Average contents of REE in sediments and suspended particles are obviously lower than that in natural rivers but higher than that in sediments of the East China Sea shelf. These indicated that sediment and suspended particle of intertidalite are mainly originated from terrestrial soil (Liang et al, 2003). According to the distribution of rare earth elements and transition elements, the Nansha Islands sea area can be divided into such three parts as near-shelf residual sediment, deep-sea sediment and carbonate sediment. Generally，REE contents have big difference in different sediments, but their distributions have such similar features as light REE enrichment and Eu deficiency. REE in sediments has the large correlation coefficient with Ti and Zr but has no obvious relationship with other metals, which reveals that the sediments in the Nansha Islands sea area are mainly from landmass (Tian et al, 2005). Based on the vertical distributions of ΣREE, ΣLREE, ΣHREE, ΣLREE/ΣHREE, δEu and δCe in sediments at the E2 core in the southern Yellow Sea, rare earth element are controlled by the same source in the last two hundred years and

the distribution of REE shows the character of upper continent. The REE model is similar to that of the eastern China upper continent, but quite different from deep sea, indicating that the Yellow Sea sediments have good relationship with the China upper continent. The REE in the southern Yellow Sea mainly comes from weathering materials of upper continent, not from seawater. (Zhu et al, 2006).

Jia et al (2003) determined the radioisotope ^{40}K, ^{137}Cs, ^{210}pb, ^{226}Ra, ^{228}Ra, ^{228}Th and ^{238}U in the Jiaozhou Bay surface sediments. The radionuclide contents in the portion of size < 0.063 mm is higher than that in size > 0.063 mm except ^{210}Pb, ^{226}Ra, ^{228}Ra, ^{228}Th, ^{238}U in the eastern bay. Radionuclide contents in surface sediments are consistent with those in the soil of drainage basin, which indicates that the sediments are mainly terrigenous in the Jiaozhou Bay. Natural decay series are disequilibrium in sediments of the Xiamen intertidal mudflats. ^{234}Th related to ^{238}U, ^{210}Pb related to ^{226}Ra are excess, respectively, while ^{222}Rn, ^{228}Ac, ^{224}Ra related to ^{226}Ra, ^{228}Ra, ^{228}Th are deficiency, respectively (Chen et al, 2005b). High values of ^{210}Pb activities were found in the central area of the Bohai Sea, the fine-grained sediment areas of the northern Yellow Sea and the mud sedimentation area of the southern Yellow Sea. However, ^{210}Pb activities are low in the Bohai Bay, the Laizhou Bays and the west coast of the northern Yellow Sea. The enrichment and spatial distribution of ^{210}Pb are mainly controlled by hydrodynamic conditions and the grain size of sediments in the Yellow Sea and Bohai Sea. The vertical distributions of ^{210}Pb activity behave like the two-segment model regularly in the fine-grained sediment areas of the Yellow Sea and Bohai Sea characterized by high ^{210}Pb activities and low sedimentation rates, reflecting that the sedimentary environments in the fine-grained sediment areas are stable (Qi et al, 2005).

Tellurium is a sort of scattered rare element on the earth. Its concentration is very low in earth's crust, only 1.0 ng/g. However, it has extremely high abundance in Co-rich crusts, marine polymetallic nodules, deep-sea sediments and aerolites. The extreme enrichment of tellurium is possibly related to interplanetary dust particles (IDPs) (Li et al, 2005a).

Iodine is an important trace element, which is highly related with human being. Iodine deficiency can lead to abnormal growth for human. In nature, iodine enriches in marine organism and sediments which is the largest reservoir. The distribution of iodine in marine sediments has a trend of increase from low latitude to high latitude (Gao et al, 2003a).

The oceanic distribution of Al is primarily controlled by external sources and can be rapid scavenged from the water column. Therefore, it is often applied as a sensitive tracer of water masses in the coastal and offshore seawater. Fluvial input has been suggested as an important source of dissolved Al in the coastal regions, whereas the partial dissolution of eolian dust has been proposed as the dominant source of dissolved Al in the surface water of the oceans. The distribution of aluminum in the Yellow Sea showed the effect of land-source input from the adjacent rivers and the Changjiang River with obvious seasonal variations. The contribution of the Changjiang River was the highest (56.6%) near the Changjiang River Estuary, then decreased seaward along the PN section. At a distance of 250 km from the Changjiang River mouth, the freshwater input was hardly seen and the intrusion of the Kuroshio waters became dominant. Combining the different inputs of the dissolved Al from the Changjiang River, atmospheric deposition, the Kuroshio waters and the Taiwan Warm Current Waters, the average residence time is about 339 ± 118 days for dissolved Al in the East China Sea Shelf (Ren et al, 2006).

5 Improvement and innovation of analytical methods in chemical oceanology

In the last 4 years, Chinese chemical oceanographers developed a serious of new analysis techniques, which have been used in the chemical oceanography.

In order to simplify the pre-operating procedure of heavy metals in sediments, sediments were dispersed into slurry, and controlled the slurry particle size < 160 mesh (≤0.088mm), ensuring the slurry dispersal, uniform and stable by stirring with electromagnetic stirrer, then measured directly. Thereinto, Arsenic, mercury and lead in sediments were determined by hydride generation atomic-fluorescence spectrometry, and copper by graphite furnace atomic absorption spectrometry (Cheng et al, 2003，2004a，2004b，2005）. Ma et al (2005) subtracted the pollution of silicate from the dissolved detrital materials by the Ti contents in alkali leachate, and made the determination of biogenic silicate in marine sediments by normal alkali extraction more accurate. Sequential extraction technique was employed by Zhao et al (2005a) to determine the biogenic silica contents of the East China Sea and the Yellow Sea core sediments after subtracting the interference of non-biogenic silica by way of slope rate corrections.

Song et al (2004a) designed a sealed airproof device of gas extraction-absorption to measure dissolved inorganic carbon (DIC). Concretely, 100~150 ml seawater was put into conical flask,

then added H_3PO_4 in it , so DIC in seawater was extracted as CO_2 gas by acidification and nitrogen stripping, then CO_2 gas was absorbed by NaOH solution. Finally, the absorbed solution was titrated by HCl standard solution. Li et al (2004c) established a sequential extraction method based on IC combined chemical strength in sediments. Inorganic carbon in sediments were divided into five forms：NaCI form (step I)，$NH_3 \cdot H_2O$ form (step II)，NaOH form (step Ⅲ)，$NH_2OH \cdot HCI$ form (step IV)and HCI form (step V).

In addition, Cai et al (2006) improved the approach of ^{234}Th determination in seawater, which made the ^{234}Th determination more quick and concise. Peng et al (2006) developed a simple and effective method to determine simultaneously endocrine-disrupting phenolic xenoestrogens and steroid estrogens in sediments by gas chromatography–mass spectrometry (GC–MS).

Acknowledgments

This paper was supported by the National Key Project for Basic Research of China （2007CB407305）, the “100 Talents Project” of Chinese Academy of Sciences and Qingdao Special Project for Outstanding Scientists (Contract No.04-3-JJ-03, 05-2-JC-90).

Reference

Bi C J，Chen Z L，Xu S Y, 2003. Chemical Associations of Heavy Metals in the Sediments near Bailonggang Sewage Discharge Outlet of Shanghai. Marjne Science Bulletin, 5(1): 52-58.

Cai L S, Fang J G, Dong S L, 2004. Preliminary studies on nitrogen and phosphorus fluxes between seawater and sediment in Sungo Bay. Marine Fisheries Research, 25(4): 57-64.

Cai P H, Dai M H, Lv D W, Chen W F，2006. An improvement in the small-volume technique for determining thorium-234 in seawater. Marine Chemistry, 100: 282–288.

Chen B, Duan J C, Mai B X, Luo X J, Yang Q S, Sheng G Y, Fu J M, 2006. Distribution of alkylphenols in the Pearl River Delta and adjacent northern South China Sea, China. Chemosphere, 63: 652–661

Chen D H, Jiang S Y, Liu J, 2005a. Geochemical characteristics and sedimentary environment of surface sediments from Xisha trough. Marine Geology & Quaternary Geology, , 25(2):37-43.

Chen H T, Liu S M, Chen S Z, Zhang J, Yu Z G, Mi T Z, 2003. Exchange of dissolved inorganic phosphate between sediment and sea water in the Laizhou Bay, Bohai Sea. Environmental chemistry, 22（2）：110-114.

Chen J F, Liu G S, Huang Y P, 2005b. Disequilibrium of natural decay series in sediments of intertidal mudflats of Xiamen. Journal of Oceanography in Taiwan Strait, 24（3）：274-282

Chen Z L, Liu J, Xu S Y, Wang D Q, Zheng X M, 2005c. Impact of macrofaunal activities on the DIN exchange at

the sediment-water interface along the tidal flat of Yangtze River Estuary. Environmental Science, 26(6): 43-50.

Chen Z L, Wang D Q, Xu S Y, Zhang X Z, Liu J, 2005d. Inorganic nitrogen fluxes at the sediment-water interface in tidal flats of the Yangtze Estuary. Acta Geographica Sinica, 60（2）：328-336.

Chen Z Q, Li Y, Pan J M, 2004. Distributions of colored dissolved organic matter and dissolved organic carbon in the Pearl River Estuary, China. Continental Shelf Research, 24: 1845–1856.

Cheng S B, Liu M, Liu H L, Xu S Y, 2006. Distribution of Polychlorinated Biphenyls (PCBs) in suspended particulate matters from the Yangtze Estuarine and coastal areas. Environmental Science, 26(1): 110-114.

Cheng X S, Qin X G, 2003. Direct determination of trace copper in marine sediment sample by GFAAS using a slurry sampling technique. Chinese Journal of Spectroscopy Laboratory, 20（4）：586-589.

Cheng X S, Qin X G, Liu F P, 2005. Determination of trace arsenic in marine sediment sample by atomic fluorescence spectrometry using a slurry sampling technology. Acta Oceanologica Sinica, 27（1）：159-162.

Cheng X S, Qin X G, Xu R, Wang J H, 2004a. Determination of trace lead in sediment samples by flow-injection hydride generation atomic-fluorescence spectrometry using a slurry sampling technique. Marine environment science, 23（2）：72-74.

Cheng X S, Qin X G, Yang Y, Wang J H, 2004b. Determination of trace mercury in marine sediment sample by atomic fluorescence spectrometry using a slurry sampling technique. Marine environment science, 22（2）：68-71.

Du J M, Zhu L M, Zhang Y H, 2004. The environment significance of trace elements for the sediments from the southern Huanghai Sea. Acta Oceanologica Sinica, 26(6): 49-57.

Gao A G, Liu Y G, Zhang D J, Shun H Q, 2003a. Latitudinal distribution of Iodin in Chukchi Sea and Bering Sea sediment. Science in China(Series D), 33（2）：155-162.

Gao X J, Chen Z L, Xu S Y, Liu L Y, 2003b. Environmental geochemical characteristics of phosphorus in intertidal sediments of the Yangtze Estuarine and coastal zone. Acta Scientiae Circumstantiae, 23(6): 711-715.

Han J B, Ma D Y, Yan Q L, Wang J Y, Xu D Y, Chen S M, Chen H X, Yan J C. 2003. Biotoxicity of Zinc in the marine sediment to amphipod Grandidierella japontca. Environmental Science, 24（6）：101-105.

Hao Y M, Li C L, Luo X J, Mai B X, Sheng G Y, Fu J M, 2006. Free and bound PAHs in a sediment core from Nam Van artificial lake of Macao. Environmental Science, 27(2): 235-240.

Hao Y M, Mai B X, Li C L, Sheng G Y, Fu J M, Wang Z S, Deng Y H, 2004. Primarily study of Alkylphenols in sediment core from Nam Van artificial lake of Macao. Environmental Science, 25(4): 129-133.

Hong H S, Wu J Y, Shang S L, Hu C M，2005. Absorption and fluorescence of chromophoric dissolved organicmatter in the Pearl River Estuary, South China. Marine Chemistry, 97: 78– 89.

Hong L Y，Hong H S，Chen W Q，Wang X H，Zhang L P, 2003. Heavy metals in surface sediments from Minjiang

Estuary—Mazu and Xiamen—Jinmen sea areas. Journal of Environmental Sciences, 15(1):1l6 - 122.

Hu J F, Peng P A, Jia G D, Mai B X, Zhang G, 2006. Distribution and sources of organic carbon, nitrogen and their isotopes in sediments of the subtropical Pearl River estuary and adjacent shelf, Southern China. Marine Chemistry, 98: 274–285.

Hu J F, Peng P A, Mai B X, Zhang G, Yin K D, 2005. Sources and relative contribution of organic matter in surficial sediments of Zhujiang River mouth. Journal of tropical oceanography, 24(1): 15-20.

Huo W M, Zeng X Z, Tian W Z, Zeng W Y, Yin M R, 2003. The REEs geochemistry of Chukchi Sea sedlment core. Chinese journal of polar research, 15（1）：21-27.

Jia C X, Liu G S, Xu M Q, Huang Y P, Zhang J, 2003. Radionuclides and minerals in surface sediments of Jiaozhou Bay. Oceanologia ET Limnologia Sinica, 34（2）：490-498.

Jiang F H, Wang X L, Shi X Y, Zhu C J, Han X R, 2003. Benthic exchange rates and fluxes of PO4P at the sediment-water interface in Jiaozhou Bay. Marine Science, 27（5）：50-54.

Jiang F H, Wang X L, Shi X Y, Zhu C J, Hu H Y, Han X R, 2004. Benthic exchange rates and fluxes of dissolved inorganic nitrogen at the sediment-water interface in Jiaozhou Bay. Marine Science, 28(4): 13-19.

Jiang F Q, Li A C, Li T G, 2006. Geochemical characteristics of transition elements in surface sediments northern okinawa trough. Oceanologia ET Limnologia Sinica, 37（1）：75-83.

Li M, Wei H P, Wang G Q, Ni J R, 2004b. Study on adsorption behavior of phosphate by sediments from the Changjiang Estuary and the Hangzhou Bay. Acta Oceanologica Sinica, 26（1）：132-136.

Li M, Wei H P, Wang G Q, Ni J R, 2005b. The influence of environmental factors on the adsorption behavior of Phosphate by suspended sediments from Changjiang Estuary. Journal of basic science and engineering, 13(1): 19-25.

Li R S, Yang H, 2004. Adsorption and release of phosphorus in sediments of the Changjiang Estuary. Marine environment science, 23（3）：39-42.

Li X G, Li N, Song J M, 2004c, Determination for the different combined-form inorganic carbon in marine sediments. Chinese Journal of Analytical Chemistry, 32(4): 425-429

Li X G, Lv X X, Sun Y M, Li N, Yuan H M, Zhan T R, Song J M, 2003. Relation of active iron and redox environments in the sediments of Bohai Sea. Marine environmental science, 22(1): 20-24.

Li X G, Song J M, Li N, Yuan H M, Gao X L, 2005c. Source and biogeochemical characteristics of nitrogen and phosphorus in Jiaozhou Bay sediments. Oceanologia ET Limnologia Sinica, 36(6): 562-571.

Li X G, Song J M, Lv X X, Yuan H M, Zhan T R, Li N, 2004d. The expression of Redox environments in sediments outside of the Yellow River Estuary. Marine Science Bulletin, 23(4): 25-31.

Li X G, Song J M, Yuan H M, 2006. Inorganic carbon of sediments in the Yangtze River Estuary and Jiaozhou Bay. Biogeochemistry, 77：177-197.

Li X G, Song J M, Yuan H M, Li F Y, Sun S, 2005d. High contents of biogenic silicate in Jiaozhou bay sediments——evidence of Si-limitation to phytoplankton primary production. Oceanologia ET Limnologia Sinica, 36(6):92-98

Li X J, Chen F, Liu J, Huang X H, 2004e. Distribution and its dissolution of carbonate in seafloor surface sediment in the Western South China Sea. Geochimica, 33(3): 254-260.

Li Xuegang, Li Ning, Gao Xuelu, Song Jinming, 2004a, Dissolved inorganic carbon and CO_2 fluxes across Jiaozhou Bay air-water interface. Acta Oceanologica Sinica, 23(2):279-285

Li Y H，Wang Y M，Song H B，Yue G L，2005a. Extreme Enrichment of Tellurium in Deep-Sea Sediments. Acta Geologica Sinica, 79(4): 547-551.

Liang T, Wang L J, Zhang C S, Ding L Q, Ding S M, Yan X, 2003. Contents and their distribution pattern of rare earth elements in water and sediment of Intertidalite. Journal of the Chinese rare earth society, 23（1）：68-74.

Liu G Q, Zhang G, Li J, Li K C, Guo L L, Liu X, Chi J S, Peng X Z, Qi S H, 2005b. Over one hundred year sedimentary record of polycyclic aromatic hydrocarbons in the Pearl River Estuary， South China. Environmental Science, 26(3):141-145.

Liu H L, Liu M, Cheng S B, Ou D N,2005c. Occurrence of organochlorine pesticides (OCPs) in suspended particle matters(SPMs)and surface sediments of the south bank of the Yangtze Estuary. China Environmental Science, 25(5): 622-626.

Liu M, Hou L J, Xu S Y, Jiang H Y, Ou D N, Yu J, Wang Q, 2005d. The characteristics of NH_4^+-N adsorption on intertidal sediments of the Changjiang Estuary in China. Acta Oceanologica Sinica, 27(5): 60-66.

Liu Q M, Liu M, Xu S Y, Hou L J, Ou D N, 2004. Nitrogen profiles in core sediment and interstitial water of tidal flats in Changjiang (Yangtze) River Estuary. Marine Science, 28（9）：13-19.

Liu S M, Zhang J, Chen H T, Zhang G S, 2005a. Factors influencing nutrient dynamics in the eutrophic Jiaozhou Bay, North China. Progress in Oceanography, 66: 66–85.

Lu B, Chen R H, Wang Z P, Zhu C, Vetter W, 2005. The distribution pattern of persistent organic pollutants and their molecule stratigraphic records in the sediments from the Arctic Ocean. Acta Oceanologica Sinica, 27（4）：167-173.

Luo X J, Chen S J, Mai B X, Zeng Y P, Sheng G Y, Fu J M, 2005a. Distribution and sources of polycyclic aromatic hydrocarbons in sediments from rivers of Pearl River Delta and its nearby South China Sea. Environmental Science, 26（4）：129-134.

Luo X J, Chen S J, Mai B X, Zeng Y P, Sheng G Y, Fu J M, 2005b. Distribution of organoehlorine pesticites (ocps) in surface sediments in Pearl River Delta and its adjacent coastal areas of South China Sea. Acta Scientiae Circumstantiae, 26（4）：129-134.

Lü X X, Song J M, Li X G, Yuan H M, Zhan T R, Li N, Gao X L, 2005a. Geochemical characteristics and early

diagenesis of Nitrogen in the Northern Yellow Sea sediments. Acta Geologica Sinica, 79(1):119-123.

Lü X X, Song J M, Yuan H M, Li X G, Zhan T R, Li N, Gao X L, 2004a. The potential ecological roles of nitrogen in the surface sediments of the South Yellow Sea. Acta Ecologica Sinica, 24（8）：1635-1642.

Lü X X, Song J M, Yuan H M, Li X G, Zhan T R, Li N, Gao X L, 2004b. Geochemical characteristics of nitrogen in different grain size sediment from the southern Huanghai Sea. Acta Oceanologica Sinica, 27(1): 64-69.

Lü X X, Song J M, Yuan H M, Li X G, Zhan T R, Li N, Gao X L, 2005b. Distribution characteristics of nitrogen in the Southern Yellow Sea Surface sediments and nitrogen functions in Biogeochemical Cycling. Geological Review, 51(2): 212-218.

Lü X X, Zai S K, Yu Z H, 2005c. Nutrient distribution and controlled factors at the surface sediment of the Changjiang Estuary and adjacent sea area. Marine Environment Science, 24(3): 1-5.

Ma H B, Song J M, Lv X X, Yuan H M, 2003. Nitrogen forms and their functions in recycling of the Bohai Sea sediments. Geochimica, 32(1): 48-54.

Ma J L, Wei G J, Jia G D, 2005. Evaluation and calibration on the detrital contamination to biogenic opal of marine sediments by alkali leachate methods. Geochimica, 34（3）：285-290.

Maskaoui A K, Zhou J L, Zheng T L, Hong H, Yu Z, 2005. Organochlorine micropollutants in the Jiulong River Estuary and Western Xiamen Sea, China. Marine Pollution Bulletin 51 (2005) 950–959

Ni J Y, Maggiulli M, Liu X Y, Wang F G, Zhou H Y, 2005. Pore water distribution and quantification of diffusive benthic fluxes of silicate，nitrate and phosphate in surface sediments of the equatorial northeastern Pacific. Geochimica, 34（6）：587-594.

Ni J Y，Liu X Y，Chen Q J ，Lin Y A, 2006. Pore—water distribution and quantification of diffusive benthic fluxes of nutrients in the Huanghai and East China Seas sediments. Acta Oceanologica Sinica, 25(1):90～99.

Peng X Z, Wang Z D, Yang C, Chen F R, Mai B X, 2006. Simultaneous determination of endocrine-disrupting phenols and steroid estrogens in sediment by gas chromatography–mass spectrometry. Journal of Chromatography A, 1116: 51–56.

Qi J, Li F Y, Song J M, 2005. Distribution of ^{210}Pb activity of sediments in the Yellow and Bohai seas. Geochimica, 34（4）：351-356.

Qi X H, Liu S M, Zhang J, 2006. Sediment-water fluxes of nutrients in the Yellow Sea and the East China Sea. Marine Science, 30(3): 9-15.

Qi X H, Liu S M, Zhang J, Chen H T, 2003. Nutrients regeneration speed of sediment in harmful algae blooms (HAB) area of East China Sea. Chinese Journal of Applied ecology, 14(7): 1112-1115.

Qiu Y W, Yan W, Wang Z D, Zhang G, 2005a. Distributions of heavy metals in seawater, sediments and organisms at Daya Bay and their ecological harm. Journal of Tropical Oceanography, 24(5): 69-76.

Qiu Y W, Zhou J L, Maskaoui K, Hong H S, Wang Z D, 2005b. Distribution of polycyclic aromatic hydrocarbons

in water and sediments from Daya Bay and their ecological hazard assessment. Journal of Tropical Oceanography, 23(4): 72-80.

Ren J L, Zhang J, Li J B, Yu X Y, Liu S M, Zhang E R, 2006. Dissolved aluminum in the Yellow Sea and East China Sea Al as a tracer of Changjiang (Yangtze River) discharge and Kuroshio intrusion. Estuarine, Coastal and Shelf Science, 68: 165-174.

Song J M, Li X G, Li N, Gao X L, Yuan H M, Zhan T R, 2004a. A simple method for determining accurately dissolved inorganic carbon in seawaters. Chinese Journal of Analytical Chemistry, 32 (6):1689-1692.

Song J M, Ma H B, Li X G, Yuan H M, Li N, 2004b. Geochemical characteristics of adsorbed inorganic nitrogen in the south Bohai Sea sediments. Oceanologia ET Limnologia Sinica, 35(4): 315-322.

Song J M，Luo Y X，Lü X X，Li P C, 2003. Forms of phosphorus and silicon in the natural grain size surface sediments of the southern Bohai Sea. Chinese Journal of Oceanology and Limnology, 21(3): 286-292.

Tian T, Wei H, Su J, Zheng C S, Sun W X, 2003. Study on cycle and budgets of nutrients in the Yellow Sea. Advance in marine science, 21（1）：1-11.

Tian Z L, Dai Y, Long A M, Chen S Y, 2005. Geochemical characteristics of rare earth elements in sediments of Nansha Islands Sea Area, South China Sea. Journal of Tropical Oceanography, 24（1）：8-14.

Wang D Q, Chen Z L, Wang J, Xu S Y, Yang H X, Chen H, Yang L Y, Hu L Z, 2006. Denitrification，nitrous oxide emission and adsorption in intertidal flat，Yangtze Estuary，in summer. Geochimica, 35（3）：271-279.

Wang H K, Huang L H, Chen G H, 2005a. Forms and distributions of phosphorus in surface Sediments of Nansha Islands Sea Area. Journal of Tropical Oceanography, 24（3）：31-37.

Wang P B, Song J M, Guo Z Y, Li P C, 2005b. Behavior of resuspended phosphorus in sea surface sediment in the simulate condition. Marine Environment Science, 24（4）：37-40.

Wang Z B, Yang S Y, Li C X, 2004. Major elemental compositions and paleoenvironmental changes of the core sediments in the southern Yellow Sea. Geochimica, 33（5）：483-490.

Wong H X, Zhang X M, Wang Y, Chen L H, Qin Y C, Wu N Y, Zhong H X,2005. The relation between the reduce of phosphorus in marine sediment and the debase of atmospheric CO_2 during ice age. Science in China (series D), 35 (11): 1053~1059.

Wu P, Yang G P, Zhao R D, 2003. Sorption behavior of phenol in marine sediments. Oceanologia ET Limnologia Sinica, 34（4）：345-354.

Wu Q H, Jia H L, 2005. The grain-size distribution of organochlorine pesticides in sediments. Journal of Guangzhou University (Natural Science Edition), 4(1): 40-45.

Wu Y S, Zhang X Q, Zhang S K, Zhang Z S, Sun P G, 2004. The analysis of biochemical yellow substance in components of the marine the Jiaozhou Bay. Acta Oceanologica Sinica, 26（4）：58-64.

Xu j R, Wang Y S, Yin J P, Wang Q J, Zhang F Q, He L, Sun C C, 2005. Transformation of dissolved inorganic nitrogen species and nitrification and denitrification processes in the near sea section of Zhujiang River. Acta Scientiae Circumstantiae，25(5)：686-692.

Xu M D, Wei H P, Li M, Huang X S, 2006. A Study on the sorption and desorption of phosphate by sediments in the Yangtze River Estuary. Journal of Taiyuan University of technology, 37(1): 48-54.

Yang Q S, Mai B X, Fu J M, Sheng G Y, Luo X J, Lin Z, 2004a. Fluxes of persistent organic pollutants from humen tidal channel of Pearl River to lingdingyang estuary. Scientia Geographica Sinica, 24(6):704-709.

Yang Q S, Ou S Y, Xie P, Mai B X, Fu J M, Sheng G Y, 2004b. Distribution and seasonal changes of polycyclic aromatic hydrocarbons (PAHs) in surface water from Humen tidal channel. Acta Oceanologica Sinica, 26(6): 37-48.

Ye X W, Liu S M, Zhao Y F, Zhang J, 2006. The distribution of biogenic silica in the sediments of the East China Sea and the Yelow Sea and its environmental signification. China Environmental Science, 24（3）：265-269.

Yuan C G, Shi J B, He B, Liu J F, Liang L N, Jiang G B, 2004. Speciation of heavy metals in marine sediments from the East China Sea by ICP-MS with sequential extraction. Environment International, 30: 769– 783.

Yue W Z, Huang X P, 2005. Distribution characteristics of phosphorus in core sediments from Zhujiang River Estuary and its environmental significance. Journal of Tropical Oceanography, 24（1）：21-27.

Zhai W D, Dai M H, Cai W J, Wang Y C, Hong H S, 2005. The partial pressure of carbon dioxide and air–sea fluxes in the northern South China Sea in spring, summer and autumn. Marine Chemistry, 96: 87– 97

Zhang X S, Zhang L J, Tan Y, 2004. Vertical distribution and study on activity of acid extracted metals in sediment of tideland. Marine Environmental Science, 23(2): 29-31.

Zhang Z L, Hong H S, Chen W Q, Wang X H, Lin J Q, Yu G, 2003. Contents of organochlorine pesticides in water，pore water and Sediment in Minjiang River Estuary of China. Environmental Science, 24(1): 117-120.

Zhao Y F, Liu S M, Ye Y W, Zhang J, 2005a. The anaIysis of biogenic siIica in the sediments of the East China Sea and the YeIIow Sea. Periodical of ocean university of china, 35（3）：423-428.

Zhao Z M, Zhang Lei, Zheng B H, Guo K Q, Qin Y W, Wang Yi, 2005b. Spatial distribution of phosphorus and nitrogen in core sediments of Bohai bay. Jour. of Northwest Sci-Tech Univ. of Agri. and For. (Nat. Sci. Ed.), 33(4): 107-111.

Zheng L B, Ye Y, Zhou H Y, Wang H Z, 2003a. Distribution of different forms of phosphorus in seabed sediments from East China Sea and its environmental significance. Oceanologia ET Limnologia Sinica, 34(3): 274-282.

Zheng L B, Zhou H Y, Ye Y, 2003b. Laboratory simulation on phosphorus releasing near the water／sediment interface in East China Sea off Changjiang Estuary. Marine Environmental Science, 22(3): 31-34.

Zhou W H，Wu Y H，Chen S Y, Yin K D, 2003. Distribution of Organic Matter, Iron, Manganese in Surface Sediments in the Nansha Islands Sea Area，South China Sea. Marjne Science Bulletin, 5(2): 14-21.

Zhu L M, Du J M, Zhang Y H, Xu J, 2006. Tracing the sediment source at E2 hole in the South Yellow Sea with rare earth element and trace element. Acta Scientiae Circumstantiae，26(3)：495-500.

Zhu M H, Ding Y S, Zheng D C, Tao P, Qu Y J, Cui Y, Gong W M, Ding D W, 2005. Bioavailability and distribution of the familiar heavy metals around rhizosphere sediment of Suaeda heteroptera, Marine Environmental Science, 24(3): 21-24.

PROGRESS OF OCEANIC REMOTE SENSING BY SATELLITE ALTIMETRY IN CHINA, 2002-2006

QIU Zhongfeng[1], HE Yijun[1], LI Haiyan[1,2] and WANG Lijing[1,2]

(1.Institute of Oceanology, Chinese Academy of Sciences, Qingdao 266071, China;
2.Graduate School, Chinese Academy of Sciences, Beijing 100039, China)

Abstract: The development of oceanic remote sensing with satellite altimetry in China is reviewed in this paper. From 2002 to 2006, Chinese researchers have been studying altimeter widely and its application. The altimeter data has been applied mainly in three aspects: sea surface height, significant wave height and sea surface wind speed.

Key words: satellite altimetry, ocean, remote sensing

Satellite altimetry is a kind of active microwave sensor, which permanently transmits signals to the earth and receives the echo waves from sea surface. Abundant information about sea surface characteristics are included in its echo signals, which includes instantaneous distances from sea surface to satellite altimetry, backscatter coefficients and wave forms of electromagnetic waves returning from sea surface. Satellite altimeter data have almost been applied to all the fields of physical oceanography. Satellite altimetry is one of the sensors used in oceanic remote sensing competently, with long-period, large-scale, high-resolution and instantaneous data.

Altimeter has been studied widely in China from 2002 to 2006. The new research results have been published continually after the successful launch of TOPEX/Poseidon (T/P) by the joined USA and France, with more of the altimeter data accumulated than before. The study fields cover marine geophysics, oceanic dynamics and monitoring of oceanic environment.

The time delay, front slope and backscatter intensity of waveform returning from sea surface are the three widely used parameters of altimeter. The time delay is used to derive sea surface height (SSH), which is defined as round-trip time between satellite altimeter and sea surface. The front slope of return waveform can be used to derive significant wave height (SWH) and the backscatter intensity can be used to derive wind speed. The following aspects summarize the progress of oceanic remote sensing by satellite altimeter in three aspects: sea surface height, significant wave height and wind speed.

I. Sea Surface Height (SSH)

SSH is defined as the height of the sea surface above the reference ellipsoid. It is computed by the subtracting satellite altitude above the sea surface from the satellite altitude above the reference ellipsoid. SSH plays a central role in researching geoid, gravity models, tidal systems, local and global current distributions, variations of sea surface and so on.

1. Tidal Retrievals and Applications

The long-term series SSH data from altimeter can be used to retrieve tides, because the orbits of the satellite altimeter will repeat precisely after a period of time.

The Least Square Fit Method (LSFM) for tidal harmonic analysis was mainly used to extract tidal coefficients from SSH data, which was introduced by Fang et al. (1986). He et al. (2002) applied this method to retrieve the tidal constants of 21 tidal constitutes from altimeter data in the China Seas. The retrieval constants have been compared with the harmonic constants extracted from the observed data in St. Shijiusuo and the amplitude differences of major constitutes were lower than 5cm. The results showed that the method was able to be used to retrieve tidal harmonic constants from altimeter data. Dong et al. (2002) also computed the harmonic constants of 12 tidal constituents by LSFM, using the T/P altimeter data from Jan.1993 to Jun.1999. The amplitude accuracies of M_2 and m_1 ($m_1=(K_1 + O_1)/2$) at the crossover points were 2.4 cm and 0.8cm，and the accuracies of the lags were 2.3º and 2.5º respectively.

Besides LSFM, the other methods have been used to extract tidal harmonic constants from altimeter data. Wang and Liu (2003) extracted the M_2 harmonic constants using the orthogonal analysis method by the 5-yr (1992-1997) T/P altimeter data. They compared the harmonic constants by this method and LSFM. And the harmonic constants extracted by the two methods were mainly consistent.

Liu et al. (2002a, 2002b) analyzed the tidal harmonic constants on the basis of the over 6 years T/P data in the Northwest Pacific and the South China Seas (SCS) by using the difference ratio relations of the tidal constitutes. The tidal harmonic constants agreed well with those extracted from the tide gauge data.

Bao et al. (2002) analyzed tidal harmonic constants using the more than 300 cycles T/P altimeter data. The tidal aliasing problem caused by the T/P data sampling rate has been taken into account. The results of comparing the computed tidal harmonic constants with those extracted from the tide gauge data indicated that the computed tidal harmonic constants were more accurate than that of the existing global ocean models.

Tides in coastal areas and semi-enclosed seas are usually difficult to be retrieved only by altimeter data, because of shallow water depths, large gradients of water depths, small spatial scales of tides and complex distributions of tides. Therefore, He et al. (2002) thought it much precise to retrieve tides in the coastal areas and semi-enclosed seas from altimeter data using numerical assimilation methods based on hydrodynamic equations.

Wu et al. (2003) assimilated the harmonic constants extracted from the T/ P altimeter data (248 periods lasting six years) into a tidal model in the SCS by using the adjoint assimilation method. The optimal open boundary conditions and the bottom friction coefficients were given and the harmonic constants of m_1 and M_2 were retrieved. The harmonic constants were coincided with those extracted from the tide gauge data. Wu et al. (2004, 2005) adopted a three dimensional numerical model (POM) to simulate the tidal movements in the SCS. Including the tide-producing potentials，they optimized the open boundary conditions and assimilated the harmonic constants

extracted from T/P altimeter data. The harmonic constants of the four main constituents (M_2、S_2、O_1、K_1) were coincided with those extracted from the tide gauge data.

Lv et al. (2002) have performed some numerical experiments on the M_2 constitute in the Bohai Sea (BhS) using the adjoint method. The M_2 tidal harmonic constants on the open boundaries of BhS were attained. The tidal harmonic constants extracted from the T/P altimeter data were also assimilated into a 2D tidal model to study the bottom friction coefficients by using the adjoint method in the China Seas (Lv et al., 2006).

Qiu and He (2005a) extracted the M_2 tidal harmonic constants in the China seas from the 10-yr T/P altimeter data along the track points, and assimilated them into a 2-D non-linear tidal model with a nudging method. The same T/P data were used to extract the tidal harmonic constants of 11 constitutes in the BhS and the Yellow Seas (YS) by Qiu et al. (2005b, 2005c). And then the adjoint method has been used to simulate the tidal system.

The same adjoint assimilation model was used to investigate the shallow water tidal constituents by He et al. (2004). The harmonic constants of the shallow water tidal constituents (M_4, M_{S4} and M_6) in the BhS and the YS were first extracted from the 10-yr T/P data and then assimilated into a nonlinear barotropic tidal model by using the adjoint method. The results showed that the computed tidal constants were more accurate than those of the other models.

Li et al. (2005a) studied the tidal energy fluxes and the dissipations of the major tidal constituents by assimilating the harmonic constants extracted from the T/P altimeter data and the tidal gauges data into a numerical model in the BhS，the YS and the East China Sea (ECS). Li et al. (2005b) also assimilated the tidal elevations of M_2 and S_2 derived from the T/P altimeter data at the crossover points into a dynamical model using a blending method. By comparing the assimilated harmonic constants with the non-assimilated ones, the assimilated ones were improved with accuracies of 14.9% for M_2 and 23.3% for S_2， respectively.

The T/P altimeter data were also used to compute the energy flux of the internal M_2 tide. The energy flux of the internal M_2 tide in the marginal seas of the northwestern Pacific and the Pacific were analyzed using the T/P altimeter from Oct. 1992 to Jun. 2002 by Tian et al. (2003) and Zhang et al. (2005), respectively.

2. Gravity Anomalies and Bathymetry Recovery

Topography is a major boundary condition of the ocean. The surface undulations reflect the disequilibria of the earth between the interior effects and outer effects. The oceanic topography can be easily attained by satellite altimeter. Because gravity anomalies can be derived from altimeter data precisely, which is closely connected with the oceanic topography in the wavelength regions 15-200km.

He et al. (2002) retrieved the gravity anomalies from the different altimeter data in the SCS. According to the relationships between gravity anomalies and topography, they retrieved the oceanic topography based on developing the local gravity model in China. Then they attained the oceanic topography in the Northwest Pacific from the Geosat/GM、ERS-1 and T/P data.

Zhai et al. (2004) proposed a modified statistical model for recovering oceanic topography using the altimeter data by the least-squares method. The model was used to compute the oceanic depth in the SCS from the altimeter-derived gravity anomalies.

The three methods (i.e., analytical and numerical inversions of the Stokes formula, and the inverse Vening Meinesz formula) used to derive gravity anomalies from altimeter data were developed by Huang et al. (2004). And the three formulae were employed to compute gravity anomalies by use of the Seasat, Geosat, ERS-1 and T/P altimeter data in the SCS.

Zhang et al. (2003) applied a combined adjustment model to compute the SCS geoid undulations by using the T/P (9-346cycle) and Geosat/ERM (1-60cycle) altimeter data. The geoid undulation difference between this model and the OSU91A model was 30cm (with spatial resolution 22km). Moreover, Gao et al. (2003) used the altimeter-derived geoid to study submarine tectonics and geodynamics.

3. Mesoscale Eddies

Oceanic mesoscale eddies are connected with the powerful energy inputs to the ocean by heavy weather processes. Oceanic mesoscale eddies are paid attention to from the 1970s, especially their instabilities and mechanisms of energy transformation. Now altimeter data are the widely used data to research mesoscale eddies and oceanic currents. And many Chinese researchers have investigated the mesoscale eddies in the SCS by use of altimeter data.

Jing and Li (2003) found a large cyclonic front eddy in the regions around the Taiwan Island in March 1996, by use of the surface drift buoy data, the altimeter data and the remote sensing SST data.

Li et al. (2003, 2004) investigated the SSH anomalies and the seasonal and interannual variations in the northeastern SCS using the 7-yr (1993-1999) T/P altimeter data. The results showed that the energy of mesoscale eddies was large, and strong anticyclone eddies were frequently appeared.

Pan and Liu (2005) analyzed the effects of oceanic eddies on the upper mixing layer in winter in the North Pacific with the ARGO buoy data, the SST data from TRMM and the T/P、ERS altimeter data. And Chen et al. (2005) attained the temporal and spatial distributions of the mesoscale eddies and analyzed the possible mechanism of the mesoscale eddies in the SCS, using the 11-yr (1993-2003) T/P, Jason and ERS1/2 altimeter data.

Hu et al. (2004) and Wang et al. (2003) also studied eddies in the SCS using the altimeter data. Wang et al. (2004) compared the T/P data with the data of the marine investigation cruises during the mid-summer, 2002.

4. Oceanic Currents and Variations of SSH

Altimeter data have also been widely used to research oceanic currents and variations of SSH. Wang et al. (2004) used the T/P (cycles 9-249), Geosat/ERM and ERS-2 (cycles 0-44) altimeter data to analyze the SSH anomalies in the China Seas. Their results showed that the SSH anomalies appeared to be a rising trend with 2-3 mm per year in the China Seas. The characteristics of SSH

anomalies were also analyzed using the T/P altimeter data in different seas (Lin and Hu 2005, Shen et al. 2003, Yang et al. 2004, Zhong et al. 2005).

Li et al. (2003b) applied a wavelet transformation method to investigate the multiple time-scale variations of SSH using the 8-yr (1993-2000) T/P data in the northeastern SCS. Wang et al. (2003) analyzed the characteristics of the SSH anomalies using the empirical orthogonal function method in the SCS, based on the SSH derived from the T/P altimeter data from Oct. 1992 to Sep. 1997.

Zhou et al. (2003) investigated the SSH anomalies of the Antarctic circumpolar current areas using the 8-yr merged T/P data from Jan. 1993 to Dec. 2000. Qiao et al. (2004a) analyzed the high frequency oscillations with the periods of less than 150 d and described the spatial distributions, using the T/P, ERS-1 and ERS-2 satellite altimeter data from Oct. 1992 to Dec. 2000.

Based on the characteristics of the T/P altimeter return waveform, Bao et al. (2004) improved the precision of the SSH derived from the T/P altimeter data in the coastal seas. Then they processed four cycles of the T/P altimeter waveform data in the SCS. By comparing the SSH with the real-time tide gauge data, the precision of the SSH derived from the T/P altimeter data was greatly improved.

Wei et al. (2002、203) compared the T/P data with the SSH computed by a fine-grid model (1/6degrees) in the SCS, ECS and Japan/East Sea. The results showed that the model-produced monthly SSH anomalies were in a good agreement with the altimeter measurements.

Qiu and Hu (2004、2005) investigated the monthly variations of the surface currents in the tropical Atlantic by use of the T/P altimeter data from Apr. 1993 to Mar. 2001.

Wang et al. (2003) studied the Kuroshio axis fluctuations using the T/P data along three descending ground tracks from 1993 to 2001. Two large meanders were found in 1993 and 2000-2001, respectively. And both of them formed V-like paths and lasted several months.

Guo et al. (2005) computed the transport volumes and variations in the Taiwan Strait from 1993 to 2001 using the AVISO'S satellite altimeter SSH anomalies data and the wind field data from the National Centers for Environmental Prediction (NCEP).

Yuan et al. (2004) computed diagnostically the circulation with the P vector method using the hydrographic data obtained in the 1998 cruise and the TOPEX/ERS-2 SSH data in the SCS.

Taking the concept of an 'assumed reference point' into account, Zhang et al. (2005) investigated the Changjiang River discharge using the 7-yr (1993-99) T/P altimetry data.

Furthermore, Qiao et al. (2004) studied the circuits of El Niño/La Niña signals using the 8-yr (1992-2000) T/P altimeter data. Chen and Lin (2005) also investigated the impacts of El Niño/La Niña on the amplitude and phase of the annual cycle using the 10-yr (1993–2002) high quality oceanic water vapor data derived from the TOPEX altimeter data.

II. Sea Surface Wind Speed (SSWS)

The dynamic processes such as sea waves and currents are caused by winds. Sea surface wind plays a significant role in modulating energy and transmitting heat flux between ocean and atmosphere. Sea waves of a centimeter scale generated by wind will change the sea surface

roughness. And a radar altimeter is sensitive to the variations of sea surface roughness with a scale larger than or equal to the radar working wavelength, which is about 2 centimeters. So the altimeter data can be used to retrieve SSWS. Simply, the backscatter cross section is inversely proportional to the SSWS. The higher the wind speed, the stronger the roughness, the wider the returned pulse, the smaller the backscatter energy and the smaller backscatter cross section. The analytical relation between backscatter cross section and wind speed is named the Geophysical Model Function.

He et al. (2002) compared 14 representative models having been published. The RMS values between all of the models and in situ wind speeds were limited in 2m/s when the wind speeds were ranging from 0 to 15m/s. But the differences were large when the wind speeds were larger than 20m/s. Then they proposed the inversion model of high wind speeds in the China Seas and the northwest Pacific Ocean. Under low wind speeds, the accuracy was less than 2m/s, and under high wind speeds, the precision was superior 15%, which was better than the other three prevalent models.

Chen et al (2003) proposed a linear composite method (LCM) to retrieve the wind speeds from the altimeter data. By comparing the computed wind speeds with the buoy measurements, the precision of the LCM is 12% better than the other algorithms. And the global wind structures under the extreme climate were derived from the TOPEX altimeter data by Chen et al. (2004)

Zhao and Ye (2004) investigated the 7 represented altimeter functions using the coincident wind speeds from the T/P altimeter data and the buoy observations. The analytical algorithm including the effects of the wave state was superior to those empirical algorithms.

Sun et al (2006) analyzed the characteristics of the wind and wave fields in the ECS using the TOPEX altimeter data. And the wind speeds estimated from the altimeter data was also used as validation or assimilation data or model inputs to research typhoon (Wang et al 2003, Zhang et al 2003, Lin et al 2003, Zhuang et al 2006).

Additionally, Huang et al (2006) studied the wind-energy inputs to the global ocean using the T/P altimeter data from 1993 to 2003. Zhou and Guo (2005, 2006) derived the sea surface roughness in the Northwest Pacific using the wind speeds estimated from the altimeter data.

III. Significant Wave Height (SWH)

Sea surface waves, which play important dynamic roles in sea-land interactions, are key environmental conditions for marine engineering and ship design. Altimeter data can provide such the wave information as spatial scales, growth status and so on.

Chen et al (2003) studied the zonal propagation velocities of the oceanic Rossby waves in the Pacific and Atlantic by analyzing the T/P and ERS-1/2 altimeter data from Oct. 1992 to Jul. 2001 using a 2-D Radon transformation method.

Han et al (2003a, 2003b) studied the SWH components using the T/P altimeter data in the South and North Atlantic from Oct. 1992 to Dec. 1998. Their results showed that the SWH of annual swells distributed like a saddle, with the low values in the equator Atlantic and high values in the

northern and southern Atlantic. And the SWH distributions were connected with the climate distributions in the Atlantic. Han et al (2003c, 2003d, 2003e) also investigated the spatial distributions and the temporal variations of the SWH in the Pacific. The variations of the SWH were obviously seasonal, which was coincided with the distributions of the wind fields. And the dominant SWH was swell in the Pacific

Han et al. (2003f) developed the Tail Distribution Method to estimate the extreme SWH at the three coastal stations by using the altimeter data. The estimated SWH were coincided with those computed by the traditional methods using the observed wave data. The extreme SWH distributed zonally in the latitude direction, which was consistent with the distributions of the wind fields.

Qi et al (2003) analyzed the relationships of the wind and wave fields in the SCS by the Empirical Orthogonal Function (EOF) and Singular Value Decomposition (SVD) using the sea surface winds and waves derived from the T/P altimeter. Their results showed that the leading five EOF modes could capture the spatio-temporal features.

Zhang et al (2003) computed the wind fields using the NCEP re-analysis wind data with an empirical typhoon model. A third-generation wind-wave model was developed by the wind fields in the SCS in 1999. A simple optimal interpolation assimilation method was then employed in the wave model. The wave model was improved after being assimilated.

For validating the results of retrieved mean wave period, Sun and song (2006) introduced the four empirical algorithms established previously. The ocean wave periods were computed and the statistical comparison among them was performed based on the over 5-yr TOPEX altimeter data in the entire ECS. The mean wave period obtained with their new distribution parameters agreed better with the wave period measured by the buoy than that computed by the other three algorithms.

Chu et al (2004a, 2004b) compared the SWH of the Wavewatch-III model with that extracted from the T/P altimeter data. Their results showed that the Wavewatch-III model can be used to simulate the sea wave fields in the SCS.

Besides the three applications mentioned above, the altimeter data was also used to estimate rainfall. Chen et al (2003) studied the global oceanic precipitation using the TOPEX and TMR data. They also studied the interactions between the warm pool and “rain pool” in the Pacific with the altimeter data.

Furthermore, many Chinese researchers put great efforts into the altimeter data processing. Based on the orbit theory of the altimeter, Liu et al (2005) attained the mean SSH using the “Weighted Averaged Distance” method. By comparing the SSH derived by the new method with that extracted by the traditional methods at the crossover points, the new method can be used to compute the SSH from the altimeter data.

Wu and Zhang (2005) sampled the altimeter data from a mass of scientific data received by the “SZ-4” Spaceship. And they analyzed the statistical characteristics of the ocean return signals.

Zhang et al (2004) introduced the vertical deflections of the altimeter data in detail. They

computed the south and west components of the along-track vertical deflections using a cycle of the T/P altimeter data. And they also computed the errors due to the vertical deflection. Their results showed that the errors caused by the vertical deflection were mainly in the range from -5 to 5 mm, and the errors were greater than 10 cm at only a few points.

Reference

[1] He Yijun et al. (2002), *Investigation and application in oceanic remote sensing with altimeter*, Beijing: Science Press(In Chinese)

[2] Fang Guohong et al. (1986), *Analysis and Prediction of Tides and Tidal Currents*. Beijing: Ocean Press(In Chinese)

[3] Dong, X.J.，Ma, J.R.，Huang, C.，Fan, Z.H.，Han, G. J. and Xu, C. J. (2002)，tidal information of the yellow and east china seas from TOPEX/Poseidon satellite altimetric data，*Oceanologia Et Limnologia Sinica*, 33(4): 386-392(In Chinese)

[4] Liu, K.X., Ma, J. R., Han, G.J., Fan, Z.H. and Xu, C.J.(2002a)， Tidal harmonic analysis of TOPEX/POSEIDON data in Northwest Pacific by introducing difference-ratio relation, *ACAT OCEANOLOGICA SINICA*, 24(4): 1-10(In Chinese)

[5] Liu, K.X.，Ma. J. R.，Xu, J.P.，Han, G.J. and Fan, Z.H.(2002b), ocean tides and sea surface height variations in south china sea by TOPEX/Poseidon altimetry, *Journal Of Tropical Oceanography*, 21(3): 55-63(In Chinese)

[6] Wang, Q.Y. and Liu, Z.L.(2003)，a new method of orthogonal analysis to extract the harmonic constants of tidal component, *Marine Sciences*, 7(9): 49-53(In Chinese)

[7] Bao, J.Y., Chao, D.B., Zhao, J.P., Wang, Q. and Liu, YC, (2004), Harmonic tidal analysis along T/P tracks in China Seas and vicinity, SATELLITE ALTIMETRY FOR GEODESY, GEOPHYSICS AND OCEANOGRAPHY, PROCEEDINGS, International Workshop on Satellite Altimetry for Geodest, *Geophysics and Oceanography*, Wuhan, 237-242

[8] Wu, Z.K., An,J.W., Lv, X.Q. and NG Lai-Ah,(2003)，a numerical model of tides in the south china sea by adjoint method, *OCEANOLOGIA ET LIMNOLOGIA SINICA*, 34(1): 101-108(In Chinese)

[9] Wu, Z.K., Tian, J.W. and Zhao, Q.(2004)，3-D numerical simulation of the South China Sea tidal waves with assimilation method, *JOURNAL OF HYDRODYNAMICS*, 19(4): 501-506(In Chinese)

[10] Wu, Z.K., Lu, X.Q. and Tian, J.W.(2005), Simulation of barotropic and baroclinic tides in the South China Sea, *ACTA OCEANOLOGICA SINICA*, 24(2):1-8

[11] Lv, X.G. and Fang, G.H.(2002)，Numerical experiments of the adjoint model for M_2 tide in the Bohai Sea, *ACTA OCEANOLOGICA SINICA*, 24(1): 17-24(In Chinese)

[12] Lv, X.Q. and Zhang, J.C.(2006), Numerical study on spatially varying bottom friction coefficient of a 2D tidal model with adjoint method, *Continental Shelf Research*, 26, 1905-1923

[13] Qiu, Z.F. and He Y.J., (2005a)，assivimation of the m_2 tides in china seas with TOPEX/Poseidon data，*OCEANOLOGIA ET LIMNOLOGIA SINICA*, 36(4): 376-384(In Chinese)

[14] Qiu, Z.F, He, Y.Jun. and Lv, X.Q.(2005b),Tidal Constituents in the Bohai and Yellow Seas from an Adjoint Numerical Model with TOPEX/Poseidon Data, *Journal of Hydrodynamics* (B), 17(3) ,275-282

[15] Qiu, Z.F, He, Y.Jun. and Lv, X.Q.(2005c), Tidal adjoint assimilation with the TOPEX/Poseidon altimetry data in the Huanghai and Bohai Seas, *ACTA OCEANOLOGICA SINICA*, 27(4),10-18(In Chinese)

[16] He,Y.J., Lu,X.Q. and Qiu, Z.F. and Zhao,J.p.(2004), Shallow water tidal constituents in the Bohai Sea and the Yellow Sea from a numerical adjoint model with TOPEX/POSEIDON altimeter data, *Continental Shelf Research*, 24, 1521-1529

[17] Li, P.L., Li, L., Zuo, J.C., C, M.X. and Zhao, W., (2005a), Tidal Energy Fluxes and Dissipation in the Bohai Sea,the Yellow Sea and the East China Sea, *PERIODICAL OF OCEAN UNIVERSITY OF CHINA*, 35(5):713-718(In Chinese)

[18] Li, P.L., Zuo, J.C., Wu, D.X., Li, L., and Zhao W.(2005b), numerical simulation of semidiurnal constituents in the Bohai Sea, the Yellow Sea and the East China Sea with assimilating TOPEX/Poseidon data, *OCEANOLOGIA ET LIMNOLOGIA SINICA*, 36(1): 24-30(In Chinese)

[19] Tian，J.W., Zhou，L., Zhang，X.Q, Liang，X.F., Zheng, Q. and Zhao, W.(2003), Estimates of M_2 internal tide energy fluxes along the margin of Northwestern Pacific using TOPEX/POSEIDON altimeter data, *Geophysical Research Letters*, 30(17): 1-4

[20] Zhang, X.Q., Liang, X.F and Zhou, L.(2005), Estimates of M_2 internal tide energy fluxes in the Pacific Ocean using TOPEX/Poseidon altimeter data, *ACTA OCEANOLOGICA SINICA*，27(5):9-14(In Chinese)

[21] Zhai, G.J., Huang, M.T., Ouyang, Y.Z., Bian, S.F., Liu, Y.C. and Liu, C.Y.(2004), A modified method for recovering bathymetry from altimeter data, SATELLITE ALTIMETRY FOR GEODESY, GEOPHYSICS AND OCEANOGRAPHY, PROCEEDINGS, International Workshop on Satellite Altimetry for Geodest, *Geophysics and Oceanography*, Wuhan, 83-89

[22] Huang, M.T., Zhai, G.J., Bian, S.F., Ouyang, Y.Z., Liu, Y.C. and Liu, C.Y.(2004), Comparisons of three inversion approaches for recovering gravity anomalies from altimeter data, SATELLITE ALTIMETRY FOR GEODESY, GEOPHYSICS AND OCEANOGRAPHY, PROCEEDINGS, International Workshop on Satellite Altimetry for Geodest, *Geophysics and Oceanography*, Wuhan, 151-159

[23] Zhang, Y.G., Zhang, J., Ji, Y.G. and Zhang, H.Q.(2003), Calculation of geoid undulations and gravity anomalies in the South China Sea by using the TOPEX/Poseidon and geosat altimeter data, OCEAN REMOTE SENSING AND APPLICATIONS, *PROCEEDINGS OF THE SOCIETY OF PHOTO-OPTICAL INSTRUMENTATION ENGINEERS(SPIE)*, Hangzhou, 521-528

[24] Gao, J.Y. and Jin, X.L.(2003), Tectonic and geodynamic pattern of marginal seas on the West Pacific inferred from multi-satellite altewetry geoid, *CHINESE JOURNAL OF GEOPHYSICS-CHINESE EDITION*, 46(5)

[25] Jing, C.S. and Li, L.(2003), First record of quasi constant cool eddy in Lanyu southeast to the TaiWan island, *Chinese Science Bulletin*, 48(15): 1686-1692(In Chinese)

[26] Li, Y.C., Cai, W.L., Li, L. and Xu, D.W.(2003a)，seasonal and interannual variabilities of mesoscale eddies in northeastern south china sea, *Journal Of Tropical Oceanography*, 22(3): 61-70(In Chinese)

[27] Li, Y.C., Li, L., Jing, C.S. and Cai, W.L. (2004)，Temporal and Spatial variety characteristics of sea surface height Northeast to the South Sea, *Chinese Science Bulletin*, 49(7): 702-709(In Chinese)

[28] Pan, A.J. and Liu, Q.Y. (2005)，Mesoscale eddy effects on the wintertime vertical mixing in the formation region of the North Pacific Subtropical Mode Water, *Chinese Science Bulletin*, 50(14): 1523-1530(In Chinese)

[29] Cheng, X.H., Qi, Y.Q. and Wang, W.Q. (2005), seasonal and interannual variabilities of mesoscale eddies in south china sea, *Journal Of Tropical Oceanography*, 24(4): 51-59(In Chinese)

[30] Wang, D.X.，Chen, J.，Chen, R.Y.，Zhu, B.C.，Guo, X.G.，Xu, J.D. and Wu R.S.(2004)，hydrographic and circulation characteristics in middle and southern south china sea in summer, 2000, *OCEANOLOGIA ET LIMNOLOGIA SINICA*, 35(2): 97-109(In Chinese)

[31] Wang, G.H., Su, J.L. and Chu, P.C.(2003), Mesoscale eddies in the South China Sea observed with altimeter data, *Geophysical Research Letters*, 30(21): 1-4

[32] Hu, J.Y. and Kawamura, H. (2004), Detection of cyclonic eddy generated by looping tropical cyclone in the northern South China Sea: a case study, *ACTA OCEANOLOGICA SINICA*, 23(2): 213-224

[33] Lin, L.R. and Hu, J.Y.(2005)，Seasonal and interannual variation of sea surface height in southeast Pacific，*Marine Sciences*，29(2): 37-42(In Chinese)

[34] Li, Y.C., Cai, W.L. and Li, L.(2003b)，The multi-scale variability of sea surface height in the northeastern South China Sea, *ACTA OCEANOLOGICA SINICA*, 25(5): 1-8(In Chinese)

[35] Shen, H., Guo, P.F., Qian, C.C. and Han, S.Z.(2003)，SEA SURFACE LEVEL VARIATIONS DURING 1993-2001, *OCEANOLOGIA ET LIMNOLOGIA SINICA*, 34(2): 169-178(In Chinese)

[36] Wang, J., Qi, Y.Q., Shi, P., Mao, Q.W. and Zhu, B.C. (2003)，characteristics of sea surface height in south china sea based on data from TOPEX/Poseidon, *Journal Of Tropical Oceanography*，22(4): 26-33(In Chinese)

[37] Yang, J., Lu J.Z., Sha, W.Y. and Chen, X. (2004), the related analisis of the sea surface height abnormlity (ssha) near the china seas, *MARINE FORECASTS*, 21(2): 29-36(In Chinese)

[38] Zhong, H.X., Xie, Z.R., Chui, S.H. and Xin, Z.B. (2005)，Research on the Sea Surface Topography in the Yellow Sea and East China Sea Based on T/P Satellite, *MARINE SCIENCE BULLETIN*, 24(5): 1-7(In Chinese)

[39] Wang, Z.T., Li, J.C., Chao, D.B. and Hu, J.G. (2004), Sea level changes detected by using satellite altimeter data and comparing with tide gauge records in China Sea, SATELLITE ALTIMETRY FOR GEODESY, GEOPHYSICS AND OCEANOGRAPHY, PROCEEDINGS, International Workshop on Satellite Altimetry for Geodest, *Geophysics and Oceanography*, Wuhan, 271-277

[40] Zhou, Q.，Zhao, J.P. and He, Y.J. (2003)，low-frequency variability of the antarctic circumpolar current sea level detected from TOPEX/Poseidon satellite altimeter data, *OCEANOLOGIA ET LIMNOLOGIA SINICA*, 34(3): 256-266(In Chinese)

[41] Qiao, F.L., TAL Ezer and Yuan, Y.L. (2004a), The zonal distribution features of high frequency oscillations in the oceans derived from satellite altimeter data, *ACTA OCEANOLOGICA SINICA*, 26(3): 1-7(In Chinese)

[42] Bao, L.F.，Lu, Y. and Xu, H.Z. (2004)，Waveform retracking of TOPEX/Poseidon altimeter in Chinese offshore，C*hinese Journal Of Geophysics-Chinese Edition*，47(2): 216-221

[43] Wei, Z.X., Fang, G.H., Choi, B.H., Fang, Y. and He, Y.J. (2002)，Sea surface height and transport stream function of the South China Sea from a variable-grid global ocean circulation model, *SCIENCE IN CHINA SERIES D-EARTH SCIENCES* ,32(12): 987-994(In Chinese)

[44] Wei, Z.X., Fang, .GH., Choi, B.H., Fang, Y. and He, Y.J. (2003), Sea surface height and transport stream function of the South China Sea from a variable-grid global ocean circulation model, *SCIENCE IN CHINA SERIES D-EARTH SCIENCES*, 46(2): 139-148

[45] Qiu, Y. and Hu, J.Y. (2004)，Monthly variation of surface currents in the tropical Atlantic derived from TOPEX/Poseidon altimeter data, *ACTA OCEANOLOGICA SINICA*，26(6): 1-12(In Chinese)

[46] Qiu, Y. and Hu, J.Y. (2005)，Seasonal Variation of Surface Currents in the Tropical Atlantic Derived from Altimeter Data, *MARINE SCIENCE BULLETIN*，24(4): 8-16(In Chinese)

[47] Wang, H.L., Guo, P.F., Qian, C.C. and Han, S.Z. (2003)，Kuroshio Meander South Of Japan Detected By Altimeter, *Journal Of Tropical Oceanography*, 22(4): 84-92(In Chinese)

[48] Guo, J.S., Hu, X.M. and Yuan, Y.L. (2005), A Diagnostic Analysis of Variations in Volume Transport Through the Taiwan Strait Using Satellite Altimeter Data, *ADVANCES IN MARINE SCIENCE*, 23(1): 20-26(In Chinese)

[49] Yuan, Y.C., Bu, X.W., Lou, R.Y., Su, J.L. and Wang, K.S. (2004), Diagnostic calculation of the upper-layer circulation in the South China Sea during the water of 1998, *ACTA OCEANOLOGICA SINICA*，26(2):1-10(In Chinese)

[50] Zhang, J.Q., Xu, K.Q., Qi, L.H., Yang, Y.H. and Watanabe, M. (2005), Estimation of freshwater and material fluxes from the Yangtze River into the East China Sea by using TOPEX/Poseidon altimeter data, *HYDROLOGICAL PROCESSES*, 19(18): 3683-3698

[51] Qiao, F.L., Yu, W.D. and Yuan, Y.L. (2004b), On the circuit and propagation of EI Nino/La Nina signals,

ACTA OCEANOLOGICA SINICA, 26(4):1-8(In Chinese)

[52] Chen, G. and Fang, L.X., (2005), Improved Scheme for Determining the Thermal Centroid of the Oceanic Warm Pool Using Sea Surface Temperature Date, *Journal of Oceanography*, 61, 295-299

[53] Chen, G., Bertrand,C., R. Ezraty and D. Vandermark (2002), A dual-frequency approach for retrieving sea surface wind speed from TOPEX altimetry, *Journal of Geophysical Research*, 107(C12):19,1-10

[54] Chen,G. (2003a), An Intercomparison of TOPEX, NSCAT, and ECMWF Wind Speeds: Illustrating and Understanding Systematic Discrepancies, *Monthly Weather Review*, 132, 780-792

[55] Chen, G., Bi, S.W. and R. EZRATY (2004a), Global structure of extreme wind and wave climate derived from TOPEX altimeter data, *International journal of remote sensing*, 25(5):1005-1018

[56] Zhao, D.L. and Ye, Q. (2004)，On altimeter wind speed model functions and retrieval of wave period, *ACTA OCEANOLOGICA SINICA*, 26(5): 1-11(In Chinese)

[57] Sun, Q., Song, J.B. and Chen, X.G. (2006)，The analysis of the characteristic of the wind and wave fields over the East China Sea by using TOPEX satellite altimeter data, *Marine Sciences*，30(4): 10-15(In Chinese)

[58] Wang, C.X., Zhang, Z.H. and Wang, K.G. (2003)，A Hindcast Study of Waves Generated by Typhoon 9914, *MARINE SCIENCE BULLETIN*, 22(1): 9-16(In Chinese)

[59] Zhang, Z.X., Qi, Y.Q., Shi, P., Li, C.W. and Li, Y.S. (2003)，Application Of An Optimal Interpolation Wave Assimilation Method In South China Sea, *Journal Of Tropical Oceanography*, 22(4): 34-41(In Chinese)

[60] Lin, M.S.，Xu, D.W. and Li, X.S.(2003)，Study of application of satellite data in monsoon and circulation of South China Sea，*Proceedings of the SPIE - The International Society for Optical Engineering*，606-617

[61] Zhuang, W.，Wang, D.X., Hu, J.Y. and Ni, W.S., Response of the cold water mass in the western South China Sea to the wind stress curl associated with the summer monsoon, *ACTA OCEANOLOGICA SINICA*, 25(4): 1-13

[62] Huang, R.X., Wang, W. and Liu, L.L. (2006), Decadal variability of wind-energy input to the world ocean, *Deep-Sea Research* II 53, 31-41

[63] Zhou, L.M. and Guo, P.F. (2005)，derivation of sea surface roughnessfrom wind speed estimated by satellite altimnter, *Transactions of Oceanology and Limnology*, 2005.4: 10-14(In Chinese)

[64] Zhou, L.M., Guo, P.F. and Wang A.F.(2006), Sea Surface Roughness Derivation from Wind Speed Estimated by Satellite Altimeter, *Marine Science Bulletin*, 8(1):61-67

[65] Chen, H.Y., Qiao, F.L. and WANG Y.G. (2003), Zonal Propagation Velocity Distribution Characteristics of Oceanic Rossby Waves, *ADVANCES IN MARINE SCIENCE*, 21(4): 387-392(In Chinese)

[66] Han, S.Z., Guo, P.F., Zhao, X.X, Zhu, D.Y. (2003a), a study on the distribution and variation of significant wave height in the Atlantic ocean using the satellite altimetry data, *Marine Science*, 27(12):50-54(In Chinese)

[67] Han, S.Z., Zhao. X.X., Zhu, D.Y. and Guo, P.F.(2003b)，a study of distribution and variation rules of SWH in the Atlantic ocean by using the satellite altimetry data, *Transactions of Oceanology and Limnology*, 22-29(In Chinese)

[68] Han, S.Z.，Qiao, F.L.，Zhu, D.Y. and Guo, P.F. (2003c)，Study of Wave Height Entropy Distribution Variabilities in the Pacific Ocean, *Advances In Marine Science*, 21(4): 424-431(In Chinese)

[69] Han, S.Z., Zhu, D.Y. and Guo, P.F. (2003d)，A Study of Distribution and Variation Rules of SWH in the Pacific Ocean by Using the Satellite Altimetry Data, *JOURNAL OF OCEAN UNIVERSITY OF QINGDAO*, 33(6):825-832(In Chinese)

[70] Han, S.Z., Zhu, D.Y. and Guo, P.F. (2003e)，a study of the distribution and variation of the wave height composition in the pacific ocean by using satellite altimetry data, *Transactions of Oceanology and Limnology*, 14-21(In Chinese)

[71] Han, S.Z., Wang, H.L. and Guo, P.F. (2003f)，A Study of Extreme SWH Estimation Method by Using

Satellite Altimeter Date, *JOURNAL OF OCEAN UNIVERSITY OF QINGDAO*, 33(5):657-664(In Chinese)

[72] Qi, Y.Q., Shi, P., Mao, Q.W. and Wang, J. (2003)，Relationship and characteristic of the sea surface wind and wave fields over the South China Sea derived from T/P altimeter, *JOURNAL OF HYDRODYNAMICS*，18(5): 619-624(In Chinese)

[73] Zhang, .X., Qi, Y.Q., Shi, P., Li, C.W. and Li, Y.S. (2003)，Preliminary study on assimilation of significant wave heights from T/P altimeter, *ACTA OCEANOLOGICA SINICA*, 25(5): 21-28(In Chinese)

[74] Sun, Q. and Song, J.B. (2006), Comparison of retrieving methods of ocean wave periods from satellite altimeter with buoy measurements, *Chinese Journal of Oceanology and Limnology*, 24(1): 6-11

[75] Chu, P.C., Qi, Y.Q., Chen, Y.C., Shi, P. and Mao, Q.W. (2004a), Validation of Wavewatch-III using the TOPEX/POSEIDON data, PROCEEDINGS OF THE SOCIETY OF PHOTO-OPTICAL INSTRUMENTATION ENGINEERS(SPIE), *Conference on Remote Sensing of the Ocean and Sea Ice 2003*, Barcelona, SPAIN,98-107

[76] Chu, P.C., Qi, Y.Q., Chen, Y.C., Shi, P. and Mao, Q.W. (2004b), South China Sea wind-wave characteristics. Part I: Validation of Wavewatch-III using TOPEX/Poseidon data, *JOURNAL OF ATMOSPHERIC AND OCEANIC TECHNOLOGY*, 21(11): 1718-1733

[77] Chen, G., Ma, J., Fang, C.Y. and Han, Y. (2003b), Global oceanic precipitation derived from TOPEX and TMR: Climatology and variability, J*ournal of Climate*,16: 3888-3904

[78] Chen, G., Fang, C.Y., Zhang C.Y. and Chen, Y. (2004b), Observing the coupling effect between warm pool and “rain pool” in the Pacific Ocean, *Remote Sensing of Environment*, 91:153-159

[79] Liu, C.Y., Huang, M.T., OUYANG, Y.Z., Wang, K.P., Zhou, J. and Li, H.B. (2005), Research on the Method of Sea Surface Heights at Normal Points in Satellite Altimetry, *HYDROGRAPHIC SURVEYING AND CHARTING*, 25(6):4-8(In Chinese)

[80] Wu, X.H. and Zhang, X.H. (2005)，The Statistical Characteristic Analysis of the Ocean Return Signal from the Spaceborne Ocean Altimete, *OCEAN TECHNOLOGY*, 24(3): 10-13(In Chinese)

[81] Zhang, Y.G., Zhang, J. and Ji, Y.G. (2004)，Correction for Deflection of the Vertical in TOPEX/Poseidon Satellite Altimetry, *ADVANCES IN MARINE SCIENCE*, 22(supply): 187-191(In Chinese)

ADVANCES IN MARINE MICROWAVE REMOTE SENSING IN CHINA

Zhang Jie[1,2]，*Meng Junmin*[1]，*Ji Yongang*[1]，*Yang Jungang*[1]

1. First Institute of Oceanography, S.O.A, Qingdao 266061, China

2. Key Laboratory of Marine Science and Numerical Modeling, S.O.A, Qingdao 266061, China

1. Introduction

Microwave sensors can observe in all-day and all-weather without the influences of cloud, rain and fog, and microwave has some penetrability. So microwave remote sensing is widely used in all kinds of scientific research domains. Monitoring and detection of ocean is one of the important applications of microwave remote sensing. Many oceanic physical phenomena and processes can be detected by microwave remote sensing. Location and speed of ships, area, thickness and age of sea ice, area of oil spill, sea surface wind field, ocean current, period and wave height of ocean wave, wavelength, period and spreading speed of internal wave and underwater bottom topography can be monitored or detected by microwave remote sensing. Furthermore, marine microwave remote sensing can also be used in the detection of sea surface temperature, salinity, ocean front, meso-scale eddy. Data of microwave remote sensing combined with some numerical models can be used in the researches on tide, El Nino/La Nina and so on.

The researches of the marine microwave remote sensing have made great developments in the development of microwave sensors and their platforms and the applications of microwave remote sensing in the monitoring and detection of ocean during the past four years.

2. Development and application of microwave remote sensors and their platform

According to their working mode, microwave sensors are divided into two kinds: active sensors and passive sensors. The active microwave sensors are composed of radar altimeter, microwave scatterometer and synthetic aperture radar, and the passive sensor is microwave radiometer. These microwave sensors have been developed one by one in China. The great achievements have been made during the past four years in the development of the platforms of microwave sensors and the long-term development programming of marine microwave satellites have been established.

Spacecraft Shenzhou-4 launched on Dec. 30, 2002 loaded the multimode microwave remote sensor which was the first spaceborne microwave sensor in China. This sensor system is original creation of China. It is composed of a five-channel microwave radiometer whose frequency is

between 6.6GHz and 37GHz, a microwave altimeter whose precision is 10cm and a scatterometer which measures wind field with orthogonal pencil scanning beam. Under the uniform management and control of data, the multimode microwave remote sensor can work in different modes according to the requirement of spacecraft and the customers and form a particular integrative system (Zhang Yunhua, 2005; Zhang Dehai, 2005; Ye Yunshang, 2005a,b). The multimode microwave remote sensor acquired a great number of scientific data during the Shenzhou-4 flight experiment. Sea surface wind filed and significant wave height were obtained by these data and it shows that the experiment by the multimode microwave remote sensor was successful during the Shenzhou-4 flight (Zhong Ruofei, 2004; Jiang Xingwei, 2005).

Environment satellite of ocean dynamics HY-2 is listed in the national space programs of China considering the operational requirement of ocean monitoring. The main payloads of this satellite are microwave remote sensors which include altimeter, microwave scatterometer and multi-channel microwave radiometer. Its main objective is to monitor and investigate ocean environment which include sea surface wind field, ocean wave, ocean current, sea surface temperature, storm surge and tide and so on, to serve for the forecast of ocean disasters and to provide in-situ data for scientific researches (Lin Mingsen, 2003; Xu ke, 2005).

Under the support of the Chinese national high technology project ‘integration and application system of airborne remote sensors’, Chinese marine monitoring plane loaded microwave remote sensors such as microwave radiometer and radar scatterometer. The study on the retrieval of sea ice, oil spill, wind filed of sea surface, sea water salinity and other parameters of ocean conditions were developed.

3. Basic research of marine microwave remote sensing

With the development of microwave remote sensors and their platform, basic research of marine microwave remote sensing had made great progresses in the past four years. On the basic research of altimeter, Guo Wei et al. (2004) successfully developed a full signal RSS for a Chinese satellite altimeter test and calibration by using the chirp regeneration technique, full de-ramp technique, ocean return spectrum digitally synthesizing technique and high speed DSP technique, and full range of time delay and full sea state simulation were achieved. As for the problem of real-time tracking and processing of altimeter, Xu Ke et al. (2004) developed a tracker for spaceborne radar altimeter based on sub-optimal maximum likelihood estimation (SMLE), by which a lot of ocean echo signal curves were obtained successfully in the airborne flight experiment. Considering the requirement of the speed for the real-time tracking and processing, Tang Changping et al. (2004) proposed a new approach to performing FFT by FPGA, by which

both the processing speed and the precision can meet the requirement of the spaceborne altimeter system. On the study of the applicability of the tracking algorithm, Wang Zhisen et al. (2003) testified that the OCOG (offset center of gravity) algorithm is an excellent tracking algorithm for radar altimeter. Wu Xiaohui et al. (2005) analyzed the statistical characteristics of the ocean return signals from the Multi-mode Microwave Remote Sensor Altimeter loaded on Spacecraft Shenzhou-4 through the data process and the statistical analysis of the IQ sampling data. Analyzing and comparing several methods of atmosphere water range correction by using the Seasat，Geosat，TOPEX and ERS-1 data, Ji Yonggang et al. (2004) pointed out that the optimal atmosphere water range correction for the altimeter of China was the isochronous radiometer correction method. Zhang Youguang (2004) studied the correction for the vertical deflection in TOPEX/Poseidon Satellite Altimetery, and his results showed that the altimetric errors due to the vertical deflection are basically in the range of -5 to 5 mm.

On the basic research of marine microwave radiometer, Guo Guanjun et al. (2005) studied polarimetric radiation of the wind-roughened sea surface using a geometrical approach with the statistical method under the assumption that the sea surface were composed of the tilted specularly reflecting facets with a statistical average of contributions from individual facets. Because computer simulation is very important for analyses, design and property test of the microwave radiometer system, Li Hao et al. (2005) simulated full-power microwave radiometer by computer and set up a system simulation model of full-power microwave radiometer. Yin Xiaobin et al. (2005) studied the emission properties of L-band (1.4GHz) microwave in the calm sea based on the emission mechanism of microwave in the calm sea and experiential formula of relative seawater permittivity.

In order to increase the precision of SAR position, considering the echo signal of ocean is weak, Hao Shengyong et al. (2005) adopted a Doppler measurement model in the design of ocean SAR to increase signal-to-noise ratio of ocean echo by decreasing the bandwidth. On the marine microwave remote sensing of GPS, Zhang Yiqiang (2006) discussed the GPS detection technique and presented the working principle of the self-developed delay mapping receiver. The first test flight experiment was done in Tianjin City near sea with the delay mapping receiver mounted on an airplane and the results of experiment had good agreement to the theory.

4. Applied research of marine microwave remote sensing

There are many complicated physical phenomena and processes in the ocean, which can be detected by the microwave remote sensing. According to the different goals of monitoring and detection, there are two primary parts in the application of marine microwave remote sensing:

microwave remote monitoring of the objects on the sea surface and microwave remote detection of the ocean dynamic processes.

4.1 Sea surface objects monitoring by microwave remote sensing

The major objects of microwave remote monitoring of sea surface are ships, oil spill and sea ice etc.

4.1.1 Ship

Ship monitoring is one of the important applications of the marine microwave remote sensing. On the basis of ships and their wakes generated by the movement of ships, location and speed of ships can be detected with SAR images. There are many researches in the ship target detection with SAR image, and most of them are focused on the two-parameter CFAR algorithm and K-distribution CFAR algorithm. Analyzing and comparing the characteristics of these two algorithms Chong Jinsong at al. (2003) proposed the adaptabilities of two methods. Song Wei et al. (2004) utilized the BP neural network method to detect ship targets on the sea surface with SAR image and avoided the problem of estimating the probability density function(PDF) of the image. Considering the different PDF distributions in different sea clutter backgrounds, Peng Shibao et al. (2006) discussed the ship target detecting capability with the wavelet transform based algorithm in the complicated clutter background. Zou Huanxin et al. (2004) developed a ship target detection method based on the feature vector matching.

The detection and accurate positioning of the ship wake linear feature in SAR imagery is of great difficulty. The conventional method is the Radon transform, which can achieve higher detection and positioning accuracy at the expenses of increased computational burden in the case of fine discretization. According to the basic properties of Radon transform and based on the multiscale matched filtering of peak waveform, Zou Huanxin et al. (2005) developed an algorithm to solve this problem. This method not only provides more reliable detection, but also enables to estimate the linear characteristic parameters with sub- pixel resolution, overcoming the computational difficulties caused by very fine discretization. Jiang Dingding et al. (2004) made the Radon transform localized, namely carried out the integral calculus by dividing line characteristics into short lines in the process of pixel grey scale integral without using the whole image. His method overcame the limitation of Radon transform and made the wake signal detected when background noise was strong, and could detect the smaller wake related to whole image size. Wang Ruifu (2006) developed an automatic detecting method of the V-image ship wake with SAR images, and his detecting experiments showed that this method was feasible.

4.1.2 Oil spill

The major microwave sensors used in the oil spill monitoring are Side-looking Airborne Radar (SLAR), Synthesize Aperture Radar, Microwave Scatter and Microwave radiometer. The main methods used in the oil spill detection with SAR image are the threshold methods at present and sometimes the wavelet transform method. Xue Haojie (2004, 2005) summarized the main characteristics of oil slicks in SAR images which were at the same time compared to that by general steps and methods of oil spill detection. Considering the computational burden with the wavelet transform method, the zero-antisymmetrical dyadic wavelet, multi-resolution analysis and multi-scale integration were used to the get oil spill edge images. Huang Xiaoxia et al. (2005) explored the segmentation of oil spills using a partial differential equation level set method, which represents the oil slick surface as an implicit propagation interface. This method can reduce the speckles and is applicable in dealing with the low contrast high noise images.

4.1.3 Sea ice

There are various sea ice in the Bohai Sea and the northern Yellow Sea every winter. Sea ice affected the normal tasks of oil platforms, ships, and ports directly. At present, one of the effective methods to observe, investigate and study the excursion rules of ice is to tail the trace of ice excursion continually and accurately utilizing the seafaring Radar. Combining the latest seafaring Radar survey techniques and cross-correlation analysis method which were developed in last several years, Sun Hequan et al. (2003) testified the reliability and practicability of the cross-correlation analysis method through analyzing the in-situ measured radar image of sea ice. Using the data gained from seafaring Radar FURUNO-1382, Zhang Meng et al. (2005) classified and testified the data of sea ice found from the observation by radar with the classification of statistical model, and tracked the movement of sea ice with numerical model to serve for the exploitation and transportation of oil. This method was applied in the operation of oil platform in ice area from December 2003 to February 2004. Li Zhen et al. (2003) retrieved several profiles of two decades ice located in the southeastern region of Antarctica with the SeaSat and GeoSat satellite radar altimeter data. Ji Yonggang et al. (2006) analyzed the backscattering distributions and texture features of different time series of the ENVISAT ASAR images of sea ice in Liaodong Bay to describe their changes, and the comparison of the results with the synchronous MODIS images proved the validation of using SAR images to monitor sea ice extent and its evolution in Liaodong Bay.

4.2 Ocean dynamic process detection by microwave remote sensing

The ocean dynamic process detection by microwave remote sensing is to detect the oceanic physical processes and the influence factors related to these processes including sea surface wind

field, ocean wave and wave height, ocean current, internal wave and underwater bottom topography etc.

4.2.1 Sea surface wind

Microwave remote sensing can provide sea surface wind field data which can not be obtained by the conventional methods. The major microwave sensors used in the sea surface wind field measurement are scatterometer, radiometer, altimeter, and SAR. Pang Aimei et al. (2002) found that there were linear relationship between the backscattering coefficient and the sea surface wind speed. The backscattering increases with increase of wind speeds periodically when the angles between the incident direction of scattering beam and wind direction changed and decreased with increase of the incident angle of antenna. Wang Zhenzhan (2003) proposed a inversion model of the sea surface wind speed by using 19.35GHz SSM/I, and inversed sea surface wind speed with the buoy data and isochronous bright temperature data of satellite. He developed a new method which can inverse the wind speed by using a signal wave band brightness temperature. Zhou Liangming et al. (2006) inversed the sea surface roughness with the TOPEX satellite altimeter wind speed data, and preliminarily solved the difficulties of understanding sea surface roughness caused by the lack of the in-situ measured data of sea surface roughness.

4.2.2 Ocean wave and wave height

As for the ocean wave SAR detection, Sun Jian, Guan Changlong (2006) carried out the observation and analysis of ocean wave diffraction in the near-shore and near-island region with SAR data by an optimized retrieval method named the parameterized first-guess spectrum retrieval method. DOONG Dongjiing (2002) pointed out that the wave parameters estimated from the nearshore SAR image are quite different from the in-situ measurements through the analyses of SAR images.

On the significant wave height detection with altimeter, Ji Yonggang et al. (2002) utilized the TOPEX altimeter significant wave height data to compare, analyze and process the significant wave height data measured by C and Ku bands in the nine regions of the China's nearshore seas, and used the three-parameter Weibull distribution method to make extreme statistical predictions and analyses of significant wave height in the Bohai Sea, the sea area adjacent to Shanghai and the eastern South China Sea. Wang Jing (2003) analyzed the data of the sea surface height of the South China Sea derived from the TOPEX/Poseidon altimeter, using the method of empirical orthogonal function, which showed the existence of two major SSHA spatial structures, i.e., a basin-scale gyre resulting from the reversion of the monsoon and a northeast-southwest double gyres pattern. Zhang Youguang(2002) developed a significant wave height(SWH) fast retrieval algorithm for airborne altimeter using the Barrack's scatter model of sea surface echo wave. Ji

Yonggang et. al (2006) processed the Spaceborne ShenZhou-4 (SZ-4) altimeter waveforms and proposed the five-region weighting waveform fit method to retrieve significant wave heights. Then the SWH data of the SZ-4 altimeter retrieved by using the proposed method were compared with those of ERS-2 and Jason-1 altimeters, and it was concluded that the SZ-4 altimeter could detect significant wave height. Yin Baoshu (2002) developed a new method to estimate the extreme significant wave height by using satellite remote sensing data, and estimated the extreme significant wave height field in the China Seas. This method leads a new way to estimate the extreme significant wave in the China Seas by using satellite remote sensing data. On the basis of the characteristics of satellite altimeter data, Han Shuzong et al. (2003) estimated the extreme significant wave height of the Northwest Pacific Ocean, and the estimation results show that they are consistent with the distribution of wind field. Zhou Qin, Zhao Jinping, He Yijun (2003) studied the low-frequency variability of the Antarctic circumpolar current sea level detected from the TOPEX/POSEIDON satellite altimeter data and described clearly the spatial and temporal variabilities of the Antarctic circumpolar current using the EOF analysis method and the empirical mode decomposition method (EMD), which showed a quantitative proportion of the variability in different scales.

4.2.3 Ocean current

Ocean current detection by marine microwave remote sensing focuses on eddies in the South China Sea recently. Li Yanchu et al. (2002) used the 5 years (1993-1997) TOPEX/POSEIDON altimeter data to investigate characteristics of mesoscale eddies to the southwest of Taiwan and the northeastern South China Sea, and found out three complete life histories of anticyclone rings with a stronger warm-core. Cheng Xuhua et al. (2005) used the 11 years (1993 -2003) TOPEX/ Poseidon, Jason and ERS1/2 altimeter data to acquire the temporal and spatial distribution characteristics of mesoscale eddies in the South China Sea, to study the seasonal and interannual variabilities and to discuss the forming mechanism of mesoscale eddies in the South China Sea. Guo Jingsong et al. (2005) used the AVISO satellite altimeter sea surface height anomaly data and the National Center for Environmental Prediction data to make a diagnostic calculation of volume transport through the Taiwan Strait and its variations during 1993-2001.

4.2.4 Internal wave

SAR is the major microwave remote sensor for the detection of internal waves. Wavelength, wave speed and period of internal waves can be acquired by SAR image. Optical remote sensing can also be used in internal wave detection besides SAR. In order to synthetizing all kinds of remote sensing for detection of internal waves, Meng Junmin (2006) synthetized ENVISAT ASAR, ERS-2 SAR, RADARSAT SAR, Landsat TM and MODIS to study the propagation features of

solitary internal wave in the northern South China Sea. That there is a pycnocline in the sea is the necessary condition for the generation of internal waves. Yang Jinsong (2005) proposed a numerical model for retrieving the pycnocline depth from SAR images, and the results of his numerical model agreed with the in-situ measurement. Ming-xia He (2006) proposed an internal wave characteristic extraction algorithm—Stationary Wavelet Transform, and the application of this algorithm in the ERS-1/2 SAR image showed that this method was more efficient than the traditional down sampling discrete Wavelet Transform.

4.2.5 Underwater bottom topography

Underwater bottom topography can be imaged by SAR. The underwater bottom topography SAR detection is one of the important applications of ocean SAR detection, and water depth can be obtained from SAR image of the shallow underwater bottom topography. Xia Changshui (2003) simulated and inversed the underwater bottom topography of the Tanngu sea area in the Bohai Sea with a scene of the RADARSAT SAR image. Yang Jungang (2003) inversed the underwater topography of Shuangzi Reefs in the Nansha Islands with three ENVISAT ASAR images and the inversion results showed that the underwater topography of the islands and reefs area could be detected by SAR image. In order to analyze the relation between the SAR backscattering section and the underwater bottom topography, Yang Jungang (2006) analyzed the correlation between the underwater topography and the SAR backscattering section with the ENVISAT ASAR image of Taiwan Shoal. Sandbanks in the Subei sea area are visible in SAR images. Meng Junmin (2006) analyzed the features of sandbanks in the Subei sea area with SAR image and TM image. Using the sea charts in 1966 and 1977, SAR image in 1995 and 2000, combining the Landsat images since 1986 and the survey data of beach profile of sandbanks in the Subei sea area in 2000, Huang Haijun (2002) interpreted and analyzed the positions of main tidal channel talwegs, and obtained four charts of the talweg positions for main tidal channels during different periods. After geometric calibration and overlay, he compared the positions of main tidal channels during 4 different periods and analyzed their changes.

4.3 Other

Microwave remote sensing can also be used in the study of sea water salinity, ocean front, tide and gravity anomaly and so on, besides monitoring oceanic surface objects and detecting ocean dynamic processes.

Shi Jiuxin et al. (2004) analyzed the factors influencing the retrieval precision of sea water salinity by remote sensing, including the selection of band, the polarization and incidence of the microwave radiometer, the temperature and salinity of sea water on the basis of the microwave

radiation model of sea surface and the dielectric constant formula of sea water. Chen Biao et al. (2002) analyzed the relationship between the short surface waves, the large scale waves and the backscattering coefficient of radar with a two-scale electromagnetic scattering model, introduced SAR imaging mechanism of ocean front and proposed a data processing technology by which the characteristic information of ocean fronts can be extracted from SAR images. To analyze the tidal characteristics of the Yellow and East China Seas by using altimeter data, Dong Xiaojun et al. (2002) carried out quality control for all the TOPEX/Poseidon Satellite altimetry data from Jan 1993 to Jun 1999, and used the project algorithm for the collinear differences. They drew the cotidal charts with the constituents obtained from the satellite altimeter data and compared them with those charts obtained from the routine tidal observations. On the basis of global mean sea surface data, together with the shipbrone gravimetric data in the China Seas, Wang Hubiao, Wang Yong et al (2005) used three methods (inverse Stokes formula, inverse Vening-Meinesz formula, least square collocation) to calculate the gravity abnormal in the China Seas and analyzed the results obtained by the three methods specially.

5. Prospect

With the resource exploitation of the ocean and the recognition of oceanic environment monitor and protection in China, the studies related to all kinds of fields of ocean are developing greatly. Marine microwave remote sensing, as one important means of monitoring and detecting ocean, will be paid more attention.

5.1 Research on the mechanism of marine microwave remote sensing

With the development of our microwave remote sensors and their platforms, we should pay more attention to the mechanism research of marine microwave remote sensing. The interaction between electromagnetic waves and micro-scale waves on sea surface is the physical basis of marine microwave remote sensing. The interaction directly influences the development of the technique of marine microwave remote sensing monitoring and detection. So the research of the ocean interface processing should be strengthened in the future and we should understand more about the interaction between electromagnetic waves and micro-scale waves.

5.2 Applied research with marine microwave remote sensing data of China

The self-designed marine microwave remote sensing satellite of China, such as the HY-2 satellite and the environment satellite, will be launched in the next several years. The HY-2 satellite loaded microwave scatterometer, radar altimeter and microwave radiometer, and environment satellite loaded SAR and so on. These will supply data much more for the study of

marine microwave remote sensing in China. The development of applied research of marine microwave remote sensing by using the satellite data of China have great significance in the advances and applications of the technology of marine microwave remote sensing in China.

Reference:

Chen Biao, Zhang Bentao, He Weiping. (2002), Detection of Ocean Fronts from Spaceborne SAR Images. Remote Sensing Technology and Application. 17(4): 177-180. (In Chinese)

Cheng Xuhua, Qi Yiquan, Wang Weiqiang. (2005), Seasonal And Interannual Variabilities Of Mesoscale Eddies In South China Sea. Journal of Tropical Oceanography. 24(4): 51-59. (In Chinese)

Chong Jinsong, Zhu Huimin. (2003), Comparison on Ship Target Detection Algorithms of SAR Imagery. Signal Processing. 19(6): 580-582. (In Chinese)

Dong Xiaojun, Ma Jirui, Huang Cheng, et al.. (2002), Tidal Information of the Yellow and East China Seas from TOPEX/Poseidon Satellite Altimetric Data. Oceanologia Etlimnologia Sinica. 33(4): 386-392. (In Chinese)

DOONG Dongjiing, KAO Chiachuen, CHUANG Zsuhsinb and LIN Hongpeng. (2002), Nearshore Wave Field Analysis Using SAR Images. China Ocean Engineering. 17(1): 45 – 60.

Guo Guanjun, Su Lin and Bi Siwen. (2005), Polarimetric microwave radiation of wind-roughened sea surfaces. ACTA PHYSICA SINICA. 54(5): 2448-2452. (In Chinese)

Guo Jingsong, Hu Xiaomin, Yuan Yeli. (2005), A Diagnostic Analysis of Variations in Volume Transport Through the Taiwan Strait Using Satellite Altimeter Data. Advances in Marine Science. 23(1): 20-26. (In Chinese)

Guo Wei, Zhang Xiaohui. (2004), Development of return signal simulator for Chinese satellite altimeter prelaunch performance assessment. Optics and Precision Engineering. 12(4): 359-366. (In Chinese)

Han Shuzong, Wang Hailong, Guo Peifang. (2003), A Study of Extreme SWH Estimation Method by Using Satellite Altimeter Data. Journal of Ocean University of Qingdao. 33(5): 657-664.

Hao Shengyong, Wang Xiaoqing, Sheng Xinqing et al. (2005), A Means of Improving Accuracy of Positioing for Ocean SAR. Journal of Electronics & Information Technology. 27(8): 1213-1216. (In Chinese)

Huang Haijun. (2002), Remote Sensing Interpretation of the Recent Migrations of Main Tidal Creeks off the Northern Jiangsu Coast. Coastal Engineering. 21(1): 24-28. (In Chinese)

Huang Xiaoxia, Li Hongga, Huang Bo. (2005), Oil Slicks Extracted by Level Set Method in Synthetic Aperture Radar Images. Journal of Remote Sensing. (5): 549-554. (In Chinese)

Ji Yonggang, Zhang Jie, Yang Yongzeng. (2002), TOPEX Significant Wave Height Data Analysis and Extremum Stratistical Prediction. Journal of Oceanography of Huanghai & Bohai Seas. 20(1): 25-33.

Ji Yonggang, Zhang Jie, Ji Guangrong. (2004), Analysis of Altimeter Wet Troposphere Range Correction. Chinese Journal of Oceanology and Limnology. 22(2): 150-156.

Ji Yonggang, Zhang Jie, Meng Junmin. (2006), SAR Monitoring of Sea Ice Evolution in Main China Offshore Sea Ice Regions. European Space Agency, (Special Publication) ESA SP, n 613, April, Proceedings of SEASAR 2006: Advances in SAR Oceanography from Envisat and ERS Missions, 4p.

JI Yong-gang, ZHANG Jie, ZHANG You-guang, et al., (2006), SZ-4 Spaceborne Altimeter Waveform Processing and Significant Wave Height Retrieval. Acta Oceanologica Sinica. 25(3): 40~47.

Jiang Dingding, Xu Zhaolin, Li Kaiduan. (2004), Ship Trace Detection of SAR Image Based on Radon Transform. Hydrographic Surveying and Charting. 24(2): 50-52. (In Chinese)

Jiang Xingwei, Lin Mingsen. (2005), An Achievements and Limitations Evaluation on M3RS Measurement System. Remote Sensing Technology and Application. 25(1) : 18-23. (In Chinese)

Li Hao, Chen Wenxin. (2005), Computer Simulation Research on Spaceborne Microwave Radiometer. Space

Electronic Technology. 3: 14-20. (In Chinese)

Li Yanchu, Li Li, Lin Mingsen et al. (2002), Observation of Meososcale Eddy Fields in the Sea Southwest of Taiwan by TOPEX/POSEIDON Altimeter Data. ACTA OCEANOLOGICA SINICA. 24(Supp.1): 163-170.

Li Zhen, Qin Xiang, Dong Qing. (2003), Ice Surface Variation in East Antarctica Surveyed by Satellite Altimetry. Journal of Glaciology and Geocryology. 25(3): 268-271. (In Chinese)

Lin Mingsen. (2003), Analyses of consumers' requirement of HY-2 satellite. Satellite Application. 11(2): 7-13. (In Chinese)

Meng Junmin, Zhang Jie, Yang Jungang. (2006), Interpretation and comparison radial sand ridges features retrieved from SAR and TM images. European Space Agency, (Special Publication) ESA SP n 611, Proceedings of the 2005 Dragon Symposium-Dragon Programme Mid-Term Results, 141-148.

Meng Junmin, Zhang Jie. (2006), Synergy ENVISAT ASAR, ERS-2 SAR, RADARSAT SAR, Landsat TM and MODIS Images to Research Propagation Features of Internal Solitary Waves in Northern of South China Sea. European Space Agency, (Special Publication) ESA SP, n 613, April, Proceedings of SEASAR 2006: Advances in SAR Oceanography from Envisat and ERS Missions, 5p.

Ming-xia HE, Haihua Chen, Lingfei Guo et al. (2006), Internal wave Extraction In SAR Ocanic Image Based on Stationary Wavelet Transform. European Space Agency, (Special Publication) ESA SP, n 611, Proceedings of the 2005 Dragon Symposium - Dragon Programme Mid-Term Results, 81-90.

Pang Aimei, Sun Yuanfu. (2002), Measurements and Analyses of Microwave Scattering of The Wind Speeds on Sea Surface. OCEANOLOGIA ET LIMNOLOGIA SINICA. 33(1): 36-41.

Peng Shibao, Yuan Junquan, Xiang Jiabin. (2006), Ship Detection in Ocean SAR Images with Complex Clutter Background. Radar & ECM. 1: 29-33. (In Chinese)

Shi Jiuxin, Zhu Dayong, Zhao Jinping, et al. (2004), Theoretic Analysis on the Retrieval Precision of Ocean Salinity Remote Sensing. High Technology Letters. 7: 101-105. (In Chinese)

Song Wei, Zhang Jie, Ji Guangrong. (2004), Ship Detection on SAR Images Based on BP Neural Network. Geo-Information Science. 6(3): 111-114. (In Chinese)

Sun Hequan, Sun Yanwei, Wang Pingrang. (2003), Measurement of Ice Drift Based on Cross-Correlation of Radar Images. Acta Oceanologica Sinica. 25(4): 135-141. (In Chinese)

Sun Jian，Guan Changlong, Liu Bin. (2006), Ocean wave diffraction in near-shore regions observed by Synthetic Aperture Radar. Chinese Journal of Oceanology and Limnology. 24(1): 48-56.

Tang Changping, Tang Yueying, Xu Ke et al. (2004), The realization and Performance Analysis of the FFT Module Based on FPGA for Spaceborne Ocean Radar Altimeter. Remote Sensing Technology and Application. 19(3): 202-205. (In Chinese)

Wang Hubiao, Wang Yong, Lu Yang, et al. (2005), Inversion of Marine Gravity Anomalies by Combinating Multi-Altimeter Data and Shipborne Gravimetric Data. Journal of Geodesy and Geodynamics. 25(1): 81-85. (In Chinese)

Wang Jing, Qi Yiquan, Shi Ping et al. (2003), Characteristics of Sea Surface Height in South China Sea Based on Data From TOPEX/POSEIDON. Journal of Tropical Oceanography. 22(4): 27-33. (In Chinese)

Wang Ruifu, Zhang Jie, Bi Zhe. (2006), An Automatic Detecting Method of SAR V-image Ship Wake. European Space Agency, (Special Publication) ESA SP, n 611, Proceedings of the 2005 Dragon Symposium - Dragon Programme Mid-Term Results, 149-154.

Wang Zhenzhan. (2003), A Model for Inversing Sea Surface Wind Speeds by Using SSM/I 19.35 GHz Vertical and Horizontal Brightness Temperatures. Ocean Technology. 22(2): 1-6.

Wang Zhisen, Jiang Jingshan. (2003), Research on a Robust Radar Altimeter Tracking Algorithm. ACTA ELECTRONICA SINICA. 31(3): 341-344. (In Chinese)

Wu Xiaohui, Zhang Xiaohui. (2005), The Statistical Characteristic Analysis of the Ocean Return Signal from the Spaceborne Ocean Altimeter. Ocean Technology. 24(3): 10-13. (In Chinese)

Xia Changshui, Yuan Yeli. (2003), Simulation and Inversion Study on the Submarine Topography in the Tanggu Sea Area Using SAR images. Advances in Marine Science. 21(4): 437-445. (In Chinese)

Xu ke, Dong Xiaolong, Zhang Dehai et al. (2005), HY-2 Radar Altimeter and Microwave Scatterometer. Remote Sensing Technology and Application. 20(1): 89-93. (In Chinese)

Xu Ke, Liu Heguang. (2004), The Realization and Airborne Flight Experiment Verification for the Tracker of the Spaceborne Ocean Radar Altimeter Based on Sub-Optimal Maximum Likelihood Estimation. ACTA ELECTRONICA SINICA. 32(6): 929-932. (In Chinese)

Xue Haojie, Chong Jinsong. (2004), Oil Spill Detection Methods in SAR Images. Remote Sensing Technology and Application. 19(4): 290-294. (In Chinese)

Xue Haojie, Chong Jinsong. (2005), Zero-Antisymmetrical Dyadic Wavelet-Based Oil Spill Detection Method in SAR Images. Journal of Electronics & Information Technology. 27(4): 574-576. (In Chinese)

Yang Jingsong, Huang Weigen, Xiao Qingmei et al. (2005), Oceanic pycnocline depth retrieval from SAR imagery in the existence of solitary internal waves. Acta Oceanologica Sinica. 24(5): 46-49.

Yang Jungang, Zhang Jie, Meng Junmin. (2006), Correlation analysis of underwater bottom topography and its SAR images. European Space Agency, (Special Publication) ESA SP, n 613, April, Proceedings of SEASAR 2006: Advances in SAR Oceanography from Envisat and ERS Missions, 6p

Yang Jungang, Zhang Jie, Meng Junmin. (2006), Underwater bottom topography detection of Shuangzi Reefs with ENVISAT ASAR images acquired in different time. European Space Agency, (Special Publication) ESA SP, n 611, Proceedings of the 2005 Dragon Symposium-Dragon Programme Mid-Term Results, 133-139.

Ye Yunshang. (2005), Electrical Design of Antenna Subsystem of Shenzhou Spacecraft's Multimode Microwave Remote Sensor. Remote Sensing Technology and Application. 20(1): 94-100. (In Chinese)

Ye Yunshang. (2005), Mechanism Design of Antenna Subsystem of Shenzhou Spacecraft's Multimode Microwave Remote Sensor. Remote Sensing Technology and Application. 20(1): 101-105. (In Chinese)

Yin Baoshu, He Yijun, Hou Yijun et al. (2002), A New Method of Return Period Wave Height Calculation. OCEANOLOGIA ET LIMNOLOGIA SINICA. 33(1): 30-35. (In Chinese)

Yin Xiaobin, Liu Yuguang, Zhang Hande, et al. (2005), Microwave Remote Sensing of Sea Surface Salinity – a Study on Microwave Radiation Theory of Calm Sea Surface. High Technology Letters. 15(8): 86-90. (In Chinese)

Zhang Dehai, Jiang Jingshan, Zheng Zhenfan et al. (2005), SZ-4 Main Payload—Multi-Mode Microwave Remote Sensor. Remote Sensing Technology and Application. 20(1): 74-80. (In Chinese)

Zhang Meng, Lin Jianguo. (2005), Application of Radar Sea Ice Monitoring and Numerical Forecast Technique to Operation in the Ice Zone of Liaodong Bay. Journal of Dalian Maritime University. 31(1): 73-76. (In Chinese)

Zhang Yiqiang, Yang Dongkai, Zhang Qishan et al. (2006), Detection Technique of GPS Sea Surface Scattered Signal. Journal of Electronics & Information Technology. 28(6): 1091-1094. (In Chinese)

Zhang Youguang, Zhang jie, Ji Yonggang. (2002), Research on Airborne Altimeter SWH Fast Retrieval Algorithm. Advances in Marine Science. 20(4): 6-10. (In Chinese)

Zhang Youguang, Zhang jie, Ji Yonggang. (2004), Correction for Deflection of the Vertical in TOPEX/ POSEIDON satellite Altimetery. Advances in Marine Science. 22(Suppl.): 187-191.

Zhang Yunhua, Jiang Jingshan, Zhang Xiangkun et al. (2005), SZ-4 Scatterometer Mode of Multimode Microwave Sensors. Remote Sensing Technology and Application. 20(1): 58-63. (In Chinese)

Zhong Ruofei, Guo Huadong, Wang Weimin et al. (2004), Data Processing and Performance Evaluation of the Microwave Radiometer Carried by Shenzhou-4. Remote Sensing for Land & Resources. 62(4): 19-22. (In Chinese)

Zhou Liangming, Guo Peifang, Wang Aifang. (2006), Sea Surface Roughness Derivation from Wind Speed

Estimated by Satellite Altimeter. Marine Science Bulletin. 8(1): 61-67.

Zhou Qin, Zhao Jinping, He Yijun. (2003), Low-frequency Variability of the Antarctic Circumpolar Current Sea Level Detected From TOPEX/POSEIDON Satellite Altimeter Data. OCEANOLOGIA ET LIMNOLOGIA SINICA. 34(3): 256-266. (In Chinese)

Zou Huanxin, Kuang Gangyao, Yu Wenxian. (2004), Detection of Ship Targets from SAR Imagery Based on Feature Vector Matching. Modern Radar. 26(8): 25-29. (In Chinese)

Zou Huanxin, Yu Wenxian, Kuang Gangyao, Zheng Jian. (2005), A Method of High Accruacy Ship Wake Positioning in SAR Ocean Imagery. Signal Processing. 21(3): 307-311. (In Chinese)

PROGRESS OF OCEAN COLOR SENSING IN CHINA

Tang J.W.[1)], Ding J.[1)], Sun L.[2)]

1 National Satellite Ocean Application Service, Beijing, China, 100081

2 National Satellite Meteorological Center, Beijing, China, 100081

1 Introduction

Ocean color remote sensing is an effective and important tool in the studies on global carbon cycling, marine environment ecology, the monitoring of water quality and pollutions, as well as open ocean fisheries. Because of historical reasons, Chinese scientists lost the opportunity to take part in the researches and applications of CZCS, the first generation of ocean color sensor in space. From the beginning of the 1990's，along with the rising of world-wide activities for second generation ocean color sensors, as represented by the SeaWiFS mission which is the mostly excellent one among them. The ground receiving station of SeaWiFS has been built up in Hangzhou, China, and the related applications have been carried out. Since then, more and more researchers have also joined in the applications of EOS-MODIS and the Chinese Moderate Resolution Imaging Spectroradiometer (CMODIS) on-board the manned spacecraft SZ-3. All these activities established a solid national foundation for further developments in ocean color sensing in China (Pan & Li, 2003).

On May 15th, 2002, the first ocean observation satellite of China, HY-1A, was launched which marked the beginning of a new era of ocean color sensing in China. Through the HY-1 mission, the manufacture ability of quantitative and high accuracy sensors has been greatly enhanced. By the support of the construction of its ground application system, the facilities and systems of satellite data receiving, processing and applications, and in-situ ocean optic instruments were established, which promoted the ocean color sensing in China to a new level. At the same time, many other national projects, funded by the National 863 Hi-Tech Program, Chinese Commission of Science Technology and Industry for National Defense, and National Science Foundation of China, have speeded up the development of ocean color sensing since 2002.

2 China's Ocean Color Sensors

2.1 HY-1 Satellite Series

The HY-1 satellites are mainly used in the observations of ocean color and sea surface temperature (SST). On board satellite HY-1A, there are two kinds of sensors: Chinese Ocean Color and Temperature Scanner (COCTS) with 10 bands, 8 of them are for ocean color and 2 for SST and Coastal Zone Imager (CZI). The technical parameters are given in Table 1.

Table 1 The parameters for HY-1A/1B satellites and sensors

	HY-1A	HY-1B
COCTS	412,443,490,520,565,670:±10nm; 765,865: ±20nm; 10.4~11.4um,11.5~12.5um Pixels:1024, Swath:1500km Resolution: 1km FOV: $\pm 45^0$	412,443,490,520,565,670,750:±10nm; 865±20nm; 10.4~11.4um,11.5~12.5um Pixels:1664, Swath:2000km Resolution: 1km FOV: $\pm 55^0$
CZI	420~500, 520~600, 610~690, 760~890 Pixels:2048, Swath:500 Resolution:250m	443, 555, 665, 685: ±10nm Pixels:2048, Swath:500 Resolution:250m
Satellite	Orbit：Near-sun-synchronous Local Pass: 8:30~9:30am	Orbit: Sun-synchronous Local Pass:10:30am

The HY-1A satellite stopped running in March, 2004. Therefore, the second one of these series, HY-1B, was launched in December, 2006. The major payload, COCTS, is actually the same to that on HY-1A, except that 765nm band has been moved to 750nm to avoid the O_2 A-band absorption and signal-to-noise ratio (SNR) has been improved. The 4 bands of CZI have been changed into ocean color bands to improve the geometrical resolutions of ocean color sensing and to enhance the abilities in red tides monitoring in China coastal areas.

2.2 Other satellite sensors capable for ocean color observation

The SZ-3 spacecraft with Chinese moderate resolution imaging scanner (CMODIS) was launched on 25th, March, 2002. It has 30 bands in the visible and near-infrared (VNIR) range with a band-width of 20nm; a shortwave infrared (SWIR) band at 2.15~2.25μm and two thermal

infrared (TIR) bands at 10.3~11.3μm and 11.5~12.5μm, respectively.

The FY-3 Meteorology Satellite will be launched in 2007, with the Medium Resolution Spectral Imager (MERSI) sensor on board, which has 8 traditional ocean color bands with wavelengths of 412, 443,490, 520, 565, 650, 685, 765,865nm, respectively, as well as 3 short infrared bands of 1.03, 1.64, 2.13μm, which can be able to provide better atmospheric correction results theoretically in turbid waters. The other parameters of MERSI are: 12-bit A/D, +/-55.4°FOV (field of view), 2048 pixels per scan line with a nadir spatial resolution of 1km.

2.3 Air-borne ocean color sensors

The Push-broom Hyperspectral Imager (PHI) is installed on the airplane for ocean surveillance in the North China Sea Branch, State Oceanic Administration (SOA), which is manufactured by the Shanghai Institute of Technical Physics (SITP), Chinese Academy of Sciences (CAS). The PHI features are: a FOV of 21° and IFOV (Instantaneous Field-of-View) less than 1.5 milli-radian, the spectral range of 420~850nm , the number of bands selected for sampling up to 124 with a resolution better than 5nm, and the SNR better than 500 for 60% reflectance targets. This sensor has been regularly used for the surveillance of coastal environments and red tides.

The Marine Airborne Multiple-band Scanner (MAMS) is installed on the airplane for ocean surveillance in the North China Sea Branch of State Oceanic Administration, which is a new generation sensor, also manufactured by the SITP after the UV-IR(Ultra-Violet and Infra-Red) scanner manufactured in the middle 1980s. The objective of the MAMS is to monitor the marine environment parameters quantitatively, and to inspect targets operationally on the sea while carrying out executions cruises. There are 8 ocean color bands identical to the bands of HY-1/COCTS; while the other 3 bands are 1 UV band and 2 TIR bands, respectively. Therefore, this sensor can be used for coastal zone pollutions, chlorophyll and suspended matter, as well as to provide simultaneous in situ data for calibration and validation (C/V) of ocean color sensors.

The South China Sea Branch of the State Oceanic Administration imported a hyperspectral imaging radiometer AISA+ from Specim Corporation, Finland, which has 224 bands in range of 400~970nm. This sensor is one of the most advanced multipurpose airborne sensors in China, with strong ability of ocean color sensing.

3 Ocean Color Algorithms and Models

Most studies of ocean color are for worldwide Case-I waters (IOCCG, 2000), whereas the corresponding studies in China mostly concentrated on the retrieval models in the coastal Case-II waters of the China seas, including chlorophyll, suspended matter, yellow substance, diffuse attenuation coefficients and transparency, water absorption and scattering coefficients, etc. There exist intrinsic differences in the bio-optical properties of various regional Case-II waters which are influenced by different land sources and bottom properties in Chinese coastal areas, so the general retrieval algorithms for the whole Chinese coastal region have not been established yet.

Up to now, most retrieval algorithms for the concentrations of water components as well as other bio-optical parameters are based on empirically statistical models. Some researchers have also proposed other new algorithms including semi-analytical algorithm, neural network(NN), genetic algorithm and statistic learning theory.

The algorithms introduced in this article are the ones based on in situ measurements or model simulated data. Some other algorithms, derived by comparing satellite products (radiances) and non-synchronous in situ measurements of concentrations, are not included here.

In recent years, along with the fast developments of China economy, many institutes have begun collecting ocean color data with the equipments and methods following NASA ocean color protocols, so that some reliable regional algorithms can be proposed on solid basis. Among the ocean color activities, the Case-II ocean color validation cruises in spring and autumn of 2003 are the most fruitful, which were carried out by the Chinese National Satellite Ocean Application Service (NSOAS) with other 6 institutes, and each of them has specific advantage on the measurement or analysis of some aspects of ocean color components. A high quality data set has been obtained and a group of ocean color retrieval algorithms have been proposed and gained common recognition by the Asian ocean color community.

Based on the 2003 cruises data, Tang et al (2004) proposed a set of statistical algorithms for the retrieval of the three-component (chlorophyll, sediment and yellow substance) concentrations for Yellow Sea and East China Sea. The algorithms are partly based on the Tassan(1994) models. The validation results of the algorithms by Tang et al (2004) showed that the accuracy was enough to derive operational data products, and the models were stable. These algorithms filled in the gap

of coastal ocean color sensing in China. Wang et al (2005,2006) have established the retrieval algorithms of diffuse attenuation coefficients at 490nm, water transparency and total absorption coefficients from Remote Sensing Reflectance(Rrs). For quantitative ocean color retrievals with broad-band sensors, Ma et al.(2005) presented the statistical algorithms for retrievals of total suspended matter (TSM), sediment and chlorophyll-a concentrations from the HY-1A CZI based on the data of spring cruise in 2003, as described above; Tang et al.(2005) tested retrieval algorithms of sediment and chlorophyll concentrations with remote sensing reflectance(Rrs) from the second China-Brazil Earth Resources (CBERS-02) satellite CCD camera data.

As for the developments of theoretical models in ocean color sensing, He et al (2004) established a semi-analytical model for transparency retrieval with the SeaWiFS data, according to the theories of in-water radiative transfer and visual contrast. But the model was not suitable for the turbid case 2 waters. Song & Tang (2006) obtained the scattering properties that are essential for semi-analytical models and derived regional relations between scattering coefficients and TSM concentrations, based on the cruise data in 2003. By using Rrs, absorption, scattering coefficients, and their relations as well as the spectral model of scattering, the total absorption coefficients in low and medium turbid waters can be retrieved, where TSM<50 mg/l. That is, the basis for regional semi-analytical models has been primarily obtained.

Shen(2006) set up a model for yellow substance retrieval for the MODIS bands in Liaodong Bay and Dalian Bay. Chen et al(2003) provided a gelbstoff retrieval algorithm in the Zhujiang River Estuary by the modeled and measured water spectra and the in situ measurements of gelbstoff concentrations. Several algorithms for chlorophyll retrieval had also been proposed in the same area (Chen et al 2002a, 2003a, 2005a). Han et al. (2003a, 2003b, 2004) researched into the spectral reflectance characteristics of suspended matter in detail.

Besides these statistical models based on the Rrs or the normalized water-leaving radiances, some researchers have also tried new methods for data analysis and modeling. Wang et al(2003) applied the spectral mix-unmix analysis to evaluate the distribution of suspended matter concentrations in the Mingjiang River Estuary with the TM data. Wen et al.(2006) used the same method to retrieve chlorophyll concentrations in the Taihu Lake with hyper-spectral data of Hyperion. Cong et al.(2005) analyzed the spectral characteristics of chlorophyll with the spectrum continuum removal method and established a retrieval algorithm with the Normalized Difference

of Pigment Index (NDPI) supported by the in situ measurements in Liaodong Bay. Zhao et al (2004a, b) presented some relations between the sun-induced chlorophyll fluorescence line height (FLH) and chlorophyll concentration for various types of phytoplanktons.

Some researchers also applied the non-linear optimization and the algebra method in semi-analytical models to the retrieval of three-component concentrations and water transparency. Using the optical models of the three ocean color components as a forward model, Zhan et al(2004) and Sun et al(2004) the presented the genetic-algorithm-based models for simultaneous retrieval of three-component concentrations for SeaWiFS and HY-1A CZI data respectively. The results showed that these algorithms were capable to overcome the difficulty of trapping in local minimum in the process of optimization method.

It is time-consuming to apply optimization method directly in processing ocean color sensing, the NN method may solve this problem with the backward error propagation training technique. Along with the accumulation of quality of *in situ* measurements in recent years, the NN method has been widely applied in ocean color retrievals.

Based on the SeaBAM and NOMAD data set, and the simulated data from radiative transfer models, Zhang et al. (2003) and Zhang & Fell(2006) tried to retrieve chlorophyll concentration and transparency in the Case-I and Case-II waters with the NN models. Their results showed that the NN models were better than the NASA OC4 algorithm in the Case-I water. Zhang & He(2002) and Huang et al. (2004) established the NN models for chlorophyll concentration in the Case-I water based on the SeaBAM data set. Based on the in situ measurements in spring, 2003, Tang & Ding et al (2005) developed a NN model for the three-component concentration retrieval simultaneously and the other 3 individual NN models for each component's concentration retrieval respectively, both using Rrs as input. Furthermore, an important conclusion was derived from the NN modeling results: it is possible to determine concentrations of TSM or sediment only with the signals of 555nm and 670nm as input. However, a sensitivity analysis showed that the NN models for chlorophyll retrieval were more sensitive to input errors comparing to sediment retrieval. Similarly, based on the same data set, Zhong et al. (2005) also set up the NN models for three-component concentration retrievals. Shen et al.(2005) tested the NN model for chlorophyll retrieval in the Zhujiang River Estuary by the *in situ* measurements in January, 2003 and 2004.

Some researchers have also introduced statistic learning theory into ocean color retrieval.

Zhan et al(2003b,2005) applied the support vector machine (SVM) method as the non-linear transfer function in chlorophyll retrieval, which was evidently better than NN in terms of model construction and training, etc. Jiang et al(2005, 2006) tried to establish a chlorophyll retrieval model by means of the statistic learning and least-square Support Vector Machine methods, which could avoid over-learning and large error from model extrapolation. Yang et al(2005) established a retrieval algorithm by means of the partial least square (PLS) method in the Yellow Sea and the South China Sea, since PLS is suitable for solving the problems of more variables with small amount samples.

4 Atmospheric Correction

As for ocean color images, the largest part of the top of atmosphere (TOA) satellite signal comes from atmospheric scattering. One of the key problems in ocean color processing is how to eliminate the atmospheric scattering in order to derive effective signal from water. In the clear open oceans, it's possible to obtain atmospheric scattering properties by assuming that the water-leaving radiances at near-infrared bands are zero, which is the black-pixel assumption. However, this assumption is not valid any more for most of the China turbid Case-II coastal water areas. The new atmospheric correction methods have to be found for turbid waters, which is one of the most challenging problems affecting the final accuracy of ocean color sensing in China.

A practical method for Case-II atmospheric correction was provided by Wei et al. (2002) & Chen et al.(2003b) by learning from Ruddicks's method, which assumed that the aerosol scatterings of two bands were known or could be derived by the adjacent clear water pixels, and the backward scatterings of the water in NIR bands were nearly constant as well as the ratio of water-leaving reflectances in two NIR bands was constant. By means of imbedding the algorithm into the SeaDAS software, the better results than those of NASA standard algorithm in the Zhujiang River Estuary and its neighboring coastal area have been derived.

Based on the in situ measured spectral relations and trial for different atmospheric correction algorithms in the Yellow Sea and East China Sea, Ding & Tang et al (2006) pointed out that the coastal waters in this area should be divided into two types: low-medium-turbid and high-turbid waters. This classification may help to improve the accuracy of atmospheric correction in low-medium-turbid water and to study particular algorithms for highly turbid water. The results

showed that in the waters where TSM was less than 20mg/l or Rrs at 670nm was less than 0.015, it's feasible to make atmospheric correction using the Arnone(1998) iteration or the Ruddick et al (2000) method, the methods were based on the fact that Rrs at NIR bands is inversely proportional to the absorption coefficients of pure water. In the highly turbid waters, Tang (2005) and Ding(2004) provided the optimization and NN methods for atmospheric correction respectively. The criterion for discriminating low and high turbid Case-II waters is that the water-leaving radiance at 490nm is negative by standard SeaDAS algorithm.

He et al.(2003) provided a simple algorithm for atmospheric correction by assuming that water-leaving radiance at 412nm was constant in highly turbid waters.

Ding (2004) designed a NN model for atmospheric correction in turbid case 2 waters, with which two aerosol parameters could be derived: aerosol scattering reflectance at 865nm and the exponential constant *c*, which was defined in Wang & Gordon (1994), from the TOA signals of SeaWiFS bands. The NN training data was based on the *in situ* measurements of Rrs and the modeled aerosol scattering. By the radiative transfer model in water-atmosphere system, Sun (2005) and Qiu (2006) established the NN models for atmospheric correction in case II waters for HY-1A/CZI and MODIS, respectively, and derive & both water-leaving radiances and optical thickness of aerosol scattering simultaneously.

Other researchers also proposed the NN models to retrieve both aerosol properties and water constituents' concentrations directly. Zhang (2002) retrieved both aerosol and three-component concentrations by use of TOA LUTs and validated it in Xiamen areas. The LUT was calculated by the atmosphere-ocean system radiative transfer model by changing sun and viewing angles, aerosol load and Junge particle size distribution, as well as three-component concentrations.

For accurate Rayleigh scattering computations, which is the basis of atmospheric correction of ocean color data, He et al (2005,2006) gave out a LUT based on Adding-Doubling method with polarization for HY-1A COCTS as well as other ocean color sensors, the results were within 1% comparing to the SeaDAS values. Zhao et al (2006a, 2006b) carried out a similar research by use of Successive Order of Scattering method. Sun et al. (2006) built a look-up table (LUT) of Rayleigh scattering computations for HY-1A CZI, a sensor with wide band-widths.

In order to eliminate the effects of absorption of gases in the atmospheric correction for CZI, Sun et al. (2005) provided an algorithm by utilizing the 6S aerosol models. Zhao et al (2005)

retrieved the aerosol thickness and size distribution from sunphotometer measurements in the Yellow Sea and East China Sea in spring, 2003, to investigate the local aerosol models.

Although many algorithms have been proposed for the Case-II atmospheric correction, it's still difficult to determine the uncertainty so far, because of the difficulties of validation in Case-II waters, such as the patchy effect, wind, the tide induced resuspension and the up-layer mixing for fast changing sediment particles.

In coastal waters, both turbid waters (bright pixel) and absorptive aerosols affect the accuracy of atmospheric correction. Li (2002) carried out some in-depth work for absorptive aerosols in Asian oceans. She firstly presented and then proved that the most important factor affecting atmospheric correction was sub-micrometer absorptive aerosols (soot-like aerosols), except desert aerosols occurring in spring (Li et al 2003). But it's still a complicated problem to apply this correction to operational data processing, especially in case 2 waters.

For hyperspectral ocean color sensing, Mao et al.(2005) presented a atmospheric correction algorithm with 1nm spectral resolution.

For atmospheric corrections in China coastal turbid waters, there may be two ways in near future: one is to make use of the longer bands, SWIR bands, other than 750 and/or 865 nm NIR band, as 1240nm and 2130nm bands of MODIS, where the water absorption coefficients are much higher to assure the black-pixel assumption even in highly turbid waters (Wang & Shi, 2005). But the difficulty to achieve the goal is that the sensor with SWIR bands is hard to be manufactured to meet the SNR requirements of ocean color sensing. The second way is to measure the Inherent Optic Properties(IOPs) more accurately to make it possible to carry out Rrs and aerosol thickness iterations or likely methods in highly turbid waters on a solid physical basis of ocean optics, for example, to measure the specific absorption coefficient of sediment by using spectrophotometer with integrating sphere (T-R method).

5 Measurements and analysis of IOPs

Several outstanding progresses have been achieved in the measurement and analysis of inherent optic properties (IOPs) of waters, which are fundamental parameters for ocean color sensing.

The optic properties of yellow substance or CDOM can be characterized by a exponential

constant, S, which determines its slope of the exponential decreasing curve of spectral absorption coefficients. Tang et al (2004) gave out a range of S between 0.011-0.022 with a mean of 0.0176, derived from the absorption coefficients measured with in situ spectrophotometer in the Yellow Sea and East China Sea, 2003.

Song et al(2006) summarized some derived models of spectral scattering properties of particles from in situ measurements of IOPs in the same cruise area in 2003. The results showed that the power-exponent *n* of particle spectral scattering decreases when the concentration increases, which varies from 2.0 in clear waters to 0.6 in turbid waters. When the total suspended matter(TSM) concentration exceeds 3mg/l, or equivalently, the backscattering coefficient at 532nm $b_{bp}(532)$ is greater than $0.013m^{-1}$, then the *n* value varies only within 0.6-1.0 with a mean value of 0.8. Besides, the relations between *n* and backscattering coefficient, and the relations between backscattering coefficient and total scattering coefficient are also given in the paper.

Cao et al(2003), Xu et al(2004), and Wang et al(2005) studied spectral absorption coefficients and regional retrieval models of suspended matter in the South China Sea and the Zhujiang River Estuary. Wu et al(2004) studied the yellow substance absorption properties in Jiaozhou Bay and gave out a range of S about 0.0131~0.0180.

Zhu et al (2004a,b) analyzed the absorption properties of non-pigment particulate matter, yellow substance, chlorophyll, as well as relations between absorption coefficients of chlorophyll and its concentration in the Yellow Sea and East China Sea based on the same cruise data in 2003. He also derived the exponential S value of 0.0103 for spectral absorption coefficients of non-pigment particulate matter in the area.

Wu et al(2006) presented the temporal and spatial distributions of phytoplankton absorption properties for the northeast continental shelf of the South China Sea based on the data of in situ measurements. She also tried to explain the seasonal variations of phytoplankton biomass and its distributions by the absorption coefficients.

In spite of the above in situ measurements, one important problem of ocean color sensing in China is lack of regular cruises for continuous optical data collection. This situation influences severely on the fine-tuning or validation of retrieval algorithms.

6 Applications Using Ocean Color Data --Transparency, Primary Productivity, and Red

Tides Detection

By the model simulated TOA signals, Tang & Ding et al (2004) analyzed the effects of atmospheric scattering on the detection of red tides or algal blooms by NDVI. The results re-confirmed that, in most cases, it is necessary to do atmospheric correction before using NDVI like ratios to detect red tides. Based on the in situ measurement data, Zhao et al(2004a; 2004b; 2005a; 2005b) analyzed the variation of spectral characteristics of chlorophyll fluorescence for different types of phytoplankton and put forward the suggestion that it needs finer resolution in the fluoroscopic spectral range in 660~710nm for detection models. Li et al(2005) proposed a detection model for red tides with the variation curve of VIS and NIR ratio.

Chen et al (2005b) evaluated the method for water quality mapping, and provided a primary classification for the Zhujiang River Estuary according to the criterion using ocean color data, further more, he tried to detect the status of eutrophication (Chen et al 2006).

Pan & Guan et al tried to derive the distributions of primary productivity (PP) in the China Seas from ocean color data (Pan et al 2005, Guan et al 2005). A retrieval model of PP has been given using the nonlinear least-squares method with the long-term in situ measurements of PP and related environmental parameters in the southern Yellow Sea and East China Sea. By the retrieved data of chlorophyll-a concentration, transparency and solar irradiance from SeaWiFS and the corresponding SST data from NOAA, the temporal and spatial distributions of PP have been derived. However, it should be pointed out that the surface chlorophyll concentration retrieved from satellite data and its stratification may not accurate enough to assure the accuracy of PP calculation, because of the complexity of ocean optic and biological properties in the China coastal waters. Also, there existed some restrictions on the time and space for the *in situ* measurements, the most PP results in the China Seas are still open to further validation.

Tang et al. (2004) studied the variations and distributions of chlorophyll concentration in the western South China Sea with seasonal winds in 1997-2002, by using the chlorophyll data from SeaWiFS, OCTS and OCI. Meanwhile, they proved the effect of strong upwelling to Chl-a concentrations by means of SST, wind speed and anomaly of SSH (sea surface height) data.

Sun&Cai(2003) analyzed the distribution and variation of chlorophyll and PP in the Bohai Sea based on the data of in situ measurements, which may be taken as a reference for the PP model development in this area. Using the SeaBAM and SeaWiFS data, Li et al. (2003) revised

the algorithms for the chlorophyll retrieval in the Case-I and Case-II waters in the East China Sea and derived the distributions of chlorophyll concentration in 1998. Furthermore, the monthly and yearly variations and distributions of PP in that area were also obtained from the calculation on the VGPM model according to relation between euphotic depth and diffuse attenuation coefficients. The results showed that the PP in the East China Sea decreased to the minimum in winter, and increased to the maximum in spring, then went down a little in summer and up a little in autumn. The daily mean of PP was about 560.03mg/m^2.d and the major effect factors were also discussed, including chlorophyll, temperature, fresh water flushing from the Changjiang River, euphotic depth and fronts, etc. Li et al. (2006) analyzed the variations of PP in the South China Sea in 1998~2002, by use of the VGPM model based on the chlorophyll data from the SeaWiFS and SST data from other sensors. It is found that the PP is highest in winter and lowest in summer.

By taking the combination of SST retrieved from AVHRR and chlorophyll from SeaWiFS as an indicator, Shang et al(2005) found that the yearly variations of upwelling current were obvious in the upwelling areas in 1985-2005, and discussed the relations between wind stress, upwelling current, nutrition and chlorophyll. Based on an analysis of the daily chlorophyll series data from SeaWiFS in August, 1998, Shang et al(2004) showed that the chlorophyll concentration responsed quickly to upwelling current in the coastal waters of Taiwan Strait during summertime, which delays 1~2 days. There exists difference in the response of chlorophyll to SST in the northern and southern areas of the strait. Zhang et al (2006) validated the ocean color products from SeaWiFS and those from MODIS for a period of 8 years by comparing them with *in situ* measurements in the large area, which shows that chlorophyll concentrations given by these two sensors have no significant difference, no matter in temporal statistics or in spatial distribution patterns. Thus, they thought that MODIS could replace SeaWiFS to assure continuity of ocean color products for research in the Taiwan Strait and the northern South China Sea.

Mao et al.(2005) implemented an operational information system for open ocean fisheries operationally, which had provided tens of quick reports every year on ocean color and SST.

7 Conclusions

Since 2002, ocean color sensing in China has been developing fast, many scientists have conducted various studies and derived plentiful results, especially in the fields of atmospheric

correction in the turbid Case-II waters, the inherent optical properties analysis as well as the in-water ocean color models, empirically or semi-analytically.

In the foreseeable future, ocean color scientists in China need to make more efforts in the following aspects:

1) The applications of high spatial resolution satellite data in coastal and inland waters, where is highly concerned by the government and public, and the ocean color sensing technique may exhibit its potential economic and social benefits. It might be the only way to advance its developments under the push of social requirements.
2) New methods of atmospheric correction for turbid waters, especially those different from Gordon algorithm for special purpose, e.g., sediment retrievals in highly turbid waters may not need accurate atmospheric correction.
3) The in-depth analysis of inherent optical properties of Chinese coastal waters.

Acknowledgements: The authors of this paper have obtained many helps from the China ocean color community, Xianqiang He, Dongzhi Zhao, Wenxi Cao, Chuqun Chen, Shaoling Shang, Yi Ma, Tinglu Zhang, Jinping Zhao, et al.

References:

Arnone, R.A., P. Martinolich, R.W. Gould, et al. Coastal Optical Properties Using SeaWiFS, Ocean Optics XIV Kailua-Kona Hawaii, Nov 10-13, 1998, *SPIE*-the International Society for Optical Engineering.

Cao W.X., Y.F. Guo，Y.Z. Yang, et al., Research on spectroradiometer equipped in water with many bands. High Technology Letters, 12(1): 96-101, 2002.

Cao W.X., Y.Z. Yang, T.C. Ke, et al., Test and analysis on optical characteristics of an underwater multi-channel spectral radiometer. Tropic Oceanology. 21(1)：1-10，2002.

Cao W.X., Y.Z. Yang, A bio-optical model for ocean photosynthetic available radiation. Tropic Oceanology. 21(3)：47-54, 2002.

Cao W.X., C. Li, T.C. Ke, et al., Hyperspectral meter for measuring inherent optical properties of sea water based on principle of double-optical-path. Optical Technology. 29(2)：139-145. 2003a.

Cao W.X., Y.Z. Yang, X.Q. Xu, et al., Spectral absorption of suspended matter and its regional model in Zhujiang River Estuary. Chinese Science Bulletin, 48(17): 1876-1882, 2003b.

Cao W.X., T.F. Wu, Y.Z. Yang, et al., Monte Carlo Simulations of the Optical Buoy's Shading Effects. High Technology Letters, 13(3)：80-84，2003c.

Cao W.X., Y.Z. Yang, X.Q. Xu, et al., Regional patterns of particulate spectral absorption in the Pearl River estuary. Chinese Science Bulletin, 48(21): 2344-2351, 2003.

Cao W.X., Y.Z. Yang, T.C. Ke, et al, Optical systems for applications in ocean color remote sensing and interdisciplinary study. SPIE, 4892: 222-232, 2003.

Chen C.Q., Z.L. Pan, P. Shi, Simulation of sea water reflectance and its application in retrieval of yellow substance by remote sensing data. Journal of Tropical Oceanography, 22(5): 33-39, 2003.

Chen C.Q., P. Shi, M. Larson, et al., Estimation of chlorophyll-a concentration in the Zhujiang River Estuary from SeaWiFS data. Acta Oceanologica Sinica, 21(1): 27-36, 2002a.

Chen C.Q., L. Joensson, M. Larson, Parameters to characterize biological conditions in marine and coastal waters retrieved from SeaWiFS data. Marine Technology Society Journal, 36(1): 14-22, 2002b.

Chen C.Q., P. Shi, Application of remote sensing technique for Monitoring the thermal pollution of the cooling-water from the nuclear power station in Daya Bay. Paper for the International Conference on the Environmental Problems of the Mediterranean Region ,EPMR, 2002c.

Chen C.Q., P. Shi, A local algorithm for retrieval of yellow substance (gelbstoff) in coastal waters from SeaWiFS data: Pearl River Estuary, China. International Journal of Remote Sensing, 24(5): 1171-1176, 2003a.

Chen C.Q., P. Shi, Q.W. Mao, Application of Remote Sensing Techniques for Monitoring the Thermal Pollution of Cooling-water Discharge from Nuclear Power Plant. Journal of Environmental Science and Health (A), A38(8): 1659-1668, 2003b.

Chen C.Q., J. Wei, P. Shi，Atmospheric correction of SeaWiFS imagery for turbid waters in Southern China coastal aeas. Proceedings of SPIE, Ocean Remote Sensing and Applications, 4892: 80-86, 2003c.

Chen C.Q., P. Shi, K.D. YIN, et al., Absorption coefficient of yellow substance in the Pearl River estuary. Proceedings of SPIE, Ocean Remote Sensing and Applications, 4892: 215-221, 2003d.

Chen C.Q., P. Shi, H.G. Zhan, et al., Retrieval of gelbstoff absorption coefficient in Pearl River estuary using remotely-sensed ocean color data. Proceedings of IGARSS05, Seoul, South Korea, 2005a. (*ISTP, EI)

Chen C.Q., P. Shi, H.G. Zhan, et al., Application of satellite data for integrated assessment of water quality in the Pearl River Estuary, China. Proceedings of IGARSS05, Seoul, South Korea, 2005b. (*ISTP, EI)

Chen C.Q., P. Shi, H.G. Zhan, Application of remote sensing technique for Long-term monitoring of thermal pollution from cooling-water discharge of nuclear power plant. Proceedings of the 9th International Symposium on Physical Measurements and Signatures in Remote Sensing. Beijing, China. 2005c.

Chen C.Q., X.B. Li, Application of Ocean colour remote sensing data for retrieval of nutrients concentration in Pearl River Estuary, Proceedings of the (3rd) International Conference on the Prevention and Management of Harmful Algal Blooms in the South China Sea, 33-38, 2006.

Chen X.X., X.Y. Ding, Study on Estimation of Chlorophyll Concentration of Surface Water in the Pearl River Estuary Using SeaWiFS Data. Acta Scientiarum Naturalium Universitatis Sunyatseni, 43(1): 98-101，2004.

Cong P.F., Z. Niu, L.M. Qu, et al. Retrieval of chlorophyll a concentration from ocean satellite HY-1. High Technology Letters. 15(11): 106-110, 2005.

Ding, J., Atmospheric correction and ocean constituents retrieval based on NN method in case 2 waters [D]. Dissertation of Doctor's Degree of Ocean University of China, 2004.

Ding J., J.W. Tang, Q.J. Song, et al., Comparisons between several methods for atmospheric correction in case 2 waters. The 5th conference of Ocean color remote sensing in case 2 waters in China, 2005(Dalian), CD-ROM, 2006.

Ding J., J.W. Tang, Q.J. Song, et al., Atmospheric correction with iteration and optimization methods in Chinese coastal turbid waters. Journal of Remote Sensing, 10(5): 732-741, 2006.

Feng C.J., C.F. Zhao, Study of the Vertical Distribution of Chlorophyll in the Ocean Based on Artificial Neural Networks. Journal of Ocean University of Qingdao, 34(3): 497-505, 2004.

Gao F., T.J. Li, Q.L. Chen, et al., The Key Techniques of Using MICROTOPS II Hand-held Sun Photometer on the Sea. Ocean Technology, 2004，23(3)：5-9.

Gordon H.R. and M. Wang, 1994. Retrieval of water-leaving radiance and aerosol optical thickness over the oceans with SeaWiFS: a preliminary algorithm. *Appl. Opt.*, 33(3), 443-452.

Guan W.J., X.Q. He, D.L. Pan, et al., Estimation of ocean primary production by remote sensing in Bohai Sea, Yellow Sea and East China Sea. Journal of Fisheries of China, 29(3)：367-372，2005.

Han Z., C.X. Yun, X.Z. Jiang, Experimental study on reflected spectrum of suspended sediment. Journal of Hydraulic Engineering, 2003a，327（12）：118-122.

Han Z., C.X. Yun, Deposition and erosion remote-sensing reverse of Dachan Bay beach in Lingdingyang estuary. Acta Oceanologica Sinica, 2003b，25（5）：58-64.

Han Z., C.X. Yun, et al., Research on reflectance spectrum of fine suspended sediment. Proceedings of the ninth international symposium on river sedimentation. Tsinghua university press, 2523-2527, 2004.

He X.Q., D.L. Pan, A practical method of atmospheric correction of SeaWiFS imagery for turbid coastal and inland waters. Proceedings of SPIE, Vol. 4892, 494-505, 2003.

He X.Q., D.L. Pan, Z.H. Mao, et al. The study on the inversing model of water transparency using the SeaWiFS data. ACTA OCEANOLOGICA SINICA. 2004，26(5)：55-62.

He X.Q., D.L. Pan, Q.K. Zhu, et al., Atmospheric correction for HY-1A/COCTS data. The conference for communications of HY-1A satellite and related technologies, Sanya, CD-ROM, 2004.

He X.Q., D.L. Pan, Q.K. Zhu, et al., Exact Rayleigh Scattering Calculation for Chinese Ocean Color and Temperature Scanner. Acta Optica Sinica. 25(2)：145-151，2005a.

He X.Q., D.L. Pan, Z.L. Yin, et al., Effects of Satellite Attitude on the Rayleigh Scattering Calculation. Journal of Remote Sensing, 9(3): 242-246, 2005b.

He X.Q., D.L. Pan, Y. Bai, General exact Rayleigh scattering look-up-table for ocean color remote sensing. Acta Oceanologica Sinica, 28(1)：47-55，2006.

Huang H.Q., X.Q. He, D.F. Wang, et al., A Study on the Remote Sensing Inversion of Ocean Chlorophyll Concentration by Using Neural Network Method. Geo-information Science, 6(2): 31-36, 57, 2004.

IOCCG (2000). Remote Sensing of Ocean Colour in Coastal, and Other Optically-Complex,

Waters. Sathyendranath, S. (ed.), Reports of the International Ocean-Colour Coordinating Group, No. 3, IOCCG, Dartmouth, Canada.

Jiang G., J. Xiao, Y.K. Zheng, et al., Retrieve the oceanic chlorophyll-a concentration in case I water by support vector machine. Computer Applications. 25(10): 2398-2400,2409, 2005.

Jiang G., J. Xiao, Y.K. Zheng, et al., Use Ocean Color Remote Sensing Data to Retrieve Chlorophyll-a Concentration Based on Statistic Learning Theory. Journal of Ocean University of Qingdao. 36(4):559-563，2006.

Jiang X.W., S.L. Niu, J.W. Tang, The System Cross-Calibration Between SeaWiFS and HY-1 COCTS. Journal of Remote Sensing, 2005，9(6)：680-687.

Li C., W.X. Cao, T.C. Ke, et al., Equipment for preventing pollution on the optical windows of marine optical buoy. Electronic Design & Application World, 6: 28-30, 2003.

Li C., T.C. Ke, Y.Z. Yang, Clock Chip PCE8563 Appilcation in Ocean Optical Buoy. Electronic & Computer Design World. 7:32-34，2003.

Li C., Y. Liu, A. Wang, et al., Exploitation of the data collecting system for CCD arrays based on CPLD. Application of Electronic Techniques, 29(6): 37-39, 2003.

Li G.S., F. Wang, Q. Liang, et al., Estimation of Ocean Primary Productivity by Remote Sensing and Introduction

to Spatio-temporal Variation Mechanism for the East China Sea. Acta Geographica Sinica. 58(4)：483-493，2003.

Li J.S., B. Zhang, Z.C. Chen, et al., Atmospheric correction for inland waters based on CBERS/CCD data with MODIS data as assistant. The 15th conference for remote sensing sciences and technologies in China, Guizhou, 2005.

Li L.P., Effects of absorptive aerosols on atmospheric correction in the East Asian Sea and related issues of ocean color remote sensing[D]. Dissertation of Doctor's Degree of Ocean University of China, 2002.

Li, L., H. Fukushima, R. Frouin, et al., Influence of sub-micron absorptive aerosol on SeaWiFS-derived marine reflectance during ACE-Asia. *J. Geophys. Res.*, 108: 4472-4482, 2003.

Li S.H., J.W. Tang, C.X. Yun, A study on the quantitative remote sensing model for the sediment concentration in estuary. Acta Oceanologica Sinica, 24(2): 51-58, 2002.

Li X.B., C.Q. Chen, P. Shi, et al., Estimation of primary production of South China Sea from 1998 to 2002 by remote sensing and its spatio-temporal variation mechanism. Journal of Tropical Oceanography. 25(3)：57-62，2006.

Li Y., S.L. Shang, C.Y. Zhang, et al., A model for redtide identification based on the relationships between remote sensing reflectances at visible bands and near-infrared bands. Chinese Science Bulletin, 2005, 50(22): 2555-2561.

Ma C.F., X.W. Jiang, J.W. Tang, et al. Inverse algorithms of ocean constituents for HY-1/CCD broadband data. Acta Oceanologica Sinica. 2005，27(4)：38-44.

Mao Z.H., Q.K. Zhu, F. Gong, Satellite remote sensing of chlorophyll a concentration in the north Pacific Fishery. Journal of Fisheries of China. 29(2)：270-274，2005.

Mao Z.H., 2005: Research of the Mechanism and Application of Ocean hyper-spectrum remote sensing. Technical report of National High-Tech Project"863"(2002AA639220)。

Mao Z.H., Q.K. Zhu, F. Gong, et al. The development of inversion models of chlorophyll-a concentration from CMODIS data. Acta Oceanologica Sinica. 28(3): 57-63, 2006.

Pan D.L., Y. Li, The Development of Marine Optical Remote Sensing and the Frontiers. Engineering Science, 2003, 5(3)：39-43.

Pan D.L, W.J. Guan, Y. Bai, et al., Ocean Primary productivity estimation of China Sea by remote sensing. Porgress of Natural Science, 2005, 15(7):627-632.

Qiu Z.F., NN based atmospheric correction in the areas with high frequency of redtides occurring of the East China Sea for MODIS data. The 5th conference of Ocean color remote sensing in case 2 waters in China , 2005(Dalian), CD-ROM, 2006.

Ruddick, K.G., F. Ovidio, M. Rijkeboer, 2000. Atmospheric correction of SeaWiFS imagery for turbid coastal and inland waters. *Appl. Opt.*, 39(6), 897-912.

Shang, S. L., C. Y. Zhang, H. S. Hong, et al. Short-term variability of chlorophyll associated with upwelling events in the Taiwan Strait during the southwest monsoon of 1998. *Deep-Sea Research II*, 2004, 51(10-11), 1113-1127.

Shang, S.L., C.Y. Zhang, H.S. Hong, et al., Hydrographic and biological changes in the Taiwan Strait during the 1997-1998 El Nino winter. *Geophysical Research Letters,* 2005, Vol.32, doi:10.1029/2005GL022578.

Shen C.Y., C.Q. Chen, H.G Zhan., Inverse of chlorophyll concentration in Zhujiang River Estuary using artificial neural network. Journal of Tropical Oceanography. 24(6):38-43，2005.

Shen H., The Research of the Optical Characteristic of CDOM and MODIS Algorithm to Estimate CDOM in the Typical Bays of China[D]. Dissertation of Master's Degree of Dalian Maritime University, 2006.

Song L.S., W. Chen, W.H. Xiang, et al., Remote sensing model for sediment information of Hangzhou Bay based

on rough sets. Journal of Hydraulic Engineering, 5:58-63, 2004.

Song Q.J., J.W. Tang, The study on the scattering properties in the Yellow Sea and East China Sea. Acta Oceanologica Sinica. 28(4)：56-63, 2006.

Sun J., X.Y. Cai, Evaluations of chlorophyll a concentration and primary production in the middle of Bohai Sea as well as the neighboring regions in spring and autumn, 1998-1999. ACTA ECOLOGICA SINICA, 23(3): 517-526, 2003.

Sun L., J. Zhang, Evaluation of Capacity to Retrieve Water Constituents in Case Ⅱ Waters From HY-1A CCD Data Using Genetic Algorithm. Advances in Marine Science. 22(B10):101-108, 2004.

Sun L., J. Zhang, Analysis of effects of gas absorption on applications of HY-1A/CCD data: data modeling and correction of Rayleigh scattering. The conference for communications of HY-1A satellite and related technologies, Sanya, CD-ROM, 2004.

Sun L., Atmospheric correction and ocean constituents retrieval based on HY-1A/CCD data [D]. Dissertation of Doctor's Degree of Graduate school of Chinese Academe of Sciences, Institute of Oceanology, 2005.

Sun L., J. Zhang, M.H. Guo, Rayleigh Lookup Tables for HY-1A CCD Data Processing. Journal of Remote Sensing. 10(3)：306-311，2006.

Sun L., J. Zhang, M.H. Guo, NN based atmospheric correction for case 2 waters. The annual conference of environment remote sensing of China, 2006, August, Yinchuan.

Sun L., M. H. Guo, Atmospheric correction for HY-1A CCD in Case 1 waters. Proceedings of SPIE Vol. 6200, Remote Sensing of the Environment: 15th National Symposium on Remote Sensing of China, Editor(s): Qingxi Tong, Wei Gao, Huadong Guo. 2006, 20-31.

Tang D.L., H. Kawamura, T.V. Dien, et al., Offshore phytoplankton biomass increase and its oceanographic causes in the South China Sea. MARINE ECOLOGY PROGRESS SERIES, Vol. 268: 31–41, 2004.

Tang J.W., X.M. Wang, Q.J. Song, et al., The statistic inversion algorithms of water constituents for Yellow Sea & East China Sea. Acta Oceanologica Sinica, 23(4): 617-626, 2004.

Tang J.W., G.L., Tian, X.Y. Wang, et al. The Methods of Water Spectra Measurement and Analysis I:Above-Water Method. Journal of Remote Sensing. 8(1)：37-44，2004.

Tang J.W., J. Ding, Q.M. Wang, et al., Research of the effects of atmospheric scattering on red tide remote sensing with normalized vegetation index. Acta Oceanologica Sinica. 2004，26(3)：136-142.

Tang J.W., J. Ding, J.W. Tian, et al. Neural network models for the retrieval of chlorophyll, total suspended matter, and gelbstoff concentrations of case-II waters in Yellow Sea and East China Sea. High Technology Letters. 2005，15(3)：83-88.

Tang J.W., X.F. Gu, S.L. Niu, et al., Cross calibration between CBERS-02/CCD and MODIS based on the water targets. Science in China, Series E, 2005, 35(Supplement I): 59-69.

Tang J.W., C.F. Ma, S.L. Niu, et al., Primary research on quantified retrieval of ocean constituents based on CBERS-02/CCD data. Science in China, Series E, 2005, 35(Supplement I): 156-170.

Tassan S. Local algorithms using SeaWiFS data for the retrieval of phytoplankton,pigments, suspended sediment, and yellow substance in coastal waters. *Appl. Opt.*, 1994,33(12): 2369-2378.

Wang G.F., W.X. Cao, D.Z. Xu, Variations in specific absorption coefficients of phytoplankton in Northern South China Sea. Journal of Tropical Oceanography. 24(5)：1-10，2005.

Wang, M. and W. Shi, "Estimation of ocean contribution at the MODIS near-infrared wavelengths along the east coast of the U.S.: Two case studies," *Geophys. Res. Lett.*, **32**, L13606, doi:10.1029/2005GL022917, 2005.

Wang X.M., J.W. Tang, J. Ding, et al., The retrieval algorithms of diffuse attenuation and transparency for the Case-Ⅱ waters of the Huanghai Sea and the East China Sea. Acta Oceanologica Sinica. 2005，27(5)：38-45.

Wang X.M., J.W. Tang, Q.J. Song, et al. The statistic inversion algorithms and spectral relations of total absorption

coefficients for the Yellow Sea and East China Sea. Oceanologia Et Limnologia Sinica. 2006, 37(3) ：256-263.

Wang X.Q., Q.M. Wang, Q.Y. Wu, et al., Estimating Suspended Sediment Concentration in Coastal Waters of Minjiang River Using Remote Sensing Images. Journal of Remote Sensing. 7(1): 54-57,T004, 2003.

Wang X.Y., T.J. Li, J.W. Tang, et al. Measurement and Analysis of AOPs in Case II Waters with Above-Water Method. Ocean Technology. 2004，23(2)：1-6.

Wang X.Y., T.J. Li, A.A. Yang, Spring Empirical Models between Apparent and Inherent Optical Properties in the East China Sea and Yellow Sea. Ocean Technology. 23(4)：123-126，2004.

Wei J., C.Q. Chen, P. Shi, A practical algorithm for atmospheric correction of SeaWiFS data. Acta Oceanologica Sinica. 2002, 24（4）：118-126.

Wen J.G., Q. Xiao, Y.P. Yang, et al., Remote sensing estimation of aquatic chlorophyll-a concentration based on Hyperion data in Lake Taihu. Journal of Lake Sciences, 18(4): 327-336, 2006.

Wu J.Y., S.L. Shang, H.S. Hong, et al., Variation of phytoplankton absorption in the northeastern South China Sea during spring and late autumn. Submitted to Journal of Marine Research, 2006.

Wu Y.S., S.K. Zhang, X.Q. Zhang, Yellow Substance in Jiaozhou Bay of China and Prospect of Its Application. Proceedings of SPIE，Hangzhou,China, 2003, 930—936.

Wu T.F., W.X. Cao, A study on shading error and correction of underwater optical measurements. Acta Oceanologica Sinica. 25(1):42-51，2003.

Wu Y.S., S.K. Zhang, X.Q. Zhang, et al. Experimental study on the optical absorption property of Yellow substance in seawater. Oceanologia Et Limnologia Sinica. 33(4)：402-406，2002.

Wu Y.S., X.Q. Zhang, S.K. Zhang, The analysis of biochemical components of the marine yellow substance in the Jiaozhou Bay. Acta Oceanologica Sinica. 2004，26（4），58-64.

Xu X.Q., W.X. Cao, Y.Z. Yang, Relationships between spectral absorption coefficient of particulates and salinity and chlorophyll a concentration in Zhujiang River Mouth. Journal of Tropical Oceanography. 23(5)：63-71，2004.

Yang Y.M., Z.W. Liu, B.Q. Chen, Retrieval of Ocean Color Constituents from Case 2 Water Reflectance by Partial Least Squares Regression. Journal of Remote Sensing. 9(2): 123-130, 2005.

Zhan H.G., P. Shi, C.Q. Chen, A Genetic Algorithm for Retrieval of Water Constituents from Ocean Color Remote Sensed Data in Case 2 Waters. Journal of Remote Sensing. 8(1)：31-36，2004.

Zhan H.G., P. Shi, C.Q. Chen, Quasi-analytical algorithm based on Bayes theory for ocean color retrievals in case 2 water. Chinese Science Bulletin, 51(2): 204-210, 2006.

Zhan H.G., Z.P. Lee, P. Shi, et al., Retrieval of Water Optical Properties for Optically Deep Waters Using Genetic Algorithms. *IEEE Trans. Geosci. Remote Sensing,* 41(5): 1123~1128, 2003.

Zhan H.G., P. Shi, and C.Q. Chen, Retrieval of Oceanic Chlorophyll Concentration Using Support Vector Machines. *IEEE Trans. Geosci. Remote Sensing*, 41(12), 2003.

Zhan H.G. Application of Support Vector Machines in Inverse Problems in Ocean Color Remote Sensing, in "Support Vector Machines: Theory and Applications", Springer-Verlag. 387～397. 2005a.

Zhan H.G., P. Shi, and C.Q. Chen, A Bayesian based quasi-analytical algorithm for inversion of *ocean* color in Case 2 waters. Submitted to Chinese Science Bulletin, 2006.

Zhang C.Y., C.M. Hu, S.L. Shang, et al. Bridging between SeaWiFS and MODIS for continuity of chlorophyll-*a* concentration assessments off Southeastern China. *Remote Sensing of Environment*, 2006, 102 (3-4): 250-263.

Zhang J., An Atmospheric Correction Algorithm of Ocean Color Satellite for Case Ⅱ Water[D]. Dissertation of Master's Degree of Hefei University of Technology, 2002.

Zhang Q.L., C.Q. Chen, P. Shi, Characteristics of Kd(490) around Nansha Islands in South China Sea. Tropic

Oceanology, 22(1): 9-16，2003.

Zhang T.L., M.X. He, A Method to Retrieve the Oceanic Chlorophyll-a Concentrations in Case I Water Based on Artificial Neural Network. Journal of Remote Sensing, 6(1), 2003.

Zhang T., F. Fell, Z.S. Liu，et al .，Evaluating the performance of the artificial neural network techniques for pigment retrieval from ocean colour in Case I waters, *J. Geophys. Res*., 108(c9), 3286, doi: 10.1029/2002JC001638, 2003.

Zhang, T., Retrieval of oceanic constituents with artificial neural network based on radiative transfer simulations techniques, *PhD thesis*, *Institut fuer Weltraumwissenschaften*, Freie Universitaet Berlin, Germany, 2003.

Zhang, T., J. Fischer，Retrieval of Oceanic Constituents from MERIS Imagery over Case II waters with Artificial Neural Network， *SP-1286/EPD*，2005.

Zhang, T., F. Fell , An approach to improving the retrieval accuracy of oceanic constituents in Case II waters, Journal of Ocean University of China, 3 (2), 2004.

Zhang, T., F. Fell, J. Fischer, Modelling the backscattering probability of marine particles in Case II waters, *in Ocean optics XVI*（Santa Fe，USA）, 2002.

Zhang, T., F. Fell, An Empirical Algorithm for Determining the Diffuse Attenuation Coefficient, Kd(490), in Clear and Turbid Waters.(2006, submitted to *limnology & Oceanography*)

Zhao D.Z., F. Du, L. Zhao, et al. On the Reflectance Spectrum of Algae in Water: Comparison of Chlorophyll Fluorescence Algorithms for Three Remote Sensing Red Tide Sensors. High Technology Letters. 14(11)：93-97，2004a.

Zhao D.Z., F.S. Zhang, F. Du, et al. Fluorescence Peak near 700nm on the Reflectance Spectrum of Algae in Water: the Relationship of Fluorescence Line Height with Chlorophyll a Concentration. High Technology Letters. 14(5)：68-72，2004b.

Zhao D.Z., F.S. Zhang, F. Du, et al. Interpretation of Sun-induced Fluorescence Peak of Chlorophyll a on Reflectance Spectrum of Algal Waters. Journal of Remote Sensing. 9(3)：265-270，2005a.

Zhao D.Z., F.S. Zhang, J.H. Yang, et al. The optimized spectral bands ratio for the relation of sun-induced chlorophyll fluorescence height with high chlorophyll a concentration of algal bloom waters. Acta Oceanologica Sinica. 27(6)：146-153，2005b.

Zhao W., J.W. Tang, F. Gao, et al. Measurement and study of aerosol optical properties over the Huanghai Sea and the East China Sea in the spring. Acta Oceanologica Sinica. 2005，27(2)：46-53.

Zhao W., M.S. Lin, G.M. Chen, et al., Study of exact Rayleigh scattering arithmetic for COCTS sensor on "HY-1" satellite. Acta Oceanologica Sinica. 2006，28(3)：139-143.

Zhao W., M.S. Lin, J.W. Tang, Study of exact Rayleigh scattering arithmetic for the ocean color remote sensing. High Technology Letters, 16(8)：876-880，2006.

Zhong J.C., X.Y. Wang, Q.L. Chen, A Retrieval Method on the chlorophyll, total suspended matter, and gelbstoff concentrations of Case II waters in Yellow Sea and East China Sea Based On Artificial Neural Network. Ocean Technology. 2005, 24(4): 118-122.

Zhou H.L., J.H. Zhu, B. Han, et al. Research on the Key Technique of the Analysis of Suspended Matter by Weighting Method. Ocean Technology. 2004，23(3)：15-20.

Zhu J.H., T.J. Li, Spectral Mode Research about Absorption Coefficient of The De-pigment Particles And Yellow Substance in Yellow Sea And East China Sea. Ocean Technology. 23(2)：7-13，2004a.

Zhu J.H., T.J. Li, Relationship Research of Phytoplankton Pigments Absorption and Chlorophyll a Concentration in in the East China Sea and Yellow Sea. Ocean Technology. 23(4):117-122, 2004b.

(Author's email: jwtang@public3.bta.net.cn)

PROGRESS AND PERSPECTIVE IN THE OCEAN INFORMATION TECHNOLOGY IN CHINA

Lin Shao-hua *Han Gui-jun*

National Marine Data and Information Service

ABSTRACT

This paper reviews the progress in the ocean information technology in China, including oceanic data quality control and processing (especially related with those of the high tech observations such as altimetry, remote sensing, ARGO, multi-beam marginal sounding beam, HF ground wave radar, and so on), databases and data mining, ocean GIS and digital ocean, ocean data assimilation and numerical analysis, ocean data exchange, assembly, sharing, management and service. The primary perspectives to the future development on the ocean information technology are also put forward.

1. Introduction

Over the last decades, significant accomplishments by individuals and groups have led to major advances in many branches of oceanography and marine science and technology in China. These advances have been driven by improved knowledge and by technological advances in observational techniques and in computing. Such advances, particularly those associated with remote sensing and complex computer models, have led to a rapid expansion in the data and information related to the ocean and the marine environment. In parallel with this evolution it has been a trend toward the increasing applied oceanography of a form which set up an efficient and effective data and information system for the ocean and marine environment, based on the underlying technology of such system, the ocean information technology (OIT), to serve the oceanographic community and beyond.

This paper reviews the progress in the OIT in China. The rest of the paper is organized as follows. In section 2, many diversity of aspects of the progress in the OIT are presented respectively, which include ocean data quality control and processing (especially related with those high tech observations such as altimetry, remote sensing, ARGO (Array for Real-time

Geostrophic Oceanography), multi-beam marginal sounding beam, HF (High Frequency) ground wave radar, and so on), databases and data mining, ocean GIS (Geographical Information Systems) and digital ocean, ocean data assimilation and numerical analysis, ocean data exchange, assembly, sharing, management and service. The primary perspectives to the future development on the OIT are put forward in section 3. In section 4 the summary is given.

2. Progress in the OIT

2.1 Quality control and processing of ocean data

Whether the users are operational or not, there is always an emphasis on quality of the oceanic data. Quality control is an important part of the ocean data processing. The "quality" of ocean data will evolve as our knowledge evolves. And the ocean quality control system needs to be revised to form a robust and effective system for both historical and real-time data. Besides conventional oceanic observations, we need to put more effort into the quality control and processing for those high tech observations due to increasing of such procedure as newly developed instruments being used. These kinds of data include altimetry, remote sensing, ARGO (Array for Real-time Geostrophic Oceanography), multi-beam marginal sounding beam, HF (High Frequency) ground wave radar, and so on.

As for altimetry data processing and information application in the China Seas, there are many studies involving tidal analysis (Liu, et al, 2002a, Dong, et al, 2002), mean sea surface (Jiang, et al, 2002), sea surface height anomaly and geostrophic circulation variations (Liu, et al, 2002b, Wang, 2004, Cheng, et al, 2004, Bao, et al, 2005, Wen et al, 2006). The along-track TOPEX/POSEIDON Geophysical Data Records (GDR) are processed, and the time series of the tidal sea surface heights referring to the mean sea surface are obtained. Two classical methods, i.e. harmonic and response analyses are implemented to estimate the tide from such datasets over China Seas (Han, et al, 2006). A high precision 2-dimensional nonlinear tidal model (external mode of the Princeton Ocean Model, Mellor, 1998) is established by incorporate tidal measurements both from tide gauges and derived T/P datasets using the variational adjoint approach.

Taking the advantages of quality control and data assembly endeavored by the international community for Argo data, the real-time and delayed-mode data are processed and handed out to users timely through on-line data services in China (http://www.argo.org.cn/english/ index.html

for China real-time Argo data, and http://www.argo-cndc.org/argo-eng/index.asp for global delayed-mode Argo data). The method of Wong et al (2003) is improved by using multiple-regression method (Ji and Wang, 2006) when sensor drifts of salinity measurements are corrected.

The multi-beam sounding systems have been used in the ocean survey more and more in China. Many aspects have been studied to process such kind of bathymetry survey data to ensure their quality (Zhao, 2002, Zhao, et. al., 2003 , Yang, et. al, 2003, Yang, et. al. 2004a, 2004b, Zhao, et. al, 2004, Tang, et. al., 2004, Tang, et. al., 2005a, 2005b, Zhou, et. al., 2005). The error of marginal beams mainly influences the quality of multi-beam sounding data. On the basis of multi-beam survey principles and the acoustics theory, Wu, et al (2005) analyzed the control factors of marginal beams quality. By considering such factors as multi-beam sonar parameters, sound profiles and sounding noises compilation, a software based man-machine conversation to process the multi-beam sounding data has been designed and established by using oriented-object method of GIS. The above method has been introduced in the topographic mapping project. Qi and Tian (2003) proposed a method of ray tracing in the depth direction to improve the quality of multi-beam sounding bathymetry measurement.

In the past decade the high frequency ground wave radar has been developed as an advanced technique for the ocean survey of surface currents, winds and waves. The calibration of radar-measured data and the methods to control the quality of radar-sensing data are widely discussed (Shi, et al, 2002, Yang, et al, 2002, Zhou, et al, 2002, Li, et al, 2003, Zhang, et al, 2003, Liu, et al, 2004,Qiao et al, 2005, Guo, et al, 2006, Wu, et al, 2006,Yu, et al, 2006.). Such monitoring data have gradually turned into a steady source of operational application for coastal area in China.

2.2 ocean data bases and data mining, ocean GIS and digital ocean

There has been accumulated massive amounts of valuable ocean multi-disciplines data through the global operations in the past decades. A significant need for automatic and intelligent knowledge discovery of these data has emerged. Routine analytical methods are unable to satisfy such a need. Data mining technology provides a promising solution for the problem. Database, data mining and visualization are the new paradigm for analyzing and understanding vast wealth

of ocean information. The applications of data mining technology to analyze the oceanic datasets are streaming out (Ma et al, 2005, Wang et al, 2005, Xia et al, 2005, Xue et al, 2005, He et al, 2006, She et al, 2006, Wang, et al, 2006). The ocean database prototype has been created under the frame of "908 Project". The studies have demonstrated the power of data mining and database in ocean data search, retrieval, display, and 3-D visualization. And also it has shown a great promise to apply such high-tech to build the component of the digital ocean in China.

The access to qualify the coastal and ocean information is critical and also it's necessary to better assess and plan for the use and protection of the ocean resources. The Ocean GIS prototype will take us further in terms of our understanding because of the way it gathers and analyzes ocean information. Given enough data, a GIS can, in fact, create a virtual ocean inside of a computer which is actually a substantial part of building prototype of the digital ocean in China. Technical issues related to the ocean GIS (also digital ocean) in the China have been comprehensively probed, and some prototypes of ocean GIS have been designed and created (Cao, et al, 2002, Chen, et al, 2002, Li, et al, 2002, Xu, et al, 2002, Shao, et al, 2003, Yan, et al, 2003, Chen, et al, 2004, He, at al, 2004, Su, et al, 2004, Han, et al, 2006, Song, et al, 2006, Su, et al, 2006).

2.3 ocean data assimilation and numerical analysis

The observations from ocean stations have been too sparse to be of practical use for retrieving the space-time evolution of the ocean. The development of modern ocean science and technology and computing techniques makes it possible to use ocean dynamics model to extract information from oceanic observations to reconstruct the structure of the ocean circulation system. This is the concept of ocean data assimilation. Taking the advance of modern ocean data assimilation methods, a state-of-the-art data assimilation system is used to reprocess all past ocean observations, combining them with short forecasts in order to derive the best estimate of the state and evolution of the ocean. Since the statistical combination of the forecast and observations is denoted in operational applications as analysis, the method is usually known as reanalysis. The ocean data assimilation and reanalysis have been given intensively attention along with the progress of such techniques acquired by international communities. Some major progress and achievement have been made in the above area. The traditional three dimensional variational (3D-Var) data assimilation method and its variations have been used in the operational system of

ocean circulation model in the China Seas (Zhang, et al, 2003, Liu, et al, 2005, He, et al, 2006, Li, et al, 2006, Wang (personal communication), Zhu, et al, 2006). The advanced methods have been studied in-depth, for instance, 3D-Var for both temperature and salinity assimilated into the ocean model (Han, et al, 2004, Yan, et al, 2004), four dimensional variational (4D-Var) data assimilation (Han, et al, 2006), Kalman Filter (Ma, et al, 2003, Zhang, et al, 2003). Li et al (2006) and He et al (2006) have recently developed two new 3D-Var methods, so called multi-grid method and sequence 3D-Var respectively, which can give the flow dependent background error covariance as the Ensemble Kalman Filter. The reanalysis products of sea level, temperature, salinity and current have been tentatively produced in China (Han, et al, 2006).

2.4 ocean data exchange, assembly, sharing, management and service

As a national oceanographic data center, The National Marine Data and Information Service (NMDIS) holds ocean historic data surveyed by the State Oceanic Administration (SOA) of China. The NMDIS has actively participated in marine data and information management activities of international organizations, such as IODE, JCOMM, GOOS, etc, and acts as China's national focal point for international oceanographic data exchanges. The NMDIS also takes charge of bilateral data exchange of marine data and information with dozens of ocean-related international organizations over 170 institutions in 32 countries and regions.

Before assembling data into data sets and data streams, we need to consider more formality and implementation of accepted procedure. We require a study of requirements, existing practices for quality control, and standards. The Chinese government has invested in such area of the OIT. And The NMDIS has taken this task into account and implementation. A series of standards are being drafted and revised to cater for ocean data assembly and sharing requirements. However, we have a long way to go to accomplish the final goal of ocean data assembly, sharing management and service. The root of the problem is obviously that agencies, government departments, and laboratories around China, have never recognized the need to commit sufficient resources. It lacks status and the investment is way too low. The real costs of such activities must be addressed. The attitude should be: preserve the resource we just spent millions collecting, make it available to others and show the added value data such efforts will achieve.

3. Perspectives in the OIT

As new technology for observing the ocean—ranging from submersible buoys to multi-spectral satellite observations —is implemented, a significant challenge will be to optimally process large volumes of this new information. This challenge implies that OIT should alongside advance the modeling technique and modern observing.

By now national programs in the OIT have been set up in China. For example, the frame of digital ocean is a key component of "908 Project". Such program is ambitious, but can be realized drawing largely on already available resources. Most importantly, the program would benefit from sharing resources at national level.

Most observations cannot be applied in ocean prediction and state assessment without being subjected to some form of process and analysis, which maximizes information content of the observations relative to the desired state representation. To continue to improve the effectiveness of rather expensive observing networks, it is necessary to both refine ways of optimizing information content of the observations. These emphasize the importance of much more investment in the OIT and also will give high expectation for great achievement both from individuals and community with great effort engaged in the development of OIT in China.

4. Summary

It is clear that, for all applications of the ocean data and information, there is a primary dependence on the technology used for extracting useful portion from the original sources. The strategy has generally been to seek increments to the data and information as new requirements emerge and as technology has changed. The information systems have been set up and it should be emphasized that we are seeking a 21st Century solution that takes advantage of leading ocean information technology and methodology. The serious challenge imposed by a rapid expansion in the ocean data and information and many new functional requirements is our ability to manage and interpret this information. What we should do at the present time is to develop a management structure of oceanic data and information at national level, to adapt to the remarkably broad range of types of data sources, storage repositories, and access mechanisms, and to make major improvements in serving the customer. Otherwise, it is shown that this is beginning to limit further progress in the OIT in China.

Acknowledgments. The authors would like to thank Li Shi for her help on the collection of references related with the OIT in China. This is partly support by the National High-tech R&D Program of China (2006AA09Z138).

References

Bao Lifeng, Lu Yang, Wang Yong, Xu Houze, 2005, Seasonal variations of upper ocean circulation over the South China Sea from satellite altimetry data of many years *Chinese Journal of Geophysics*, 48(3), 543-550.

Cao Wenzhi, Hong Huasheng, Zhang Yuzhen, Ding Yuanhong, Yue Shiping, 2002, Testing AGNPS for water quality modeling in agricultural catchments in southeast of China, *Acta Scientiae Circumstantiae*, 22(4), 537-540.

Chen Chuqun, Pan Zhilin, Shi Ping, 2003, Simulation of sea water reflectance and its application in retrieval of yellow substance by remote sensing data, *Journal of Tropical Oceanography*, 22(5), 33-39.

Chen Ge, Fang Chaoyang, 2002, Application of RS and GIS technologies in the analysis of global sea surface wind speed, *Journal of Remote Sensing*, 6(2), 69-74.

Chen Yilan, Zhou Xinghua, Zhang Weihong, 2004, Discussion about two technical problems of establishing MGIS, *Engineering of Surveying and Mapping*, 13(4), 40-42.

Cheng Luying, Xu Houze, 2004, Sea level variation over china seas from TOPEX/Posidon crossovers data, *Journal of Geodesy and Geodynamics*, 24(2), 106-109.

Dong Xiaojun, Ma Jirui, Huang Cheng, Fan Zhenhua, Han Guijun Xu Congjin, 2002, Tidal information of the yellow and east China seas from TOPEX/Poseidon satellite altimetric data, *Oceanologia Et Limnologia Sinica*, 33(4), 386-392.

Du Yan, Qi yiquan, Chen Ju, Shi Ping, Zhu Bocheng, 2003, Current analysis at a continuous observation station in the East China Sea, *The Ocean Engineering*, 21(1), 28-34.

Du Yan, Wang Dongxiao, Chen Rongyu, Mao Qingwen, Qi Yiquan, 2004, Vertical structure of ADCP observed current in the western boundary of the South China Sea, *The Ocean Engineering*, 22(2), 31-38.

Guo Peifang, Hou Yijun, Han Shuzong, Zhou Liangmin, Zhan Xianglun, 2006, Comparison and error analysis of remotely measured waveheight by high frequency ground wave radar, *Chinese Journal of Oceanology and Limnology*, 24(1), 28-34.

Han Guijun, Li Wei, He Zhongjie, Liu Kexiu, and Ma Jirui, 2006, Assimilated tidal results of tide gauge and TOPEX/Poseidon data over the china seas using a variational adjoint approach with a nonlinear numerical model, *Advances in Atmospheric Sciences*, 23(3), 449–460.

Han Guijun, Ma Jirui, Liu Kexiu, 2006, The advance and progress of data assimilation method research and operational application in China. Technical Report, NMDIS 2006-05-01.

Han Guijun, Jiang Zhu, and Guangqing Zhou, 2004, Salinity estimation using the T-S relation in the context of variational data assimilation, *Journal of Geophysical Research*, 109, c03018, doi: 10.1029/2003JC001781.

Han Litao, Zhu Qing, Hou Chengyu, 2006, Issues related to the construction of the virtual marine environments, *Marine Science Bulletin*, 25(4), 85-91, 96.

He Guangshun, Li Sihai, 2004, Constructing spatial information database for digital ocean, *Marine Information*, 1, 1-4.

He Hong, Xiao Jianhua, Xiao Weiping, 2006, The research on the incremental updating algorithm for mining association rules, *Natural Science Journal of Xiangtan University*, 28(3), 36-39.

He Xianqiang, Pan Delu, Bai Yan, Gong Fang, 2006, General exact Rayleigh scattering look-up-table for ocean color remote sensing, *Acta Oceanologica Sinica*, 28(1), 47-55.

He Zhongjie, Yuanfu Xie, Wei Li, Dong Li, Guijun Han, Kexiu Liu, and Jirui Ma, 2006, Application of sequential three dimensional variational method on Argo in a global ocean model, *The collection of Argo application papers*, Ocean Press, 183-192.

Ji Fengying and Wang Fan, 2006, A calibration method of Argo floats based on multiple regression analysis, *Chinese Journal of Oceanology and Limnology* , 24(2), 118-124.

Jiang Xingwei, Niu Shengli, Tang Junwu, Shao Yan, 2005, The system cross-calibration between SeaWiFS and HY-1 COCTS, *Journal of Remote Sensing*, 9(6), 680-687.

Jiang Weiping, Li Jiancheng, Wang Zhengtao, 2002, The satellite altimeter data derived mean sea surface WHU2000, Chinese Science Bulletin, 47(15), 1187-1191.

Li Guowei, Ke Hengyu, Zhang Yi, 2003, Processing of step frequency signal in a high frequency ground wave over-the-horizon radar, *Journal of Wuhan University (Natural Science Edition)*, 49(3), 396-400.

Li Wei, Yuanfu Xie, Zhongjie He, Kexiu Liu, Guijun Han, Jirui Ma, and Dong Li, 2006, Application of multi-grid method on Argo data assimilation, *The collection of Argo application papers*, Ocean Press, 193-203.

Li Xiao, Zhang Jiangfeng, Lin Zhong, He Chenggen, 2002, Secondary Development of Thematic GIS Based on MapX+Visual basic--taking the development of a marine function zoning MIS as an example, *Journal of Fujian Teachers University* (Natural Science), 18(4), 105-109.

Liu Kexiu, Ma Jirui, Han Guijun, Fan Zhenhua, Xu Chongjin, 2002a, Tidal harmonic analysis of TOPEX/POSEIDON data in the Northwest Pacific by introducing difference-ratio relations. *Acta Oceanologica Sinica*, 21(1), 33-44.

Liu Kexiu, Ma Jirui, Xu Jianping, Han Guijun, Fan Zhenhua. 2002b, Sea surface height anomaly and geostrophic circulation variations in the South China Sea from TOPEX/POSEIDON altimetry. *Acta Oceanologica Sinica*, 21(3), 345-354.

Liu Lei, Wu Xiongbin, Chengfeng, 2004, Ocean surface currents detection at the Eastern China Sea by HF surface wave radar, *Chinese Journal of Radio Science*, 19(z1), 139-141.

Liu Lei, Wu Xiongbin, Chengfeng, 2006, Algorithm for vector current measurements based on stream function method, *Journal of Wuhan University(Natural Science Edition)*, 52(3), 366-370.

Liu Yimin, Zhang Renhe, Yin Yonghong, And Niu Tao, 2005, The application of ARGO data to the global ocean data assimilation operational system of NCC, *Acta Meteorologica Sinica*, 19(3), 355-365.

Ma Chaofei, Jiang Xingwei, Tang Junwu, Wang Xiaomei, Li Tongji, Huang Haijun, Ren Jingping, 2005, Inverse algorithms of ocean constituents for HY-1/CCD broadband data, *Acta Oceanologica Sinica*, 27(4), 38-44.

Ma Ronghua, Ma Xiaodong, Pu Yingxia ,2005, Spatial association rule mining from GIS database, *Journal of Remote Sensing*, 9(6), 733-741.

Ma Zhaipu, Huang Daji, Zhang Benzhao, 2003, Study on the theory of reducing Kalman filter gain matrix with SVD decomposition, Journal of Zhejiang University(Engineering Science), 37(1), 87-93.

Mellor, G. L., 1998: Users guide for a three-dimensional primitive equation numerical ocean model .Program in Atmospheric and Oceanic Sciences, Princeton University, Princeton, NJ 08544-0710, 56pp.

Pan Delu, He Xianqiang , Zhu Qiankun, 2004, In-orbit cross-calibration of HY-1A satellite sensor COCTS, *Chinese Science Bulletin*, 49(23), 2521-2526.

Qi Na, And Tian Tan, 2003, Ray tracing in multibeam swath bathymetry, *Journal of Harbin Engineering University*, 24(3), 245-248.

Qiang Yong, Jiao Licheng, Bao Zheng, 2005, Super-resolution estimation of the ocean surface current for the HF ground wave radar, *Journal of Xidian University*, 32(1), 75-79.

Qu Liqin, Guan Lei, He Mingxia, 2006, The Global Availabilities of SeaWiFS, MODIS and Merged Chlorophylla Data, *Periodical of Ocean Universit*y of China, 36(2), 321-326.

Shao Quanqin, Zhou Chenhu, Shen Xinqiang, Yang Chongjun, 2003, Operational GIS and RS technology & methods for marine fishery, *Journal of Remote Sensing*, 7(3), 194-200.

She Xiangyang, Xue Huifeng, Lei Xuewu, Tang Guoan, 2006, The remote sensing image classification research based on mining classification rules on the spatial database, *Journal of Remote Sensing*, 10(3), 332-338.

Shi Yubing, Yang Zijie, Chen Zezong, Wan Xianrong, 2002, The present operational status and developing trend of HF ground wave radar for ocean surface condition monitoring, *Telecommunication Engineering*, 42(3), 128-133.

Song Yuanfang, Wang Xingtao, Zhai Shikui, 2006, Applications of GPS, GIS and RS technology to the sustainable development of marine resources and marine environment, *Journal of Ocean University of Qingdao*, 36(1), 26-30.

Su Fenzhen, Du Yunyan, Pei Xiangbin, Yang Xiaomei, Zhou Chenghu, 2006, Constructing digital sea of China with the datum of coastal line, *Geo-Information Science*, 8(1), 12-15, 20.

Su Fenzhen, Zhou Chenghu, Yang Xiaomei, 2004, Definition and structure of marine geographic information system, *Acta Oceanologica Sinica*, 26(6), 22-28.

Sun Ling, Zhang Jie, Guo Maohua, 2006, Rayleigh lookup tables for HY-1A CCD data processing, *Journal of Remote Sensing*, 10(3), 306-311.

Tang Qiuhua, Chen Yilan, Zhou Xinghua et al. 2004, Formation of seafloor image for Multibeam Sonar and its application, *Hydrographic Surveying and Charting*, 24(5): 9-12.

Tang Qiuhua, Chen Yongqi, Zhou Xinghua et al. 2005 , Seafloor Classification with the approach of GA-based LVQ neural network. *The Pacific Congress on Marine Science and Technology*, 73-85.

Tang Qiuhua, Zhou Xinghua, Liu Zhongchen et al. 2005 , Processing multibeam backscatter data. *Marine Geodesy*, 28(3), 251-258.

Wang Haiqi, Wang Jinfeng, 2005, Research on progress of spatial data mining, *Geography and Geo-Information Science*, 21(4), 6-10.

Wang Qimao, Ma Chaofei, Tang Junwu, Guo Maohua, 2006, A Method for detecting red tide information using EOS/MODIS data, *Remote Sensing Technology and Application*, 21(1), 6-10.

Wang Qimao, Lin Mingsen, Guo Maohua, 2006, Error analysis of sea surface temperature retrieved from the HY-1 satellite data, *Advances in Marine Science*, 24(3), 355-359.

Wang Qimao, Jin Zhengang, Sun Congrong, 2003, Sea surface temperature retrieval using the HY-1 satellite data, *Marine Forecasts*, 20(3), 53-59.

Wang Zhengtao, Li Jiancheng, Chao Dingbo, Jiang Weiping, 2004, Correlativity Study Between El Ni(n)o Phenomenon and mean sea level abnormal variations in Equator Pacific area using multi-satellite altimetric data, *Geomatics and Information Science of Wuhan University*, 29(8), 699-703.

Wang Dandan, Liu Tongming, Zhang Jing, 2006, H-C: an algorithm for mining frequent closed itemsets based on H-Struct, *Journal of Jiangsu University of Science and Technology (Natural Science Edition*), 20(4), 60-63.

Wen Hanjiang, Zhang Chuanyin, 2006, EOF analysis of sea level anomaly time series derived from ERS-2 and TOPEX altimeter data, *Geomatics and Information Science of Wuhan University*, 31(3), 221-223.

Wong, A.P.S. , Johnson, G.C., Owens, W.B., 2003. Delayed mode calibration of autonomous CTD profiling float salinity data by Θ–S climatology. *Journal of Atmospheric and Oceanic Technology*, 20, 308–318.

Wu Xiongbin, Yin Wei, Cheng Feng, Ke Hengyu, 2006, Statistics analysis of HF broad-beam sea-echo spectra, *Chinese Journal of Radio Science*, 21(3), 432-436.

Wu Ziyin, Jin Xianglong, Zheng Yulong , Li Jiabiao , Yu Ping, 2005, Integrated error correction of multi-beam marginal sounding beam, *Acta OceanoloGica Sinica*, 27(4), 88–94.

Xia Dengwen, Wang Hong, Shi Suixiang, 2005, Design on flow of visualization modeling system for ocean remote sensing information extraction, *Acta Oceanologica Sinica*, 27(3), 97-103.

Xia Dengwen, Shi Suixiang, Wang Daling, Yu Ge, 2005, Study on the techniques of marine data warehouse and data mining, *Marine Science Bulletin*, 24(3), 60-65.

Xue Huifen, Zhou Yanxia, 2005, A study on the application of warehouse technology to ocean environment information management, *Marine Science Bulleti*n, 24(3), 66-72.

Xiong Xuejun, Hu Xiaomin, Yu Fei, Jiao YuTian, 2006, Blanking optimizing and error control of data processing for lowered acoustic doppler current profiler, *Ocean Technology*, 25(1), 107-110.

Xu Kehui Sun Xiaogong Liu Zhan Feng Landi, 2002, Critical technique of coastal zone GIS based on components GIS MapObjects, *Journal of Ocean University of Qingdao*, 32(5), 770-776.

Yan Changxiang , Zhu Jiang, Li Rongfeng, et al. 2004 , Roles of vertical correlations of background error and T-S relations in estimation of temperature and salinity profiles from sea surface dynamic height. *Journal of Geophysical Research*, 109, C08010, doi:10.1029/2003JC002224

Yan Shiqiang, Xiong Deqi, Teng Guangwei, 2003, Projection conversion of graphic and its application in marine numerical prediction based on GIS, *Journal of Zhejiang Ocean University*, 22(4), 321-326.

Yang Fanlin, Liu Jingnan , Zhao Jianhu, 2003, Multi-beam Sonar and Side-scan Sonar Image Co-registering and Fusing, *Marine Science Bulletin*, 5(1), 16-23.

Yang Fanlin, Liu Jingnan , Zhao Jianhu, 2004, Detecting outliers and filtering noises in multi-beam data, *Geomatics and Information Science of Wuhan University*, 29(1), 80-83.

Yang Fanlin, Liu Jingnan, and Zhao Jianhu, 2004, Pre-processing of Side-scan Sonar Image using data fusion method, *Geomatics and Information Science of Wuhan University*, 29(5), 402-406.

Yang Shaolin, Ke Hengyu, Tian Jiansheng, Wu Shicai, Yang Zijie, 2002, Self-calibration method of channel amplitude of HF ground wave radar based on sea echo, *Journal of Electronics and Information Technology*, 24(9), 1233-1237.

Yu Wei Tian Jiansheng , 2006, New method to pick up sea echo signal in HF radar*s, Systems Engineering and Electronics*, 28(8), 1161-1163.

Yuan Yaochu, Zhao Jinping, Wang Huiqun, Lou Ruyun, Chen Hong, Wang Kangshan, 2002, The results and chart analysis of shallow current of top 450m and deep current observed with ADCP in the Northeast of South China Sea, Science in China (SERIES D), 32(2), 163-176.

Zhang Renhe, Liu Yimin, Yin Yonghong Shi Li, 2004, Utilizing ARGO data to improve the ocean data assimilation and the relative physical processes in ZC ocean model, *Acta Meteorologica Sinica*, 62(5), 613-622.

Zhang Tong, Han Guijun, 2003, A study on data assimilation of sea temperature with Kalman Filter, *Marine Science Bulletin*, 22(5), 50-57.

Zhang Yi, Ke Hengyu, Wen Biyang, Wu Xiongbin, 2003 A new method to estimate signal number by echo's phase, *Journal of Wuhan University (Natural Science Edition*), 49(1), 137-140.

Zhang Xiaoyu, Lin Yian, Tang Renyou, Pan Delu, Wang Difeng, Gong Fang, 2005, Preliminary study of concentration distribution of total particulate phosphorus in estuary by remote sensing technology, *Acta Oceanologica Sinica*, 27(1), 51-56.

Zhao Wei, Lin Mingsen, Tang Junwu, Niu Shengli, 2006, Study of exact Rayleigh scattering arithmetic for the ocean color remote sensing, *Chinese High Technology Letters*, 16(8), 876-880.

Zhao Wei, Lin Mingsen, Chen Guangming, Tang Junwu, Niu Shengli, 2006, Study of exact Rayleigh scattering arithmetic for COCTS sensor on "HY-1" satellite, *Acta Oceanologica Sinica*, 28(3), 139-143.

Zhao Jianhu, 2002, Study of the process method for the multi-beam sounding bathymetry data and image, Ph.D. dissertation, Wuhan University.

Zhao Jianhu, Liu Jingnan, 2004, Weaken systematic error in depth data of MES, *Geomatics and Information Science of Wuhan University*, 29(5), 394-397.

Zhao Jianhu, Liu Jingnan, 2003, Development of method in precision multibean acoustic bathymetry, *Geo-Spatial Information Science*, 6(3), 971-74.

Zhou Hao, Wen Biyang , 2002 , Mapping ocean surface vector currents by dual HF ground wave radars, *Oceanologia Et Limnologia Sinica*, 33(1), 1-7.

Zhou Xinghua ,Chen Yongqi et al. 2005, Seafloor Classification of Multibeam Sonar Data Using Neural Network Approach, *Marine Geodesy*, 28 (2): 201-206.

Zhu Hao, Liu WenYao, LiangJie, Hao Yongjie, 2004, Implementation of ELMS algorithm on ADCP signal processing system, *Ocean Technology*, 23(3), 41-45.

Zhu Jiang, Zhou Guangqing, Yan Changxiang, Fu Weiwei and You Xiaobao, 2006, A three-dimensional variational ocean data assimilation system: Scheme and preliminary results, *Science in China Series D-Earth Sciences*, 49(11), 1212-1222.